THE GEOLOGY AND GEOCHEMISTRY OF THE AREA WEST OF LOCH KILLIN, INVERNESS-SHIRE

K.H.Whittles

Submitted for the degree of Ph.D.

1981

ORIGINAL COPY TIGHTLY BOUND

ABSTRACT

The area under study, which lies west of Loch Killin, Inverness-shire, was mapped during the years 1975-1978.

The continuous sequence of pelitic and psammitic metasediments comprises four formations and each is characterised by dominant lithotypes and distinctive minor metasedimentary facies. Lithotypes are described for each formation. Sedimentary structures are described in some detail, allowing an insight into the depositional environment.

The area has been subjected to polyphase folding and four phases (F_1-F_4) are determinable. Morphology and distribution are considered for each fold phase. Geometrical analysis is applied to selected folds. Production of the regional foliation (S_1) accompanied F_1 with later fabrics forming with subsequent deformational episodes. The S_1 fabric is analysed graphically (using selected smaller areas)thus elucidating trends and the influence of later phases of folding.

All lithotypes are described petrographically and the petrology of both white and green calc-silicates is discussed in some detail, with reactions postulated to account for mineral assemblages. The white calc-silicates are further used to establish metamorphic zones which aid in assessing the metamorphic grade in the absence of a full sequence of Barrovian zonal index minerals. Timing of metamorphism is related to deformational episodes using textural information and two major metamorphic peaks (M_1 and M_2) are isolated.

Minor intrusive bodies of the Newer Granites and two petrographically distinct suites of granophyres occur in the area. Selected samples are described and compared. Small suites of amphibolites and meta-appinites are also studied.

Abstract-continued.

Chemical analyses of 115 samples are presented and the geochemical study appraises the results from various suites in order to link chemical and mineralogical variations, to discover the chemical bases for differences between groups and to compare Killin rock types with similar lithologies from other regions.

ACKNOWLEDGEMENTS

My grateful thanks are due to many people, but primarily to John Winchester for advice and constant encouragement throughout my stay at Keele and afterwards. Also at Keele, I thank all friends and colleagues for excellent company and lively discussions. A special debt of gratitude is due to all technical staff in the Department of Geology, under the guidance of Mike Stead. Financial assistance from the University for fieldwork expenses is also acknowledged.

Access to selected computer programs was readily provided by Steven Daly, for which I am most grateful.

Finally, I thank Cath, my wife, for her help with the typing and for her patience.

NOTES

i) The scale of field photographs is indicated by the following:

Hammer shaft-32 centimetres

Hammer head-14 centimetres

Long edge of clinometer-10 centimetres

Lens cap-5 centimetres

ii) The pocket at the rear of the thesis contains the 1:10,000 field map of the Killin area.

CONTENTS

INTRODUCTION

i) Physical Geography of the Killin area.

The area studied lies 5 kilometres south-east of Loch Ness and covers approximately 80 square kilometres. It is situated in the south-western Monadhliath mountains, lying between latitudes 57° 12' to 57° 4' N and longitudes 4° 35' to 4° 25' W. The area is approximately triangular and has at its apex Whitebridge, a small village connected by minor roads to Fort Augustus in the west and Foyers to the south.

Rivers are the main features which delineate the area (Figure 1), in the east the Rivers Fechlin and Killin and south of Sronlairig Lodge, the Allt Odhar. On the north-western side the boundary is formed by the Cumrack Burn with its right-bank tributary, the Allt Vungie south of Loch nan Eun. The southern and south-western limits are partly followed by the River Tarff and the Allt Doe.

The largest loch is Loch Killin which lies in a typically U-shaped valley. Small lochs are numerous, especially in the western part of the area, the larger ones being Loch nan Eun and Dubh Lochan. All valleys are U-shaped and dissect a plateau which forms much of the area and is covered by extensive peat bog. This is especially true in the south and south-east around and below Carn Easgann Bana and the Allt à Choire Odhar. Exposure here is poor but isolated outcrops are seen in peat bogs or in small burns. To the west of Glen Brein exposure improves especially around Cairn Vungie where

Figure 1 Main geographical features of the Killin area

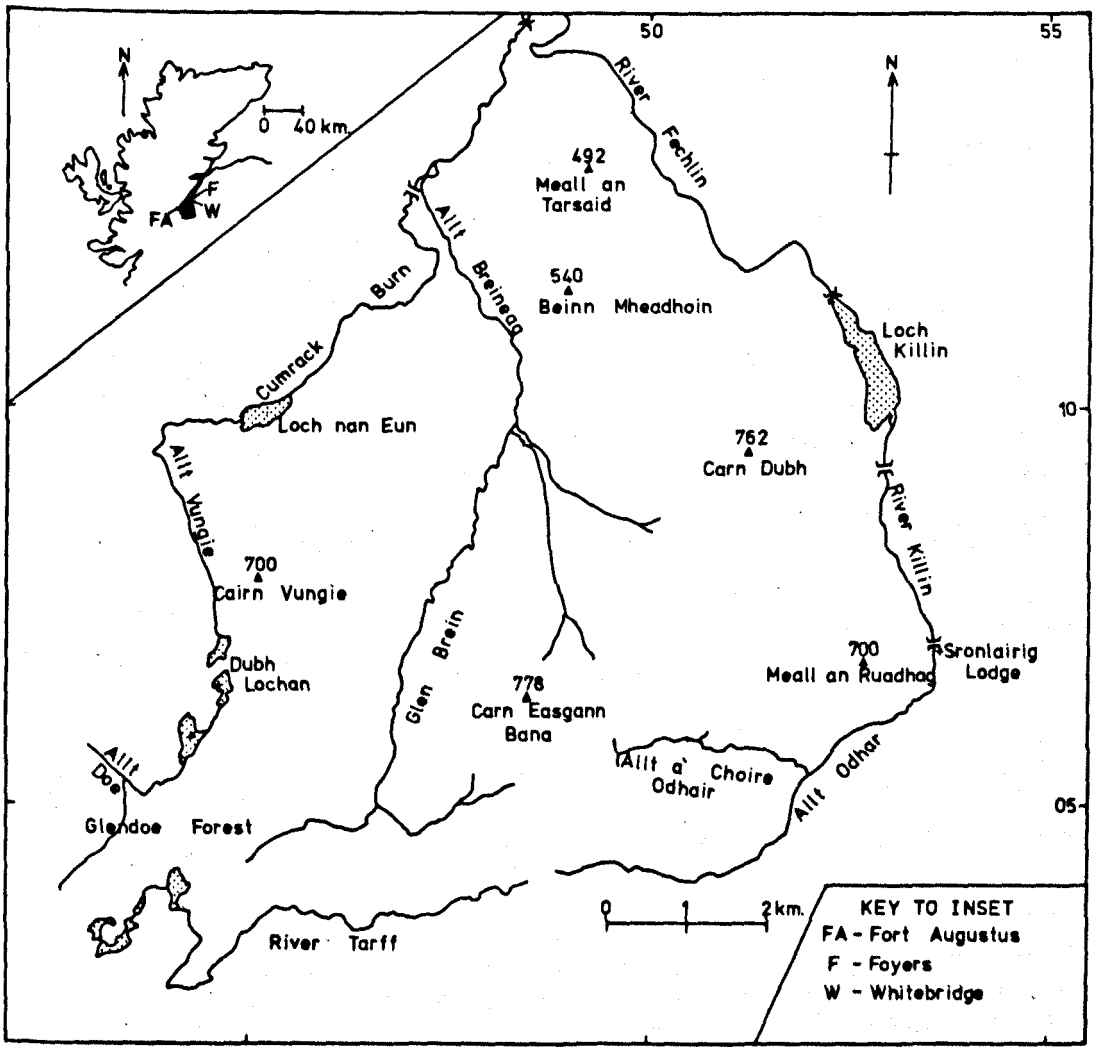
N
0 40 km
F
FA
W
50
55
N
River Fechlin
492
Meall an Tarsaid
Allt Breineag
540
Beinn Mheadhoin
Burn
Cumrack
Loch Killin
Loch nan Eun
762
Carn Dubh
10
Allt Vungie
River Killin
700
Cairn Vungie
Dubh Lochan
Glen Brein
778
Carn Easgann Bana
700
Meall an Ruadhag
Sronlairig Lodge
Allt Doe
Glendoe Forest
Allt a' Choire Odhair
Allt Odhar
05
0 1 2km.
River Tarff
KEY TO INSET
FA - Fort Augustus
F - Foyers
W - Whitebridge

low ridges alternate with small lochs. Exposure elsewhere is reasonable, particularly in the eastern rivers and the area north and west of Loch Killin.

Access to the area in the north-east is by a road which approximately parallels the River Fechlin and Loch Killin. South of Loch Killin the road is private but continues to Sronlairig Lodge. From the lodge paths skirt the Allt Odhar and the southern parts of the area. The central and western parts of the area are reached by paths which run alongside the Allt Breineag and the Allt Vungie respectively.

Although the major valleys are all U-shaped and glacial deposits are abundant, they do not form part of this study. Alluvium covers much of the northern reaches of the Cumrack Burn west and north of Meall an Tarsaid and the River Killin. The latter possesses a flood plain almost 600 metres wide which is now used as pasture.

ii) History of Research.

Anderson produced the earliest geological description of the area in 1956. He produced a very broad stratigraphic division into Eilde Flags and Monadhliath Schists and equated the Highland succession with that of the Lochaber District produced by Bailey (1934). Description of the structures was limited primarily to to the major features eg. the Corrieyairack Syncline which repeats the succession in the Killin area.

Information about the Newer Granites is provided by three authors, especially Anderson (1956) who mentioned all three intrusive granites in the Killin area. Mould (1946) instigated research on the Foyers Granite and

Marston (1971) provided a detailed study of the Foyers intrusion. No detailed study of the Allt Crom Granite has been documented.

Reference has been made to the study of white calc-silicates in the Western Moines. This minor lithology was studied initially by Kennedy (1949) and subsequently in increasing detail by Winchester (1970, 1972, 1974 b & c) and Tanner (1976). Work by Winchester on the metamorphic zones of Fannich Forest and Freevater Forest provide the base for similar work in the Killin area.

CHAPTER ONE-STRATIGRAPHY

1.1 Nomenclature

The term 'Moine' itself has no stratigraphic significance (Johnstone,1975), in the past it has been used in a regional sense. It would therefore seem logical to refer to such rocks as the Moinian Metamorphic Assemblage (Anderson,1948) or the Moine Succession (Johnstone, 1975), implying a sequence of lithologies.

Subdivision of an assemblage produces major groups composed of formations (Harland et al.,1972). The group of rocks covering much of the Monadhliath Mountains and forming the 'cover' to the Central Highland Division basement, is not named in this thesis but has been termed the Grampian Division (Piasecki,1980) to conform with the existing nomenclature of the subdivisions of the Moinian Assemblage proposed west of the Great Glen.

Rocks to the east of the Great Glen (underlying the Dalradian and collectively known as the 'Central Highland Granulites', Anderson,1948), have been regarded as part of the Moinian Assemblage for some time. Although similarities have been noticed (e.g. Johnstone,1975) no definite stratigraphical correlations across the Great Glen Fault have been proven. The rocks studied in this thesis may form part of the Grampian Division (Piasecki,1980) but the status of this Division within a regional stratigraphy is largely outside the scope of this thesis.

The four tectono-stratigraphic units described here can therefore be termed formations but correlation with possible equivalents in earlier works is difficult

because of the multitude of names produced by numerous authors over the past years. Examples are provided by Anderson (1948) and later by Piasecki (1975).

The term 'Monadhliath Schist' was first applied by Anderson (1948,1956) following traverses across the Monadhliath mountains. Subsequent work equated the schists of the central region (south of the Great Glen) with those of the Lochaber region further southwest, although the connection remained unproven. Hence the use of 'Monadhliath Semi-pelite' in this thesis is for ease of recognition and not for purposes of correlation with earlier proposed successions.

1.2 Stratigraphic Column

1.2.1 Introduction

The succession consists of four tectono-stratigraphic units within the Grampian Division. Their distribution is shown in Figure 2a. Throughout the area (with one locality excepted) bedding (S_0) represented by calc-silicate bands and compositional changes in the major lithologies was seen to be parallel to the prevalent tectonic foliation (S_1). Primary sedimentary features are occasionally preserved and substantiate the S_0/S_1 fabric. The continuity of the tectono-stratigraphic sequence is confirmed by the lack of evidence for major tectonic discontinuities or mylonites and the gradational nature of boundaries between the formations. The four formations are distinguished firstly by their dominant lithotype and secondly by characteristic subsidiary associations. Calc-silicate bands, which occur as two major distinct lithological types with one subsidiary

Figure 2a Distribution of tectono-stratigraphic units

Figure 2b Lithologies and sedimentary structures in the succession (see also Figure 3)

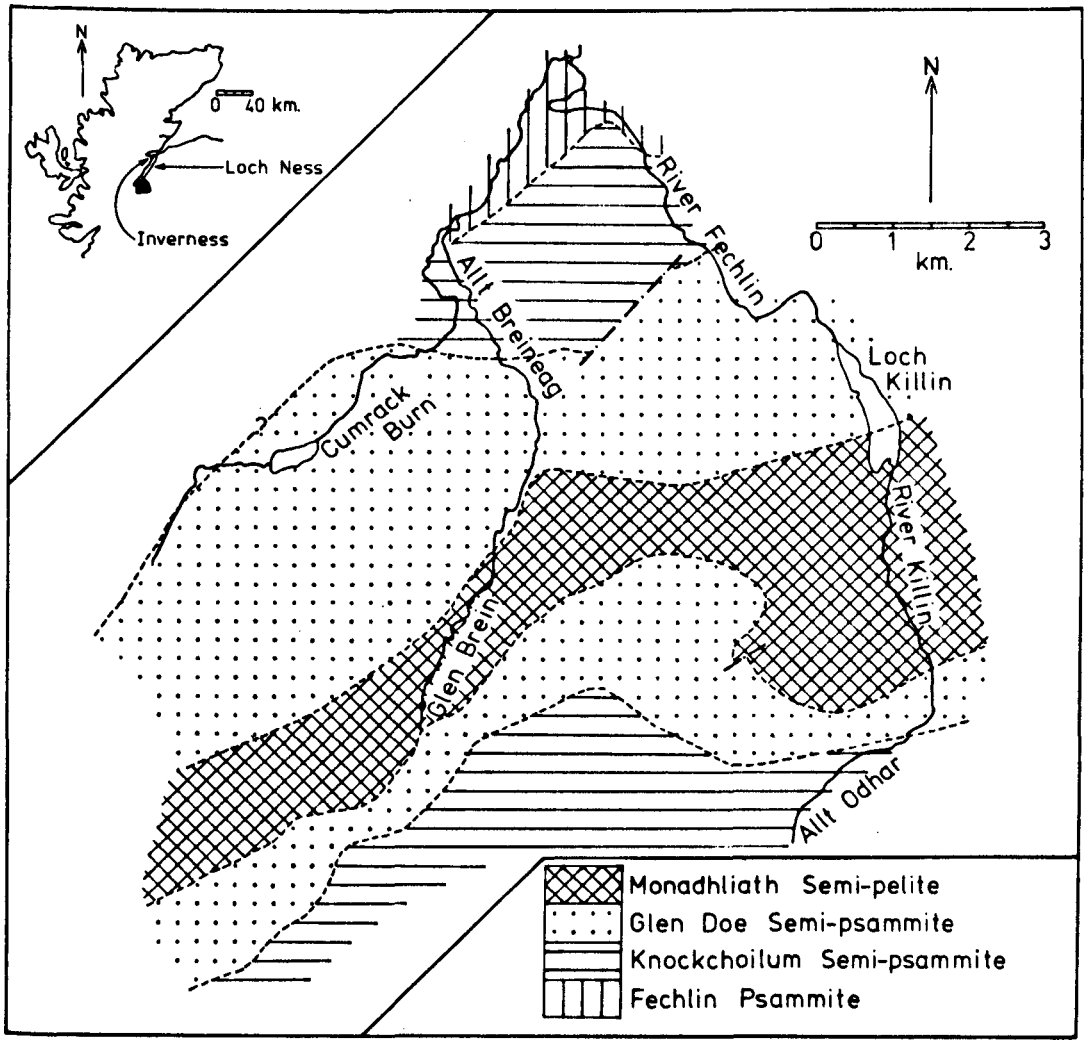

Succession	Lithology	Sedimentary structures
Monadhliath Semi-pelite	semi-pelite with white calc-silicate and psammitic bands	cross-bedding:cross-lamination: convolute bedding:loading: cut and fill.
Glen Doe Semi-psammite	semi-psammite with pelitic, semi-pelitic and white calc-silicate bands	cross-bedding:cross-lamination: convolute bedding:grading.
Knockchoilum Semi-psammite	semi-psammite with semi-pelitic and green calc-silicate bands	cross-bedding:convolute bedding:cut and fill.
Fechlin Psammite	massive psammite and semi-psammite with green calc-silicate lenses	cross-lamination:loading: grading.

(not to scale)

Figure 3 Range and abundance of minor lithologies

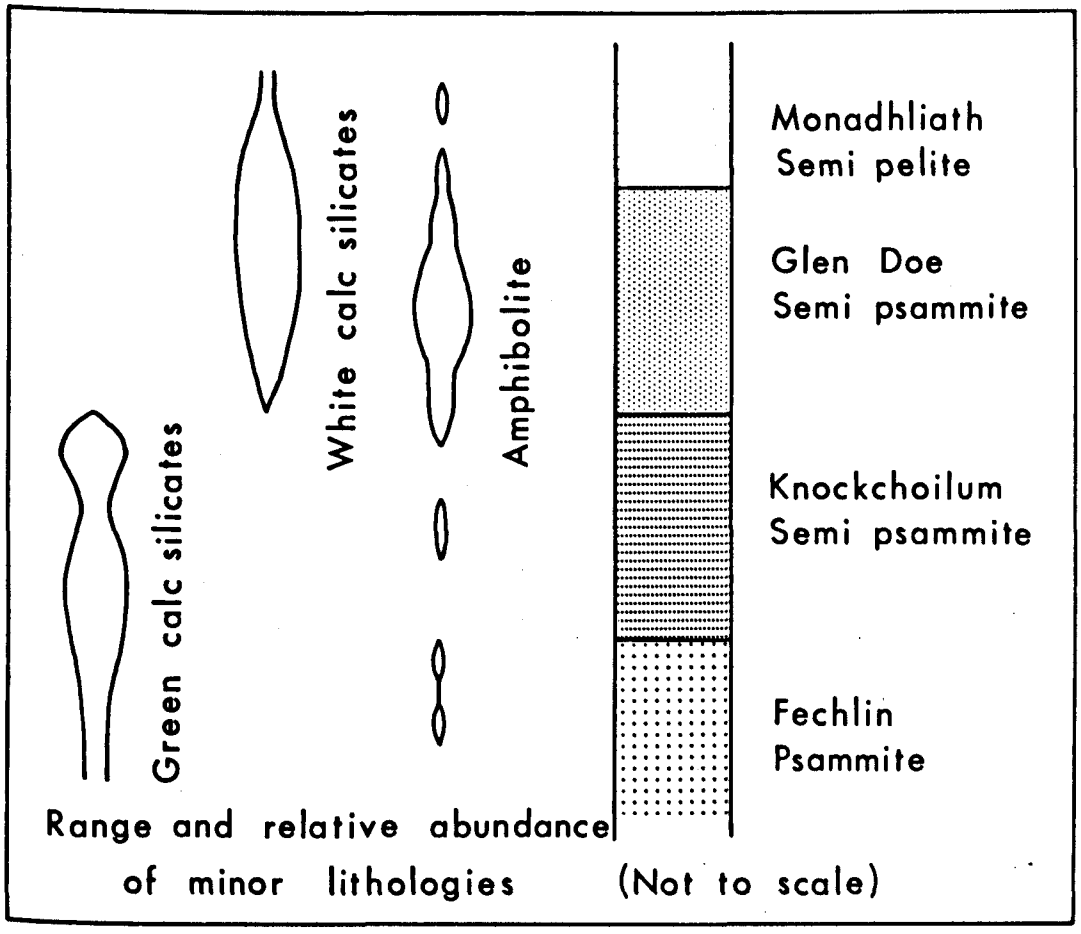
Green calc silicates
White calc silicates
Amphibolite
Monadhliath
Semi pelite
Glen Doe
Semi psammite
Knockchoilum
Semi psammite
Fechlin
Psammite
Range and relative abundance of minor lithologies
(Not to scale)

type (Arnipol type; MacGregor,1948), are restricted to specific units (cf.Figure 2b) and can be used to position unit boundaries.

Detailed descriptions of the two major calc-silicate types are given in Chapter 3 but their salient features can be summarised here. Named after their overall field appearance, both'green' and'white' types occur predominantly as thin (4cm. thick) bands or lenses. The major minerals in the white calc-silicates are quartz, garnet, amphibole, clinozoisite and plagioclase whilst the green calc-silicates contain quartz, amphibole, pyroxene, zoisite/epidote and some plagiocase.

1.2.2 Fechlin Psammite Formation (~950 metres thick)

This unit, which forms the base of the sequence, is confined to the northern part of the area and the main outcrop is seen in the River Fechlin. Further north still, (grid reference 145490), the unit is extensively veined and altered by granitic material which is probably related to the Foyers Newer Granite. The effect of this and other granitic intrusions on the country rocks will be discussed later (Chapter 6).

Lithotypes:

(i) Psammite: The meta-sandstones or psammites are planar bedded with a sheet-like bed form. A more detailed sedimentological discussion is set out in Chapter 2. The psammites are coloured beige or grey and the partings in the rock vary from 5 centimetres in thickness thus imparting a flaggy aspect, up to 1.5 metres producing massive beds. Within each psammite bed the pelitic content

varies, in some cases present as thin pelitic laminae and in other examples as a definite increase in mica content throughout the bed, in a more homogeneous nature, producing a semi-psammite. The pelitic laminae are thin (2 millimetres thick) and may be regarded as a relict planar fabric (S_0) and in many cases they delineate primary features other than bedding e.g. cross-bedding and cross-lamination.

(ii) Semi-psammite: This forms one of several subordinate lithologies occurring as bands (<15 centimetres thick) within psammite sequences or as thinner bands comprising a more substantial unit (>30 centimetres thick). The change from psammite to semi-psammite is denoted by an increase in biotite content. Garnet is absent from both these lithologies.

(iii) Quartzite: Laterally discontinuous grey quartzites occur at only two horizons. Reaching a maximum thickness of 5 metres, both exhibit well-defined jointing.

(iv) Calc-silicates: Although uncommon, green calc-silicates occur sporadically throughout the unit usually as lenses. Characteristically weathering brown, they rarely exceed 3 centimetres in width and 10 centimetres in length. Their overall light-olive green colour is uniform over the width of the lens, but the margins often show a white quartz-rich selvage, sometimes with pink garnets (1.5 millimetres diameter), and a subsequent gradation into the host psammite or semi-psammite.

1.2.3 Knockchoilum Semi-Psammite Formation (<2000 metres thick)

This semi-psammite unit covers extensive areas on both the northern and southern limbs of the major Corrieyairack syncline, part of its upper junction in the northern outcrop being fault-bounded. It is distinguished from the Fechlin Psammite by an increase in pelitic material up the succession producing a higher proportion of semi-psammite and semi-pelite bands. Green calc-silicates are also present but occur primarily as bands, not lenses.

Lithotypes:

(i) Semi-psammite: Bands up to 20 centimetres in width are common, some with thin (<3 millimetres thick) pelitic partings. The semi-psammites are various shades of grey in colour and often show a 'salt-and-pepper' appearance due to the distribution of quartz with biotite.

(ii) Semi-pelite: Bands occur up to 5 centimetres in in width and, with an increase in mica content, grade into pelite. Throughout the unit the bands may form a pelitic sequence reaching 50 metres, which then grades back into the semi-psammite. Small pink idioblastic garnet porphyroblasts (1 to 3 millimetres in diameter) occur in all lithologies but are most common in the pelitic bands.

(iii) Quartzite: Grey quartzite bands, 5 metres thick, were observed in three locations, two of which may be

stratigraphic equivalents. The beige to grey quartzites are similar to others elsewhere in the area, and are strongly jointed. In one occurrence the quartzite unit was divided by a thin (4 centimetres thick) pelitic band.

(iv) Calc-silicates: As in the Fechlin Psammite formation, green calc-silicates are present throughout and these are identical to those of the psammite unit except for their dimensions. Here they occur as bands up to 2.5 centimetres thick, commonly traceable for several metres, but lenses are rare.

1.2.4 Glen Doe Semi-Psammite Formation (<1400 metres thick)

This unit outcrops on both limbs of the Corrieyairack syncline and shows a disparity in total apparent thickness. Lithologically, this unit is very similar to the underlying Knockchoilum Semi-psammite but with one important difference; the presence, in the former, of white calc-silicate bands.

Lithotypes:

(i) Semi-psammite: With partings between 6 and 10 centimetres in thickness, semi-psammite comprises flaggy sequences (<50 metres thick) with semi-pelite thinly interbanded (4 centimetres thick). The semi-psammite is usually coloured dark grey and often the arrangement of quartz grains and small aggregates of mica produces a mottled appearance. Garnets are uncommon.

(ii) Pelite and Semi-pelite: Both lithologies are

common throughout as thin (<5 centimetres thick) bands in semi-psammitic sequences. Subhedral garnets are often present reaching diametres of 3 millimetres. Often associated with thin (<5 millimetres thick) quartzose bands, these pelites weather a rusty brown.

(iii) Psammite: Bands of psammite are more common in this unit than in the Knockchoilum Semi-psammite. However, they are not sufficiently consistent features to be useful in distinguishing between the units. Coloured grey and frequently massive (bands >50 centimetres thick), this lithotype often outcrops over several metres.

(iv) Quartzite: Several occur but all are of limited lateral extent. The major development is on the western shore of Loch Killin, immediately below the boundary with the Monadhliath Semi-pelite. The quartzite is beige to grey in colour and in places reaches 10 metres in thickness with strong jointing. However, over a distance of 200 metres quartzite is the dominant rock type constituting a subsidiary lithology. It is not possible to trace this quartzite westwards for more than 1500 metres, where it grades into relatively more pelitic lithologies. This is undoubtedly the quartzite mapped initially by Anderson (1956) and named the Eilde Quartzite. Piasecki (1975) also discovered a poorly exposed impersistent quartzite in the Findhorn district which he likewise equated with the Eilde Quartzite. It is considered that the discontinuous nature of this and many other quartzites, and the lack of correlation of the Monadhliath Semi-pelite with the Eilde Schist, renders definite correlation with the Eilde Quartzite of Lochaber extremely dubious.

(v) Calc-silicates: White calc-silicate bands occur in this unit and most cluster near the upper boundary (with the Monadhliath Semi-pelite) both on the northern and southern limbs of the Corrieyairack syncline. The calc-silicates are very distinctive in the field occurring as thin (<4 centimetres thick) bands, usually coloured white or, more rarely, grey. They characteristically contain hornblende and clinozoisite and garnet (see Chapter 3). Hornblende occurs as dark green blades and garnet as dominantly euhedral pink to red porphyroblasts up to 4 millimetres in diameter. Clinozoisite commonly exists in bladed or tabular form. Banded calc-silicates are less common, the bands being visible as a colour difference related to the phase content.

1.2.5 Monadhliath Semi-pelite Formation (c. 700 metres thick)

This uppermost unit of the succession, occupying the core of the syncline, is distinguished by the pronounced increase in the proportion of semi-pelite and pelite, the boundary with the Glen Doe Semi-psammite being completely gradational. Psammitic lithologies become subsidiary and white calc-silicate bands are not only more common but also better developed.

Lithotypes:

(i) Semi-pelite: This lithotype totals approximately 65% of the whole unit exposed. With individual bands rarely exceeding 7 centimetres in thickness, semi-pelite units may reach thicknesses of up to 1 metre. The semi-

pelite contains small red to brown, dominantly euhedral, garnets (2 millimetres in diameter) and in places a great number of quartz-rich laminations. Such development produces an interbanding of pelitic and quartzose layers on a small scale, individual laminations reaching 3 to 4 millimetres in thickness.

(ii) Pelite: A substantial 'wedge' of dominantly pelitic schist is discernible around the southern end of Loch Killin, extending for approximately 1100 metres laterally and 750 metres perpendicularly to the strike trend. No tectonic discontinuities are associated with the pelitic wedge which must therefore reflect an initial variation in composition in the original sediment. Small pink euhedral garnets occur but cannot be described as very common. Lack of garnets in pelites or semi-pelites must be due to compositional variation between bands i.e. insufficient iron and magnesium. Staurolite or aluminium silicate minerals were not found in any pelitic lithologies.

(iii) Psammitic lithologies: Semi-psammite bands form a frequent subsidiary lithology, usually thinly banded (5 to 10 centimetres thick) and often intimately interbanded with semi-pelite. Psammites are less common in this unit, as are quartzites.

To the south of Killin Lodge, semi-psammites become more apparent but are not sufficiently developed to warrant inclusion as a separate subsidiary lithotype within the formation.

(iv) Calc-silicates: White calc-silicates are abundant as bands commonly 4 to 5 centimetres thick but

reaching 9 to 10 centimetres in thickness. A more comprehensive petrological description is given later (Chapters 3 and 4). The bands are very similar in appearance to those described from the Glen Doe Semi-psammite.

All unit boundaries show a transitional change over many metres (<150 metres) with no evidence of tectonic discontinuity.

1.3 Lithological Variations

Throughout the sequence, apart from an initial vertical alternation of lithologies producing inter-banding, there is also a transitional change of rock types laterally, related to the original depositional conditions.

Within a semi-psammite unit, pelitic content varies considerably but tracing individual semi-psammitic beds to monitor the transition is very difficult due to both lateral variation in composition and to the lack of continuous outcrop. The task is somewhat simplified by choosing a distinctive lithology e.g. a thin (<50 centimetres thick) quartzite band which affords an excellent example that, with better exposure, may well be applicable to the thicker developments of quartzite. Towards the edge of the quartzite, intercalations of psammite and semi-psammite occur, accompanied in some instances by a thinning of the quartzite suggesting an initial lens shape.

The 'wedge' of pelitic schist within the Monadhliath Semi-pelite is probably a similar development. The lack

of tectonic features associated with the schist suggest a lateral lithological transition with the adjacent semi-pelitic rocks.

1.4 Stratigraphical Correlations

1.4.1 Correlation of the Moines Assemblage west of the Great Glen Fault with the sequences east of the Great Glen.

The Moine succession west of the Great Glen fault consists of a threefold division-the Morar, Glenfinnan and Loch Eil Divisions-a subdivision erected by Johnstone et al.(1969). Of these three, the Loch Eil Division outcrops in the east (cf. Figure 6 of Johnstone, 1975) and is adjacent to the Great Glen Fault for its entire length on the mainland of Scotland.

The rocks east of the Great Glen Fault possess a lithological similarity which has led previous workers to equate them with the Moines west of the Great Glen Fault.

Local successions in the North-western Highlands (e.g. Ramsay and Spring,1962; Powell,1964) illustrate the similarity in lithologies throughout the Moine outcrop. The schist formations contain subordinate psammitic rocks and calc-silicate bands, and these have their equivalents, superficially, in the Killin area. Likewise the Fechlin Psammite formation shows similarities to the western psammitic formations. However, the general equivalence is still not proven and if any reference is to be made, the Killin sequence is better placed with the Grampian Division (Piasecki,1980)

Isotopic data has now produced 'Morarian' and

'Grenvillian' dates east of the Great Glen Fault (Piasecki & van Breeman,1979,1979a) comparable to those existing in the western Moines. Grampian Division rocks form a cover to Grenville age rocks of the Central Highland Division (op. cit.) and unless a proven 'Grenville' age for Loch Eil and Morar Division Moines is produced, then one of these latter two divisions may form a likely equivalent to part of the Grampian Division.

1.4.2 Correlation of the Monadhliath Semi-pelite with the Leven Schist

The equivalence of the Monadhliath Semi-pelite (Monadhliath Schist of previous authors) with the Leven Schist was accepted after its postulation by Anderson (1956), and it appeared in many subsequent publications. The quartzite intermittently present near the base of the formation was thus correlated with, and frequently called, the 'Eilde' Quartzite (Piasecki,1975).

Detailed mapping to the south-west of the Killin area (Haselock, pers. comm.) has suggested that at least two breaks occur in the continuity of outcrop between the Monadhliath Semi-pelite and the Leven Schist. Also, the two units do not occur at the same stratigraphic level. Mapping between Glen Roy and the Corrieyairack Pass has shown the Monadhliath Semi-pelite to thin southwards and to lie stratigraphically beneath the Leven Schist from which it is separated by a thick sequence of semi-psammites (Haselock & Winchester, in press). The Leven Schist consists of grey-green phyllite and mica schist (Hickman,1975) but phyllitic lithologies are absent in the Killin area. The presence of distinct 'calcareous

strata' which indicate the proximity of the Ballachulish Group do not find their equivalent in the Monadhliath formation. Calc-silicate bands are abundant in the latter, but occur throughout the formation as discrete bands. Correlation between the two formations is therefore difficult, especially since major facies changes must also be postulated (Anderson,1956; Hickman,1975).

If all this evidence is correct, there is no justification for equating the Leven Schist and Monadhliath Semi-pelite stratigraphically and hence little evidence for including the Monadhliath Semi-pelite as part of the Dalradian Assemblage, unless the entire Grampian Division is interpreted as an integral part of the Dalradian Assemblage.

1.4.3 Equivalence of 'Moine' with Torridonian

This possibility has been raised several times, especially with regard to the Moine Assemblage of the Northern Highlands. Although work in the Killin area provides no information, a brief summary of relevant evidence is included here.

No reliable date yet exists for deposition of western Moine sediments although Long and Lambert (1963) suggested a maximum of about 1000 m.y. Brook *et al.* (1977) recorded a whole rock age of 1002±94 m.y. for the metamorphism of the Morar Pelite at Druimindarroch. A further date from the Upper Morar Psammite of 820 m.y. (Moorbath,1969) would seem to comply with these dates. A minimum depositional age of 730 m.y. has also been postulated in the Knoydart-Morar

area (Giletti et al.,1961; Long & Lambert,1963).

Ages from the Torridonian provide dates of 965 and 785 m.y. for the Lower and Upper Torridonian respectively (Moorbath,1969) and therefore possible equivalence with either part cannot be ruled out. However, because the picture is complicated by the movement along the lines of the Moine Thrust, Sgurr Beag Slide and Great Glen Fault, any correlation between the Torridonian and any part of the Grampian Division is equally almost impossible to prove.

CHAPTER TWO-SEDIMENTARY STRUCTURES

2.1 Introduction

Relict sedimentary structures are found in all four formations (Figure 2b). They include cross-bedding and cross-lamination, cut and fill structures, graded and rhythmic bedding and examples of soft-sediment deformation.

Preservation depends on two factors; (a) the lithology and (b) the amount of tectonic deformation, hence the formation in which most primary structures are seen is the relatively competent Fechlin Psammite in which deformation has been less penetrative than in the more pelitic sequences. This also applies to quartzite beds. The terminology used for thickness is that of Ingram (1954); beds >1 centimetre, laminae <1 centimetre.

Since these rocks have been affected by regional metamorphism all of the minerals present have been recrystallised. The internal structures preserved, such as cross-bedding and cross-lamination, are outlined by pelitic laminae which now occur as discrete planes of biotite (and muscovite). It may be assumed that the mica grew from primary bands of sediment which were rich in alumino-ferromagnesian minerals, for example, a shale band within sandstone. Since recrystallised metamorphic minerals outline the relict structure of the original sediment the term 'blasto-psammitic' may be applied (Spry,1969).

2.2 Cross-bedding (Plate 1)

Cross-bedded semi-psammitic beds within alternating semi-psammitic and semi-pelitic sequences occur throughout

Plate 1 Cross-bedding from the Killin area

Plate 2 Cross-lamination

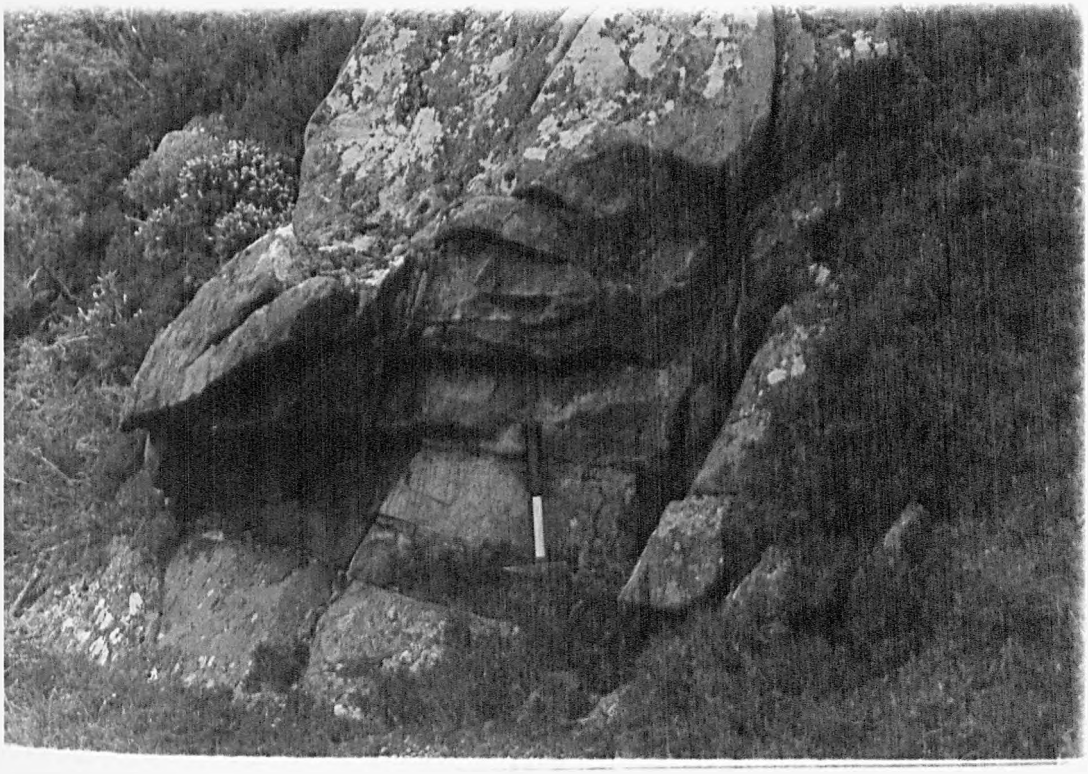

the area. The cross-bedding is defined by concave-upwards pelitic laminae, maximum thickness 3 millimetres, often slightly flattened by subsequent tectonic deformation. The laminae are tangential to the bases of the beds, and truncated at the tops (which are therefore erosive). The maximum thickness of these isolated, tabular (McKee & Weir, 1953) sets is approximately 35 centimetres and they extend laterally up to a maximum of 3 metres. In both style and scale, these cross-bedded sets resemble those described from the Moines of Sutherland and Ross-shire (Wilson et al., 1953). Few examples of cross-bedding from the Killin area afforded surfaces for precise measurements to be taken to enable determination of the palaeocurrents. Only four such measurements were possible and from these, only random directions were obtained, unlike the southerly derivation determined in Sutherland (op. cit.)

2.3 Cross-lamination (Plate 2)

Thin cross-laminated cosets with individual set thicknesses of 3 centimetres are common within banded semi-psammitic beds. Some units, where the tops of the inclined pelitic laminae are truncated, resemble the cross-bedding on a smaller scale. The structures are laterally impersistent occurring over a maximum of 40 centimetres, and the sets show truncated surfaces.

2.4 Cut and Fill Structures

These are the least common sedimentary structures, only two good examples being recorded, from the Monadhliath Semi-pelite and the Knockhoilum Semi-psammite. The former example (Figure 4) has an irregular base cut into the

Plate 3 Scour channel exhibited in pelite with white calc-silicate bands

Figure 4 Scour from the Monadhliath Semi-pelite (from Plate 3)

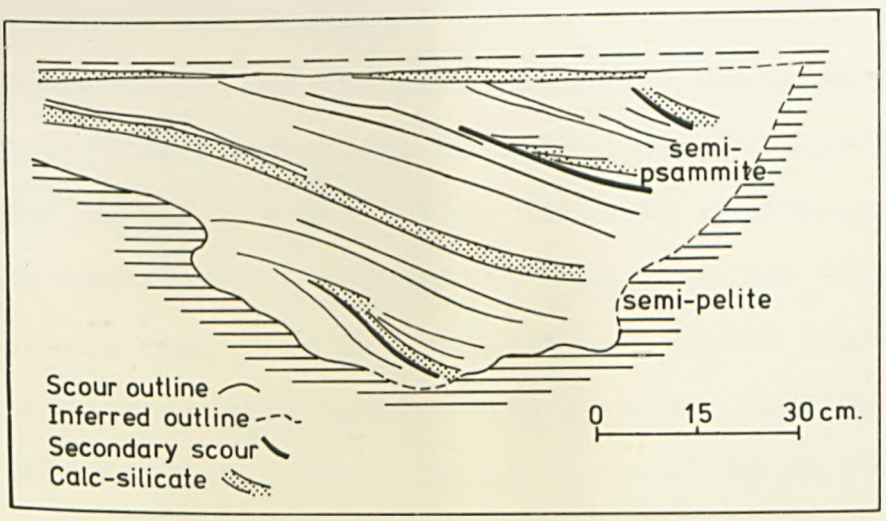
semi-
psammite
semi-pelite
Scour outline
Inferred outline
Secondary scour
Calc-silicate
0
15
30 cm.

underlying pelite, the fill consisting of semi-psammite and white calc-silicate bands. The scour is asymmetrical, measuring 130 centimetres in width and 55 centimetres at its maximum depth. The fill is coarse and cross-statified at a low angle with respect to the planar scour top. Within the scour, several areas show a steepening of the bedding and these probably represent secondary scours. The edges of the scour are locally steep and this would have led to secondary scouring of unconsolidated sediment. The bedding of the fill is similar to epsilon cross-bedding (Allen, 1965) which is generally believed to record accretion on the side of a laterally migrating channel.

The second example which occurs at the top of a banded semi-psammite is 35 centimetres wide and 8 centimetres deep in the centre, the overall shape being symmetrical. The scour clearly truncates pelitic laminae in the host semi-psammite and the fill is of coarser psammite with no internal features (Plate 4).

2.5 Graded and Rhythmic Bedding (Plate 5)

Within the Fechlin Psammite a sequence of rhythmically-banded psammites and semi-psammites contains both reverse and normal grading. Gain or loss of pelitic material (depicted by changes in biotite content) represents an original variation in mud content and thus may reveal original grading. Each bed exhibits a couplet consisting of a lower coarsening upwards and an upper fining upwards unit. This couplet (Figure 5) is observed in at least twelve consecutive beds and therefore warrants the term rhythmic bedding.

The two couplets illustrated in Figure 5 each have a

Figure 5 Graded couplet from the Fechlin Psammite

Figure 6 Flattening of load structure

Figure 7 Erosion surface within convolute lamination

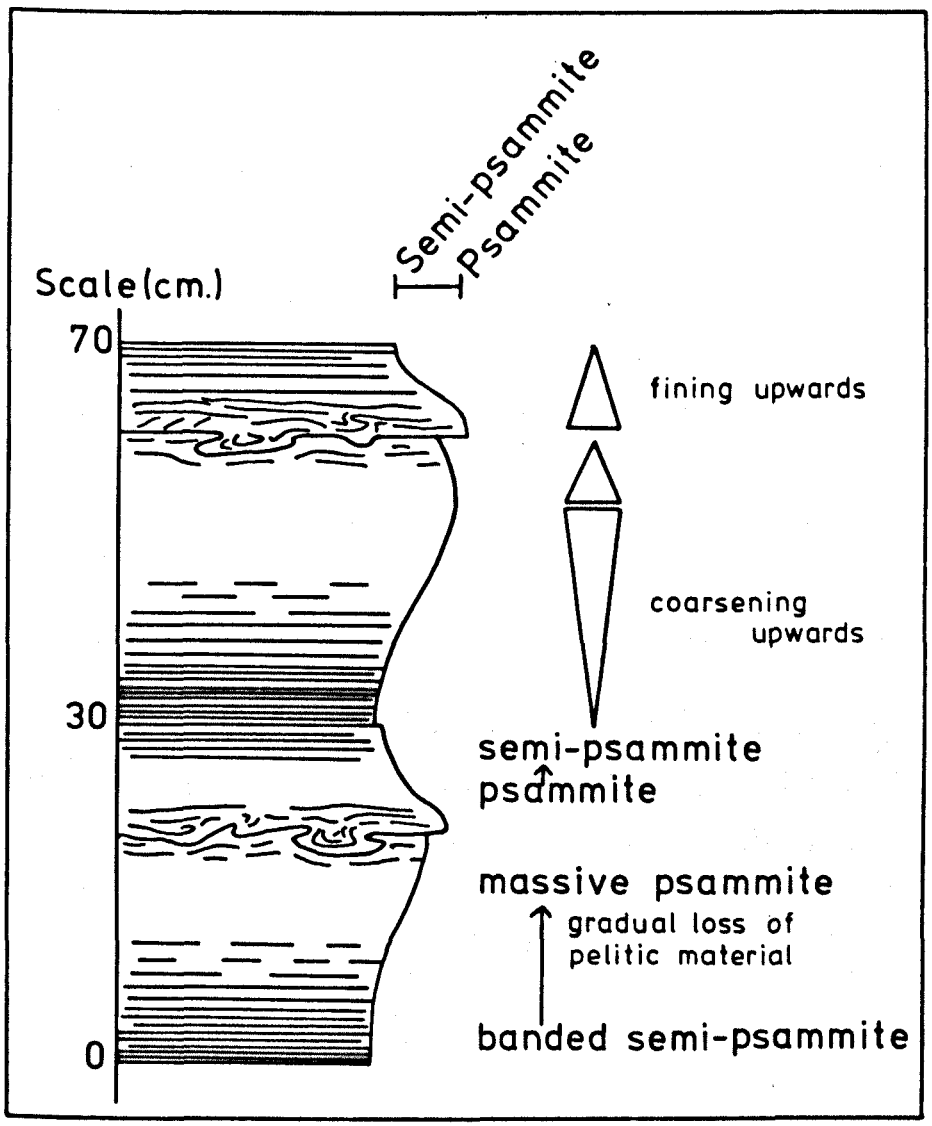
Semi-psammite
Psammite
Scale(cm.)
70
30
0
fining upwards
coarsening upwards
semi-psammite
psammite
massive psammite
gradual loss of pelitic material
banded semi-psammite

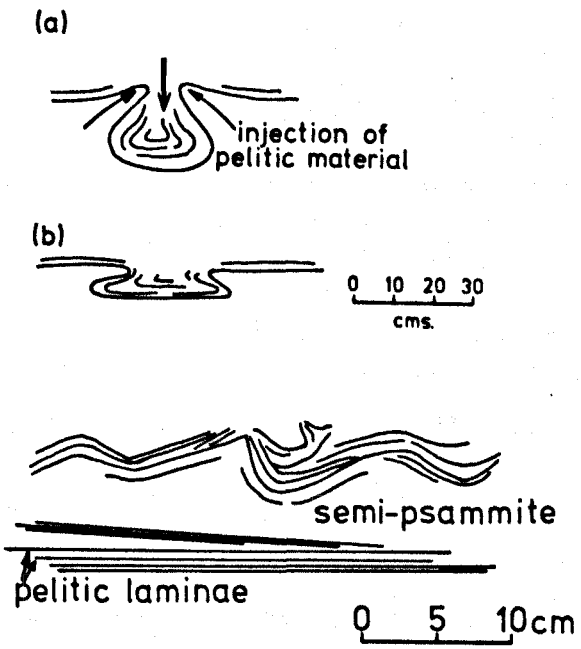
(a)
injection of pelitic material
(b)
0 10 20 30
cms.
semi-psammite
pelitic laminae
0 5 10cm

Plate 4 Small channel scour in semi-psammite

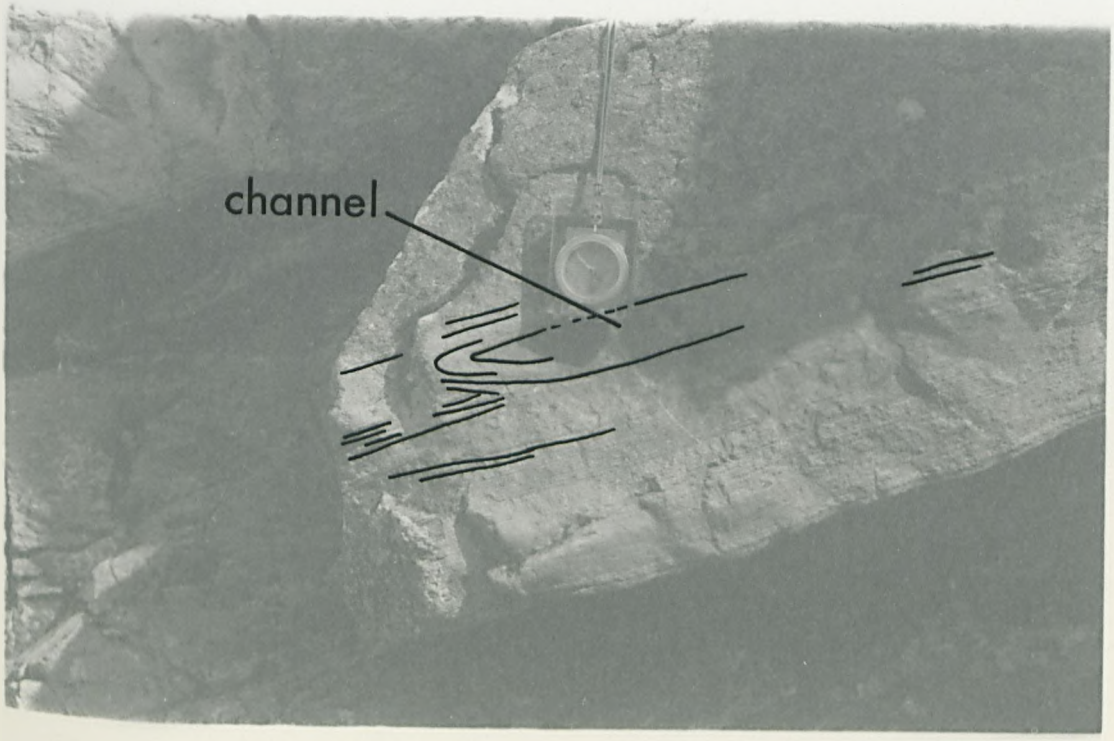
channel

Plate 5 Graded sequence, with loads, in the Fechlin Psammite formation

Plate 6 Loaded white calc-silicate bands

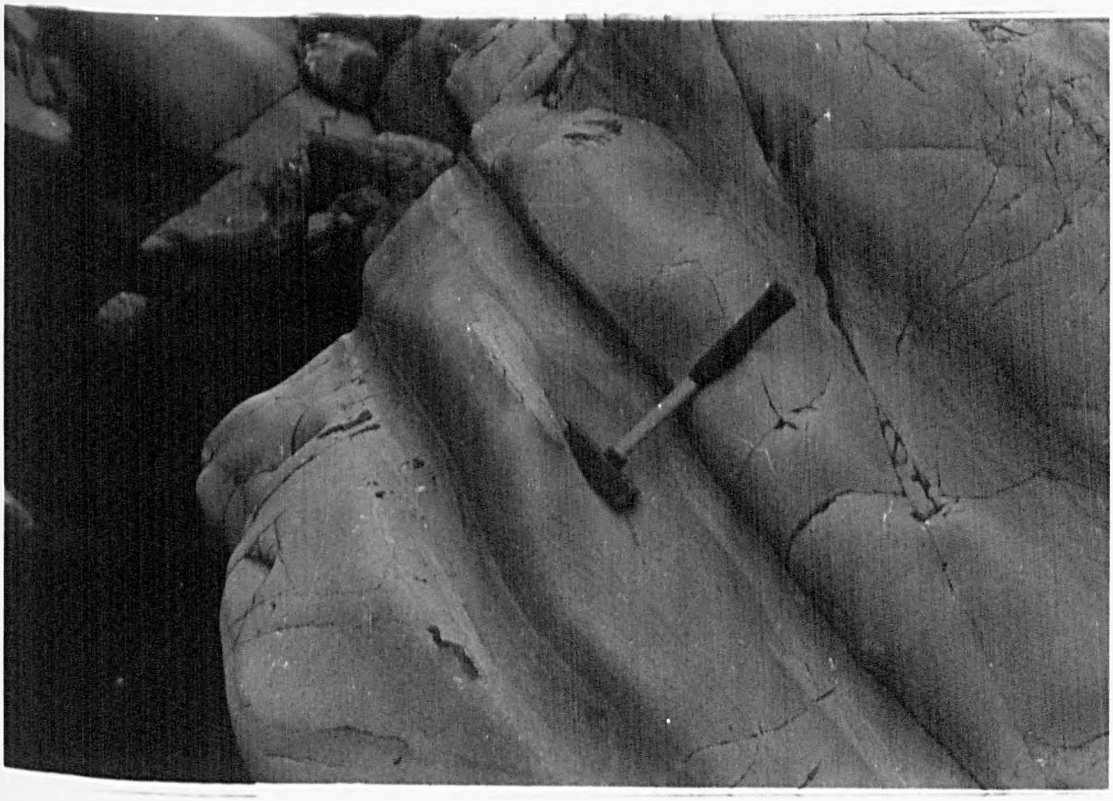

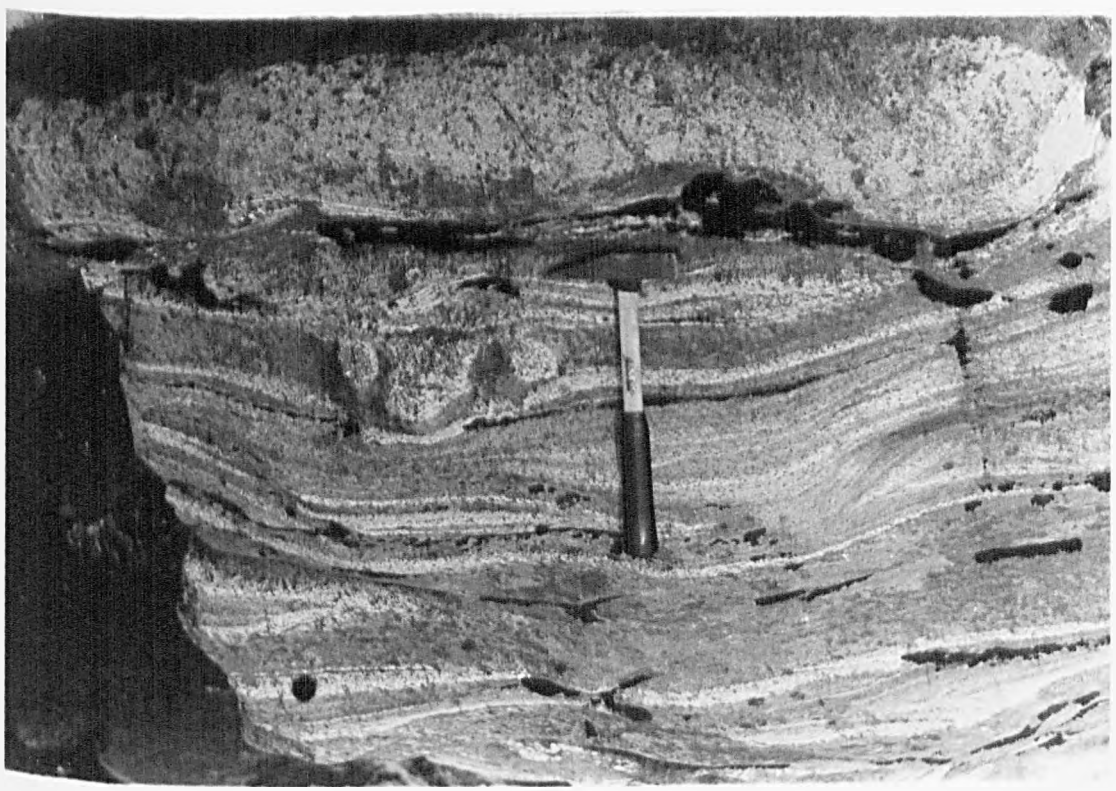

lower unit which is an average 20-25 centimetres thick and exhibit an erosional base underlying semi-psammite which shows dominantly planar lamination. The semi-psammite grades into psammite with a loss of pelitic material, until below the upper half of the couplet it reverts to a semi-psammite. The upper part exhibits normal grading and its psammitic base is invariably loaded down into the underlying semi-psammite.

It is not possible to give a precise interpretation of the processes of deposition of these beds. Any process proposed must account for the production of the couplet. However, although a complete Bouma (1962) sequence has not been observed in the fining upwards units, they do tend to resemble turbiditic deposits.

2.6 Soft Sediment Deformation

2.6.1 Load Structures

The best developed load structures are those previously mentioned from the Fechlin Psammite, where the psammitic base of the upper unit of the couplet has loaded down into the underlying more pelitic parts (Plate 5). The pelitic laminae of this upper psammite are correspondingly deformed though subsequent tectonic deformation has flattened the original shape of the loads (Figure 6) and rotated the associated injection structures. In some units loading has progressed to the extent of producing isolated load-balls (see Plate 5) where loads have become detached from their parent bed. These features suggest rapid deposition and the trapping of much pore fluid (Reineck and Singh, 1975) giving a liquefied bed for a short

period soon after deposition.

A further example of loading occurs in the Monadhliath Semi-pelite (Plate 6). Here three pods ranging in depth from 5 to 10 centimetres (in the direction of loading) extend down from a thin white calc-silicate band. Although tectonic deformation is intense in this area, these features cannot fully be explained as tectonic in origin because their long axes are parallel or sub-parallel to the direction of maximum compression; thus it would seem that they are related to some primary feature. The three pods have clearly been more resilient to deformation than the relatively less competent pelitic matrix. They may represent recrystallised calcareous nodules but their shape makes their interpretation as load structures a more obvious choice. They appear very similar lithologically and geometrically to pseudo-nodules (Kuenen,1958) and may have developed from an originally thicker portion of a marl bed (now calc-silicate).

2.6.2 Convolute Lamination

This structure occurs in layered psammite units of the Glen Doe and Knockchoilum Semi-psammite formations. Careful examination reveals internal erosion surfaces (Figure 7) suggesting an origin from cross-laminated units.

This mode of genesis is commonly recognised and attributed to a combination of sediment liquefaction and the shear stress produced by currents at the sediment surface (Kuenen,1953; Sanders,1965; Allen,1977). The troughs are broad and open whilst the crests are sharp and peaked and appear in places to be'ruptured', probably due to the

expulsion of water (Pettijohn, Potter and Siever,1972).

2.7 Interpretation

The structures and sequences are not considered unique to a specific environment. Deposition in deep marine conditions could produce many of the features described but the association of predominantly tractional features including abundant cross-beds, with calc-silicate bands (originally impure carbonate sediment) is more readily compatible with a shallow to marginal marine environment. This is similar to the suggestions of some earlier studies in the Moinian Assemblage west of the Great Glen Fault (Wilson *et al.*,1953; Johnstone,1975).

In fact each feature can be attributed to one of several depositional environments. Storm dominated offshore or fluvial conditions could produce cross-bedding, channels, grading and possibly convolute lamination (Johnson *et al.*, 1978), whilst shallow marine sedimentation could account for most of the structures seen in the Killin area (Johnson,1977).

The overall picture would therefore suggest shallow marine/sub-tidal conditions subject to the effects of storms resulting in the production of graded beds, where each coarse sandstone may represent a storm event.

CHAPTER THREE-PETROGRAPHY OF METASEDIMENTS

3.1 Psammitic and Pelitic Lithologies

Samples have been studied from all the formations and the information has been compiled here to present an overall picture. Where necessary, individual cases are cited. Each constituent mineral is described for psammitic and pelitic lithologies respectively.

3.1.1 Quartz

Quartz forms a ubiquitous constituent of all the metasediments. Most samples from the Fechlin Psammite formation show the effects of nearby granitic intrusions. Quartz has recrystallised into sub-grains, or exhibits large grains (up to 0.45 millimetres long) with strained extinction. Foliation trends are disrupted by the intrusions, a feature paralleled by the truncation of micas in thin section. Quartz-quartz boundaries are curved or embayed thus suggesting non-attainment of equilibrium (Spry,1969), further substantiated by the disparity in grain size. Contacts between granite veins and semi-psammites are delimited by clearer, larger quartz grains.

In ordinary psammitic and semi-psammitic samples, quartz is invariably strained with development of sub-grains and disequilibriate boundaries. Grains are commonly elongate with a length to width ratio up to five (length < 1.0 millimetres).

Pelitic lithologies contain less quartz, which usually occurs as bands alternating with sheaths of close-packed micas. Quartz grains are often elongate and although most samples do exhibit strained grains with curved or embayed

mineral boundaries, some also show straight boundaries with triple points suggesting an approach, if only partial, to equilibrium.

3.1.2 Biotite

In the Fechlin Psammite formation biotite occurs as elongate flakes (<2.5 millimetres x 0.4 millimetres) exhibiting pleochroism from pale to dark brown, and as very dark brown or bottle green tabular grains (<1.0 millimetres x 0.5 millimetres) showing little pleochroism. In the remaining formations, there is considerably less biotite in the psammites and it is associated with quartz in a granoblastic-polygonal texture. The higher proportion of biotite in the Fechlin samples may be due to the proximity of granitic intrusions, resulting in a partial mobilisation of potassium over short distances.

In semi-psammitic samples, biotite forms flakes exhibiting pleochroism from pale to medium brown. Often it is seen as small flakes growing across, and possibly from another biotite flake. All semi-psammites show development of a planar fabric due to mica alignment, a feature also well-illustrated in the pelitic lithologies.

In all pelitic samples studied in detail, biotite is a major constituent and is usually present as close-packed sheaths, often associated with muscovite. Biotite occurs as elongate flakes and laths (2.75 millimetres x 0.5 millimetres). The fabric is often folded in micro-crenulate style producing fanned extinction in the micas. Zircons form common inclusions in biotite flakes, exhibiting pleochroic haloes around the inclusions.

3.1.3 Muscovite

In the more psammitic lithologies, muscovite usually forms a minor constituent occurring as small flakes reaching a maximum of 1 millimetre in length, aligned with the major planar fabric.

In pelitic samples muscovite occurs more abundantly, as flakes interleaved with biotite often surrounding garnets.

3.1.4 K-feldspar

K-feldspar is common in all psammites, occurring primarily as orthoclase, but with some subsidiary microcline. Samples close to late igneous intrusions show large orthoclase crystals reaching 3.5 millimetres in length and 1.5 millimetres in width. Simple twins are frequently seen and many grains are cloudy and flecked with small grains of secondary sericite. In the remaining psammites, orthoclase occurs as smaller (<2.0 millimetres long) equant grains and constitutes a much smaller volume than it does in samples close to granitic intrusions. Microcline occurs only in very small amounts as inequant grains showing vague cross-hatch twinning. It is hard to distinguish because in many samples, growth of sericite obscures the properties of the feldspar. Insufficient information is therefore available to comment reliably upon the distribution of microcline.

In more semi-psammitic samples, orthoclase is the primary mineral again exhibiting cloudiness. Habit varies from 'interstitial' between quartz and biotite, to larger grains with straight or curved feldspar-feldspar interfaces.

In pelitic samples orthoclase is present as small (approximately 0.4 millimetres long) cloudy grains within

mica sheaths. Microcline, where determinable, is again subsidiary.

3.1.5 Plagioclase

In the psammites plagioclase is not common, occurring primarily as short (<1.0 millimetres long) stubby grains showing multiple albite twins. Not all grains were sufficiently clear to enable determination of the An content. However, where possible, the content was approximately determined using the Michel-Levy method. Most was seen to fall within the oligoclase-andesine range.

Plagioclase varies in its abundance in the semi-psammites sometimes forming the dominant feldspar, occurring mainly as grains with multiple twins or, less commonly, pericline twins. Most of the plagioclase is in the compositional range oligoclase to andesine, An_{29}-An_{47}, although some showed an albite composition. Crystals usually exhibit a stubby, rectangular outline and are often cloudy with incipient alteration. Zoning was rarely seen.

Semi-pelitic and pelitic lithologies contain little plagioclase but scattered, often elongate grains were seen surrounded by micas. The grains are distinctive in that they are clear with well-developed twinning on the Albite law, and are less altered than in more psammitic lithologies. The composition, where determinable, falls in the oligoclase-andesine range, An_{26}-An_{41}, although the Glen Doe samples do show more albite-rich grains.

3.1.6 Garnet

In the psammites of the Glen Doe and Monadhliath

formations red-brown garnet (1.4 millimetres x 1.0 millimetres) occurs only as scattered xenoblastic granules outlining the crystal shape. In the semi-psammites it is more common, reaching diameters of 1.5 millimetres. The subidioblastic garnets are often granular, without zoning, but may be pseudomorphed by chlorite, biotite and magnetite.

Deep red to red-brown garnets in pelitic lithologies are xenoblastic to subidioblastic, and reach diameters of 4.25 millimetres. In samples 716 and 6204 (Grid references 467094 and 438053, respectively) the garnets are without exception idioblastic and show a zonal development indicating at least two periods of growth (see Section 8.3.1).

Inclusions occur in many garnets and consist primarily of quartz although calcite was also recorded. All garnets in sample 716 contain quartz inclusions but in only a few are any distinctive inclusion trails produced.

3.1.7 Accessory Minerals

Accessory minerals are few in the psammites. Pyrite and magnetite occur most frequently. Pyrite is the dominant opaque mineral, usually associated with subsidiary magnetite, and both occur as anhedral, irregular grains reaching a maximum of 1.5 millimetres in length. In some samples a core of pyrite is rimmed either by haematite or limonite and occurs mainly in the psammites and pelites. The semi-psammites contain magnetite, often with a limonite core, and pyrite is either subordinate or absent.

Sample 6243 (Grid reference 531061) is a psammite

which contains numerous pyrite cubes reaching 2.5 millimetres in diameter. Their formation must post-date the major deformational episodes since there is no development of pressure shadows. The only visible products of deformation are occasional deformation twins (pressure twins of Ramdohr,1969), and cracks within the pyrite crystals which are infilled by calcite. This idiomorphic growth of pyrite after deformation is recorded elsewhere e.g. Sulitjelma and the Schiefergebirge of the Rhine (op. cit.).

Apatite is common as small rounded grains with moderate relief and low birefringence. Chlorite is rarely seen in any of the lithologies but in samples 716 and 6204 post-tectonic chlorites cross the foliation and contain opaque inclusions in continuity with the external fabric.

Tourmaline occurs in six pelitic samples usually as small hexagonal cross-sections rarely exceeding 0.1 millimetres in diameter (Plate 7). Some grains are zoned with dark green centres and brown rims and pleochroism is marked. Sample 666 (Grid reference 504126) shows differing tourmaline habits with both hexagonal cross-sections and large, pale yellow tabular grains (Plate 8). The latter is crowded with quartz inclusions and in some aspects resembles staurolite.

3.2 Quartzites

Quartzites form a subsidiary lithotype and six samples have been selected for this study.

3.2.1 Quartz

Quartz occurs in a variety of habits. Small

Differing habits of tourmaline exhibited in Killin samples

Plate 7 Small hexagonal grains in pelite

Plate 8 Tabular grain with quartz inclusions

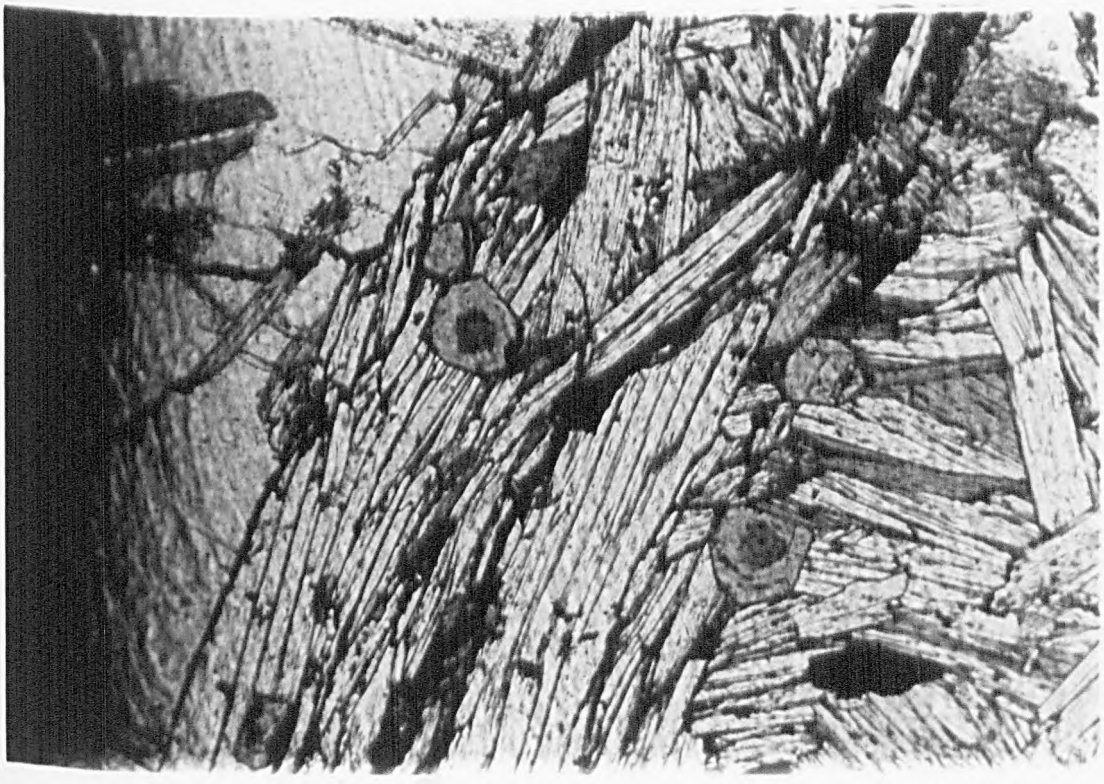

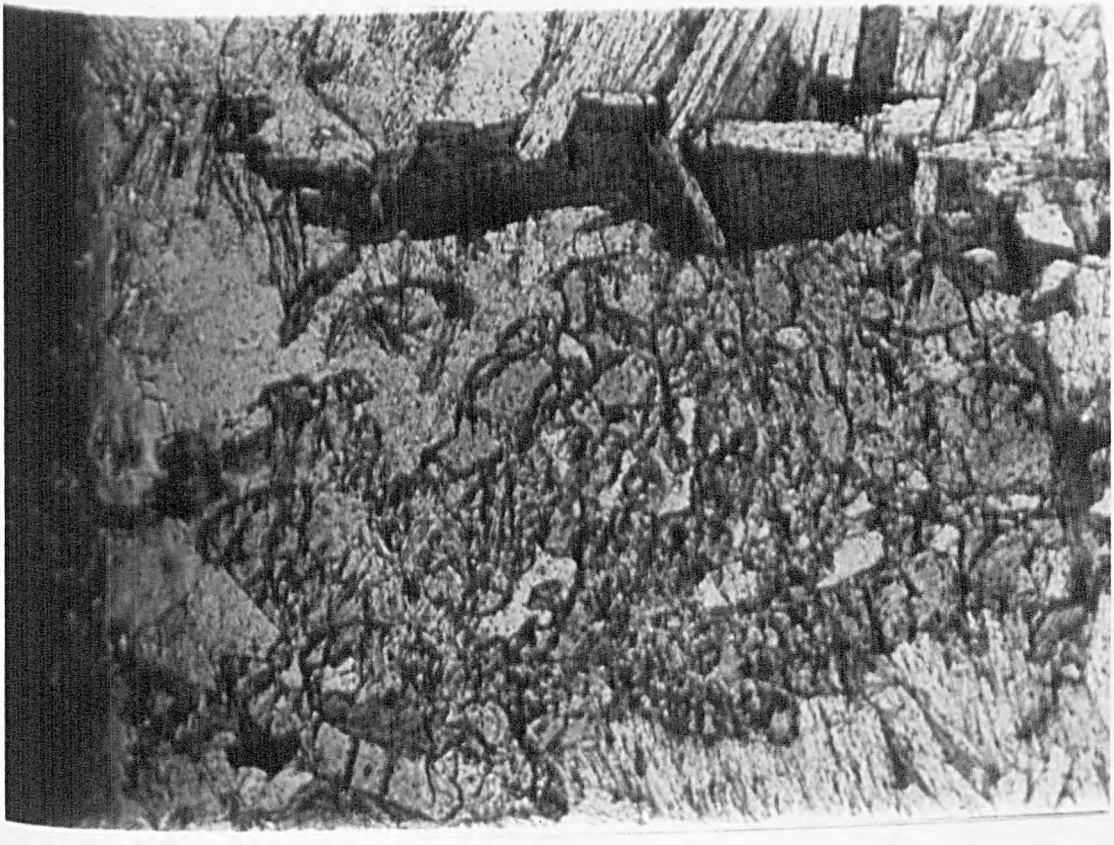

rounded grains (average diameter 0.25 millimetres) are common with curved quartz-quartz boundaries and the grains are often pervaded by a fine, opaque mineral dust. Some samples possess larger grains which occasionally reach 4.0 millimetres in length and in these the boundaries are lobate to cuspate. Straining is apparent in some larger grains from the slightly undulose extinction, but formation of sub-grains is not well developed.

3.2.2 Muscovite

This is usually the only mica present, occurring as small rectangular flakes. Grains rarely exceed 0.5 millimetres in length unless forming part of one of the few aggregates.

3.2.3 Orthoclase

K-feldspar is represented by orthoclase and this forms the dominant feldspar in all but one of the samples examined. Simple twins are apparent in most grains. The rounded to sub-rounded grains show curved grain boundaries and many are cloudy due to incipient alteration to sericite.

3.2.4 Plagioclase

Plagioclase shows a similar cloudiness due to sericitisation but several grains show multiple twins (on the Albite law). The composition range is oligoclase to andesine An_{29}-An_{34}, the latter being dominant. Most of the grains are sub-rounded and rarely exceed 0.5 millimetres in length.

3.2.5 Accessory minerals

Remaining minerals occur in exceedingly small proportions, as scattered grains, with opaque minerals alone being found in all six samples. In one specimen, the fine grains could be identified as haematite and magnetite.

Sphene, chlorite and biotite were also recorded, with small rounded grains of orthite present in one quartzite from the Glen Doe formation.

3.3 White Calc-silicates

Occurring in both the Monadhliath Semi-pelite and Glen Doe Semi-psammite formations, this distinctive metasedimentary facies can be classified on mineral assemblages as shown in Table 3.1. Fifty five samples have been studied and Figure 8 shows the distribution of the groups.

Important mineral phases will now be described in the various groups, moving sequentially through the groups.

3.3.1 Biotite

Group A-1: In all six samples, biotite exhibits a normal dark to pale brown pleochroism. Grain size varies between samples and three different habits are seen. These are stubby prisms (0.4 millimetres x 0.2 millimetres), thin slivers (0.5 millimetres long) and laths with dark cleavage planes due to opaque grains (former up to 3 millimetres long). Associated minerals are normally chlorite and hornblende and in sample 747, biotite is growing at the expense of hornblende in the

Figure 8 Distribution of white calc-silicate assemblages (group assemblages are defined in Table 3.1)

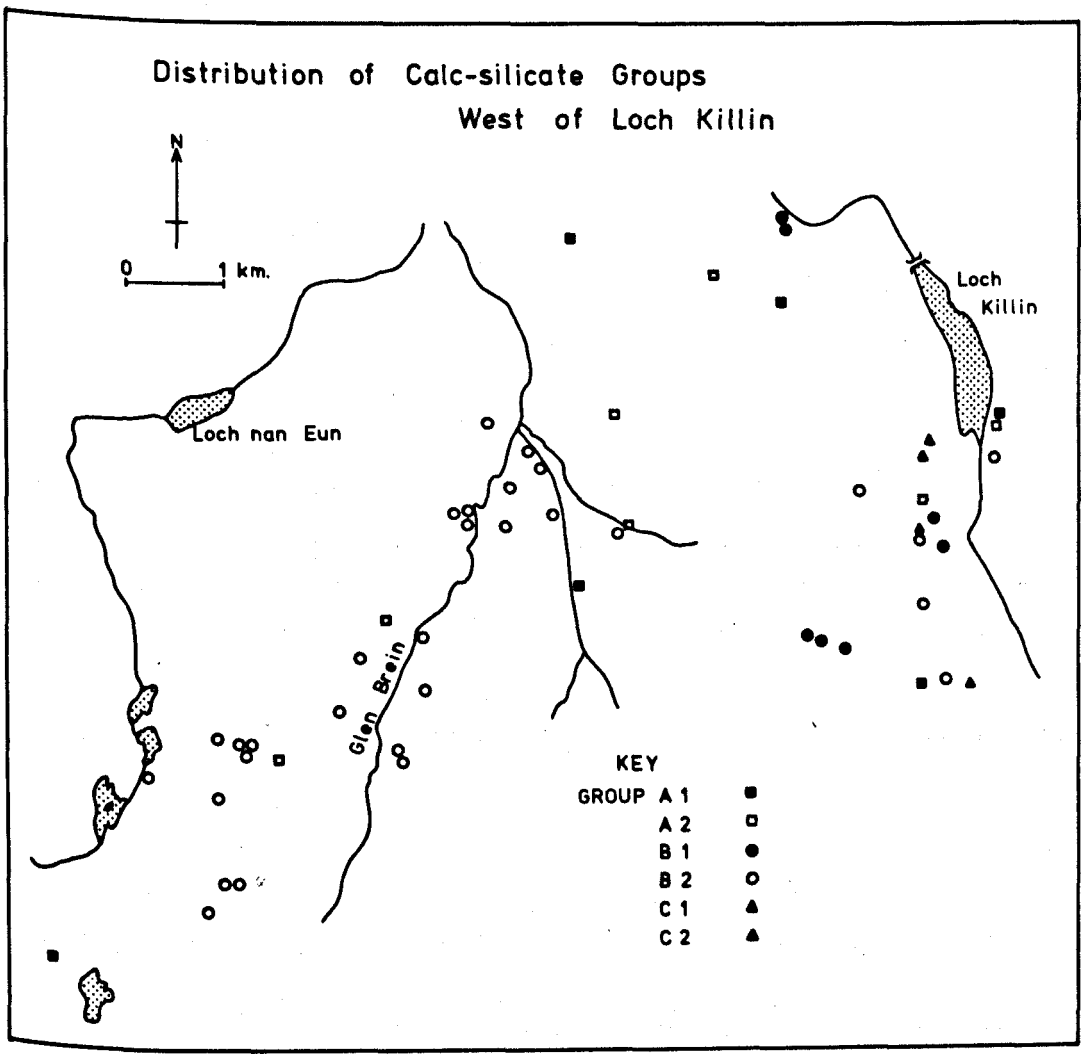
Distribution of Calc-silicate Groups
West of Loch Killin
N
0
1 km.
Loch nan Eun
Glen Brein
Loch
Killin
KEY
GROUP A 1
A 2
B 1
B 2
C 1
C 2

presence of calcite, probably in a mechanism similar to that proposed by Winchester (1974 (c), reaction 2; and section 4.1.3).

Group A-2: All biotite in this group is remnant and is found either with chlorite or as small laths partially surrounded by hornblende. Therefore this assemblage shows phases which are marginal to group B-2. No grains greater than 1 millimetre in length are seen.

3.3.2 Amphibole

Group A-1: Hornblende exhibits pleochroism from pale to dark green. Many samples contain quartz inclusions imparting a spongy texture to the grains. The maximum dimensions noted are 3 millimetres length and 1.5 millimetres width. The hornblende forms close associations with quartz and sericite, biotite and chlorite. In sample 724, a small amount of blue-green amphibole is present. This may be actinolitic amphibole and it occurs with hornblende-biotite intergrowths, the biotite often with an opaque core.

Group A-2: Predominantly pale to medium green hornblende occurs either as single spongy crystals (2 millimetres x 0.75 millimetres in size) or as aggregates (Plate 9) reaching 4.5 millimetres x 1.5 millimetres in size and composed of smaller individual grains (0.5 millimetres x 0.2 millimetres). Sericite commonly encloses subidioblastic hornblende laths.

Group B-1: In this group, hornblende is again very spongy with quartz inclusions. The hornblende grains reach 2.5 millimetres in length and 1 millimetre in width. In

Plate 9 Aggregates of hornblende grains in white calc-silicate

Plate 10 Growth of hornblende from biotite

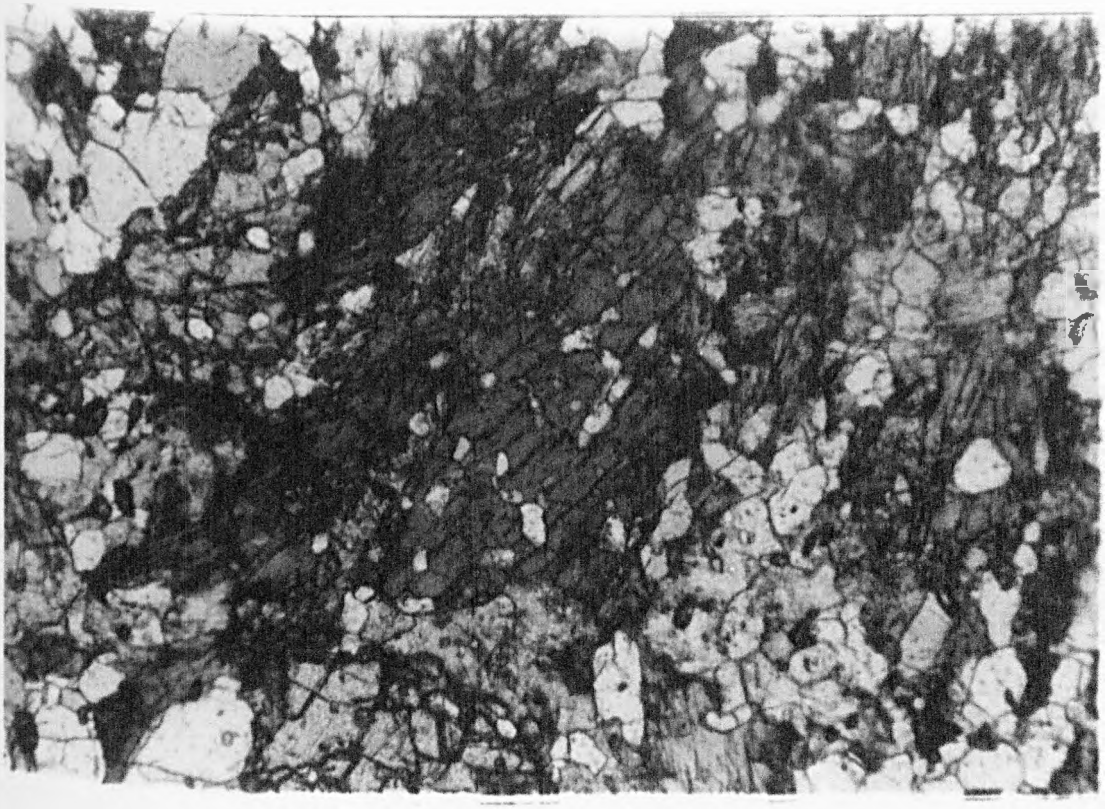

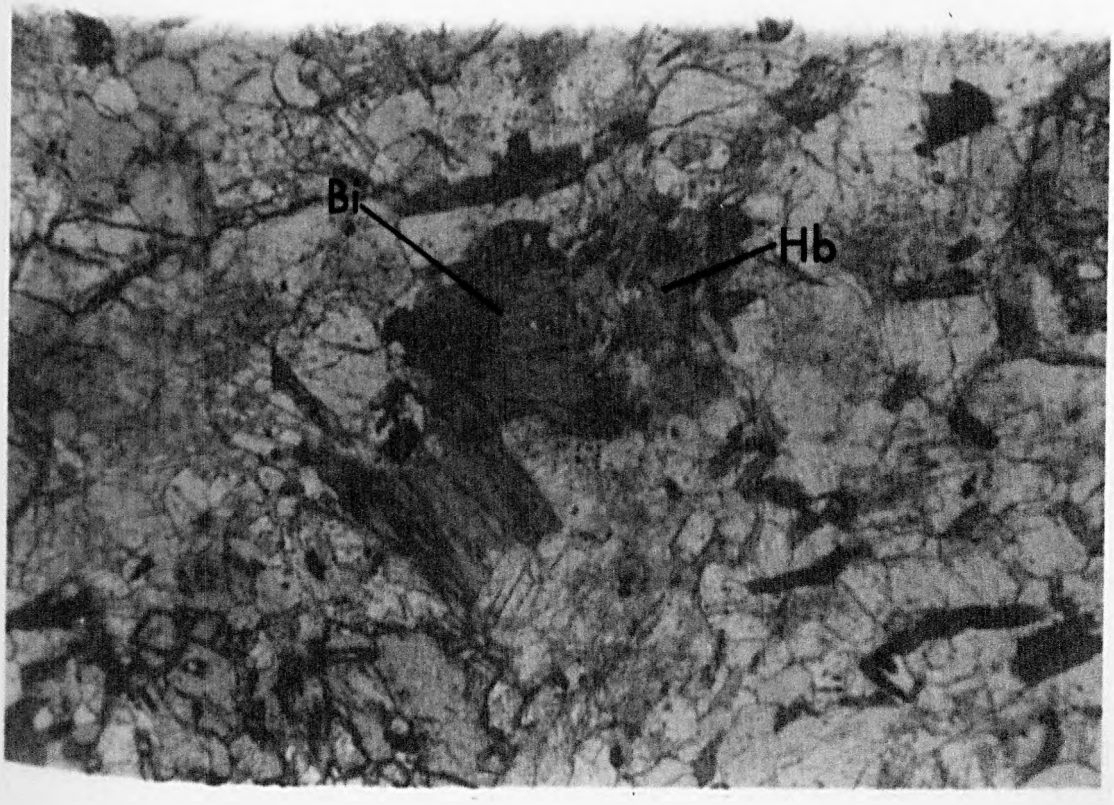
Bi
Hb

two samples (6116 and 6156) the hornblende is in contact with xenoblastic biotite and is probably growing from it (Plate 10). Chlorite has partially replaced hornblende in sample 674 but is seen little in other specimens.

Group B-2: Table 3.2 shows the major properties of hornblende in this group and from this the major features can be discerned. Most samples contain both single grains and grain aggregates, the former averaging 2.2 millimetres in length with a maximum of 7 millimetres and the latter 3.5 millimetres, with a maximum of 11 millimetres. Most grains are spongy, the inclusions being predominantly quartz, but in some instances including clinozoisite and occasionally garnet. Quartz, clinozoisite and sericite are common associates and secondary biotite very occasionally forms along basal cleavage planes of hornblende.

Group C-1: In both samples, aggregates of small prismatic grains of hornblende form elongate bands reaching 4 millimetres in length. Sericite is intimately associated with these hornblende bands and they alternate with similar bands of quartz. No relict plagioclase is visible within much of the sericite but this is presumably the source.

Group C-2: Spongy to skeletal hornblende occurs in both samples reaching 4 millimetres in length in sample 6224. Clinozoisite laths are partially enclosed by hornblende in sample 6113 and the former commonly borders the pale green amphiboles.

Group	Major Mineral Phases	Samples
A-1	Bi:Hb:Sodic Plag.	68,698,6229,724,747,7412.
A-2	Bi:Hb:Sodic Plag:Clzo.	67,6111*,6121*,6210*, 7413,7416,7528.
B-1	Hb:Sodic Plag.	673,674,6116,6117,6156, 6157,6160.
B-2	Hb:Sodic Plag:Clzo.	691,692,6114,6125*, 6136,6141,6142,6143,6146, 6152*,6155,6175,6207, 6208,6209,6212,6213,6216, 6221,6222*,6228,73,75, 730,751,765,7526,7527, 7553,7554,7555.
C-1	Hb:Calcic Plag.	6225,6227.
C-2	Hb:Calcic Plag:Clzo.	6113,6224.

* signifies clinozoisite is rare.

Table 3.1 White Calc-silicate Groups and Assemblages

No.	Grain	Maximum size		Inclusions
		single	aggregate	
691	s,a	0.7 x 0.2	1.0 x 0.4	qtz^{a}
692	s,a	1.5 x 0.8	1.9 x 0.4	qtz^{s,a}
6114	s	3.0 x 0.9		qtz;clzo
6136	s,a	1.0 x 0.4	4.0 x 0.6	qtz^{s,a};clzo^{a}
6141	s,a	1.5 x 0.5	2.0 x 0.4	qtz^{s,a}
6142	s,a	4.0 x 1.0	4.0 x 4.0	qtz^{s}
6143	s,a	0.5 x 0.2	4.0 x 0.5	qtz^{s}
6146	s,a	3.5 x 0.75	4.25 x 1.0	qtz^{s,a}
6152	a		2.0 x 0.75	qtz
6155	s,a	2.5 x 0.5	2.25 x 0.75	qtz^{s,a}
6175	s,a	0.5 x 0.1	3.0 x 1.0	qtz^{a}
6208	s,a	4.0 x 1.0	5.0 x 2.0	qtz^{s,a}
6209	s,a	1.0 x 0.25	1.0 x 0.4	qtz^{s,a};clzo^{s}
6212	s	4.0 x 0.5		qtz;clzo
6213	s	0.75 x 0.15		qtz
6216	s,a	5.0 x 1.0	3.0 x 1.5	qtz^{s,a}
6221	s,a	0.35 x 0.2	1.5 x 0.5	qtz^{a}
6222	s,a	7.0 x 1.75	4.5 x 1.0	qtz^{s,a};gt/bi^{s}
6228	s,a	2.1 x 0.5	5.0 x 1.0	qtz^{s,a}
73	s,a	2.1 x 0.4	3.5 x 0.5	qtz^{s,a};gt^{s}
75	s	2.0 x 0.75		qtz
730	s,a	3.5 x 1.0	6.0 x 3.0	qtz^{s}
751	s,a	4.0 x 2.0	11.0 x 0.5	qtz^{s,a}
765	s	1.0 x 0.75		qtz
7526	s,a	3.0 x 0.4	4.0 x 1.25	qtz^{s,a}
7527A	s,a	3.5 x 1.0	4.0 x 1.5	qtz^{s,a}
7553	s,a	3.75 x 0.8	3.5 x 1.5	qtz^{s,a}
7554	s,a	0.5 x 0.15	4.0 x 1.5	qtz^{a}
7555	s,a	1.25 x 0.3	3.75 x 0.6	qtz^{s}

s = single, a = aggregate; qtz = quartz; clzo = clinozoisite; gt = garnet; bi = biotite.
Superscript by inclusion mineral(s) refers to the relevant grain. Sizes are in millimetres.

Table 3.2 Properties of Amphibole in Group B2

3.3.3 Clinozoisite

Group A-2: Apart from sample 6121, in which clinozoisite occurs as isolated grains within garnet, the common form is that of tabular blades reaching 1 millimetre in length. Small clinozoisite grains are present in sample 67, usually within garnet, and in sample 6210 some of the clinozoisite may have formed from the breakdown of garnet since the latter has a somewhat corroded 'relict' texture. If this reaction occurred then it may be a sign of retrogression. Evidence of retrogression elsewhere in the area is not common and would therefore suggest that this clinozoisite is not a retrograde feature. The corroded garnet occurs at the calc-silicate margin (with the host semi-psammite) whilst all other garnets in the calc-silicate band are idioblastic or sub-idioblastic. This would also suggest that the feature is not retrogressive, but possibly a product of local metasomatic reactions at the margin of the calc-silicate.

Group B-2: Table 3.3 illustrates the habit and size of clinozoisite grains in this group. Grains average 0.5 millimetres in length and rarely exceed 1 millimetre. In four samples, a second generation of granular clinozoisite may exist, impinging upon the earlier tabular form (Plate 11). The four samples are scattered over the area, and therefore show no geographical sequence. Two of the four samples have been analysed but show no chemical similarities, although all four are not dissimilar mineralogically.

The growth of clinozoisite occurred during the D_1 phase of deformation resulting in its incorporation in the S_1 fabric, with amphibole, quartz and biotite, if

Plate 11 Possible second generation of clinozoisite in white calc-silicate

Plate 12 Clinozoisite grains within the S_1 fabric

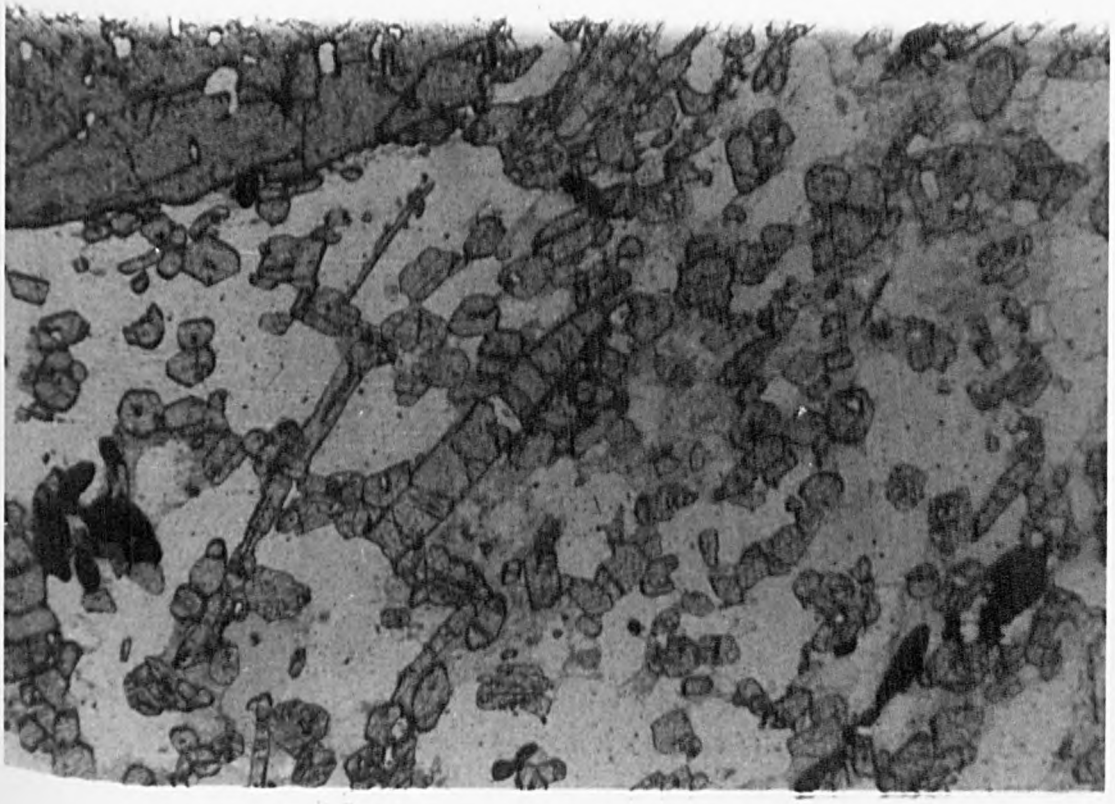

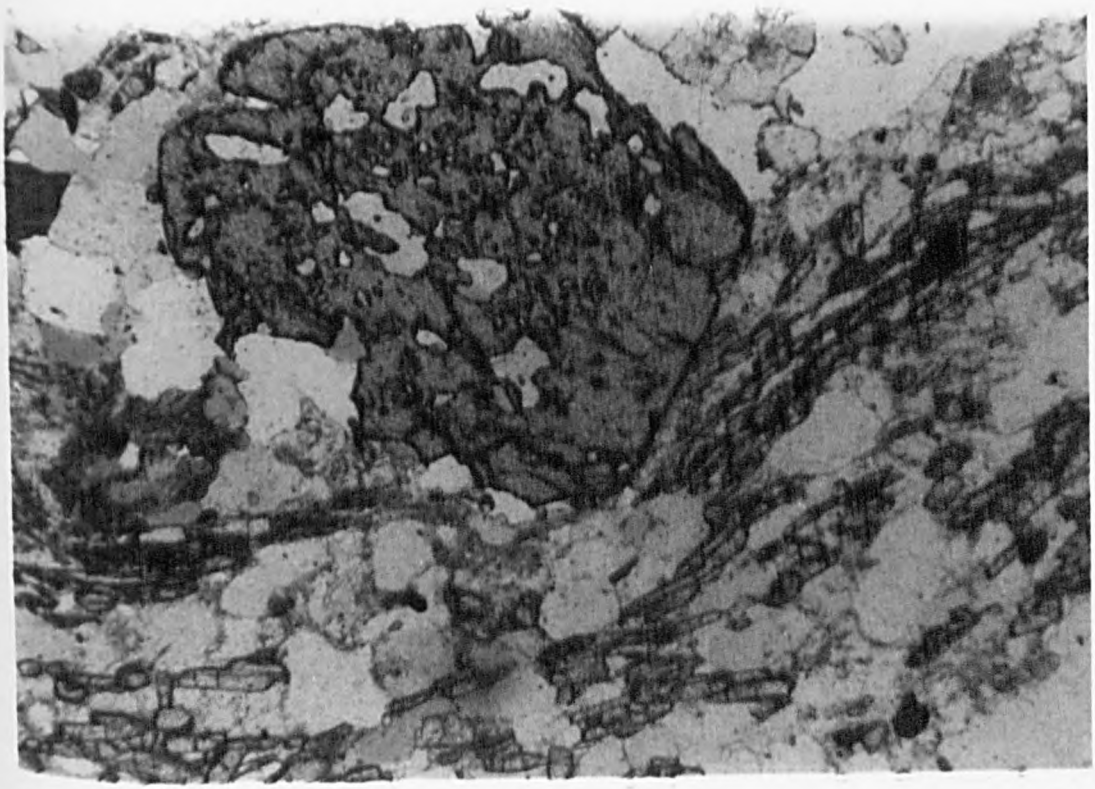

Number	Habit(s)	Maximum Size (mm.)
691	g/t	1.0 x 0.25
692	g/t	0.5 x 0.1
6114	t/p^2	0.75 x 0.15
6136	g/t	0.5 x 0.1
6141	(g)t/p	1.6 x 0.75
6142	g/t	0.35 x 0.05
6143	g/t/p	0.4 x 0.1
6146	g/t	0.7 x 0.1
6152	g/t	0.3 x 0.1
6155	g/t	0.3 x 0.2
6175	(g)t	1.1 x 0.2
6207	g/t/p	1.2 x 0.3 0.8 x 0.5
6208	g/t	0.3 x 0.1
6209	g/t	1.2 x 0.3
6212	g/t	0.5 x 0.3
6213	g/t	0.4 x 0.1
6216	g/t(p)	0.8 x 0.25
6221	g(t)	0.5 x 0.1 0.4 x 0.3
6222	g/t/p	0.4 x 0.1 0.3 x 0.2
6228	$g/t/p^2$	0.4 x 0.3 0.6×0.2^2
73	g/t	0.4 x 0.05
75	g/t(p)	0.5 x 0.2
730	g/t(p)	0.5 x 0.1
751	t/p^2	0.7 x 0.2
765	g(t)	0.6 x 0.4
7526	g/t	0.35 x 0.1
7527A	g/t	0.6 x 0.2
7527B	g/t	0.35 x 0.08
7553	(g)t	1.5 x 0.3
7554	g(t/p)	0.4 x 0.15
7555	$g/t/p^2$	0.8 x 0.1

g = granular; t = tabular; p = platy. 2 = possible 2nd generation. Habit in parentheses indicates the subsidiary form.

Table 3.3 Properties of Clinozoisite in Group B2

present. Any further and distinct growth must therefore be post-F_1. Direct evidence for growth during D_2 is absent since there is no cross-alignment of mineral grains. Development of second generation clinozoisite in a handful of samples would infer such growth in other samples but this was not observed.

To establish the presence of a second clinozoisite generation a more detailed survey would be required with sections taken mutually at right angles to determine the angular relationship of grains which possibly cut the S_1 fabric.

Group C-2: All the properties and features described above are exhibited in samples 6113 and 6224. A further texture seen in sample 6224 is that of tabular zoisite enclosed by later hornblende. Since both minerals conform to the S_1 foliation, this arrangement must indicate relative growth during the first metamorphic episode.

3.3.4 Garnet

Group A-1: Most samples contain xenoblastic garnets (maximum diameter 2.5 millimetres), showing sieve textures with inclusions predominantly of quartz and calcite. Sample 724 contains no garnet but some small chlorite-sericite magnetite pseudomorphs.

Group A-2: All garnets in this group are idioblastic to subidioblastic (maximum diameter 2.5 millimetres) and more euhedral than those in group A-1. Inclusions themselves form several assemblages:-

(i) quartz + chlorite

(ii) calcite + quartz

(iii) (calcite) + clinozoisite

(iv) chlorite + sphene + quartz + opaque (magnetite) When associated with biotite, assemblage (iv) forms a near complete replacement of the garnet.

Group B-1: Garnets of this group are very similar to those of group A-2 (maximum diameter 2.5 millimetres), but in some cases possess inclusion-free rims. This simple zonation is not a common feature.

Group B-2: Table 3.4 shows the occurrence of garnet in this group, indicating form, size and inclusions present. The average diameter is 1.95 millimetres and the maximum 4.0 millimetres. Inclusions, particularly quartz, are present in all samples.

Group C-1: Reaching a maximum diameter of 2 millimetres, garnets in these two samples show a subidioblastic to xenoblastic shape sieved with quartz and some clinozoisite (sample 6225) inclusions.

Group C-2: Skeletal garnets, somewhat similar to group C-1, characterise this assemblage and may be present as scattered, partially linked granules. In sample 6113, the garnet remnants are intergrown with tabular clinozoisite.

3.3.5 Plagioclase

Plagioclase usually forms granoblastic aggregates with quartz and often shows multiple twins (Albite twin law). Often partial or total sericitisation may obscure twin planes and form elongate blebs of white mica. Nevertheless, approximate anorthite content can be determined in most samples using the mean of a number (six or more where possible), of good twinned samples

Figure 9 Plagioclase variation in the white calc-silicate groups

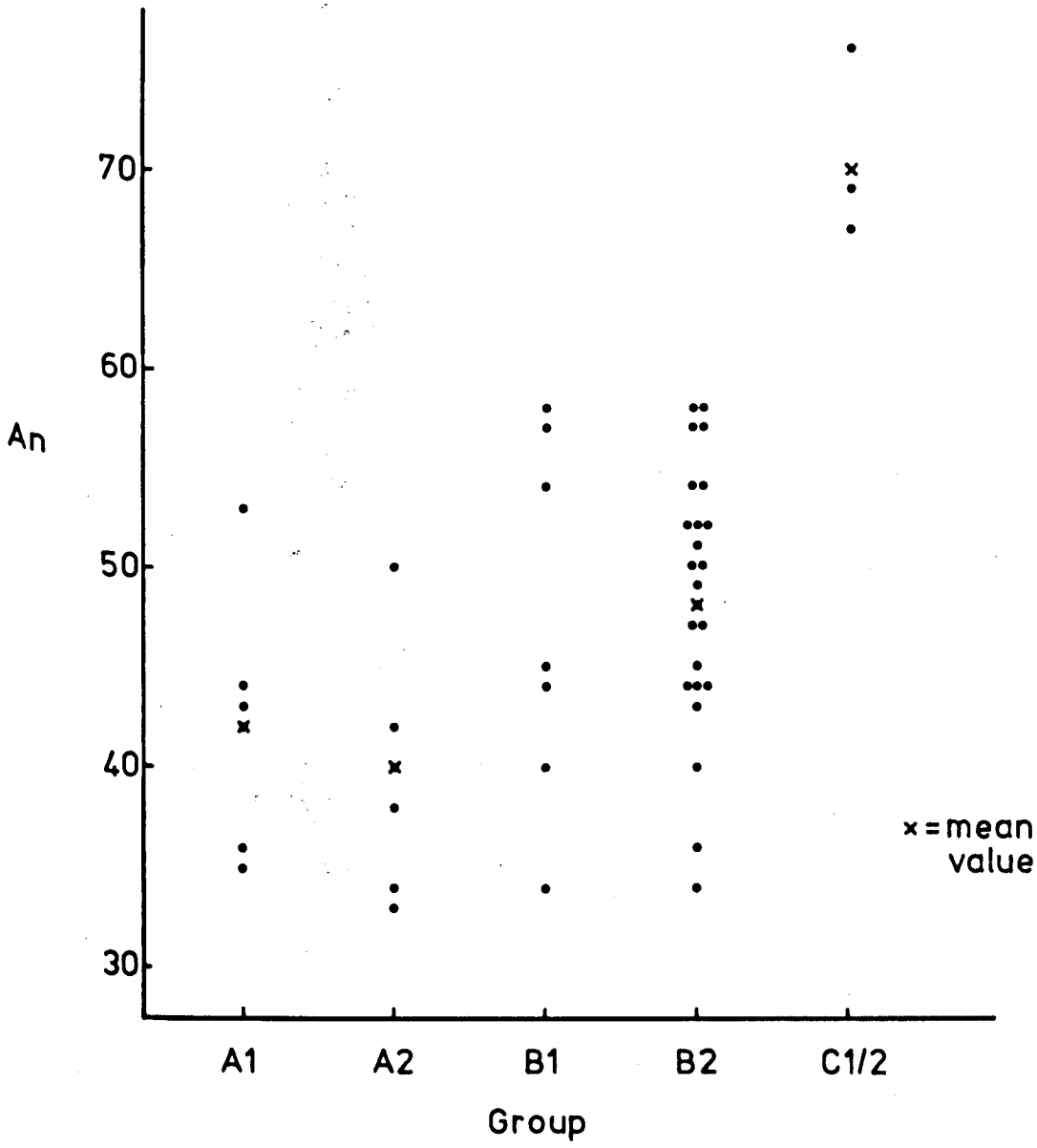

Graphical Representation of Plagioclase An ranges within groups.

No.	Outline	Texture	Inclusions	Max. Diam. (mm.)
691	S	s	qtz:chl:op	1.2
692	S	s	qtz:op:bi	2.0
6114	X	s/g	qtz:cc:chl:clzo	3.5
6136	S	s	qtz:cc:op	3.0
6141	S	g	qtz:chl:op	1.75
6142	I/S	s	qtz:chl:op:sph	2.0
6143	S	g	qtz:cc:chl	2.0
6146	S	g	qtz:chl:op	2.5
6152	S	g	qtz:chl	2.0
6155	S	g	qtz:cc:chl:op	2.0
6175	S	g	qtz:cc:chl:bi	2.0
6207	S	g	qtz:chl	3.0
6208	S	g	qtz:chl	2.25
6209	S	s/g	qtz	3.75
6216	I/S	s/g	qtz:cc:chl:op	2.0
6221	X	sk	qtz	1.75
6222	I/S	s	qtz:cc:op	1.5
6228	S/X	sk/g	qtz:cc	4.0
73	S	s	qtz:sph	1.5
75	I/S	s	qtz:cc:op	3.5
730	S/X	s/sk	qtz:sph:clzo	2.25
751	I/S	s	qtz:chl:op	2.25
765	S	g	qtz:chl:op	1.65
7526	S	s	qtz:op	1.75
7527A	I/S	s	qtz:op	2.0
7527B	I/S	s	qtz:chl:op	1.5
7553	S	sk	qtz:chl:op	1.75
7554	S	g	qtz:chl:op	1.5
7555	S	sk	qtz:chl:bi	2.0

S = subidioblastic, I = idioblastic, X = xenoblastic.
s = sieve, g = granular, sk = skeletal.
qtz = quartz, chl = chlorite, cc = calcite, bi = biotite,
clzo = clinozoisite, op = opaque mineral, sph = sphene.

Table 3.4 Properties of Garnet in Group B2

(Michel-Levy method). Table 3.5 shows the range within each calc-silicate group.

GROUP	NUMBER	RANGE	MEAN
A-1	6	An 42-53	42
A-2	5	34-50	39
B-1	7	34-58	46
B-2	25	34-58	48
C-1	2	69-76	73
C-2	1	67	67

Table 3.5 Ranges and Means of An content in Calc-silicate Groups (see also Figure 9)

3.3.6 Accessory minerals

Sphene is common, primarily as anhedral grains (0.1 to 0.4 millimetres in diameter). Also present is magnetite, commonly as a fine'dust' incorporated into sericite, mantling quartz.

Apatite also occurs as very small rounded grains. Zircon is rare.

3.3.7 Textural note

Textures in the white calc-silicates are very similar throughout all the groups and samples. Amphibole and biotite define the major fabric which, with elongate quartz aggregates, enclose spongy garnets thus forming augen structures. If clinozoisite is present, either as tabular or bladed grains, then these too enclose garnets (Plate 12).

Clinozoisite also forms granoblastic intergrowths with quartz (Plate 13), the latter forming inequant grains

Plate 13 Granoblastic fabric composed of quartz and clinozoisite

Plate 14 Elongate quartz aggregates associated with 'stringers' of sericite

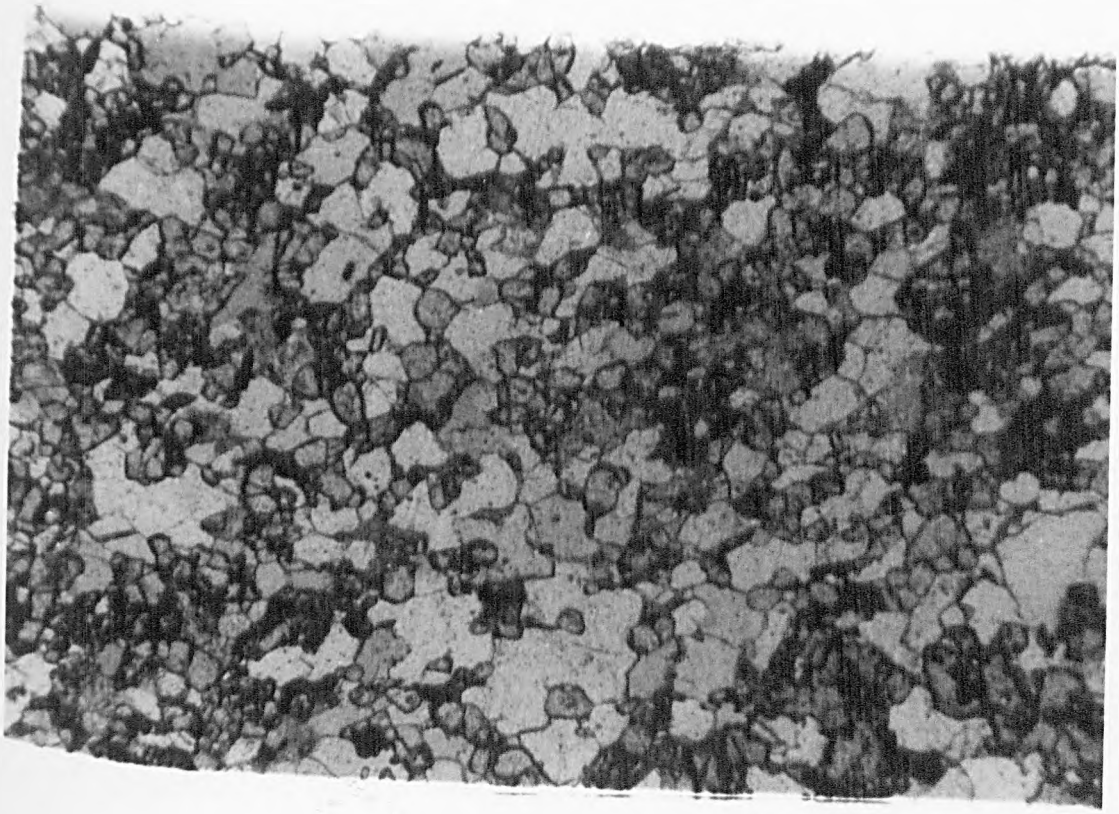

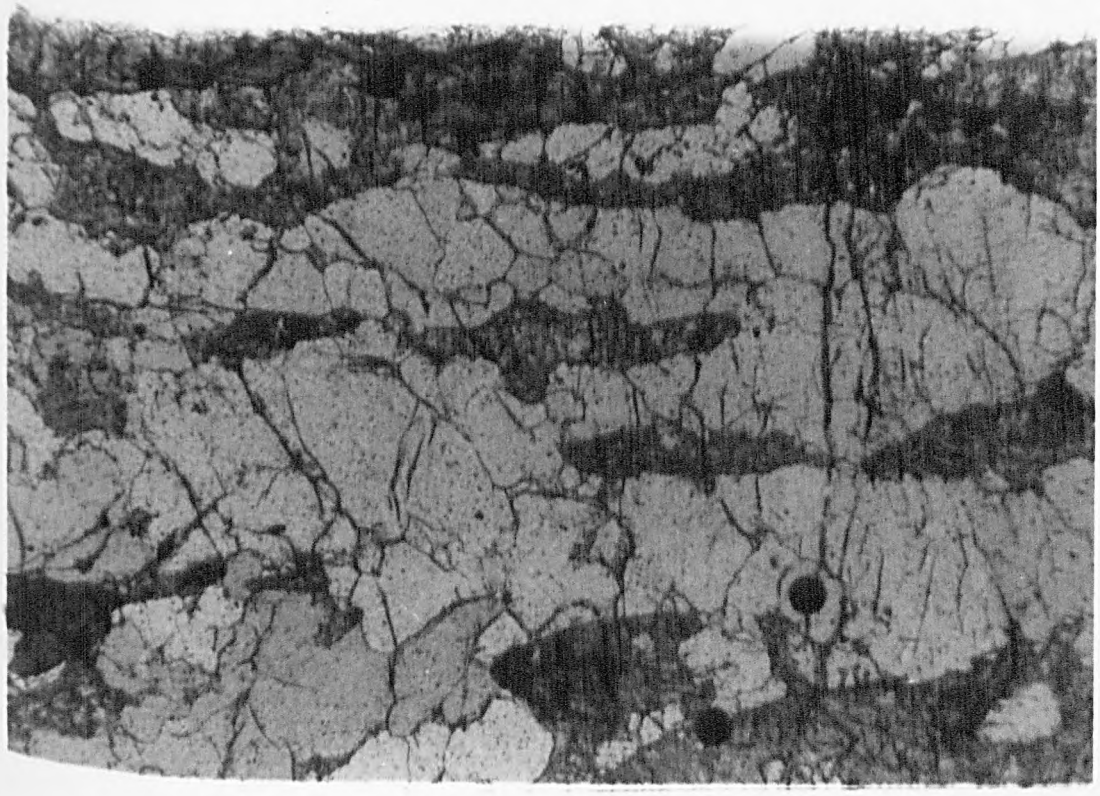

which exhibit two states of strain. Large grains (>3.0 millimetres in diameter) show some strain while others form aggregates of sub-grains. Large-grain aggregates show some approach to equilibrium with a proportion of straight boundaries (and some triple points) whilst the smaller grains display curved or embayed quartz-quartz boundaries.

In group C assemblages, elongate quartz aggregates (>5 millimetres long) with embayed boundaries, alternate with sericite 'stringers', presumably derived from secondary alteration of feldspar (Plate 14). The sericite also forms isolated blebs within quartz, and may enclose small grains of hornblende.

3.4 Green Calc-silicates

Green calc-silicates form a distinctive, accessory lithotype in both the Fechlin Psammite and the Knockchoilum Semi-psammite formations (see Sections 1.2.2 and 1.2.3). The green colour results primarily from the presence of scattered amphibole, commonly associated with clinopyroxene.

3.4.1 Assemblage Groups

In addition to amphibole and pyroxene, the green calc-silicates also contain quartz, some biotite, plagioclase, which is invariably sericitised, and minerals of the epidote group, namely epidote itself with associated subsidiary clinozoisite. Several consistent differences between the green and white calc-silicate groups are noticeable. Hornblende is the only amphibole

present in the white calc-silicates whilst it is one of three amphiboles in the green group. Garnet, common in the white calc-silicates, is rare in the green calc-silicates and clinozoisite is a less common primary constituent of green calc-silicates than it is in the white ones.

Unlike the white calc-silicates it is difficult to subdivide the green equivalents on a mineralogical basis. More samples are required to provide a positive distinction. The lack of fresh plagioclase renders any differentiation on anorthite content dubious.

Table 3.6 indicates the minerals present in the twenty-one samples examined. In the marginal selvages, the amphibole and clinopyroxene characteristic of the calc-silicates decrease in proportion and biotite becomes correspondingly more dominant. This produces a group of samples which can be considered gradational to semi-psammites and it is represented in Table 3.6 by three samples.

3.4.2 Quartz

Quartz is abundant in green calc-silicates and depending upon the other constituent minerals and their proportions, tends to occur in various habits. In calc-silicates where both amphibole and biotite are scattered throughout, the quartz forms large, inequant, strained grains which show undulose extinction. Many large grains break down to form sub-grains (strain assisted 'high-energy' nucleation: Spry, 1969) with distinctively embayed quartz-quartz boundaries. This texture is usually

Major Component

Number	Qtz	Hb/Trem	Act	Clpx	Ep	Clzo	Ser	Pl
640	x	(x)	(x)	(x)			x	(x)
650	x	x					x	(x)
651	x	xHb	(x)	x			x	x
653	x	x	(x)	x			x	(x)
662	x		(x)	x	x		x	
664	x	xHb	(x)	x			x	
686	x		(x)	x	x	x	x	(x)
696	x	(x)Hb	x	x			x	(x)
697(i)	x	(x)Hb	x	x			x	(x)
697(ii)	x		x				x	
699	x	(x)	x				x	(x)
6102	x	(x)Hb					x	(x)
6103	x		(x)	x	x		x	
6104	x	(x)Hb	(x)	x	x		x	
6241	x	(x)Hb					x	
6242	x	(x)Hb					x	
750	x	x	x	(x)			x	
752	x	x	x		x	x	x	(x)
755	x	x				x	x	
758	x	x	x	x	x	(x)	x	
761	x	x			x	x	x	

Accessory

Number	Gt	Bi	Chl	Sph	Cc	Op
640	(x)	x	x	(x)	x	x
650	(x)		x	x	x	x
651				x		x
653	(x)			x		
662	(x)			x		x
664	(x)			x		x
686	x	(x)				x
696		(x)		(x)	x	(x)
697(i)	(x)			x	x	(x)
697(ii)	(x)	x		(x)	x	
699	(x)	(x)		(x)	x	(x)
6102	x	(x)	x	x		(x)
6103				x		
6104	(x)			(x)	(x)	(x)
6241		(x)	x	x		x
6242	(x)	x	x	x		(x)
750	(x)		x	x		x
752	x	x	x			(x)
755	(x)	x	x	x		
758				x	x	(x)
761	(x)	x	x	x		

Key

Qtz-quartz
Hb-hornblende
Trem-tremolite
Act-actinolite
Clpx-clino-pyroxene
Ep-epidote
Clzo-clino-zoisite
Ser-sericite
Pl-plagioclase
Gt-garnet
Bi-biotite
Chl-chlorite
Sph-sphene
Cc-calcite
Op-opaque mineral

(x) signifies very small quantities: dominant amphibole is identified thus: x.
Samples 6102, 6241, and 6242 are gradational with the host semi-psammite. Apatite occurs as small rounded grains in samples 650, 651, 699 and 6103.

Table 3.6 Minerals Occurring in Green Calc-silicates

associated with pyroxene-free calc-silicates with a lower sericite (after plagioclase) content.

Samples with clinopyroxene and sericite often contain small, slightly elongate grains of quartz isolated in a sericite matrix. A third habit is that of dominantly rounded to sub-rounded quartz grains and sub-grain aggregates. Quartz-quartz boundaries are curved or embayed, often with sericite along the boundaries in cuspate patches.

3.4.3 Amphibole

Amphibole is present in all the green calc-silicates, primarily either as hornblende, or, what is probably blue-green actinolitic amphibole. (Small quantities of tremolite may also be present). It is a primary constituent with grains parallel to the calc-silicate margins which usually mirrors the major S_1 foliation.

The actinolitic amphibole occurs as small needles or typical basal sections with a strong blue-green colour (unlike hornblende) and an extinction angle in the range 11 to 15°. Although the petrological identification ideally requires confirmation by microprobe analysis, this amphibole will be referred to as actinolite on the petrologic evidence since it is clearly distinct from other amphiboles in the green calc-silicates.

In twelve out of fifteen samples the actinolite is closely associated with clinopyroxene and in many cases is nucleating on the pyroxene. Although some acicular actinolite parallels aligned biotite in the adjacent semi-psammite or psammite, there is an incipient cross-

fabric developing (in the marginal selvage zone) composed of small actinolite needles (Plate 15) relating to a later tectono-metamorphic event.

3.4.4 Clinopyroxene

Clinopyroxene occurs in twelve samples and is associated with actinolite in each one. The clinopyroxene always occurs as granular to elongate grains (Plate 16). Based on extinction angle (c.40°), the pyroxene is diopsidic but further evidence would be required to identify it positively. Under plane polarised light it is characteristically pale green with high relief. Elongate stringers of sericite (probably after plagioclase) are also associated with the clinopyroxene and often partially enclose the grains.

3.4.5 Biotite

Biotite occurs in eleven samples but often in minor quantities. In assemblages with amphibole only as the major ferromagnesian constituent, biotite forms very small flakes associated with chlorite and is clearly residual (and possibly secondary).

Where the amphibole is actinolitic, the biotite forms a nucleus from which the amphibole grows. In amphibole-clinopyroxene assemblages, biotite is an accessory as small flakes either within hornblende (and therefore probably residual), or in amphibole-biotite fibrous aggregates.

Biotite also occurs as large plates which form a greater component (e.g. samples 752 and 755) of the calc-silicate, where the calc-silicate is less calcareous and

Plate 15 Small needles of actinolitic amphibole forming a cross-fabric

Plate 16 Typical clinopyroxene from green calc-silicates

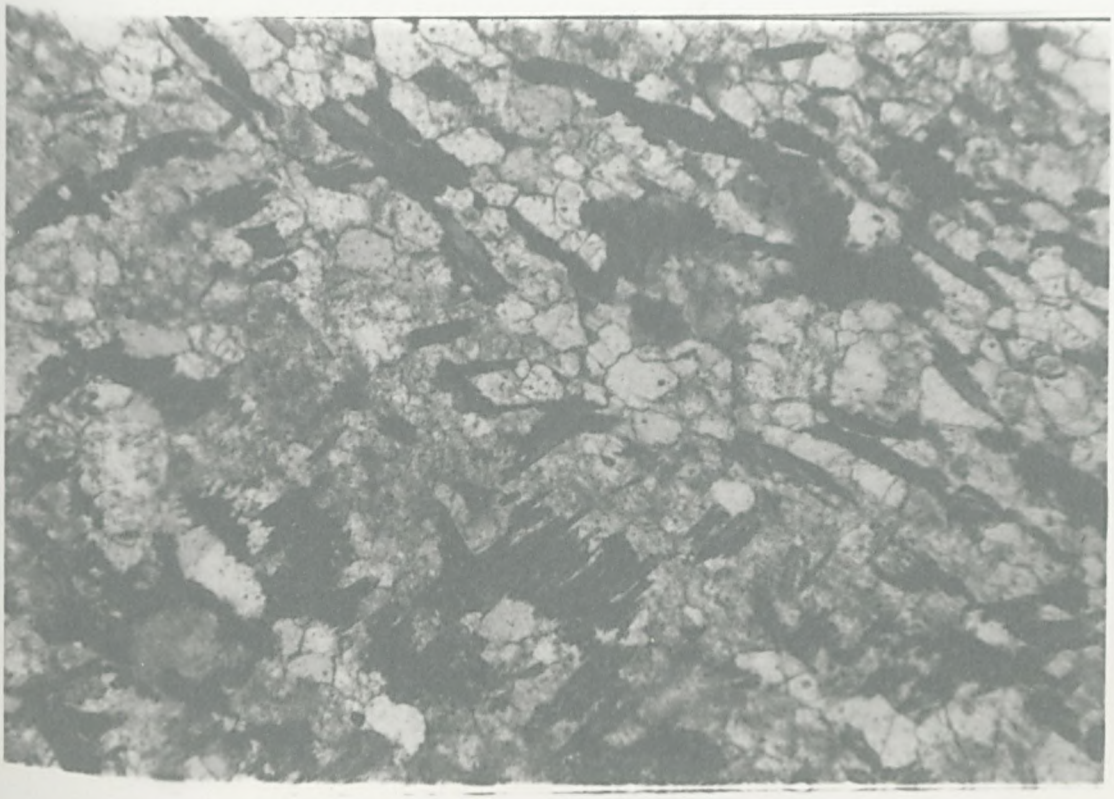

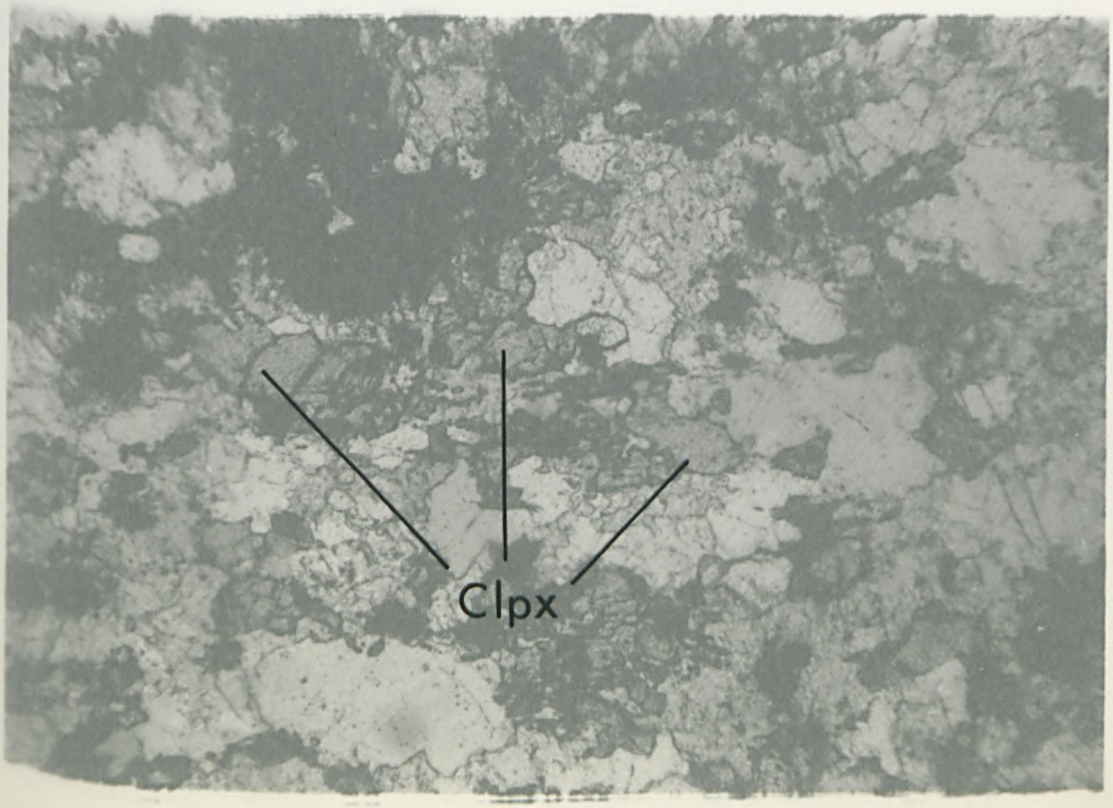
Clpx

therefore is gradational with the host semi-psammite.

3.4.6 Epidote

Members of the epidote group occur in some green calc-silicates, usually associated with clino-pyroxene. Epidote forms small granules scattered throughout, and may occur as the core to unzoned clinozoisite from which it may be distinguished by the pale, yellow-green colour.

In sample 758, the clinozoisite forms a web usually enclosing sphene or sericite and itself enclosed either partially or totally by amphibole laths (Plate 17).

3.4.7 Plagioclase

Plagioclase remains only as a few isolated grains within secondary sericite. Elongate stringers of sericite alternate with quartz and/or amphibole bands and pyroxene and quartz grains are often totally surrounded by sericite.

Sericitisation of plagioclase tends to obscure the twin planes in the original plagioclase, rendering even approximate determination of composition very difficult. The sericitisation of the plagioclase feldspar is so universal that it is probably a late stage hydration effect.

3.4.8 Garnet

Garnet occurs in all but five samples and when present it is invariably in very small quantities. Less garnet seems to have developed than in the white calc-silicates and existing garnets are skeletal or granular. Quartz, sphene, sericite and chlorite may form

Plate 17 Thin clinozoisite webs enclosing green calc-silicate minerals

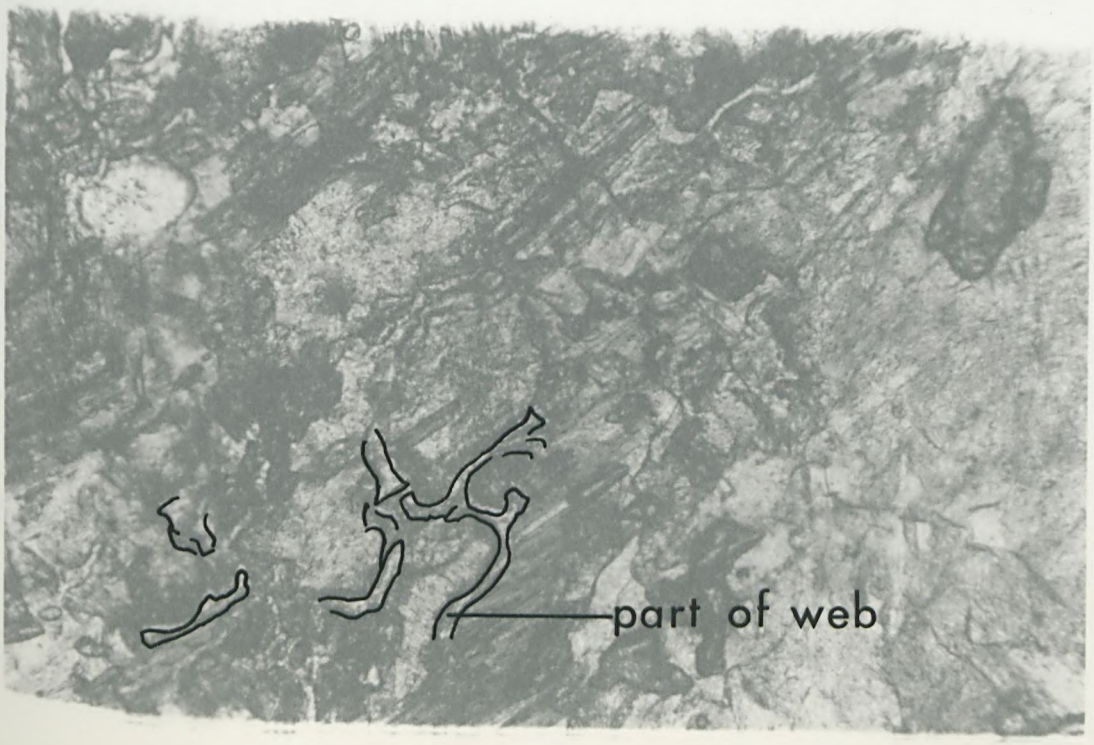
part of web

aggregates with grains of garnet and may be products of garnet replacement in a complex hydration reaction.

Some subidioblastic garnets are recorded (mean diameter 1.75 millimetres) but these are very spongy with abundant inclusions of quartz and rimmed by sericite and quartz.

3.4.9 Accessory minerals

These include sphene, pyrite and magnetite (with pyrite dominant), apatite and calcite, the last often occurring as late thin veins cross-cutting the calc-silicate bands. Granular sphene is common and in one sample forms small bands (<1.5 millimetres thick) of densely packed grains at the calc-silicate/semi-psammite boundary.

Apatite is rare, no more than a few rounded grains occurring in any one sample. Pyrite grains are scattered throughout the bands with separate subsidiary magnetite.

CHAPTER FOUR-CALC-SILICATE PETROLOGY

4.1 White Calc-silicates

4.1.1 Previous research

White calc-silicate bands form a widespread but subsidiary lithotype in both the Glen Doe Semi-psammite and the Monadhliath Semi-pelite (see Sections 1.2.4 and 1.2.5).

For the last thirty years their presence has been acknowledged and their mineralogy used to attempt to estimate metamorphic grade in pelitic sequences lacking orthodox zonal minerals. Kennedy (1949) provided the first detailed study of this metasedimentary lithotype from western Inverness-shire and north-west Argyll. He distinguished four zones based on index minerals:

1) zoisite-(calcite)-biotite
2) zoisite
3) anorthite-hornblende
4) anorthite-pyroxene, in order of increasing grade. He also subdivided the first zone into three assemblages based on the presence or absence of zoisite and calcite.

a) zoisite-calcite
b) zoisite-calcite-hornblende
c) zoisite

Kennedy differentiated each major zone on mineral associations, and proposed three reactions as being transitional between groups.

Zone Transition	Reaction
1/2	biotite + calcite (zoisite)= hornblende
2/3	2 zoisite = 3 anorthite + $Ca(OH)_2$
3/4	hornblende = 4 pyroxene

These reactions and groups were equated with Eskola's facies (namely from the epidote-amphibolite to the pyroxene hornfels facies) and also with zones in pelitic schists. This last comparison Kennedy based on Barth's (1936) work when he stated anorthite-hornblende granulites to be isofacial with the sillimanite zone. Kennedy therefore equated zones 1 and 2 with the garnet zone and he found further corroboration from work in the Trondheim region by Goldschmidt (1915).

For several years after Kennedy, no further information was forthcoming save for a mention of the presence of calc-silicates by Anderson (1956), notably in the Monadhliath Mountains. Winchester undertook detailed studies of calc-silicate mineralogy, petrography and metamorphism in Fannich Forest. Minerals present in the calc-silicates (Winchester, 1970, 1972) mirrored those described by Kennedy but assemblages equivalent to only the first two of Kennedy's zones were found in Fannich. Tanner (1976) also studied the mineralogy and geochemistry of calc-silicates around Morar and Knoydart and distinguished three major zones trending approximately north-south over the area. Table 4.1 shows zonal assemblages and their correlation with the distinctions made by Kennedy.

Kennedy, 1949.	Winchester, 1970, 1972.	Tanner, 1976.	
1 Zo,cc,bi	Zo,bi±na plag	Alb,zo,cc,bi	1
		Olig,zo,cc,bi(hb)	2a
2 Zo	Zo,hb±na plag	And,zo,bi(hb)	b
		And,zo,hb(bi)	c
3 An,hb		Byt/an,hb(zo,bi)	3a
4 An,px		Byt/an,px(Hb)	b

Key: zo-zoisite,cc-calcite,bi-biotite,hb-hornblende, px-pyroxene;alb,olig,and,byt,an-albite to anorthite plagioclase.

Table 4.1 Correlation of White Calc-silicate Zonal Assemblages

In the Killin area three groups are discernible based on mineral assemblages seen in thin section. Each can be subdivided on the presence or absence of clinozoisite and equivalents to the first three groups of Table 4.1 are seen.

		Kennedy	Tanner
A 1	Bi-hb-sodic plag		
2	Bi-hb-sodic plag-clzo	1/2	2(a)
B 1	Hb-sodic plag		
2	Hb-sodic plag-clzo	2	2(c)
C 1	Hb-calcic plag	3	3(a)
2	Hb-calcic plag-clzo		

The presence of each mineral, its habit, size and texture have been described in Chapter 3. Associations of minerals

with each other will now be discussed and reactions will be postulated to account for variations seen.

4.1.2 Calcite in calc-silicates

Calcite occurs in only twelve out of sixty-three calc-silicates studied in thin section, and in two of those is present in very small amounts ($\ll$0.5 volume %). Of the remaining ten samples, nine contain calcite as inclusions within garnet thus indicating the primary nature of the calcite. When occurring outside garnet, the calcite is invariably associated with chlorite or biotite, and also sphene, sericite and quartz.

The comparative scarcity of assemblages containing calcite outside garnet renders elucidation of its role rather difficult. One noticeable feature is that in all such samples, there is no calcite associated with the clinozoisite-rich areas thus lending weight to the reaction:

$$3\ An + Cc + H_2O \longrightarrow 2\ Zo + CO_2 \qquad (1)$$

(Winchester,1972; Storre & Nitsch,1972; Ghent & DeVries, 1972; Hewitt,1973; Hoy,1976).

Elsewhere, chlorite is associated with, and growing at the expense of, hornblende in the presence of calcite and sericite, and complex intergrowths of chlorite, calcite, sphene, opaques and garnet are seen. In the latter case, more than one reaction must be taken into account for the present assemblage. The occurrence of a sphene rim upon an opaque core is repeated throughout sample 674 (Grid reference 511118) always in the presence of calcite and quartz, thus suggesting:

$$Ilm + Cc + Qtz \longrightarrow Sph + CO_2 \qquad (2)$$

Associated with this in some samples is the chloritisation of garnet, a process difficult to express by reaction but approximating to:

$$Gt + H_2O \longrightarrow Chlorite + Qtz \qquad (3)$$

Chloritisation often occurs in the core of the garnet or along fractures.

The inverse reaction illustrated by reaction (1) was postulated by Winchester (1970,1972) in Fannich but refuted by Tanner in 1976 on the grounds that more sodic plagioclase is produced. In the Killin area evidence is scarce due to the intense sericitisation of plagioclase in these examples, which makes the existence of more Na-rich plagioclase hard to prove or disprove. However, one sample does show corroded clinozoisite adjoining sericite in the presence of calcite, the latter appearing to fill in areas between clinozoisite laths.

4.1.3 Ferromagnesian minerals in calc-silicates

Biotite occurs in group A (Table 3.1) in all thirteen samples but in group A-2 tends to a more remnant form. However, in all assemblages biotite participates in few prograde reactions. Hence evidence of the reaction quoted by Kennedy (1949):

$$Biotite + Calcite\ (Zoisite) \longrightarrow Hornblende \qquad (4)$$

is rare. Only one sample (7411 collected by J.A.W. Grid reference 490082), shows amphibole definitely growing from biotite in the form of acicular grains clustering on brown biotite with adjacent calcite, quartz and sericite (Plate 18). Although other samples show biotite and hornblende in juxtaposition, quartz is the only assoc-

Plate 18 Amphibole radiating from biotite in a white calc-silicate

Plate 19 Growth of biotite along the basal cleavage of hornblende

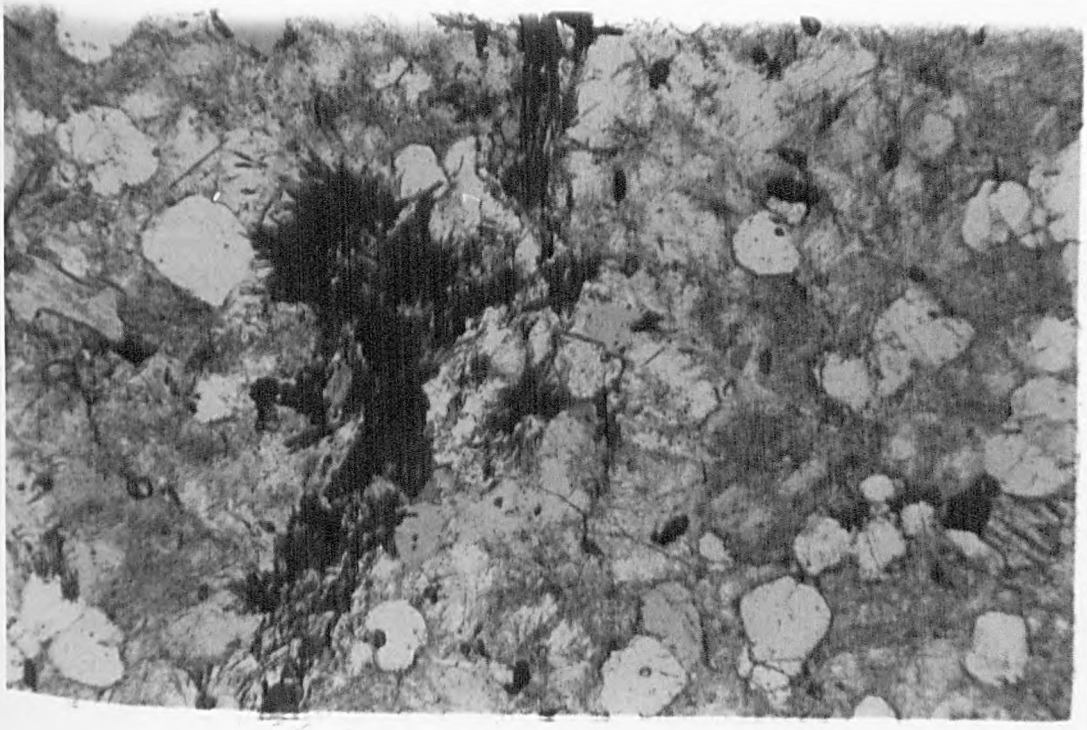

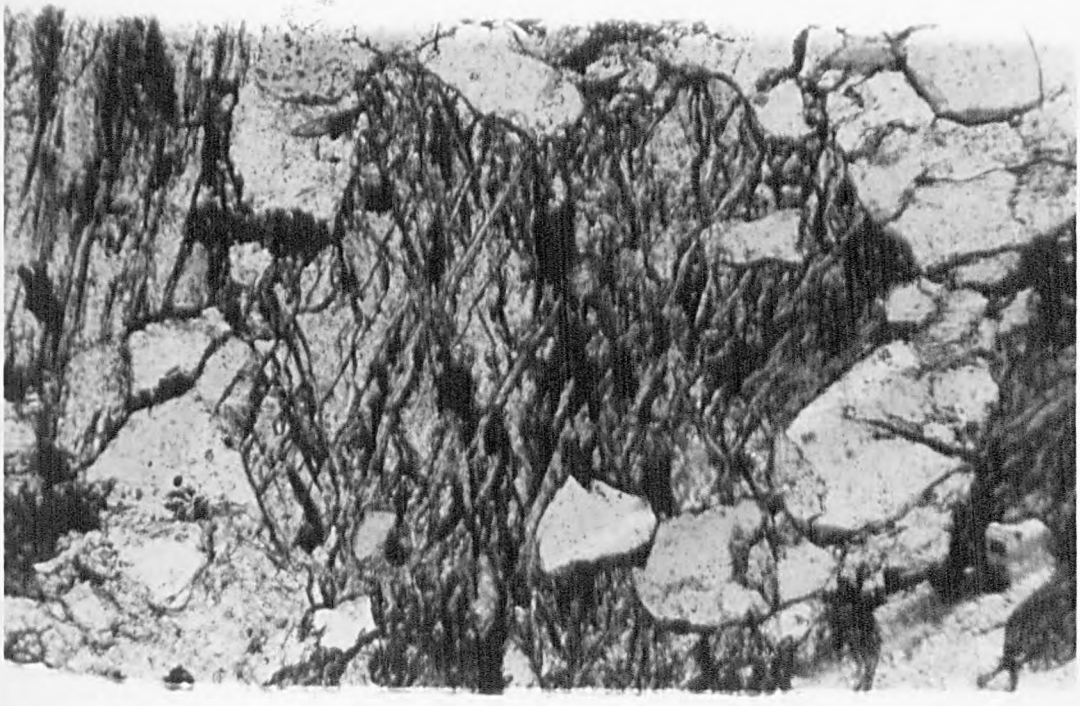

-iated mineral thus implying that all the reacting calcite has been consumed or that the two minerals are merely in physical contact.

The retrograde growth of biotite from hornblende was seen extensively by Winchester in Fannich and the introduction of potassium into the calc-silicates from microcline in adjoining pelites was postulated:

$$\text{Hornblende} + \text{Microcline} \longrightarrow \text{Biotite} + \text{Anorthite} + \text{Quartz} \qquad (5)$$

In the Killin area this retrograde production of biotite is seen in a few examples, occurring along the cleavages of basal sections (Plate 19). Two factors are apparent, firstly that no products other than quartz and biotite are seen, and secondly that the alteration occurs on the calc-silicate margin but not in the centre. These two observations would suggest that potassium is indeed introduced from the country rock and also that the reaction is achieved via pore fluid (cf. Tanner,1976).

4.1.4 Clinozoisite and Plagioclase (in some instances, the former in association with epidote)

Clinozoisite is present in most calc-silicates and appears to form from calcite, plagioclase and garnet. Reaction (1) illustrates the prograde formation of clinozoisite, with the production of more sodic plagioclase, the clinozoisite occurring as both granules and tabular grains. This reaction was also noted by Ferry (1976) in Maine. Most clinozoisite however, is closely associated with sericitised plagioclase, small needles of the former being completely enclosed by sericite. The sericitisation process is the latest involved since larger grains of

white mica trend across the foliation, the latter outlined by clinozoisite laths and elongate quartz grains. This post-dates the partialbreakdown of plagioclase to produce clinozoisite.

In some samples there are clinozoisite and hornblende-plagioclase bands, the former associated with sieved and somewhat granular garnets. The garnets are more anhedral within the clinozoisite-rich areas and there is an associated decrease and near loss of plagioclase compared to the hornblende areas. A reaction involving the removal of plagioclase and depletion of garnet is therefore suggested:

$$5\ An + Gross + 2H_2O \longrightarrow 4\ Zo + Qtz \quad (6)$$

Na plag. absorbed $\longrightarrow$ c. rock

(Ghent & DeVries,1972; Winchester,1972; Höy,1976). Within the clinozoisite areas very small grains (0.01 millimetres long) of plagioclase are seen but the mineral edges are decomposed. Also, fairly good albite twins are noted in the centre of grains which have a sericitised and decomposed outer rim suggesting an incomplete reaction.

Clinozoisite is frequently seen adjacent to, or enclosed by garnet which is breaking down in the presence of calcite, quartz and sometimes sericite. Where sericite is involved, reaction (6) may again be invoked but many examples exhibit only calcite and quartz with garnet and clinozoisite. The clinozoisite often has a distinctive, additional but continuous rim of more epidotic material implying further growth of the mineral but with a greater iron content. On the introduction of water, the grossular

component of the garnet may break down thus:

$$H_2O + 5\ CO_2 + 3\ Ca_3Al_2Si_3O_{12} \longrightarrow \quad (7)$$

$$2\ Ca_2Al_3Si_3O_{12}(OH) + 5\ CaCO_3 + 3\ SiO_2$$

(after Narayanan Kutty & Anantha Iyer, 1977). The iron necessary for production of an epidote rim seen in some samples may have two sources. In one example the margins of a hornblende lath lose their colour and exist as 'ghosts' implying loss of iron taken up in epidote. The alternative is that an iron-bearing component of the garnet (e.g. almandine) releases iron on breakdown. It is noticeable that sphene is often present when clinozoisite is forming but its role, if any, in the formation of new epidote minerals is not discernible.

Plagioclase is present in most calc-silicates studied in thin section either as twinned or sericitised grains. In Fannich, Winchester (1970,1972)found that thirty percent of the calc-silicates contained no plagioclase and he considered that this was due to completion of reaction (6). A specimen previously described (see preceding page) contains clinozoisite-rich areas with a consequent depletion in plagioclase but rarely does this apply to the whole of any calc-silicate from the Killin area. Only specimen 6120/1 (Grid reference 502113) contains no plagioclase, the sample being crowded with fresh clinozoisite and clear quartz, with garnet and hornblende. Specimen 6120/2 from the same rock shows a few partially sericitised grains on the margin of the calc-silicate, as does sample 744 (Grid reference 472069). The absence or depletion of plagioclase does seem to be associated with an abundance of clinozoisite but that the reaction is

controlled to some extent by the original chemistry also seems probable.

Determination of plagioclase composition in forty-nine samples was attempted (using symmetrical extinction), the majority being from group B-2. Tanner (1976) subdivided his assemblages on 'jumps' in plagioclase composition, a feature not readily apparent in the Killin area. No equivalent of zone one of Tanner is seen; thus An values start just above the oligoclase junction. Zones A1 to B2 in Killin show a progressive increase in anorthite content when the mean value is taken for each group. However, there is no substantial overlap between groups. Four values from groups C1 and C2 do however, show a considerable increase in anorthite content (Figure 9), and there is a jump with no An values recorded between An_{58-67}. The groups have a mean value of An_{70}, the higher value being attributable to increasing grade (Winchester, 1970; Tanner, 1976).

4.1.5 Garnet

Garnets occur in all the calc-silicates examined. No garnets from Killin have been analysed but those studied by Winchester (1970, 1972) were found to be calcic almandine. Most garnets studied contain inclusions, primarily of quartz and calcite but sphene and opaque grains are sometimes present.

The production of garnet from magnetite and anorthite may have occurred in some samples (specifically from group B-1), although as noted by Tanner (1976), this reaction tends to be characteristic of higher grades and

may not be readily applicable.

$$4 \text{ Magnetite} + 6 \text{ An} + 6 \text{ Qtz} \longrightarrow 2 \text{ Calcic Almandine} + 2O_2 \qquad (8)$$

(Muecke,1969; Winchester,1970,1972). In such samples, smaller and much fresher garnets occur amongst larger ones which in some cases have complete, or near complete rims. Sample 6210 (group A2) also contains blades of clinozoisite presumably enclosed during garnet growth. However, reworking of the garnet thus enclosing changing suites of minerals, as described by Tanner (1976), has not been observed.

Retrograde changes involving garnet have been discussed in previous sections (4.1.4), the products including chlorite, zoisite and clinozoisite. Instances of this reaction are however not particularly common, and no general retrogression in the area seems indicated by the mineral assemblages and textures.

4.2 Origin of the Calc-silicates

The field appearance of both white and green calc-silicates confirms their sedimentary origin. The bands or lenses are parallel to the S_0/S_1 fabric and sedimentary structures substantiate this conformity. Their origin would therefore seem to be as calcareous nodules or bands, the differences between the two groups being an initial disparity in chemical components (see Section 7.4.1).

The presence of calc-silicates in the Western Moines is acknowledged by many authors including Kennedy (1949), Butler (1965) and Winchester (1972) but few postulate their origin. Similar studies have been made elsewhere such as

that of Vidale (1969) in New England, Ghent and DeVries (1972) in British Columbia, Thompson,P.H. (1973) in Canada and Thompson,A.B. (1975) in Vermont. However, in many accounts, very little basic descriptive information is presented. Both Ghent and DeVries (1972) and Thompson (1973) describe epidotic calc-silicates, in the latter case formed due to metamorphism of calcareous psammites. Both also describe assemblages very similar to those exhibited by the Killin green calc-silicates. Apparently marginal to these are Arnipol types (see Section 4.4), initially described and named by MacGregor (1948) and attributed by Winchester (1975) to the metamorphism of epidotic grits. Unlike the Arnipol calc-silicates, garnet is present in the Killin green calc-silicates and the epidote does not appear to be primary. This may suggest a slightly different initial sediment composition.

Vidale (1969) and Vidale and Hewitt (1973) studied zoned calc-silicates produced experimentally by metasomatic diffusion, with subsequent comparison to natural examples. Petrographic evidence for metasomatism in natural samples is given by Vidale as the symmetry of mineral assemblage zones (and zone width) about the band centre. The low number of mineral phases and discrete changes in composition of zones from the band centre to the enclosing schist are also quoted.

Comparison with Killin white calc-silicates reveals several differences which tend to discount metasomatic diffusion as the dominant process. On the whole, near-equilibrium assemblages are observed and reactions therefore proceeded

nearer to completion in contrast to Vidale's assemblages which were 'quenched' either by a drop in temperature or a loss of pore fluid. Killin calc-silicates tend not to develop zoning to any great extent but where zonations are seen, these are invariably asymmetrical and irregular. The only comparable feature is a marginal selvage of biotite, but this is a comparative effect due to its paucity in the body of the calc-silicate. Many calc-silicates show a gradation into the host rock with an increase in biotite content and a loss of calcium aluminium silicates. This may in part be due to an initial lithological gradation, but in most cases the bands are relatively homogeneous.

The zoning discussed by Vidale and Hewitt (1973) owes its origins to fluid gradients. The enclosing pelitic schist provides a reservoir of water and the calcareous band (in this study impure limestone) a source of carbon dioxide. Subsequent migration of carbon dioxide and water produces a gradient with zoned phase assemblages, each being one local equilibrium. It is noticeable that white calc-silicates occur in host rocks with differing pelitic contents and therefore water capacities. The assemblages produced are nevertheless remarkably constant over the area and within the bands.

That some migration of elements occurred during the formation of the Killin calc-silicates is implied by occasional textural features. However, a wholescale system of diffusion is negated by the very morphology and occurrence of the bands.

4.3 Green Calc-silicates

Occurring dominantly as thin bands and lenses in psammitic and semi-psammitic lithologies, the green calc-silicates form a metasedimentary facies hitherto undescribed (see Sections 1.2.2, 1.2.3 and 3.4).

They consist of quartz, plagioclase, amphibole ± garnet, ± pyroxene and ± epidote. Subdivision into groups is not possible on the available information (Section 3.4.1). Minerals are here discussed and possible reactions for their formation are postulated.

4.3.1 Biotite

Biotite occurs in several samples (Table 6, Chapter 3) but in few is it present in significant proportions. Sample 697(ii) contains biotite, which mostly forms nuclei on which actinolitic amphibole grows (Plate 20) in the presence of excess calcite. Sphene is often present (although in small quantities), with the biotite and actinolitic amphibole surrounded partially or totally by a mosaic of feldspar. Due to alteration, any feldspar twins are very poor, but some may be potash feldspar. This may therefore suggest the reaction:

$$\text{Bi} + \text{Cc} + \text{Qtz} \longrightarrow \text{Act} + \text{Sph} + \text{K-feldspar} + CO_2 + H_2O \quad (9)$$

(Thompson, 1973)

A reaction proposed by Hewitt (1973) will produce a similar assemblage:

$$\text{Bi} + \text{Cc} + \text{Qtz} \longrightarrow \text{Amph} + \text{K-feldspar} + CO_2 + H_2O \quad (10)$$

and reaction (10) is substantiated by reaction 5 of

Plate 20 Actinolitic amphibole nucleating on biotite

Plate 21 Granular garnet enclosing and enclosed by calcite

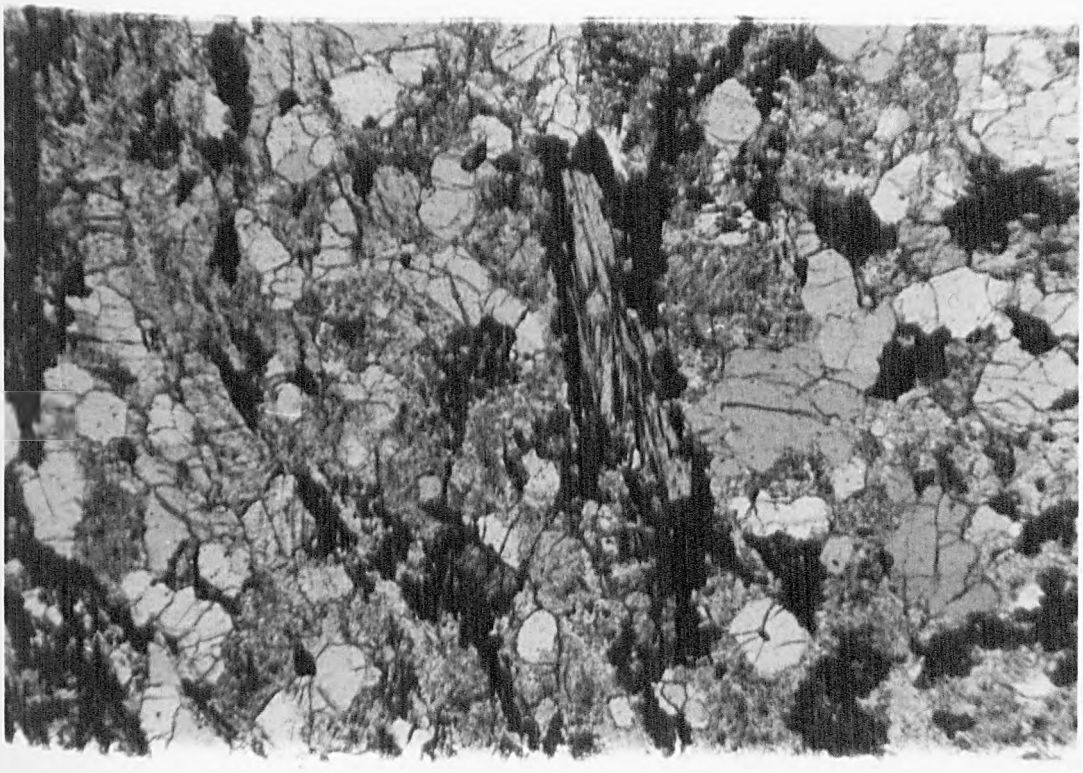

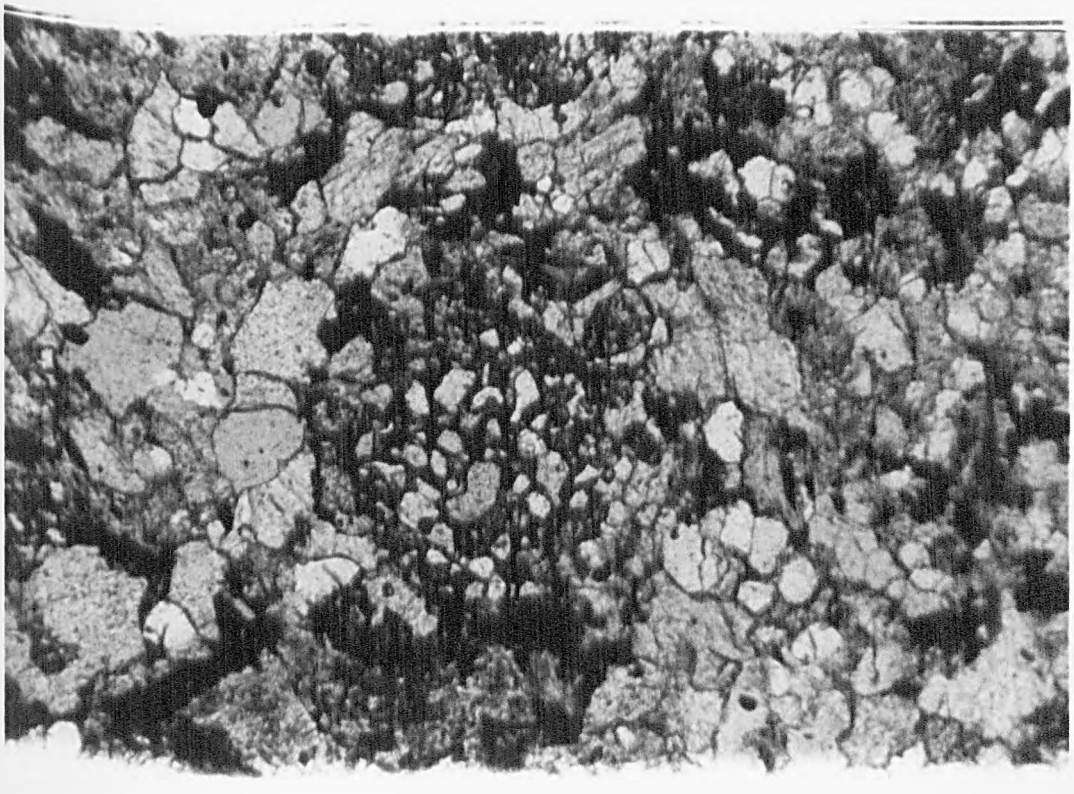

Carmichael (1970). In the remaining samples, biotite occurs as a few scattered grains usually associated with actinolitic amphibole and the biotite is clearly a residual phase, taking part in an amphibole-producing reaction.

4.3.2 Amphibole

Amphibole is present in all the green calc-silicates and three 'classes' are seen:

(i) primary hornblende

(ii) primary actinolitic amphibole

(iii) secondary actinolitic amphibole

Groups (i) and (ii) are separated on petrographical grounds (Section 3.4.3). The hornblende forms large spongy grains with numerous inclusions of predominantly quartz. Its formation is taken to be as shown in reaction (10). Primary actinolitic amphibole is seen growing from biotite (reaction 9), although only in five samples does it constitute a major part of the calc-silicate.

By far the commonest occurrence of actinolitic amphibole is derived from clinopyroxene. The clinopyroxene, which may be diopside (Section 3.4.4), is totally or partially surrounded by needles or typical basal sections of actinolitic amphibole. This would suggest that slight localised retrogression occurred (Section 8.3.3) within the green calc-silicates since water is introduced:

$$5\ Di + 3\ CO_2 + H_2O \longrightarrow Act + 3\ Cc + 2\ Qtz \quad (11)$$

(Carmichael, 1970; Thompson, 1973; Hoy, 1976). The reagents and products of this incomplete reaction are seen over a small area in the green calc-silicate bands. A high pCO_2,

from original green calc-silicate chemistry and associated reactions may have contributed to the process. Calcite is invariably associated with amphibole and clinopyroxene, although not all calcite present in some samples necessarily owes its origin to this reaction.

4.3.3 Clinopyroxene

Clinopyroxene (possibly diopside) occurs in twelve samples and in all is associated with secondary actinolitic amphibole. In three samples however, the pyroxene is surrounded by sericite with only very small quantities of actinolitic amphibole present.

The same agents responsible for the alteration of diopside in reaction (11), may also have participated in the sericitisation of feldspars. The presence of feldspar may have buffered the production of actinolitic amphibole from diopside in the three samples mentioned, producing pyroxene (-actinolite)-sericite-calcite-quartz assemblages.

4.3.4 Epidote minerals

Both epidote and clinozoisite are found in the calc-silicates, nearly half the samples containing one or both of these minerals, and their presence is the result of several processes. (Compared to the white calc-silicates, the green variety contain much less clinozoisite). Bladed grains of clinozoisite are seen within totally or partially sericitised feldspar, possibly formed by reaction (1):

$$Cc + 3\ An + H_2O \longrightarrow 2\ Zo + CO_2$$

Due to sericitisation of plagioclase, it is difficult to determine any relationship between anorthite and clinozoisite content.

The usual occurrence of epidote minerals is as xeno-

blastic grains or thin dendritic growths enclosing other mineral grains. Some samples (e.g. 686) contain epidote and clinozoisite associated with clinopyroxene, garnet and sericite. Small amounts of actinolitic amphibole are also seen in such assemblages. Two reactions, both of which suggest the introduction of water, are implied:

$$5\ Di + 9\ An + 4\ H_2O \longrightarrow 6\ Zo + Ac + 2\ Qtz \quad (12)$$

(Strens, 1965; Hoy, 1976)

$$Gross + 5\ An + 2\ H_2O \longrightarrow 4\ Zo + Qtz \quad (13)$$

(Ghent & DeVries, 1972; Hoy, 1976)

Epidote and clinozoisite dominate the assemblages in some (752, 755 and 761) samples with biotite forming a subsidiary constituent. All three samples show a diffuse nature with calc-silicate assemblages scattered throughout a plagioclase-quartz-biotite host. A common texture consists of granular epidote or clinozoisite surrounded by slivers of biotite, actinolitic amphibole and calcite with plagioclase (and sericite) and sporadic small grains of potash feldspar. At least two limited reactions may have proceeded here with biotite breaking down to form actinolitic amphibole (reaction 9) and some potash feldspar, the released water participating in the conversion of plagioclase to zoisite (reaction 1).

4.3.5 Garnet

Garnet is anhedral in all the green calc-silicates and absent from some samples. In samples without epidote minerals, the garnets are granular and skeletal surrounded predominantly by calcite (Plate 21), with quartz, sericite and rare amphibole. This suggests the

reaction:

$$\text{Gross} + 2\ CO_2 \longrightarrow 2\ Cc + An + Qtz \qquad (14)$$

quoted by many authors. In epidote-bearing assemblages, garnet is either absent or forms only a few relict granules. That it has broken down to form epidote seems probable.

The composition of the garnets in these calc-silicates is unknown but grossular may be found in regionally metamorphosed impure calcareous rocks (Deer, Howie & Zussman, 1962) hence metamorphism of sediments with substantial amounts of magnesium and calcium should lead to production of garnet with a high proportion of the grossular molecule. Analysed garnets from 'white' Moinian calc-silicates elsewhere have all been Ca-rich almandines (Winchester, pers. comm.) and no true grossular occurs, but some compositional variation should be expected based on the chemical and mineralogical differences between the white and green groups.

4.3.6 Feldspar

Both plagioclase and potash feldspar participate in several reactions but few samples show good examples of either mineral and differentiation between them is rendered difficult.

However, in the epidote-bearing assemblages scattered grains of plagioclase are found from which the anorthite content can be determined. Using the symmetrical extinction method of Michel-Levy for multiple albite twins and the method of F.E. Wright (1911) for combined Carlsbad-albite twins, a few values were obtained.

A similar procedure used by Ghent and DeVries (1972)

revealed that an increase in anorthite content could be correlated with an increase in metamorphic grade, as indicated by associated pelitic assemblages. This was also noted by Kennedy (1949), in 'white' calc-silicates.

In the Killin area there is a scatter of values and although the higher anorthite contents group in the north-east (albeit with some lower values), no definite trend emerged.

4.4 Arnipol Calc-silicates

The rarest group of calc-silicates in Killin are those designated by MacGregor (1948) as 'Arnipol' type, named after their first locality. Arnipol calc-silicates have subsequently been recorded by Tanner (1970,1976) and Winchester (1975). The bands or lenses generally average 1 or 2 centimetres in width and rarely exceed 10 centimetres. The distinguishing feature is that unlike their white counterparts garnet and zoisite are absent but epidote is abundant. MacGregor (1948) described them as ".....dominantly white or pink quartzo-feldspathic rocks, with local greenish streaks.....without garnet.....and rich in epidote."

Winchester (1975) noted that the epidote, accompanied by sphene occurred as rounded or sub-angular granules enclosed by biotite, hornblende, quartz or plagioclase.

Only one sample (6174) which occurs in the Killin area can be considered to belong to this group. It contains grains of epidote within predominantly hornblende, now substantially chloritised and, atypically, garnet forms a minor constituent. Similar intermediate types were also

noted by Winchester (op. cit.). Calcite is present and plagioclase forms a minor phase. The An content of the feldspar was noted by MacGregor as oligoclase and Winchester as An_{16} to An_{36} but in the Killin sample it is more calcic (An_{42}).

CHAPTER FIVE-STRUCTURAL ELEMENTS IN THE KILLIN AREA

5.1 Introduction

Description of the diverse structural elements will involve use of specific abbreviations denoting particular planar fabrics or linear features. Fabric is defined as a combination of both textural and structural elements (Whitten,1966), thus including the spatial and geometric configuration of all recurring properties constituting a rock (Turner and Weiss,1963;Hobbs, Means and Williams,1976). All planar fabrics are distinguished by S with a numerical suffix, hence S_0 is primary bedding and S_1 is the first tectonic foliation and regional schistosity. The letter F similarly refers to different fold generations, and L to the associated lineations formed during the relevant deformational phases, D.

S_0, or primary bedding, is rarely seen either in the field or thin section. The dominant planar fabric throughout the whole area is the S_1 foliation and it is within this that later generation folds have developed. This regional foliation is axial planar to small scale, isoclinal, intrafolial F_1 folds which have parallel, often attenuated, limbs and thickened hinges which are especially visible in folded calc-silicates.

Three subsequent fold generations are discernible but of these only one (F_3) shows good development of a planar fabric (S_3 crenulation cleavage).

Lineations associated with early deformations are rare, the dominant element being the L_3 crenulation lineation.

5.2 Deformational Synopsis (see Figure 10)

The D_1 episode is, in many ways, the major deformation of the area in that it produced the regional foliation. No major fold structures are evident in the area under study but scattered examples of minor folds are seen. Trend and plunge of F_1 axes (Figure 11), where measurement is possible, are variable depending upon later folding. All F_1 folds are recumbent isoclines with thickened hinges and attenuated limbs which are pinched out in the foliation. Intense flattening is therefore inferred and during this episode the S_1 foliation and subsequent parallelism of this and the S_0 fabric developed. Discordance of S_1 to S_0 is rare, although S_0 is apparent in thin section.

The D_2 episode which is most apparent in a central east-west trending belt, formed close minor folds during ductile deformation. The stratigraphy of the area was folded into a close synform, the Monadhliath semi-pelite forming the core. this major fold matches the Corrieyairack Synform of Piasecki (1975) and is considered to be its south-westerly equivalent. Minor folds reflect the trend of the major structure and a flattening event produced near similar styles (see Section 5.7) with a weak axial planar cleavage. Axial planes are steep to sub-vertical, trending approximately east-west.

Refolding of the Corrieyairack Synform occurred in the third deformation with a resultant change in trend of the fold to a more south-westerly direction. Trending approximately north-east/south-west, the F_3 folds are upright, dominantly symmetrical, open crenulate in style, with an

Figure 10 Major structural elements of the Killin area

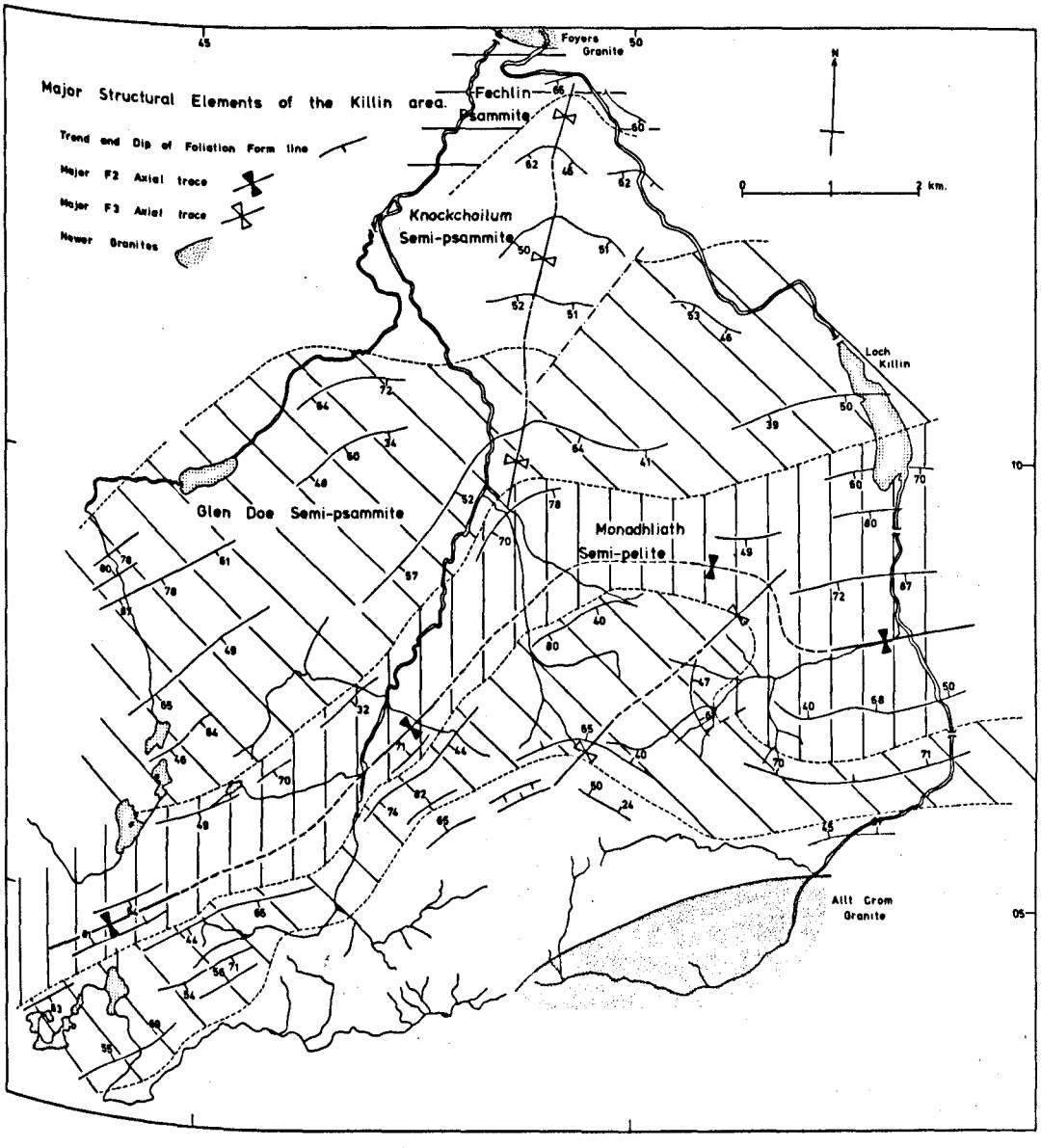
Major Structural Elements of the Killin area.
Trend and Dip of Foliation Form line
Major F2 Axial trace
Major F3 Axial trace
Newer Granites
Foyers Granite
Fechlin Psammite
Knockchoilum Semi-psammite
Glen Doe Semi-psammite
Monadhliath Semi-pelite
Loch Killin
Allt Grom Granite
N
0
1
2 km.
45
50
10
05

Figure 11 Orientation of F_1 fold axes

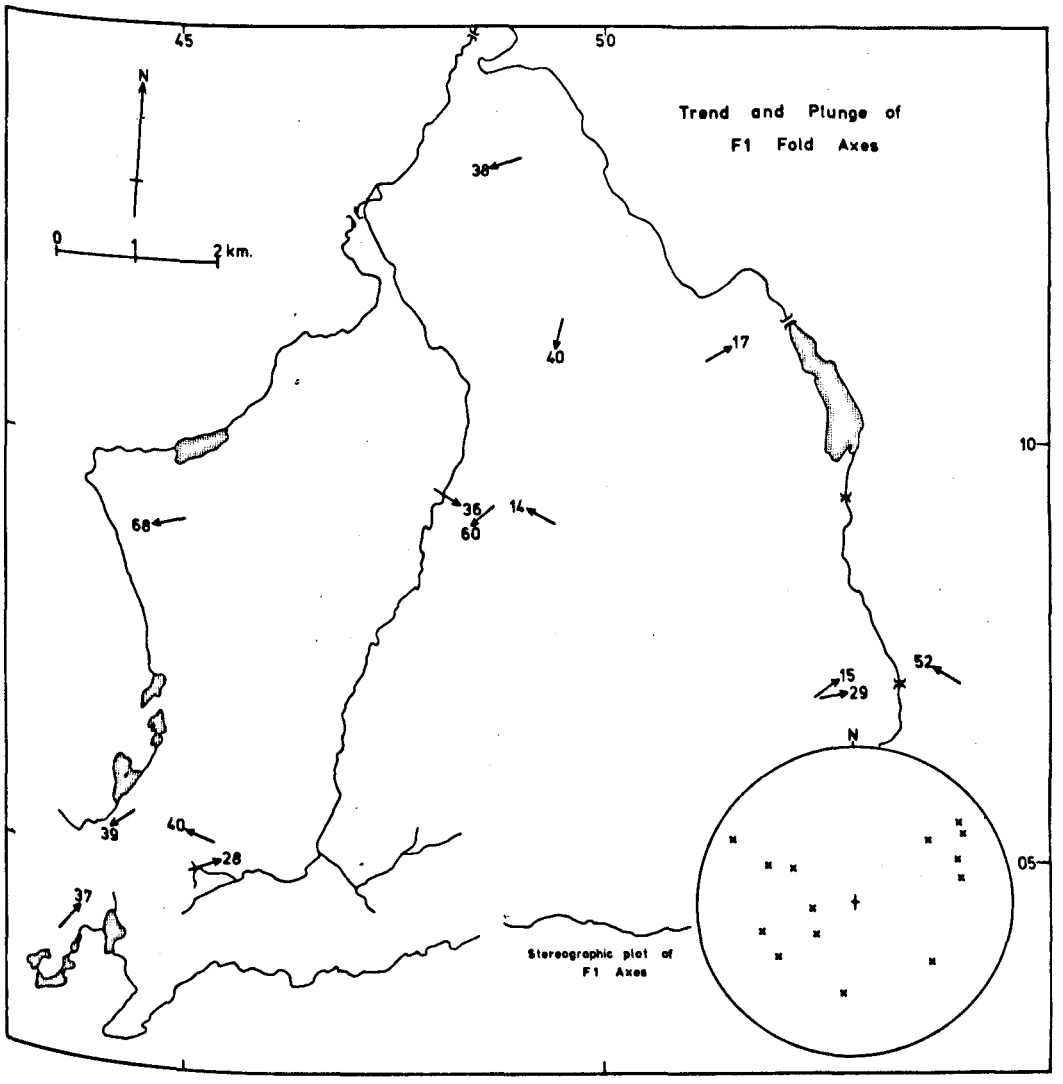
45
50
10
05
N
0
1
2 km.
Trend and Plunge of
F1 Fold Axes
38
40
17
36
60
14
68
15
29
52
39
40
28
37
N
Stereographic plot of
F1 Axes

axial planar crenulation cleavage. They occur mainly in the northern and central parts of the area. Axial planes are steep to sub-vertical and the majority dip south-east.

F_3 axial trends change considerably south of an arbitrary line (see Figure 17) and plunge directions are reversed. Although no mesoscopic evidence is apparent the presence of major F_4 structures is nevertheless inferred. Probably occurring as warping with resultant alteration of trend in minor F_3 axes, little additional evidence is apparent for this deformation. Minor structures are restricted to a few individual kinks with varying axial trends, which impart little information save to show that deformation was relatively brittle.

Subsequent deformation was limited to faulting and jointing, a dominant trend being north-east to south-west.

5.3 Linear Features-Folds

5.3.1 F_1 folds

The earliest linear features seen in the Killin area are sporadic, isoclinal, intrafolial folds. These are outlined by calc-silicate bands (see Chapter 1) or early quartz veins and the regional schistosity (S_1) is axial planar to them. S_1 is outlined by prismatic amphibole in the calc-silicates. All examples of F_1 folds possess substantially thickened hinge zones and attenuated limbs (Plate 22). The intense flattening of these folds and consequent production of the S_1 foliation has produced very attenuated fold limbs. Rarely do these exceed 3 centimetres in thickness, and overall fold length does not exceed 60

Plate 22 Examples of F_1 fold morphology, outlined by white calc-silicate bands

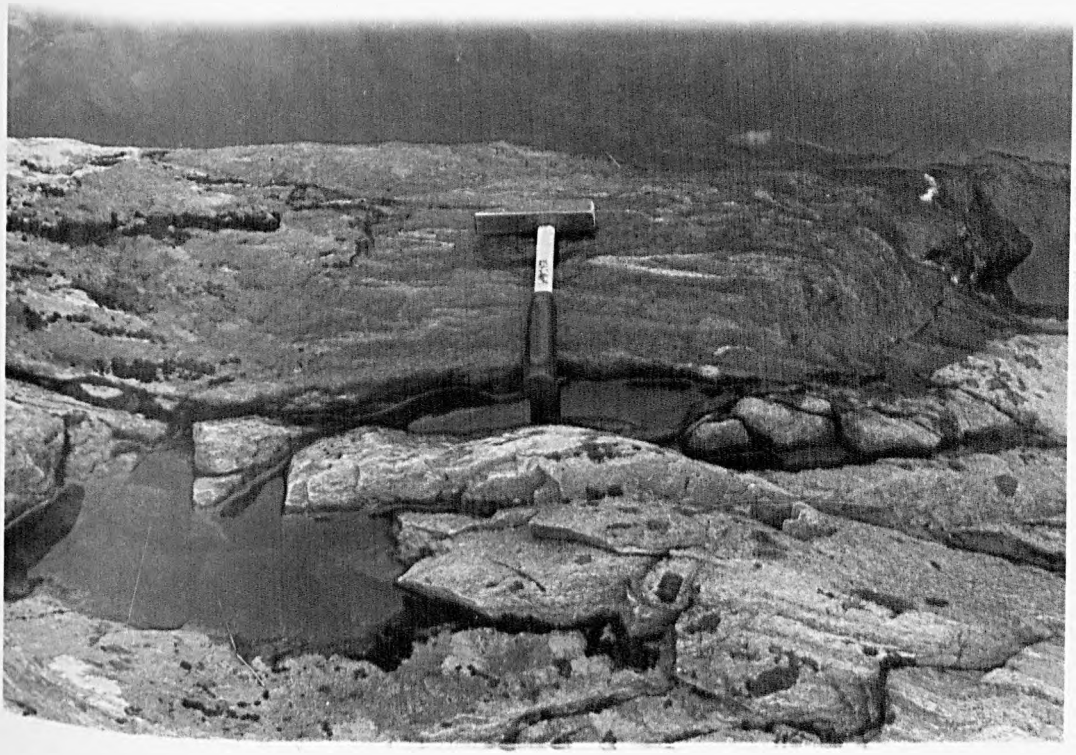

centimetres. Their attitude is dominantly recumbent.

Occasionally pelitic laminae within psammitic or semi-psammitic beds delineate F_1 folds but these are less common than folded calc-silicate bands.

Since the regional foliation is axial planar to these folds, measurement of axial trends is difficult unless a pelitic bed contains a substantially harder folded band. Fourteen such axes have been obtained and Figure 11 shows their distribution, orientation and subsequent stereographic plot. With so few measurements no clear trends are likely to emerge but there may be a bi-planar distribution, and the line of intersection of the two planes is very nearly parallel to the F_3 trend (plunging 23° to 184). However, since major episodes of deformation post-date S_1, it seems more likely that this distribution is a function of the paucity of information.

5.3.2 F_2 folds

A total of 87 minor F_2 fold axes have been measured, the majority of them from the belt which traverses the centre of the area in an east-north-east/west-south-west direction. All are associated with the major F_2 Corrieyairack Synform.

The wavelength of minor F_2 folds is commonly 30 to 50 centimetres (Plate 23) depending upon the lithologies involved and the associated degree of flattening. All folds are isoclinal to close (Fleuty, 1964) with an average inter-limb angle of 35° to 50°, and monoclinic symmetry. These asymmetrical, near cylindrical folds possess rounded to sub-rounded hinge zones and in many cases show considerable

Plate 23 F_2 fold outlined by quartz veins

Figure 12 Poles to 22 F_2 axial planes
(North point is marked by vertical line)

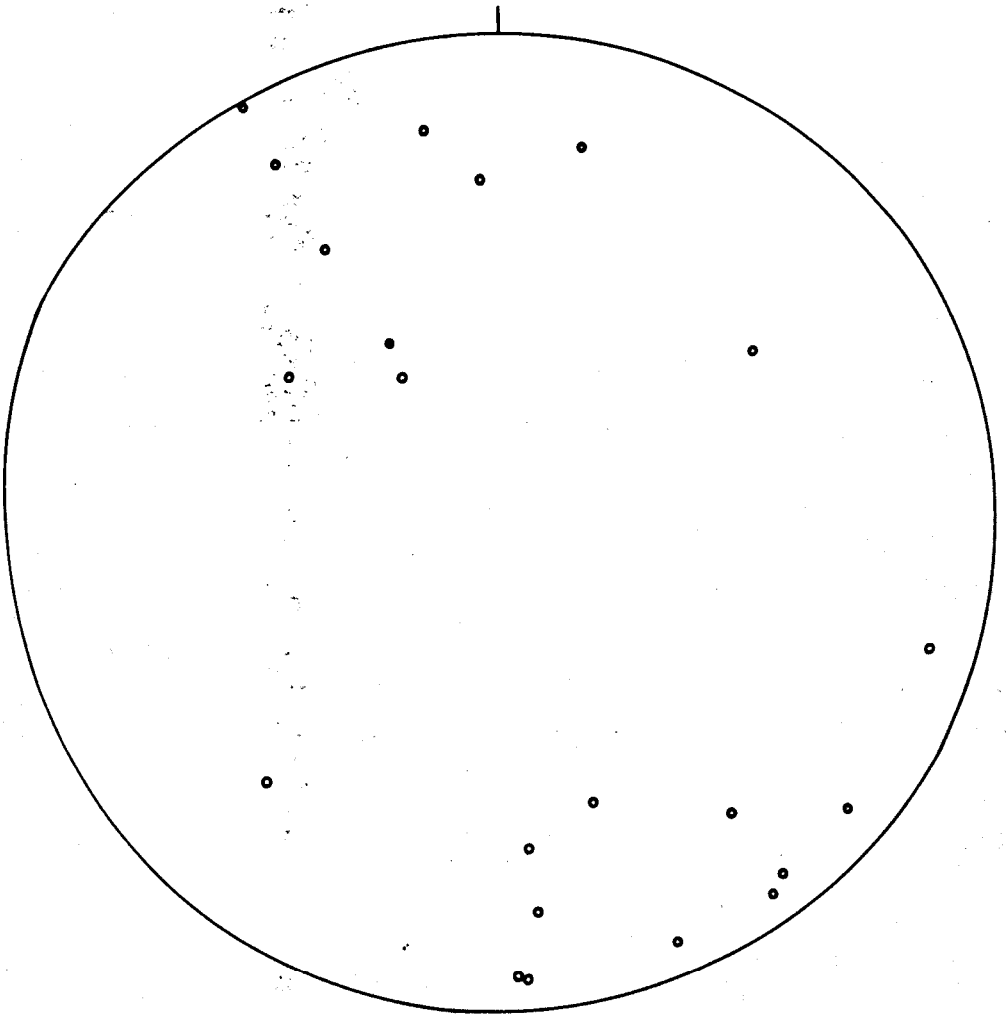

Figure 13 Axial plane trends for F_2 and F_3 folds

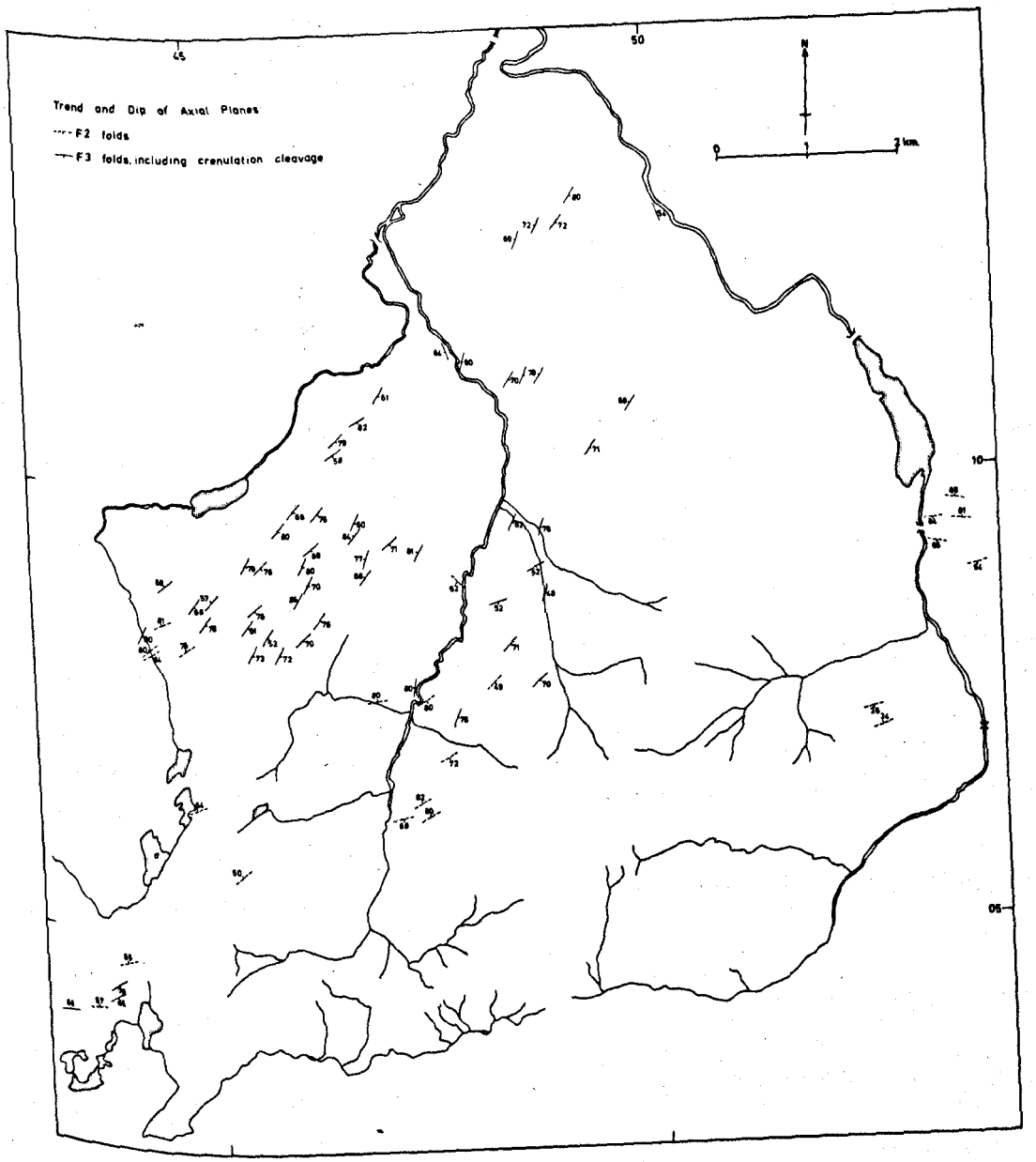
Trend and Dip of Axial Planes
F2 folds
F3 folds, including crenulation cleavage
45
50
10
05
N
0
1
2 km

thickening in this region with attenuation of limbs, shown to some extent in Plate 23.

F_2 axial planes are steep to sub-vertical and trend approximately east-north-east/west-south-west. Dips from 22 readings are split between north-west and south-east (Figure 12) producing a bimodal distribution. This change of dip direction is noticeable south-east and south of Loch Killin (Figure 13) where both regional foliation and F_2 axial planes steepen in the axial region of the major F_2 synform.

The majority of these folds are moderately plunging (Fleuty, 1964) although there are several changes of plunge across the belt of minor fold axes (Figure 14). A stereographic plot (Figure 15) shows the uneven bimodal distribution with most of the 87 readings plunging east-north-east and the remainder west-north-west. Girdles may be drawn through the plotted points although the great circle so constructed for the westerly-plunging folds is rendered rather arbitrary by the low number of readings. Subsequent intersection of these two planes produces an axis very nearly co-axial to the mean F_3 trend. Hence the distribution and the undulation in F_2 fold axes is attributable to the effect of the D_3 deformation.

5.3.3 F_3 folds

Features developed during the D_3 deformation now dominate the northern part of the Killin area. Minor F_3 fold axes are common throughout, except around Loch Killin, and are related everywhere to major structures.

Figure 14 Minor F_2 fold trends

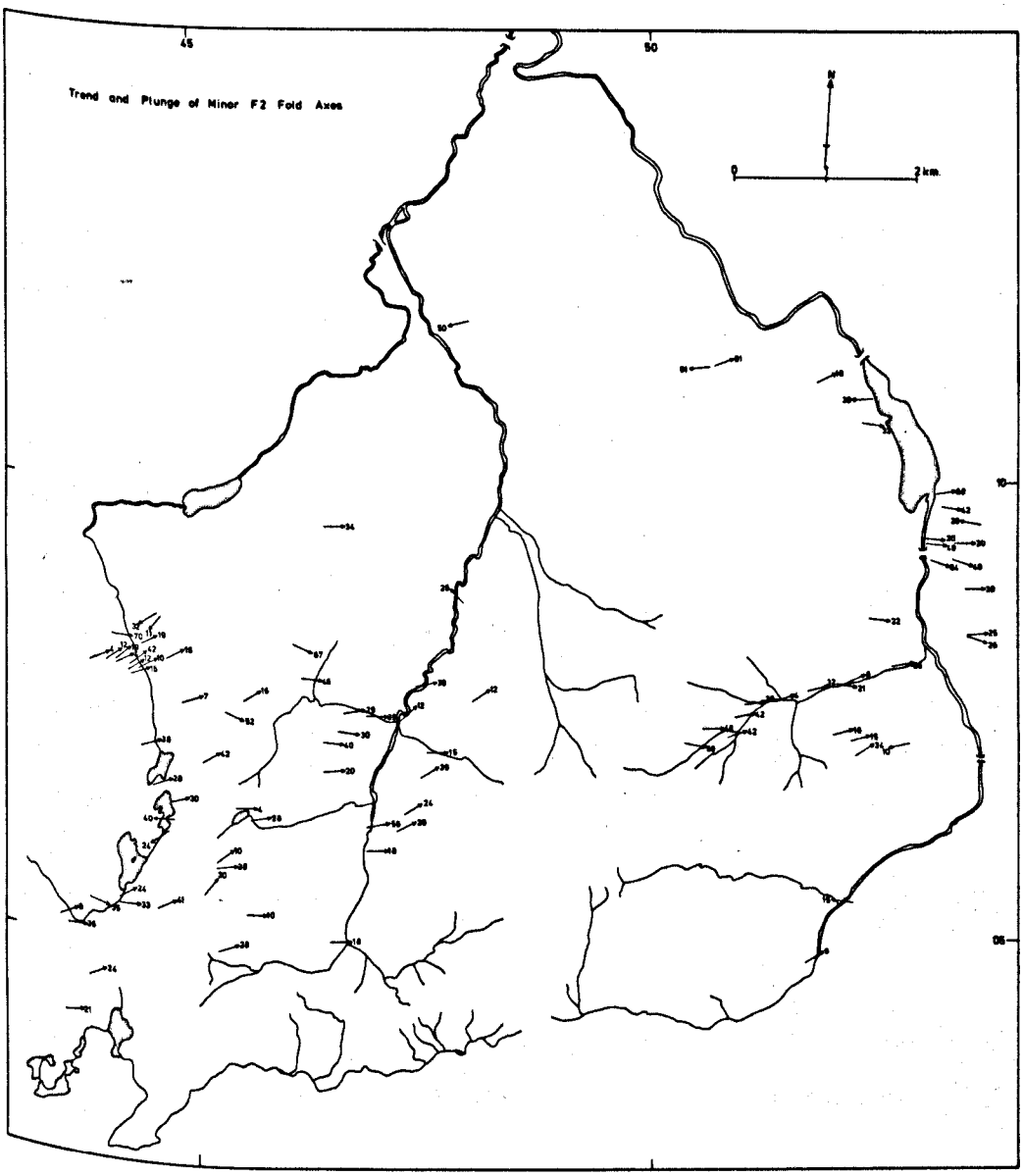
Trend and Plunge of Minor F2 Fold Axes
45
50
N
0
2 km.

Figure 15 Stereographic plot of 87 F_2 fold axes
(North point is marked by vertical line)

Figure 16 Contoured stereographic plot of 231 F_3 fold axes
(North point is marked by vertical line)

Contours at 1, 3, 5 and 7%

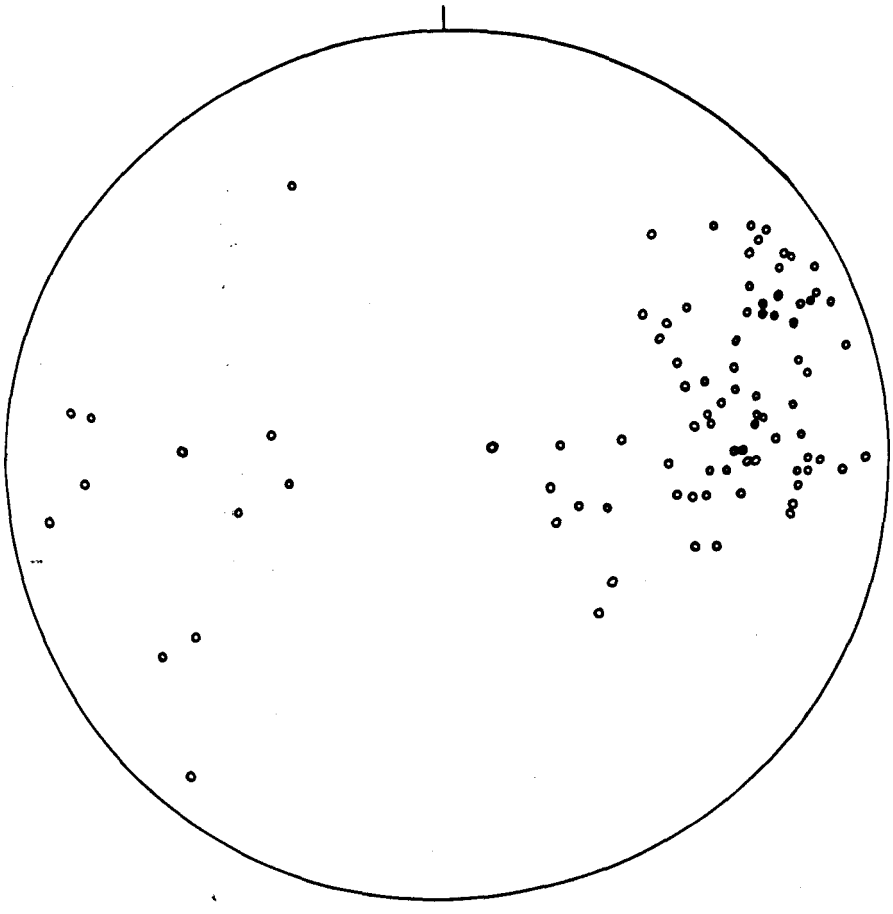

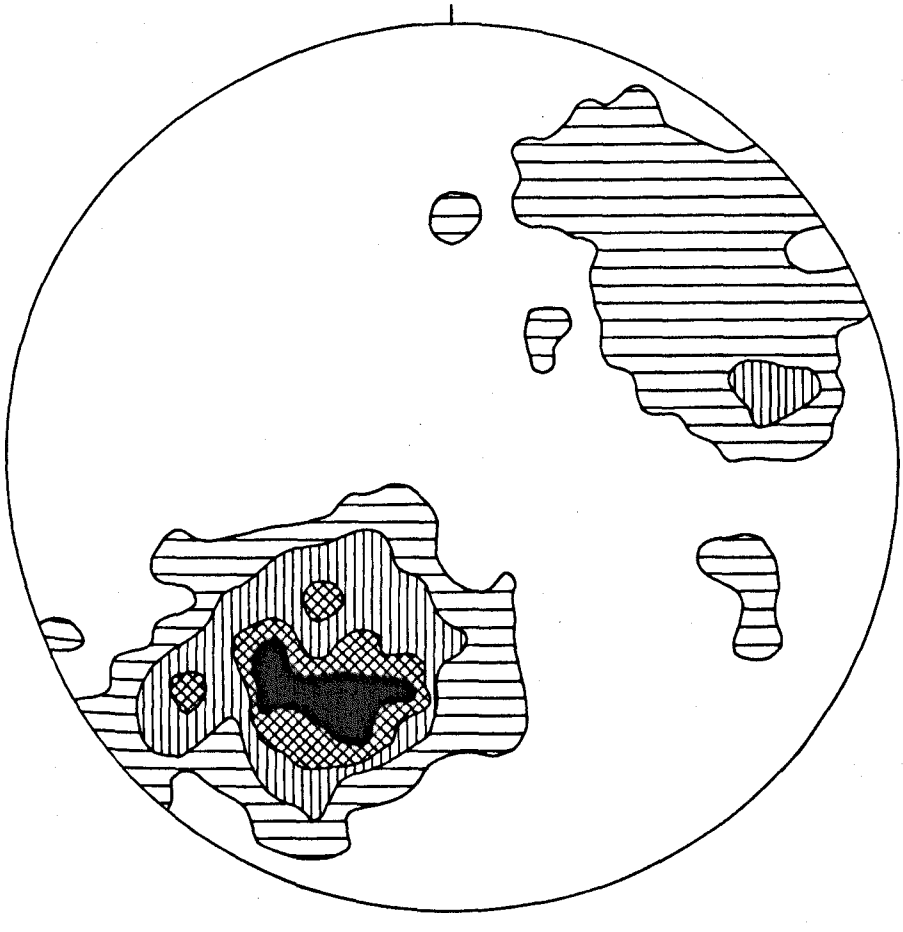

The major axes which plunge south-south-west are repeated about a median line throughout the area (Figure 10) which is responsible for the alteration of the trend of the major F_2 synform.

The amplitude of F_3 folds is highly variable and it is not possible to state a finite value since all are interrelated. It can be said that there is a range of wavelengths from less than 5 millimetres, to several kilometres for the overall structures, all folds being crenulate in style and possessing monoclinic symmetry.

Profiles show the folds to be dominantly open or gentle (Fleuty,1964). The hinge zones tend to be angular and the small degree of flattening (see Section 5.7.4 and Plate 24) leaves hinges and limbs of competent bands relatively uniform in thickness. The folds are mainly cylindrical but Plate 25 shows a departure from this pattern with the offset of fold crests and hinges over relatively short distances.

The trend of minor F_3 fold axial planes is shown in Figure 13. A fairly constant trend is maintained about a north-east/south-west direction and most dips are to the south-east, this being mirrored by the crenulation cleavage. Both the cleavage and the axial planes of the F_3 folds are steep to sub-vertical across most of the area.

The F_3 axes have an average plunge of 36° and Figure 16 shows their distribution. The axes form a bimodal distribution with a considerable number of points in the north-east quadrant. This is related to the change of plunge direction which is most noticeable in the south-western corner of the area although scattered axial undulations do occur

Plate 24 Small scale F_3 folds

Plate 25 F_3 fold crests

Figure 17 F_3 fold trends

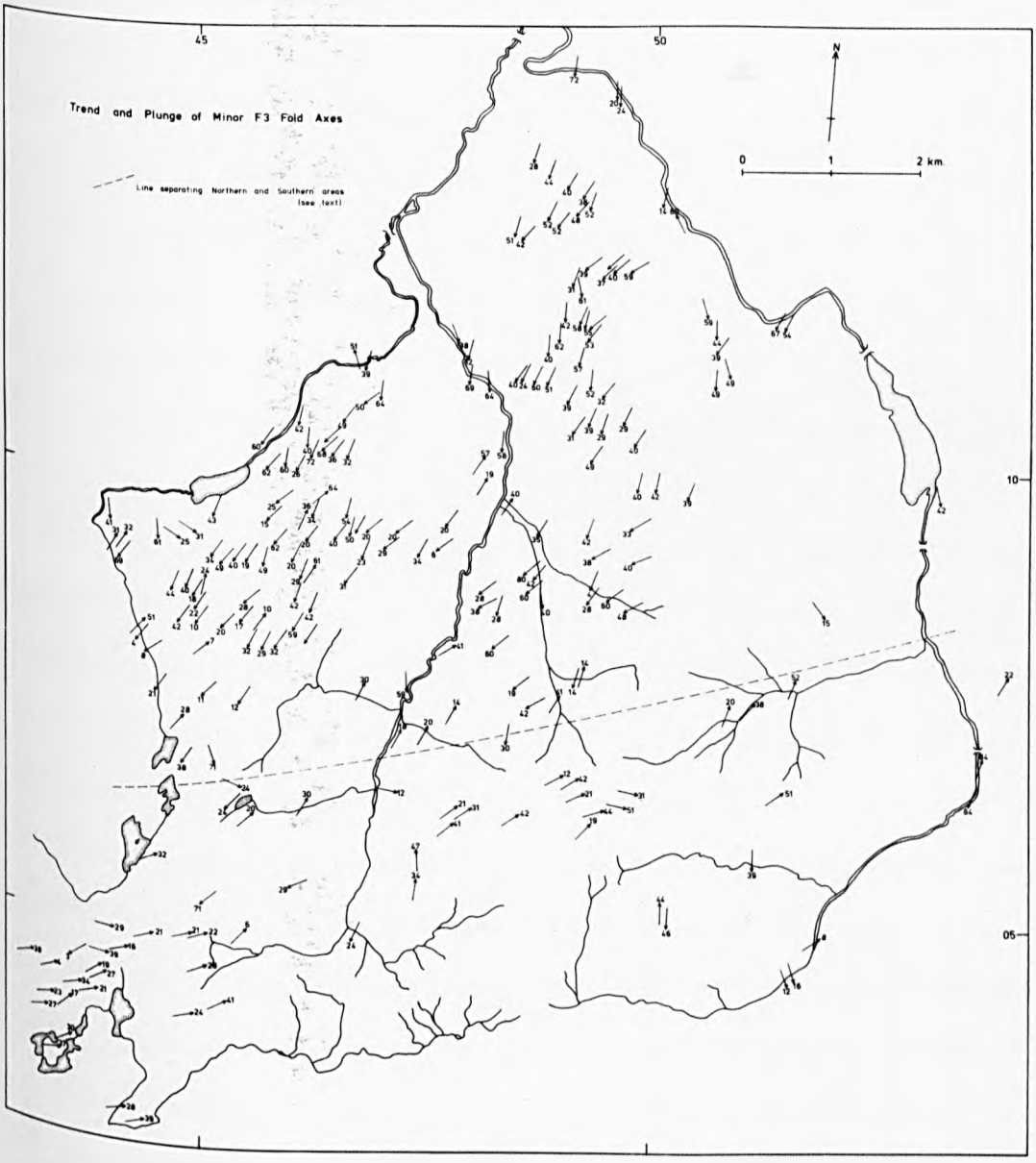
Trend and Plunge of Minor F3 Fold Axes
Line separating Northern and Southern areas (see text)
N
0
1
2 km
45
50
10
05

elsewhere. An arbitrary line may be drawn subdividing the area into two (Figure 17), the northern part exhibiting mostly south-westerly plunges and the southern part mainly easterly plunges. The changes in orientation must be related to a later deformation and this is evident from the stereographic plot of F_3 axes (Figure 16), which shows the division about an east-south-east direction. The arbitrary line dividing the fold axes is influenced by the availability of data and its direction cannot therefore be accurately fixed. Even so, the line is subparallel to the constructed trend which affects the F_3 folds. Hence it is apparent that a fourth deformation consisting of major, open folds exists.

All exposures in the extreme south-eastern corner are considerably affected by the Allt Crom granite. The regional foliation is disrupted and it seems likely that forceful intrusion has produced a disorientation of linear structural elements. The intense veining and feldspathisation of host lithologies suggests that the granite, which outcrops to the south-east, is at no great depth in this area. It is thus feasible that the disruption of F_3 axes was induced by the intrusion. The trend is approximately parallel to the northern, bulbous margin of the granite and on moving further west, its effects become less obvious. A few F_3 trends within this area deviate from this pattern, the majority being north-south or northwest-southeast. At this particular point, the effective dislocation caused by the intrusion could have been essentially vertical rather than oblique, as might be found on the flanks of the granite.

Plate 26 Muscovite crystal illustrating an early stage of kink formation

Plate 27 Muscovite crystal illustrating a later stage of kink formation

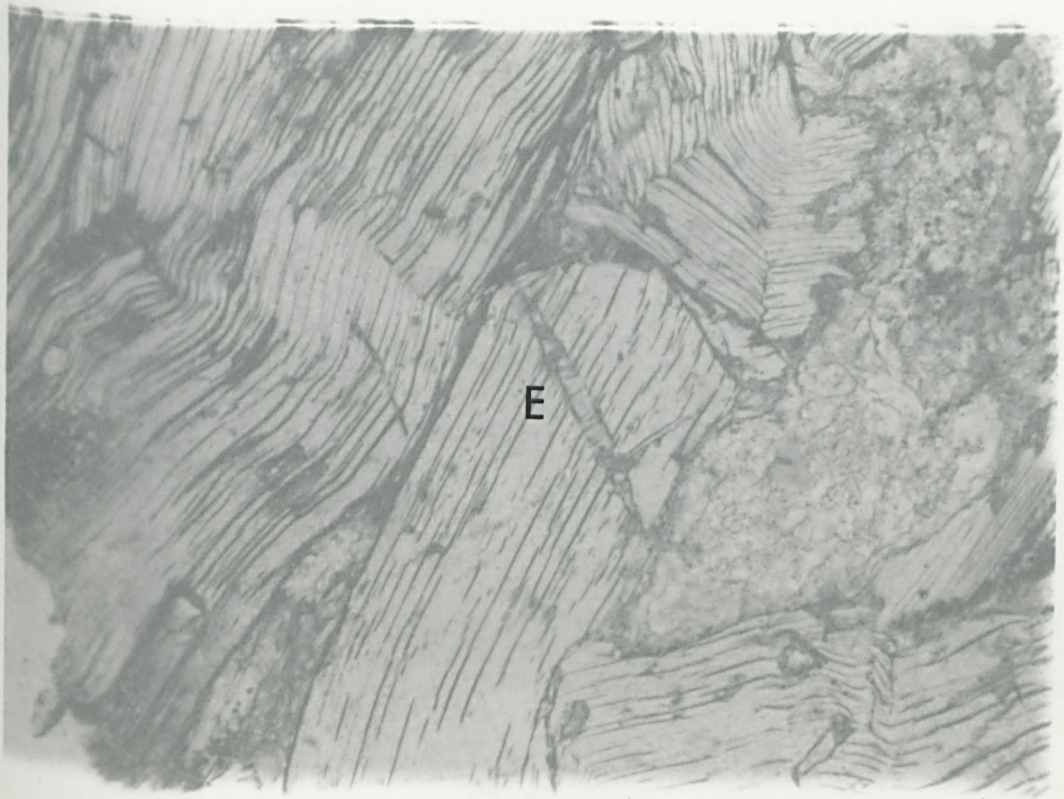
E

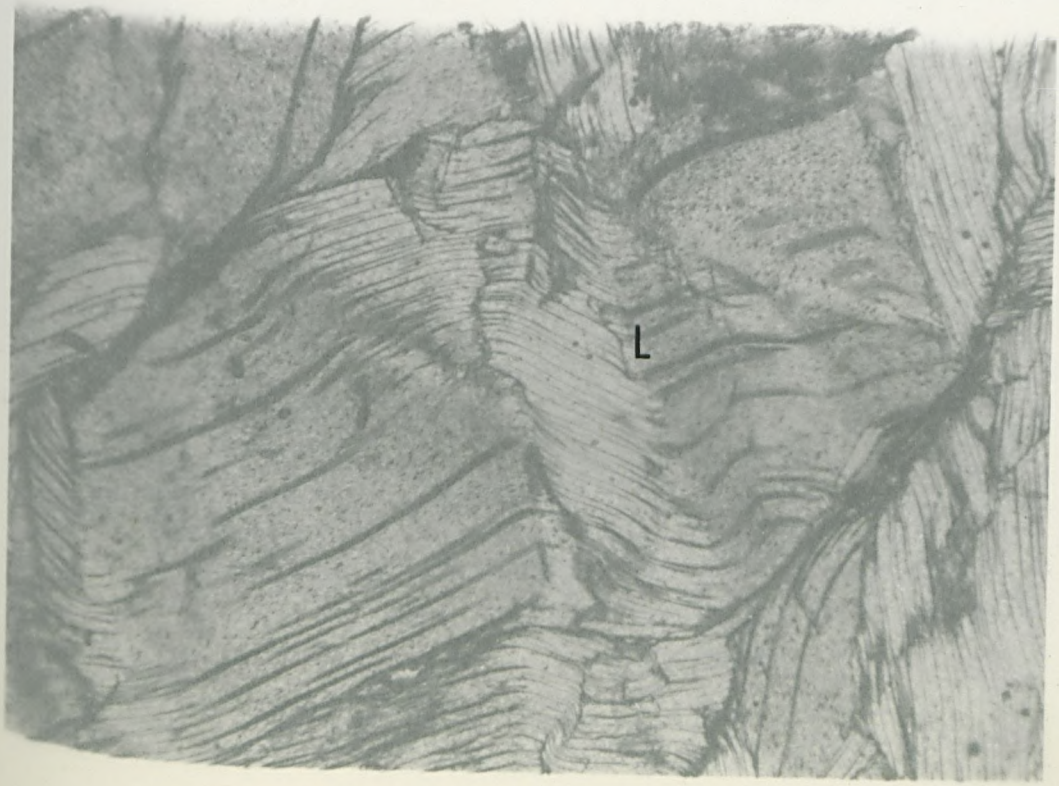
L

5.3.4 F_4 folds

Elsewhere, occurrence of F_4 structures in the field is scarce and is limited to a small number of minor kinks. Major structures are responsible for the undulation in F_3 fold axes (see Section 5.3.3), but are discernible primarily by graphical methods.

The axial trend of the kinks varies, from east-north-east to south-east and west-north-west. All show an angular deflection of the foliation but no conjugate sets are seen thus determination of the direction of compressive stress is not feasible.

The D_4 deformation is better shown in thin section by kinked muscovite crystals. Plates 26 and 27 show selected crystals, but the grains are disoriented.

Internal deformation usually occurs by flexural slip along the layering and constant orthogonal thickness is thus maintained (Ramsay,1967). It is now suggested by several authors (Cobbold et al,1971;Gay and Weiss,1974), that kinks begin as buckles which are subsequently modified to angular form. Migration of axial surfaces (Ramsay,1967) proceeds from an initial kink with lateral and longitudinal growth. Plates 26 and 27 illustrate this concept with kinks in an early stage of formation (marked E on Plate 26) and a later stage, (designated L on Plate 27), with boundary migration in the latter.

5.4 Linear Features-Lineations

Lineations do not form a persistent or common tectonic feature in the Killin area. Two are discernible, the earlier (L_2) a mineral alignment associated with F_2 folds, and a crinkle lineation (L_3) associated with microcrenulations comprising F_3 folds.

Both distribution and trend (Figure 18) of these lineations is therefore very similar to those of the minor folds. Second lineations are dominant in the east near Loch Killin and in the west, whilst third generation ones predominate in the central and northern areas.

The L_2 lineation is an axial alignment of minerals, invariably biotite with muscovite. A stereographic plot (Figure 19) shows the similarity in trend to the minor F_2 folds. Of the thirty readings, six show a plunge to the west-north-west due to the effect of the later folding.

L_3 lineations show a similar parallelism to the minor F_3 fold axes and reflect later tectonism in the same way, due primarily to F_4 warping. However, there is considerable fanning of lineation trends and this probably reflects a degree of conicalness in the F_3 folds over the whole of the area.

5.5 Boudinage

Although not common, examples of boudinage have been seen. Usually they occur within early quartz veins, and reach thicknesses ranging up to 40 centimetres. Pinch and swell of thin quartz veins was also noted.

Substantial flattening and therefore lateral stretching must have been responsible for their production, and since

Figure 18 Trend and distribution of lineations

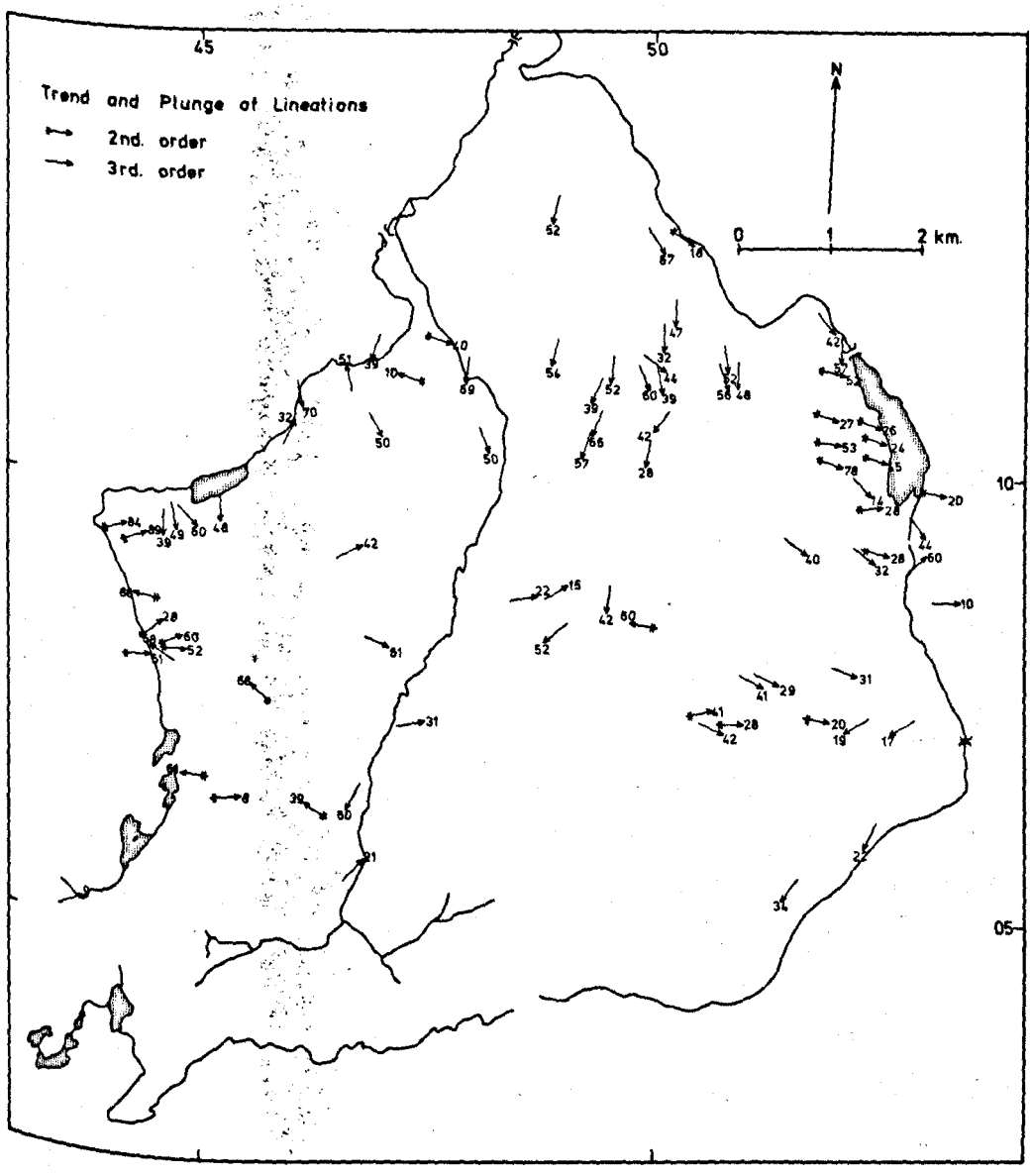
Trend and Plunge of Lineations
2nd. order
3rd. order
N
0
1
2 km.
45
50
10
05

Figure 19 Stereographic plot of lineations
(North point is marked by vertical line)

x - L_3 lineation

o - L_2 lineation

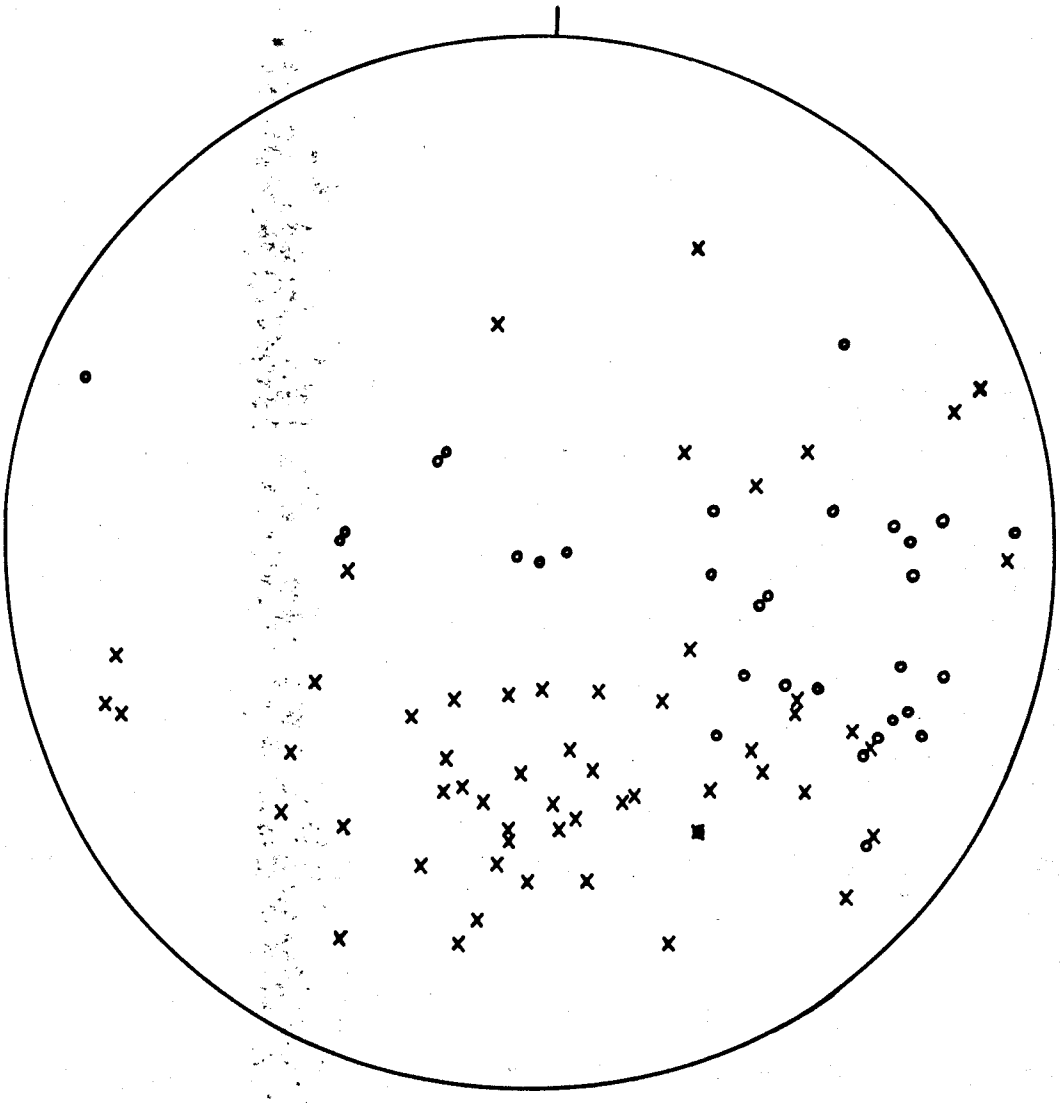

all lie within the S_1 foliation it is probable that they formed during the intensive flattening of the D_1 episode which ultimately produced the foliation.

Reaching a maximum length of 4 metres, the area of necking in some boudins is clearly seen to contain a pelitic infill, the latter flowing under the compressive stress (Plate 28). This illustrates the pre-D_1 nature of the quartz vein since the host pelite has infilled the 'neck' produced during deformation. Boudins folded in later deformational episodes were occasionally noted, on the limbs of F_2 and F_3 folds. Where the folds involved a high degree of compression further separation of the boudins may have occurred after folding (Plate 29).

The axes of boudinage show two trends (080 and 180) implying that the axes have been rotated during subsequent tectonic events.

5.6 Refolding

As with any multiply folded area, examples of refolding occur throughout. This brief section outlines the dominant styles. The most common is the refolding of F_1 isoclines by open crenulate F_3 folds, usually illustrated by calc-silicates or quartz veins. Development of the S_3 crenulation cleavage fades on approaching the isoclinal fold hinge. Occasionally the more competent bands show small discrete fractures sub-parallel to the direction of the S_3 cleavage (Plate 30).

Figure 20 shows the refolding of an isoclinally folded calc-silicate band with the F_1 axis now parallel to the F_3 axis. This is a type three interference pattern of Ramsay

Plate 28 Necking of quartz boudins

Plate 29 Folded quartz boudin (upper left of lens cap)

Plate 30 Crenulations with development of cleavage and fractures

Plate 31 Refolded white calc-silicate bands

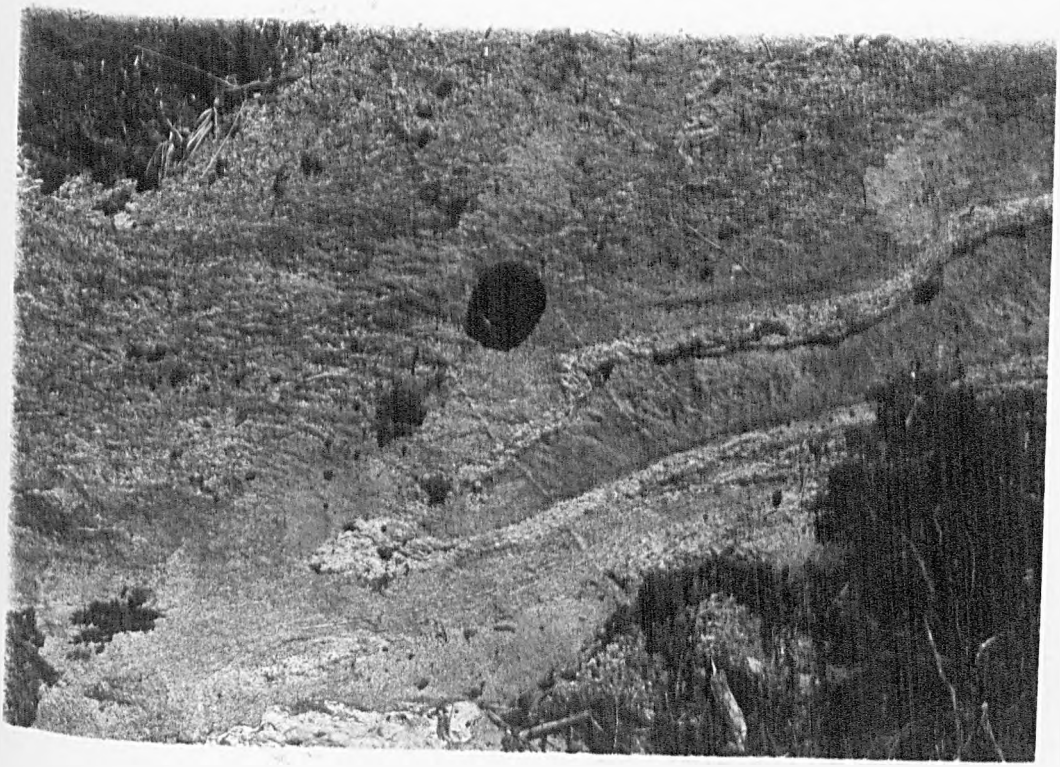

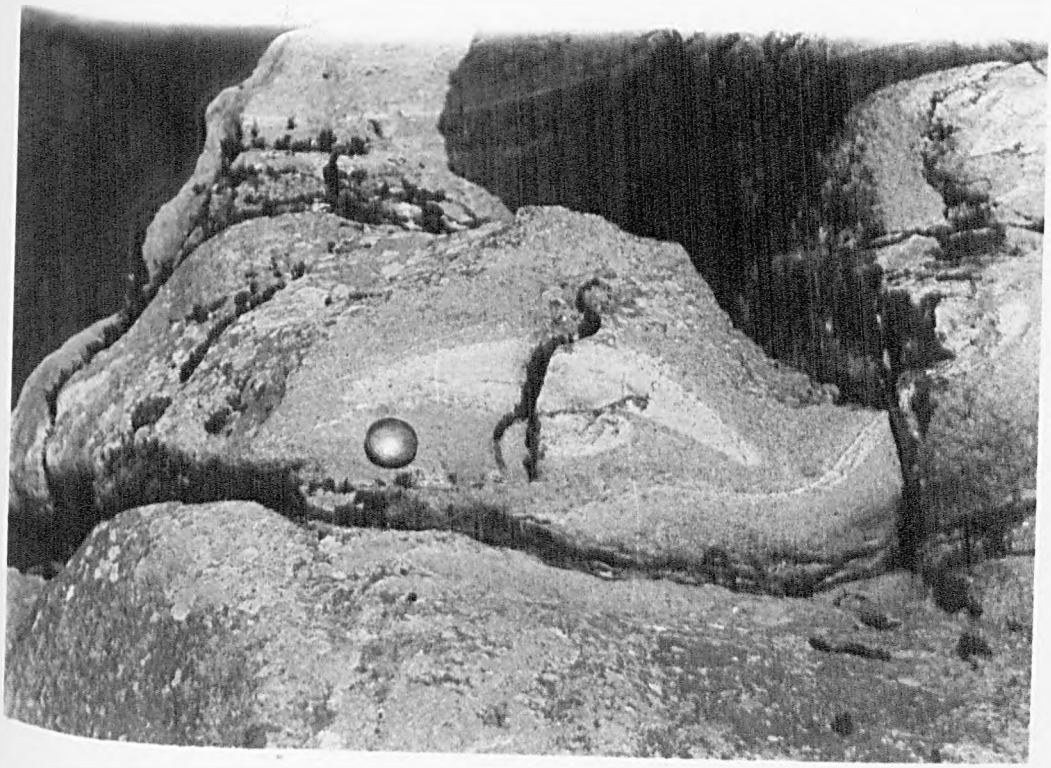

(1967) with the 'a' direction of superimposition orientated at a high angle to the first fold axial surface. This is the most common refolding pattern in the Killin area with isoclinal F_1 closures often occurring on the limbs of tight F_2 folds.

Plate 31 shows a refolded calc-silicate which closely resembles the type two structures of Ramsay (op.cit.). The central crescent shape is surrounded by a further calc-silicate band suggesting a section through an arched fold. In this instance, the F_1 axial plane and limbs are both folded, the former making a large angle with the imposed 'a' direction which is again the F_3 fold trend.

Figure 21 again illustrates a type three pattern which is outlined by calc-silicate bands, but in this case all three trends are present, each being folded by progressively younger folds, F_3 being the most recent. Axial traces of the first and second generation are now sub-parallel with the S_3 trace superimposed at a high angle to both S_1 and S_2. Intense flattening is apparent in the formation of S_1 and S_2, their traces paralleling the regional foliation.

5.7 Geometrical Analysis of Folds

5.7.1 Introduction

Analysis of folded layers is possible using several geometrical properties which are constructed upon fold profiles. Construction of dip isogons (Elliot,1965), enable fold classification according to isogon patterns (Ramsay,1967).

Dip isogons are lines which connect points of equal gradient through successive fold layers (and occur as such

Figure 20

Refolding patterns from the Killin area

Figure 21

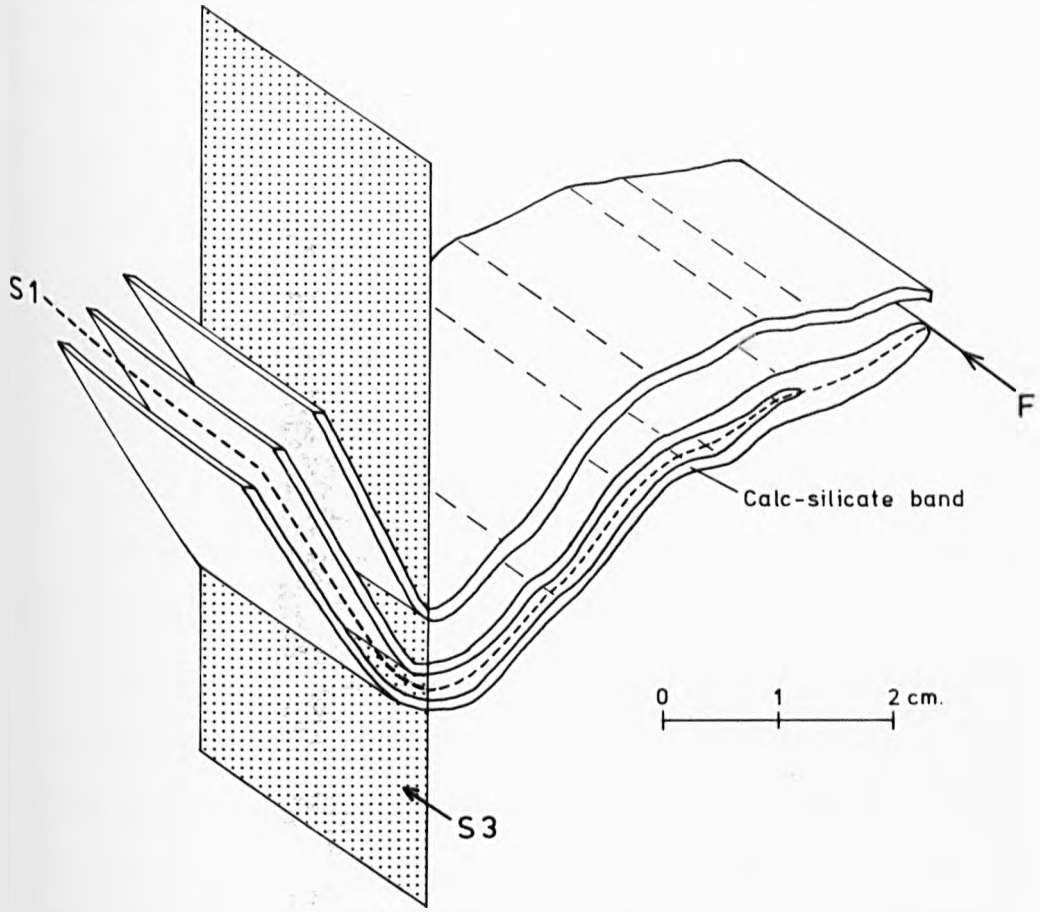
S1
F
Calc-silicate band
0 1 2 cm.
S3

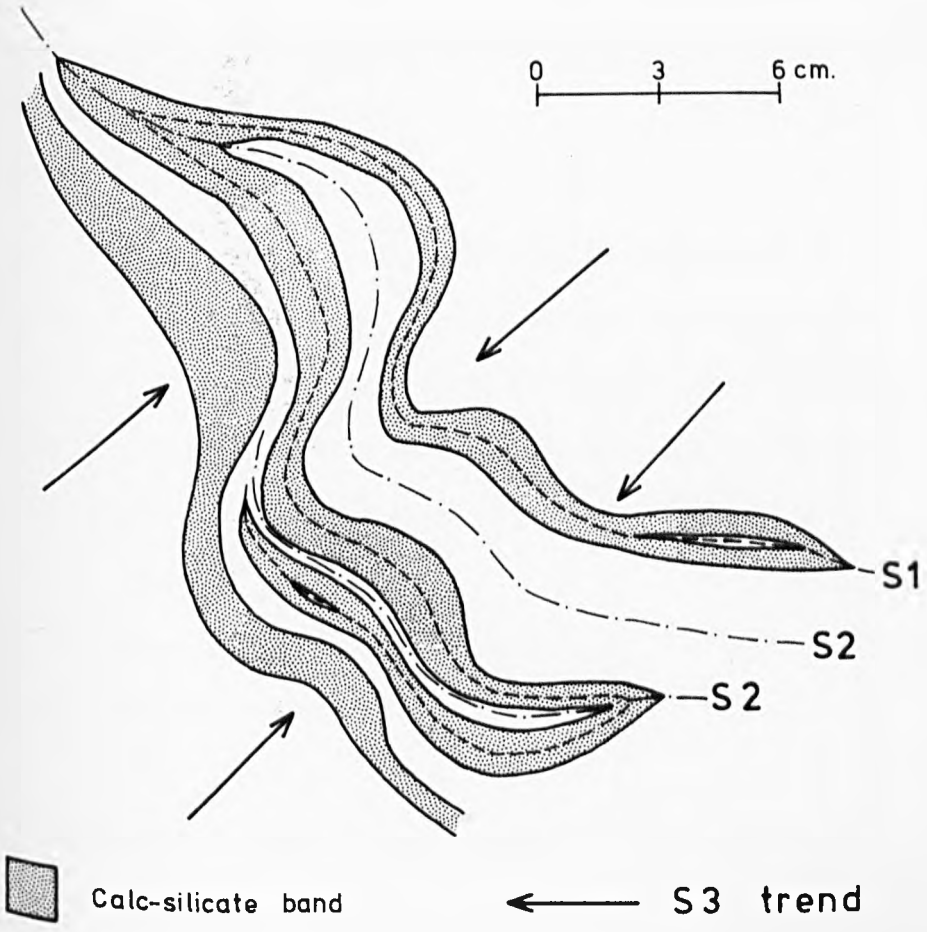
0 3 6 cm.
S1
S2
S2
Calc-silicate band
S3 trend

in subsequent examples), and the relative orientation of the isogons with respect to each other and the axial trace, determines curvatures of layer boundaries. Study of isogon patterns produces three basic fold classes (op. cit.) depending on fold arc curvatures. If in tracing isogons from the outer to inner arc of a folded layer there is convergence on each other and on the axial trace, this is indicative of class 1 geometry. Class 2 shows parallel isogons and class 3 divergent ones, class 1 being the only group which can be subdivided on the degree of isogon convergence.

A further parameter used to describe fold shape is t, the orthogonal thickness (op. cit.). Using a fold profile (Figure 22), the thickness t_α between two folded surfaces can be determined by constructing tangents to each of these, making an angle $90^\circ-\alpha$ with the fold axial trace. 't_o' is the thickness measured at the fold hinge zone and the ratio of the two, t_α/t_o, produces a useful parameter t'_α. Graphical representation of t'_α vs.α produces five fields or lines relating to the different fold classes.

A second graph may be constructed in the same way but using T, the thickness between surfaces parallel to the axial trace (Figure 22). The relationship between the two thickness parameters is expressed as:

$$t_\alpha = T_\alpha \cos\alpha$$

and in a true similar fold (class 2), the thickness t should follow the relationship:

$$t'_\alpha = \cos\alpha$$

The final parameter used is ϕ_α (Huddleston, 1973) which is measured in conjunction with the dip isogons. ϕ_α is

Figure 22 Fold profile illustrating the parameters used in analysis

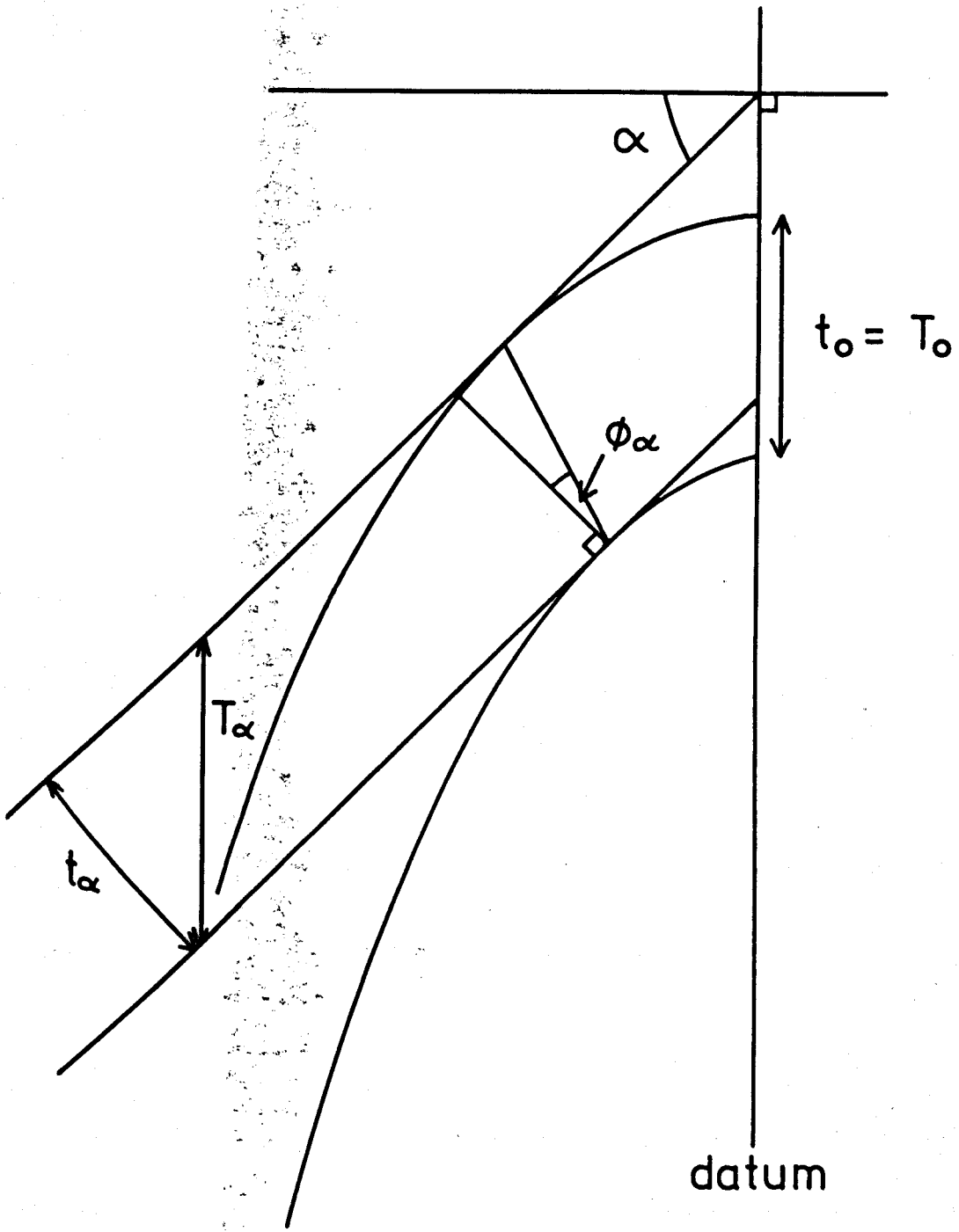
α
$t_o = T_o$
ϕ_α
T_α
t_α
datum

defined as the angle between the isogon and the normal to the tangents bounding fold surfaces (Figure 22). In a plot of ϕ and α sign conventions are necessary for both parameters. α is positive for antiform right limbs and synform left limbs and negative for the other limbs. ϕ is positive if the isogon is "deflected" in an anticlockwise sense relative to the perpendicular from the inner to outer arc, and negative if "deflected" in a clockwise direction (op. cit.).

ϕ_α is a very useful parameter since it reflects changes in fold geometry. Curvature changes in complex folds are determined using $dt'/d\alpha$ and $d^2t'/d\alpha^2$ against α plots (Ramsay, 1967), but plotting of ϕ_α against α reveals a curve very similar to that of the first differentiated plot (Huddleston, 1973). Also, ϕ_α is independent of the datum position unlike t'_α , and is therefore less liable to errors since a datum change results in a constant angular difference. Subsequent graphs of ϕ_α and α again show a subdivision into five fold classes.

Examples of F_2 and F_3 folds follow and each is analysed in the manner described. F_1 folds are not studied on account of their extreme deformation which has produced tight isoclines with attenuated limbs. Such deformation renders geometrical analysis unnecessary.

5.7.2 Analysis of F_2 folds

Fold one is composed of five layers, all but one, (number five), being semi-psammitic in composition and reaching a maximum thickness of 7 centimetres. From the crest of layer one to that of layer five is a distance

of 57 centimetres and $\lambda/2$ averages 22 centimetres. This slightly asymmetric fold has dominantly rounded crests (Fleuty, 1964), with interlimb angles for individual layers varying from 35° to 75°, the overall profile being tight to close (op. cit.).

Figure 23 shows the isogon orientation for each layer and the results are summarised in Table 5.1:

Layer	Hinge	Right limb	Left limb
1	parallel (2)	convergent (1B)	divergent (3)
2	parallel (2)	convergent (1C)	convergent (1A)
3	parallel (2)	convergent (1C)	divergent (3)
4	parallel (2)	divergent (3)	convergent (1B)
5	divergent(3)	divergent (?)	divergent (3)/ convergent (1A) at high α

Table 5.1

The noticeable property is that the fold displays class 2 geometry at the hinge with a combination of classes 1 and 3 along the limbs. Layers one to three have been analysed using the graphical methods already described. The t'_α graph shows layer one (Figure 24) to be class 3 from the hinge zone until α reaches 25°, class 2 up to 50° and class 1C thereafter. This is substantiated by the T'_α and ϕ against α plot.

Layer two lies in the 1C field for all three graphs with a slight fluctuation in gradient of the right limb between 40° and 55°. This is illustrated in the ϕ_α against

Figure 23 Isogon orientation on the profile of Fold 1

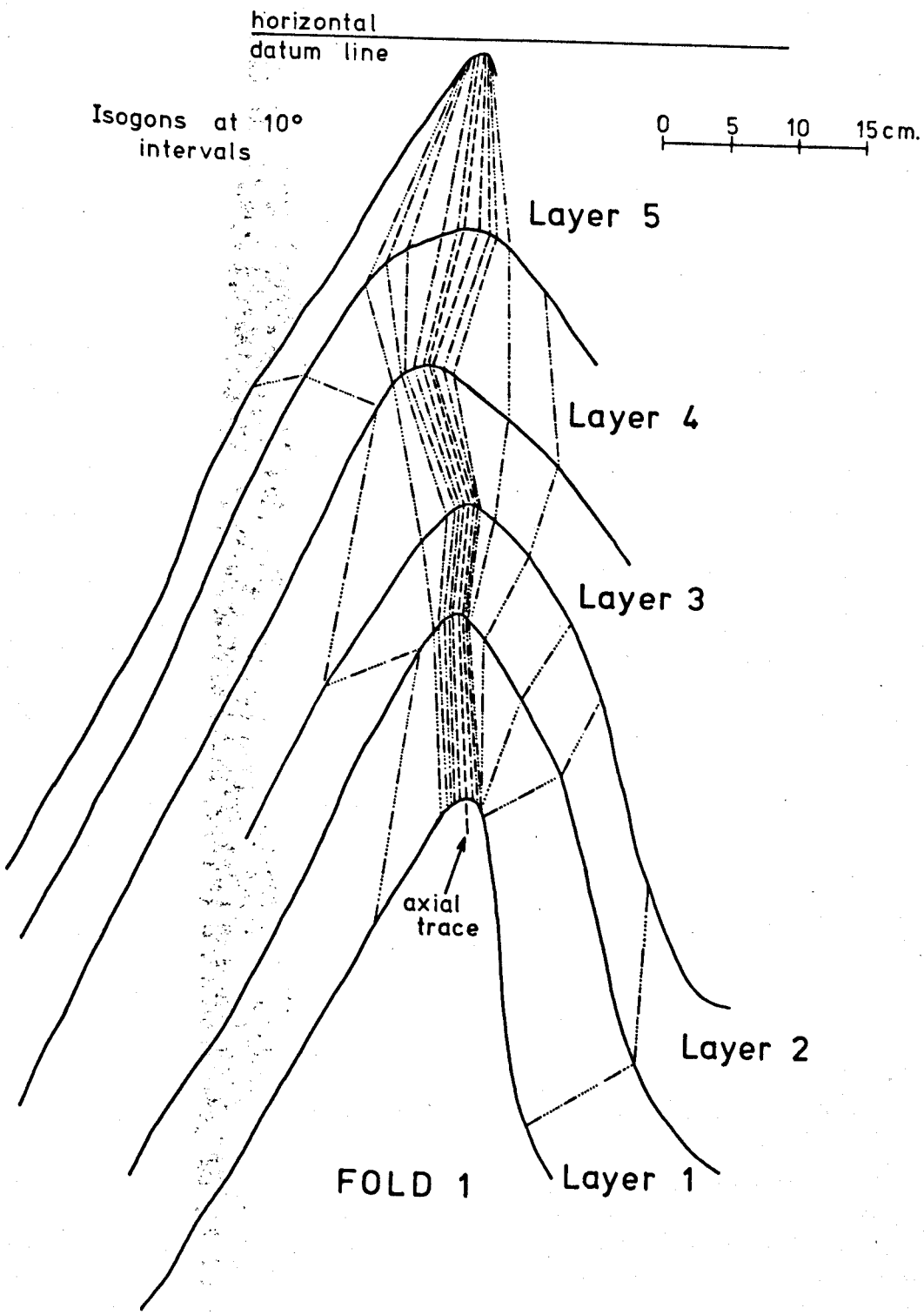
horizontal
datum line
Isogons at 10°
intervals
0 5 10 15 cm.
Layer 5
Layer 4
Layer 3
axial
trace
Layer 2
Layer 1
FOLD 1

Figure 24 Graphical plots for Fold 1, layer 1

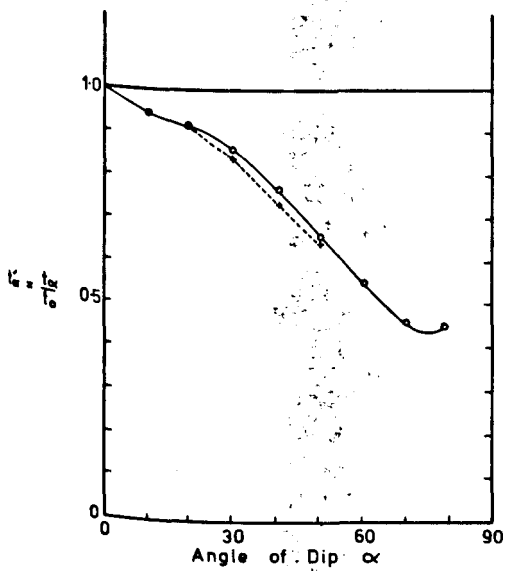
1·0
0·5
0
0
30
60
90
Angle of Dip α

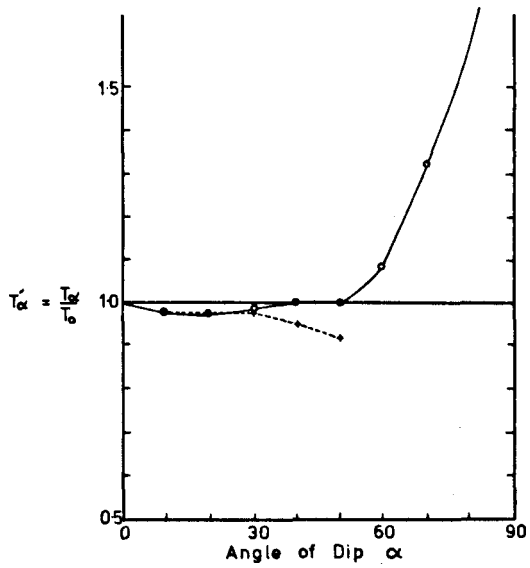
1·5
1·0
0·5
0
30
60
90
Angle of Dip α

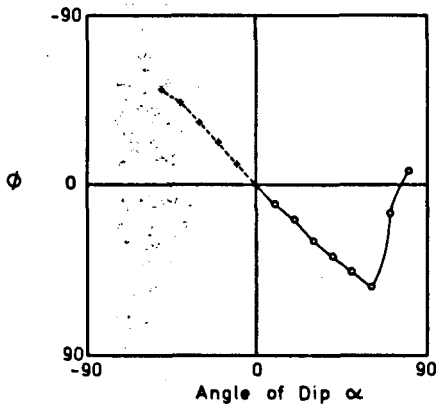
-90
0
90
-90
0
90
Angle of Dip α

LAYER 1

Figure 25 Graphical plots for Fold 1, layer 2

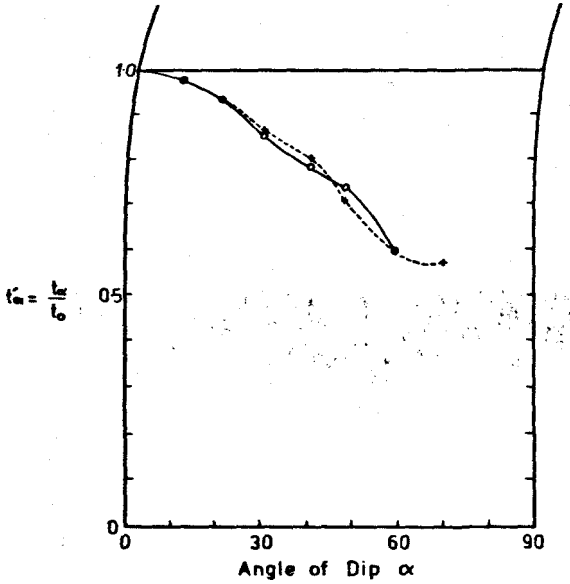
1·0
0·5
0
0
30
60
90
Angle of Dip α

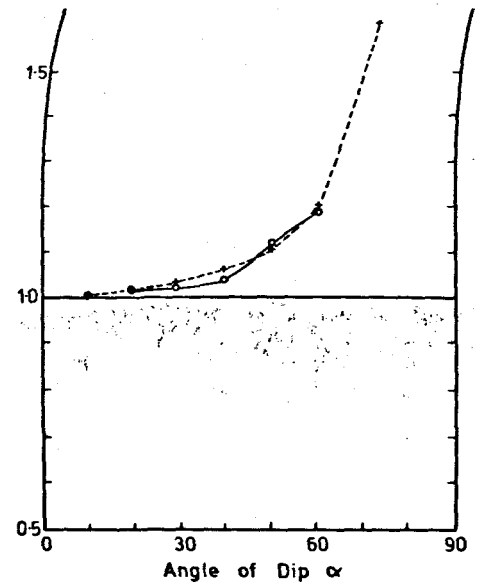
1·5
1·0
0·5
0
30
60
90
Angle of Dip α

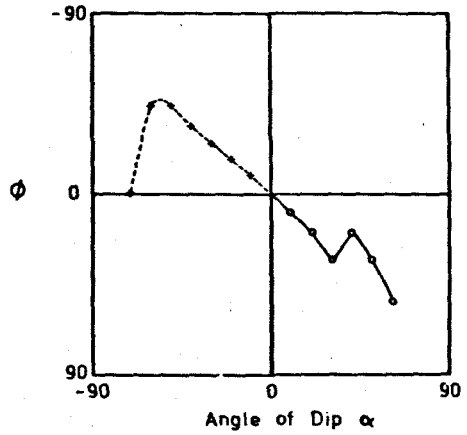
-90
0
90
-90
0
90
Angle of Dip α

LAYER 2

α plot and is due to a slight thickening of the limb (Figure 25).

The right limb of layer three is seen to be consistently class 1C (Figure 26) whilst the left one fluctuates gently about the class 2 to class 3 boundary, for low values of α, and moves into the class 3 field when α is 45° or more.

Fold two is slightly asymmetric with rounded crests and interlimb angles from 45° to 56°. Total thickness along axial trace (1) is 80 centimetres, two layers (one and three) being semi-psammitic in composition and two, slightly more pelitic. $\lambda/2$ averages 35 centimetres for this close to open fold (Fleuty, 1964).

Figure 27 shows the fold with isogons constructed at 20° intervals and the results are summarised in Table 5.2:

	Axial trace (1)		Axial trace (2)	
Layer	Left limb	Right Limb	Left Limb	Right limb
1	convergent	convergent	weakly convergent	weakly convergent
2	divergent	parallel/ convergent	divergent + (convergent)	divergent
3	convergent	parallel	convergent	weakly convergent

Table 5.2

The isogons illustrate an alternation of fold layer shape, layers one and three showing dominantly class 1C orientation, whereas layer two displays class 3 geometry.

All three layers have been analysed using the t'_{α},

Figure 26 Graphical plots for Fold 1, layer 3

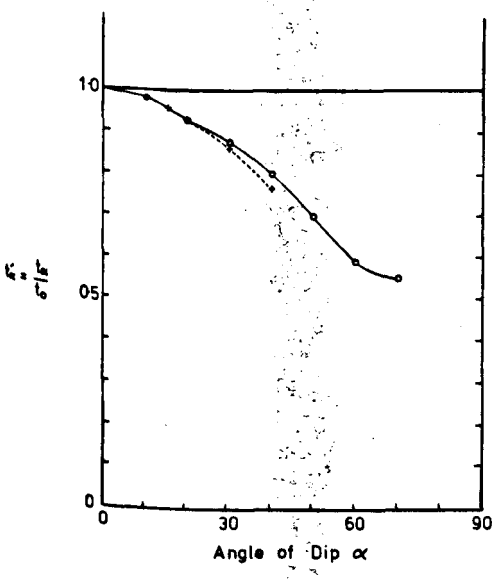
1·0
0·5
0
0
30
60
90
Angle of Dip α

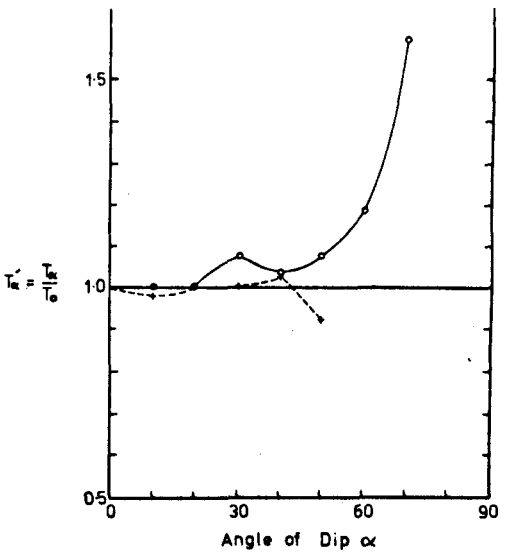
1·5
1·0
0·5
0
30
60
90
Angle of Dip α

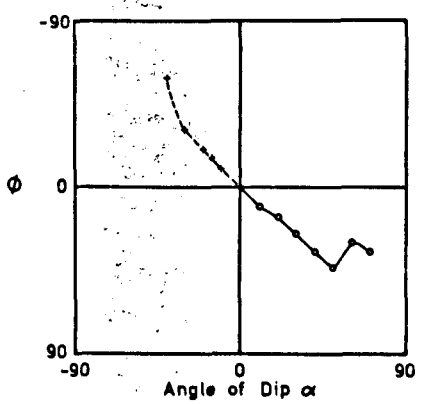
-90
0
90
-90
0
90
Angle of Dip α

LAYER 3

Figure 27 Isogon orientation on the profile of Fold 2

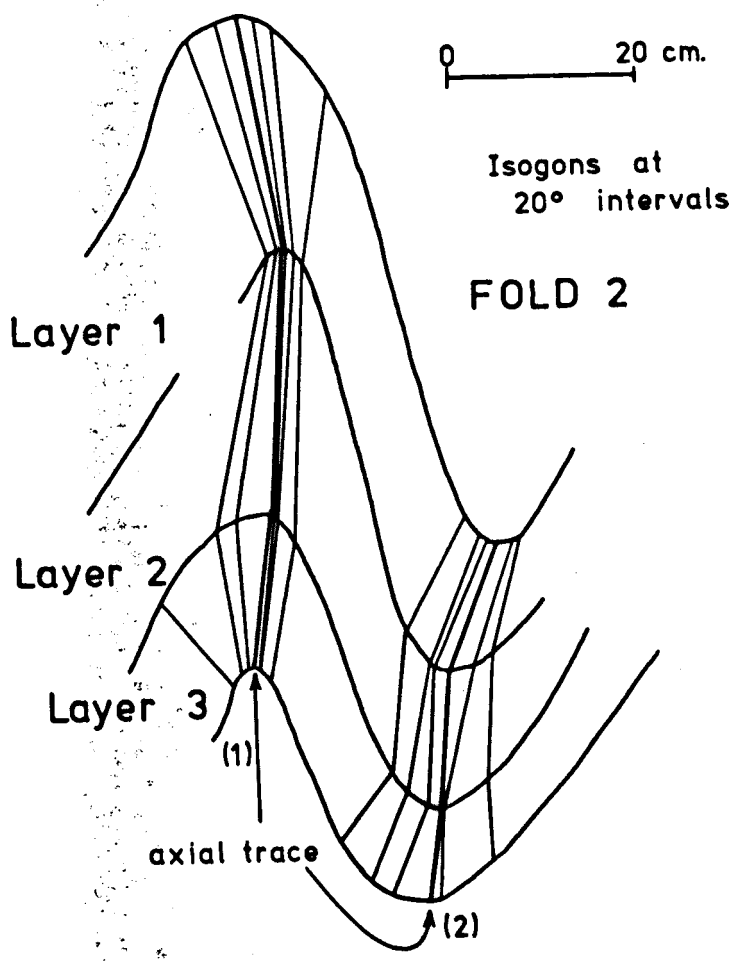
0
20 cm.
Isogons at
20° intervals
FOLD 2
Layer 1
Layer 2
Layer 3
(1)
axial trace
(2)

T'_α and ϕ (Figure 28) for the intermediate limb of the fold, layer one showing class 1C geometry in all three plots. Layer two shows a near perfect similar fold plot for values of α up to 40°, but diverges into the class 3 field at higher angles. The third layer shows gentle changes in slope from class 3 geometry at low angles ($\alpha < 35^\circ$), to class 1C at higher values of α.

5.7.3 Interpretation

Although graphical analysis of six fold layers cannot be considered to be representative of all F_2 folds, the styles throughout are reasonably constant and this process therefore serves to interpret, if only partially, their mechanism of formation.

The variations in fold style are the products of the type and amount of deformation and the differing competency of the folded layers.

All six analysed layers show a predominance of class 1C geometry with subordinate classes 2 and 3 and as such may be indicative of buckling of competent layers with subsequent flattening (Ramsay,1962;1967). Layer parallel shortening would lead to the initial development of buckle folds. This would produce parallel (class 1B) folds in more competent beds. Less competent material produces accomodating fold styles. Plots of t'_α against α can be superimposed on a similar graph indicating the variation in λ_2/λ_1 in flattened parallel folds (Ramsay,1967 p. 413). Determination of the superimposed strain is feasible only when a t'_α plot produces points falling along a similar curve.

Figure 28 Graphical plots for Fold 2

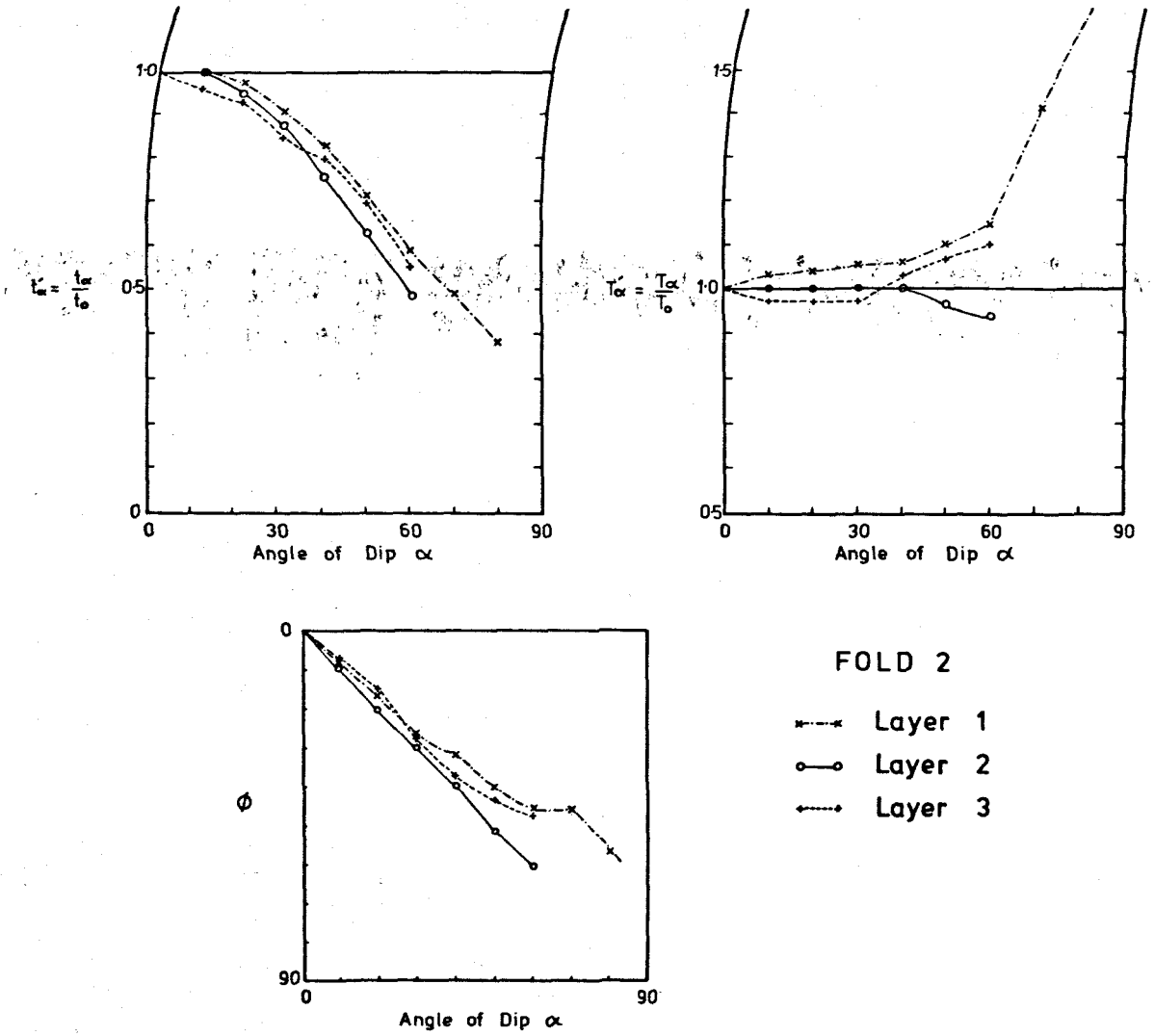
$t'_\alpha = \frac{t_\alpha}{t_o}$
1·0
0·5
0
0
30
60
90
Angle of Dip α
$T'_\alpha = \frac{T_\alpha}{T_o}$
1·5
1·0
0·5
0
30
60
90
Angle of Dip α
φ
0
90
0
90
Angle of Dip α
FOLD 2
Layer 1
Layer 2
Layer 3

In both fold one and two, no plot of t'_{α} against α produces a perfect curve on the λ_2/λ_1 variation diagram. Only layer three of fold one shows a curve which is constant enough to warrant use of this method. Values of from 25° to 63° show a flattening of 65%. The fold hinge and limb extremities both show a divergence from this value.

In fold two, layer two shows a near perfect similar fold line and layer one shows a fairly constant value of 65%. Deviations from these near constant curves can be explained by deformation continuing by processes other than flattening. An original fold profile which did not approximate to class 1B would also produce curves transgressing the λ_2/λ_1 lines.

Fold one would therefore have been compounded of class 3, 1C and both 1C and 3 for layers one two and three respectively. Fold two shows a basic alternation of styles i.e. classes 1C and 3 (more pelitic) which together produce a fold that closely follows the class 2 trend. These are produced by modification of different layers with near 1B and 1C geometry which, after superposition of homogeneous strain, take up a near class 2 geometry when considered together (Ramsay,1967). Thus the buckled layers have undergone deformation by a combination of processes. Features associated with dominantly flexural slip mechanism e.g. tension fissures, are not seen in F_2 folds and this leads to the suggestion that the tangential longitudinal strain is the major factor. As noted by Ramsay (op. cit.), it is unlikely for this process to take

Figure 29 Isogon orientation on the profile of Fold 3

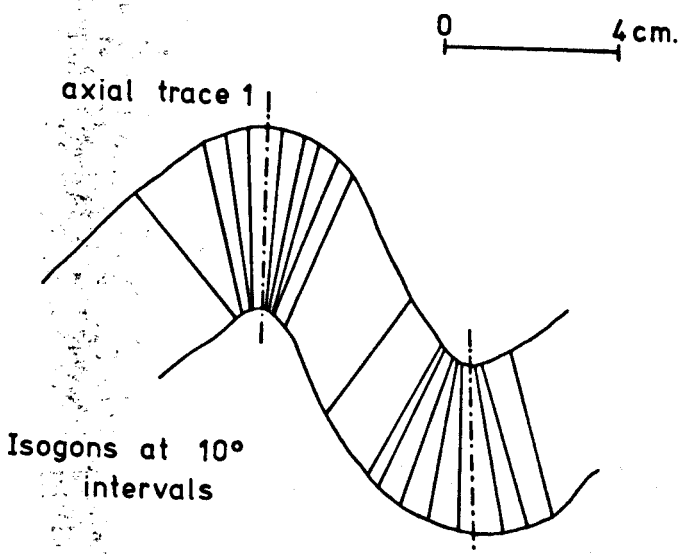

FOLD 3

place alone and it will therefore be accompanied by some flexural slip.

Folds thus developed would change in style due to flattening and associated with this, the F_2 cleavage would have formed. Although this is not a dominantly penetrative fabric it probably formed in this way, parallel or sub-parallel to the F_2 axial planes.

5.7.4 Analysis and interpretation of F_3 folds

To give some indication of the F_3 fold style one particular fold has been selected. Figure 29 shows the profile, the style being dominated by a major competent psammitic band within incompetent pelitic and semi-pelitic layers.

The isogon pattern produced for the psammitic band, which clearly resembles a cleavage fan (Figure 29), shows the 1C geometry of the layer and this is substantiated graphically (Figure 30). The curves produced in the t_α plot are almost identical for both limbs (about axial trace 1), and a sufficiently constant trend is obtained for determination of the amount of flattening. In this case a value of 35% is obtained for superimposed homogeneous strain, substantially less than in the tentative values gained for the F_2 folds. Associated pelitic and semi-pelitic bands show typically accommodating styles with fold hinge thickening and limb attenuation, both consistent with class 3 geometry.

A combination of all these properties again suggests tangential longitudinal strain as the prime factor in F_3

Figure 30 Graphical plots for Fold 3

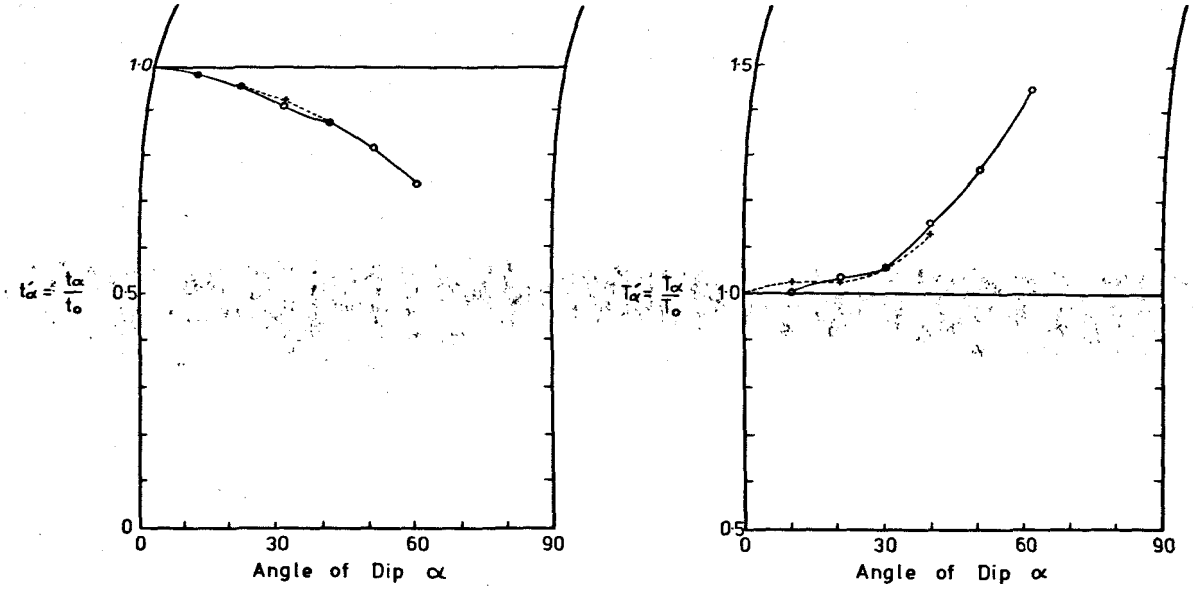
$t'_\alpha = \frac{t_\alpha}{t_o}$
1·0
0·5
0
0
30
60
90
Angle of Dip α
$T'_\alpha = \frac{T_\alpha}{T_o}$
1·5
1·0
0·5
0
30
60
90
Angle of Dip α

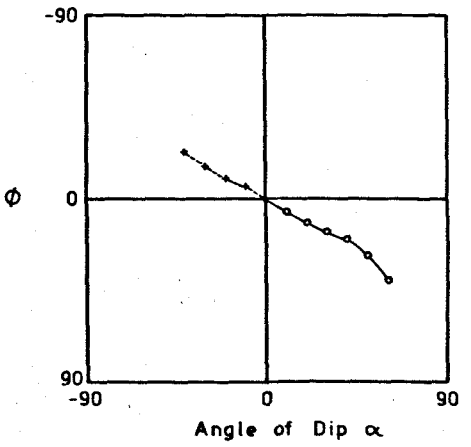
-90
φ
0
90
-90
0
90
Angle of Dip α

FOLD 3

fold formation. Study of F_3 fold geometry tends to be more difficult than for F_2 folds due to the open crenulate style of the former, and the fact that the F_3 folds are seen mainly in thinly multilayered sequences. This brief analysis does, however, serve to elucidate some of the factors involved.

5.8 Foliation

Foliation is defined here as parallel, penetrative elements (Fairbairn, 1949) produced by a combination of physical discontinuities between compositionally differing bands and a preferred orientation of mineral grains (Hobbs, Means and Williams, 1976). It is a product of deformation but often coincides with the original S surface. Hence the planar fabric developed in this area can be often designated as S_0/S_1.

5.8.1 S_0 fabric

S_0 bedding surfaces are revealed by calc-silicate bands and sedimentary structures. All these primary features have their enveloping planes parallel to the regional foliation, thereby substantiating the S_0/S_1 fabric. In the absence of such features, S_0 is rarely seen but it is hinted at in the alternations of semipelitic and semipsammitic units so characteristic of the area which may reflect compositional differences between individual beds in the original sediments. These are almost everywhere parallel to the S_1 fabric.

However, in the hinges of isoclinally folded calc-silicates, S_0 and S_1 are clearly discordant. Only on one other occasion was S_0 recorded in the field, where a dominantly pelitic rock contained a psammitic band which had a clear

angular discordance with the foliation. In thin section, aligned biotite and muscovite grains define the foliation (S_1) in the pelitic unit and they have been crenulated by later folding. In the psammitic band, rarer micas still outline a planar element which is sub-parallel to both the S_1 foliation and the S_0 boundary. This sample is thought to illustrate the refraction of the foliation caused by a difference in competence between the bands.

Two additional samples may show evidence of S_0 in thin section, both as quartz inclusions in garnets. In both cases there is a tripartite division based on inclusion size. In sample 6210, a white calc-silicate band with the paragenesis quartz-garnet-hornblende-clinozoisite-andesine, the rim of the garnet contains inclusions ranging up to 0.15 millimetres in diameter. The centre band has sizes up to 0.01 millimetres and the remaining division is relatively inclusion free (Plate 32). This arrangement is mirrored in sample 721, the garnet occurring in a pelitic band within a thin (<10 centimetres thick) quartzite. For these inclusions to represent original quartz-rich or poor bands there must have been little or no metamorphic segregation and static garnet growth. In both examples, the boundaries between inclusions show a slight angular discordance with the S_1 fabric.

5.8.2 S_1 fabric

Within the Killin area, there is no evidence for the existence of the major folds with which the S_1 tectonic fabric may be associated. However, the mechanism which produced S_1 strain and possible sliding to the north-

Plate 32 Three-fold division of garnet based on inclusion size

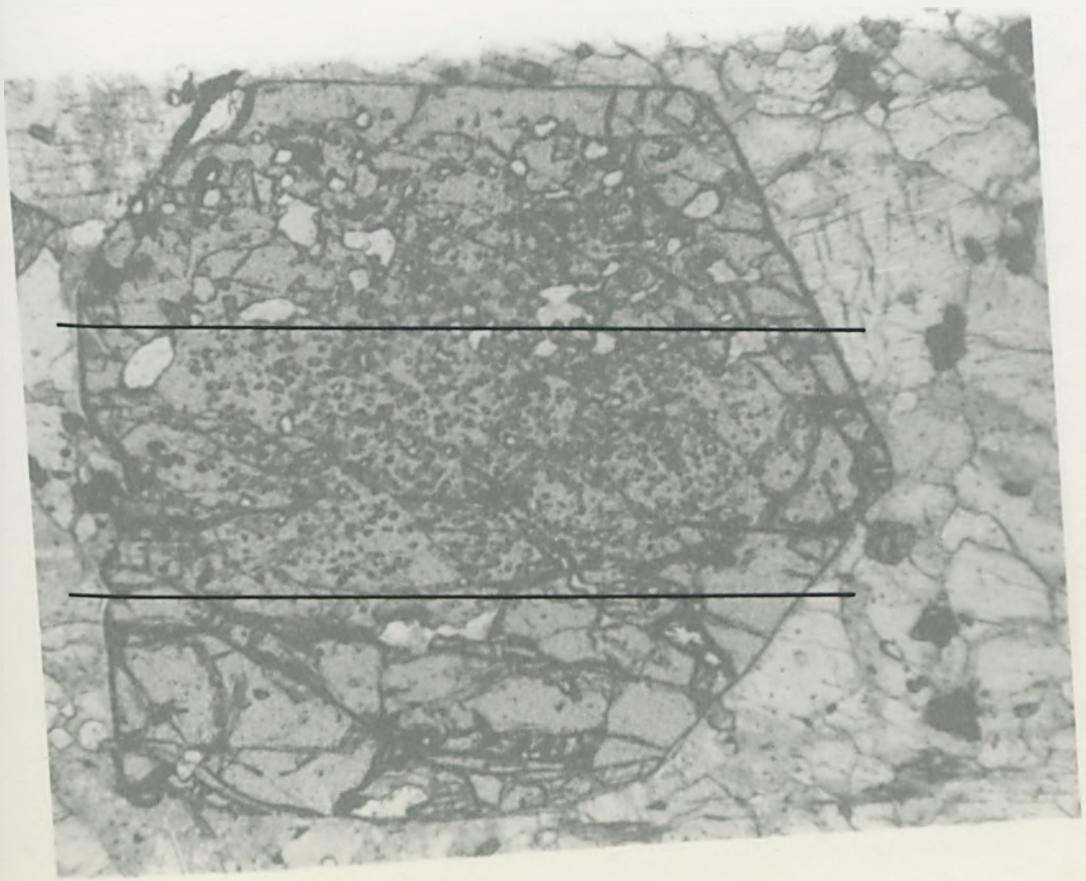

west (Parson,1979) and south (Haselock,pers.comm.) may also have been responsible for the regional foliation. No major stratigraphic inversion or recumbent folds were revealed to exist within the Killin area.

Microscopic: In pelitic and semi-pelitic schists the foliation is defined by platy mica grains both in hand specimens and thin section. In more quartzose semi-pelites micaceous laminae alternate with quartzose bands, the latter containing elongate quartz grains with length to breadth ratios reaching 6. In psammites the foliation is less evident but examination of thin sections reveals alignment of mica crystals and slight parallelism of the long axes of quartz grains. In all lithotypes, early garnets form augen structures within the S_1 foliation but in few cases are any distinctive quartz inclusion trails developed. Where they are visible, straight trails are discordant to the S_1 fabric and provide further evidence for the S_0 fabric.

In calc-silicate bands prismatic amphibole, and in many cases tabular clinozoisite, delineate the S_1 fabric.

Mesoscopic: The foliation varies in direction about two dominant trends, namely northeast-southwest and northwest-southeast. A contoured stereographic plot of poles to 1280 foliation planes (Figure 31) shows most of the readings to be in the north-westerly quadrant with a subsidiary cluster in the south-easterly quadrant. This indicates the dominance of the northeast-southwest trend but division into four sub-areas (Figure 32) outlines the trends in more detail and affords evidence of the effects of later folding episodes.

Sub-area one (Figure 33) shows the predominance of

Figure 31 Contoured stereographic plot of poles to 1280 foliation planes
(North point is marked by vertical line)

Contours at 0.5, 1, 2, 3, 4 and 5%

Figure 32 Division of area into foliation sub-areas

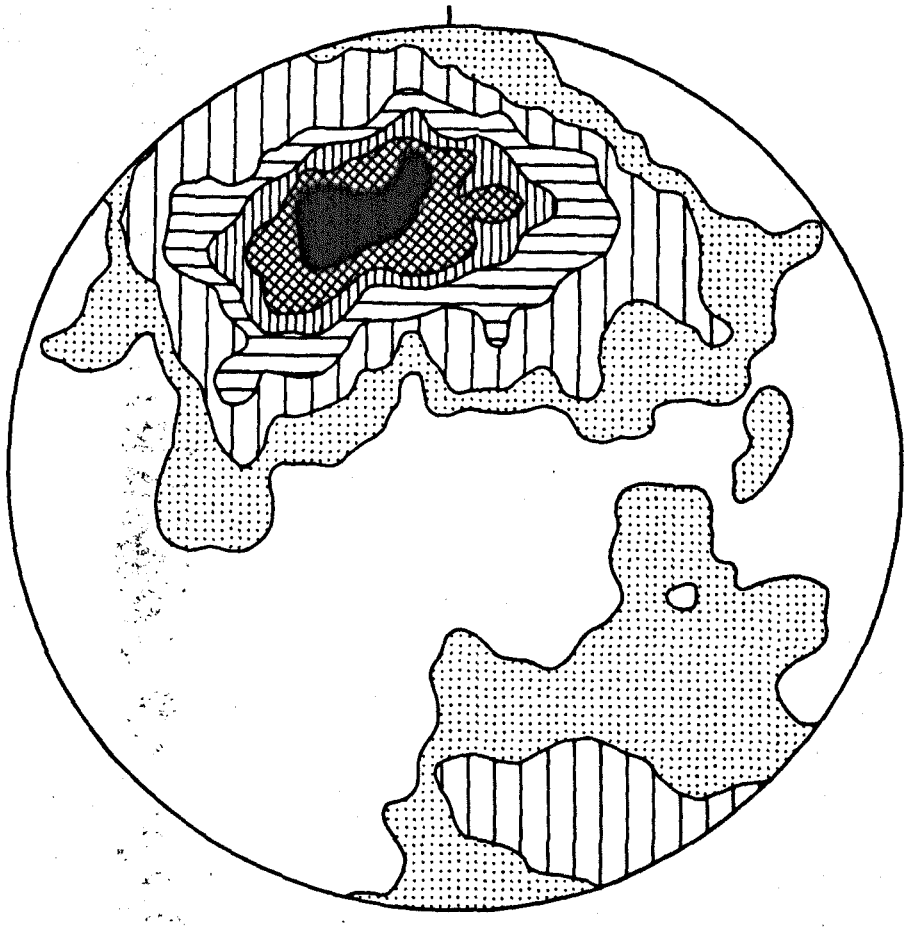

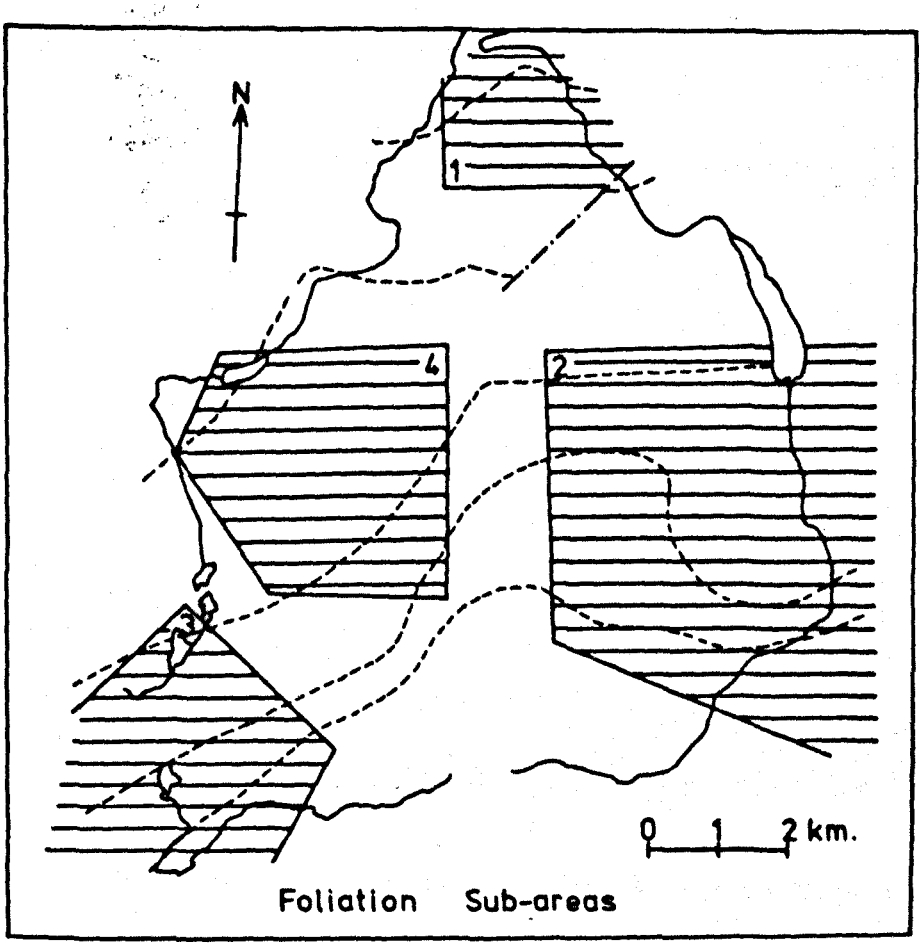
N
1
2
4
0 1 2 km.
Foliation Sub-areas

Figure 33 Contoured stereographic plot of poles to foliation planes in Sub-area 1
(North point is marked by vertical line)

Contours at 2, 4, 6 and 8%; n=88

Figure 34 Contoured stereographic plot of poles to foliation planes in Sub-area 3
(North point is marked by vertical line)

Contours at 1, 3, 5 and 6.5%; n=153

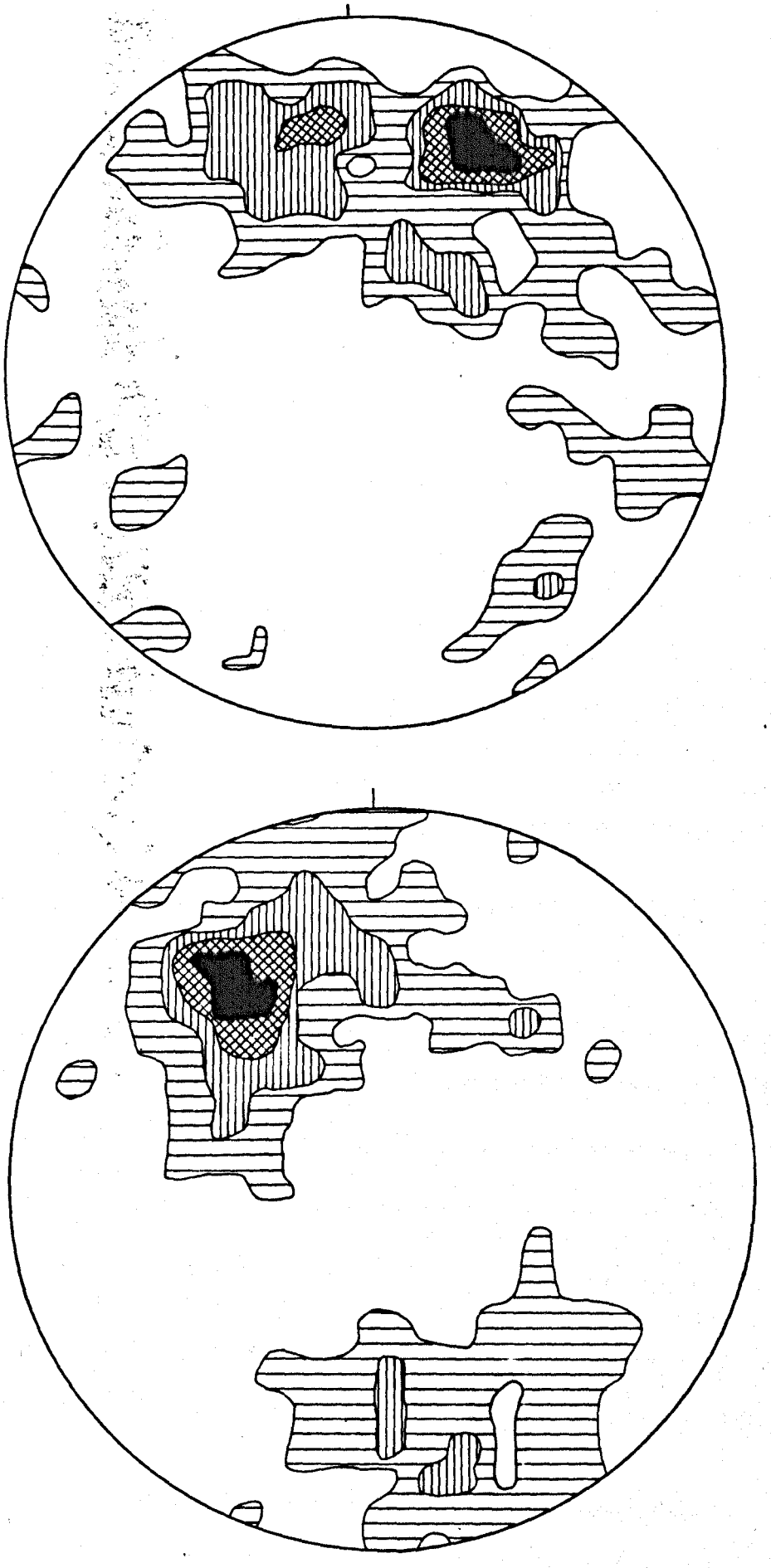

southerly and south-westerly dips producing a girdle, the axis of which corresponds to the F_3 direction. Sub-areas three and four (Figures 34 and 35) show a similar distribution but with a dominant south-easterly dip and the former shows some bimodal distribution about the F_3 axial trend. A combination of F_2 and subsidiary F_3 folds produces a rather more diffuse plot in sub-area two (Figure 36) with the foliation dipping east, south-east, and north-west about the F_2 folds, and also south-west about the F_3 structures.

5.8.3 S_2 fabric

The development of an S_2 fabric is very weak, being limited to a few occurrences scattered throughout the area. Approaching the hinge zone of folded white calc-silicate bands, prismatic hornblende crystals are aligned parallel or sub-parallel to the axial plane of the fold. However, due to the competent nature of individual calc-silicates this does not produce a strong penetrative fabric.

Folds in psammitic and pelitic lithologies also show a very weak fabric which is best developed in pelitic bands. The more psammitic bands show a poor fracture cleavage with subsequent cleavage refraction into more pelitic bands.

5.8.4 S_3 fabric

This is the dominant of all the minor fabrics developing an axial planar or sub-axial planar element to open F_3 crenulate folds. Although associated with some large folds, the crenulations are small scale (λ=1 millimetre to 15 millimetres) and occasionally, a good crenulation

Figure 35 Contoured stereographic plot of poles to foliation planes in Sub-area 4
(North point is marked by vertical line)

Contours at 1, 3, 4.5, 6 and 7.5%; n=190

Figure 36 Contoured stereographic plot of poles to foliation planes in Sub-area 2
(North point is marked by vertical line)

Contours at 1, 3, 5 and 7%; n=205

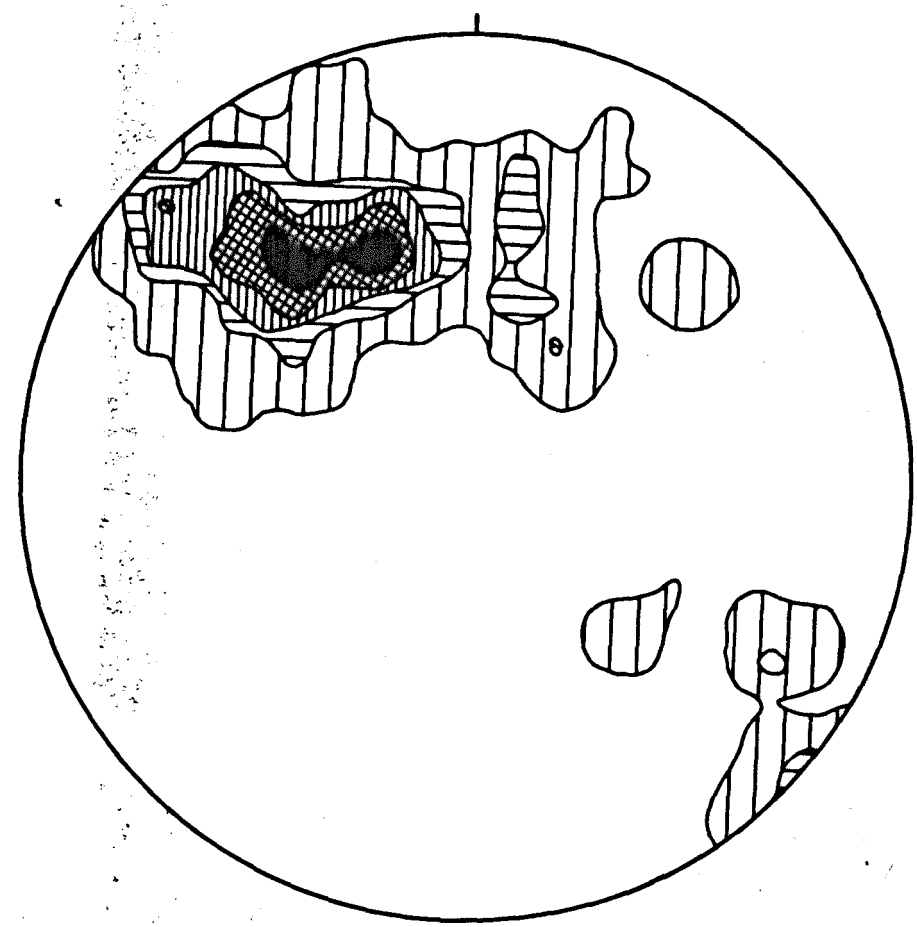

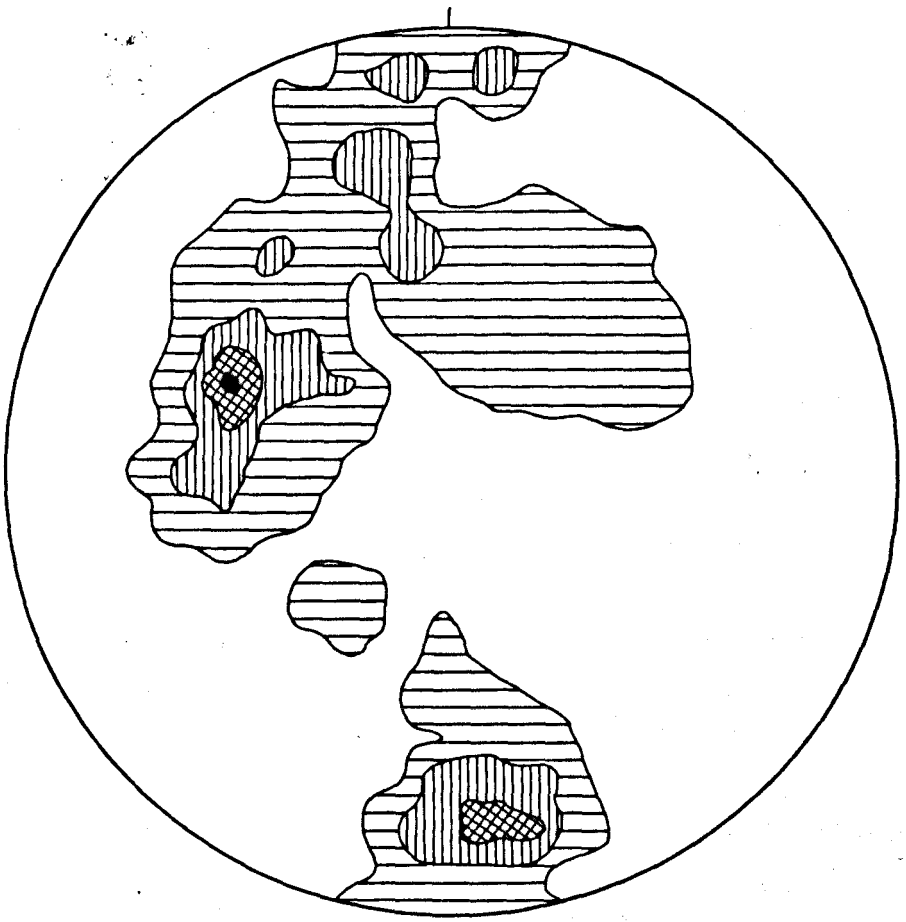

cleavage is developed due to transposition of the S_1 foliation. The dominantly asymmetric crenulations are found in the more finely banded or intensely foliated units. Plate 33 shows the crenulations and a developing crenulation cleavage in a semi-pelitic outcrop. Micas of the S_1 fabric are folded and fractured about F_3 profiles and are sometimes recrystallised and realigned along the crenulation or strain-slip cleavage planes, indicating both mechanical rotation and growth. The crenulation cleavage and associated axial planes dip predominantly to the south-east.

The crenulation cleavage consists of planar to subplanar domains of orientated micas, elongate quartz grains and opaque minerals which produce a parting in the rock. The planes coincide with the limbs of microfolds (crenulations) and constitute zones of mineral orientation and growth. The formation of the cleavage is dependent upon the existence of orientated flaky minerals, subsequently folded (Gray,1977).

Figure 37, taken from a thin section, illustrates crenulations and the associated fabric produced in a semi-pelitic schist. Developed by buckling of the fine mica layers (Cosgrove,1976), there is an associated redistribution of minerals (op.cit.) to produce zonal crenulation cleavage (Gray,1977). The intermediate cleavage trace in Figure 37 consists of, in two dimensions, a triangular area where predominantly muscovite and biotite lie at a high angle to the cleavage trace. This feature, the sub-parallel nature of the cleavage traces and their zonal, rather than discrete nature (op.cit.), suggests that this particular example is at a relatively early stage in its development.

Figure 37 Microcrenulation with development of S_3 fabric

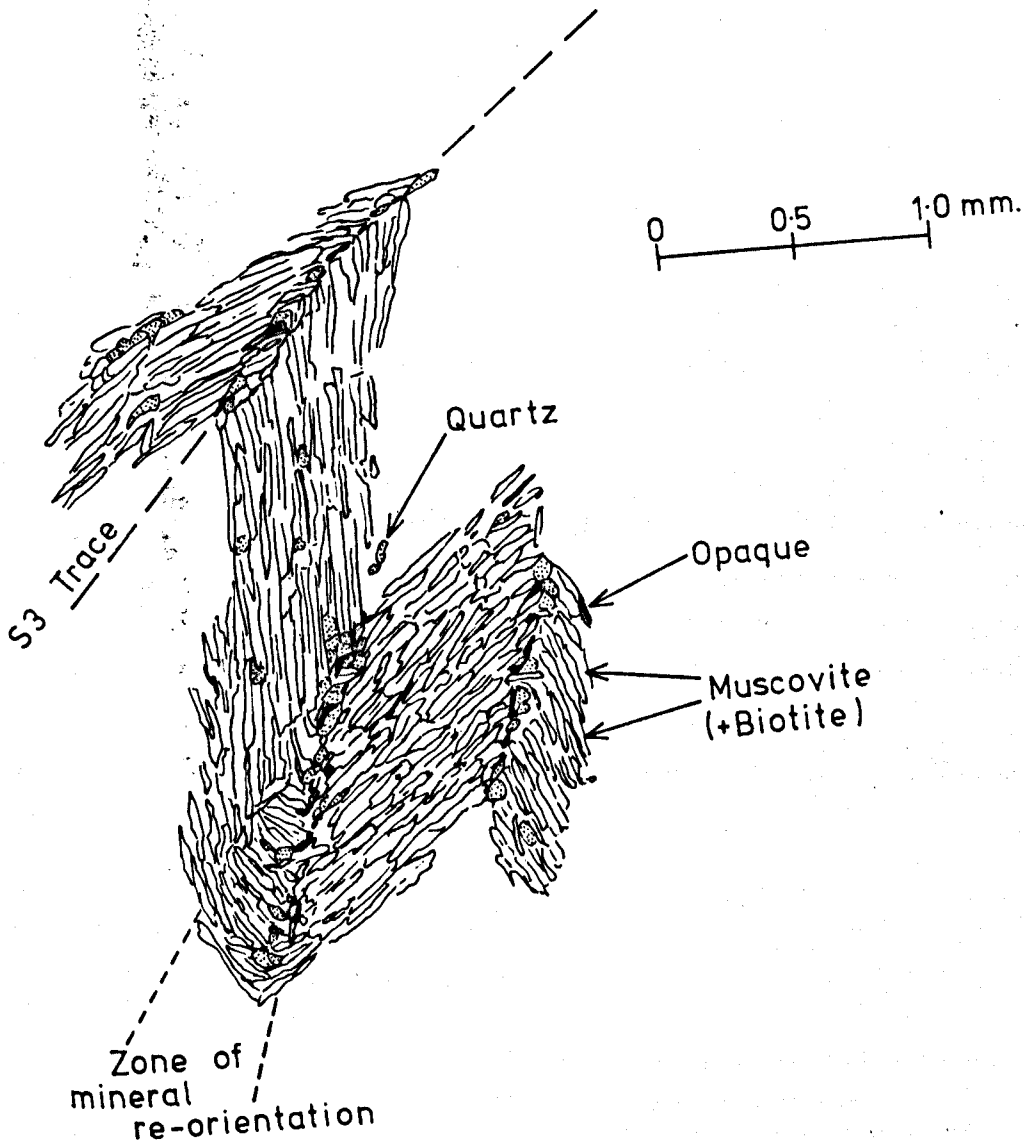
0
0·5
1·0 mm.
Quartz
Opaque
Muscovite
(+Biotite)
S3 Trace
Zone of
mineral
re-orientation

Plate 33 Crenulations and developing crenulation cleavage

5.9 Jointing

Systematic joints (Price,1966) are developed throughout the area. Although seen in all lithologies they are concentrated in the more competent quartzite and psammite bands. The thicker white calc-silicate bands also exhibit good minor jointing.

The majority of the joints appear to be related to the later F_4 phase of warping (see Sections 5.2 and 5.3.4). The main trends are outlined below (see also Figure 38):

165-180° ac joints

075-090° bc joints(longitudinal)

015-030° }
045-060° } shear joints
105-120° }

The shear joints tend to produce a cluster with the 015-030 direction being dominant. Sets trending 045-060 may be related to the late stage northeast-southwest faulting.

Many joints are vertical or sub-vertical and few possess a dip less than 65°, the average being 72°. There is some late chloritisation of micas along joint planes and epidote is also seen within areas veined by the granites.

Figure 38 Joint rose diagram (for metasediments)

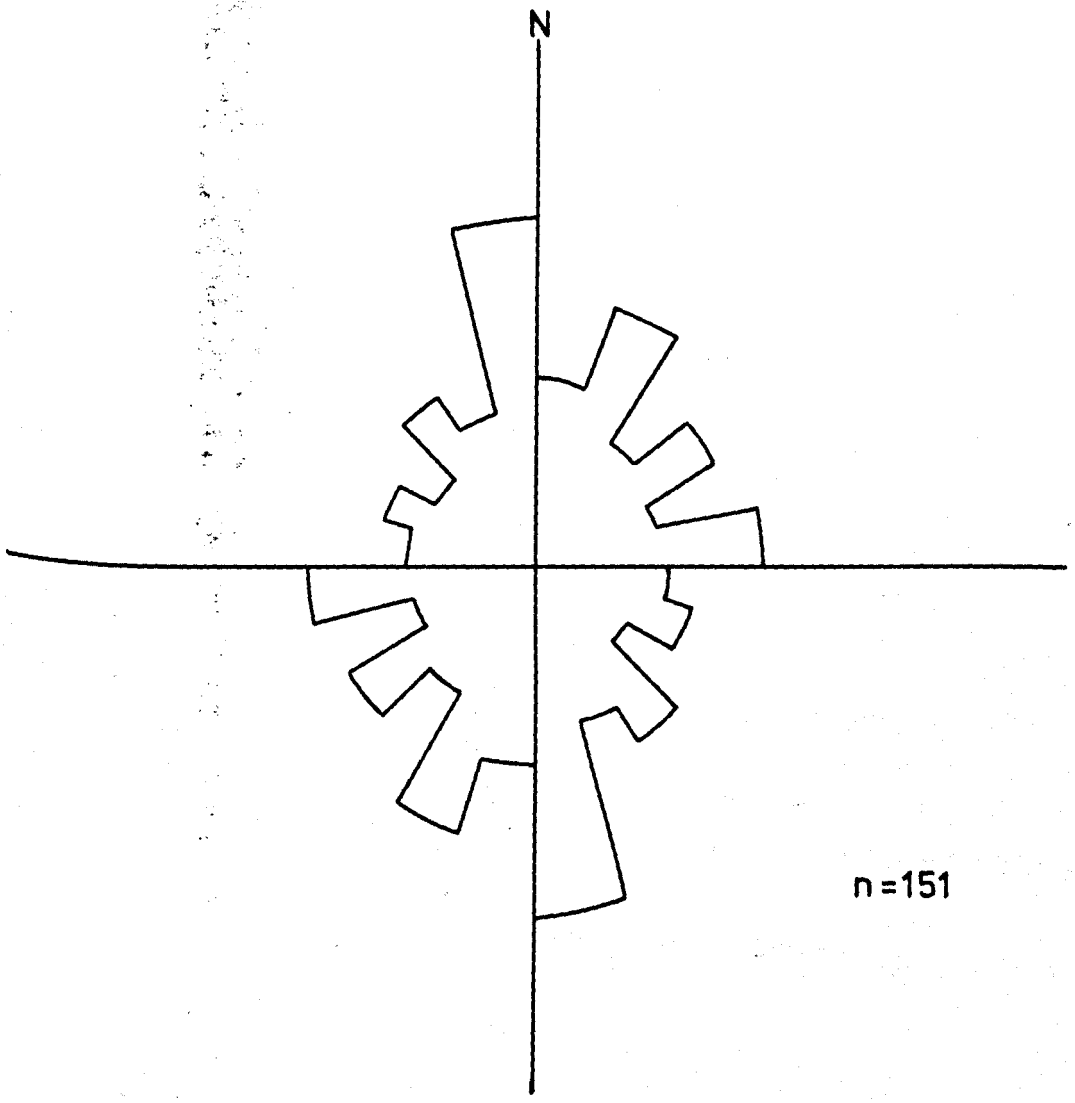
N
n=151

5.10 Faulting

Minor faults with displacements of two or three metres occur throughout the area. They are easily distinguished by the displacement of distinctive bands, such as white calc-silicates, which can be used as markers. However, the gradational lithologies render the location of major faults difficult.

One major fault (the Glen Doe fault, in the northern part of the area) displaces the boundary between the Glen Doe and Knockchoilum semi-psammites. Difficulties arise because only one marker is available from which the movement can be estimated. There is an apparent sinistral movement with a displacement of 1900 metres, although some vertical displacement also occurred. The fault appears to die out rapidly to the north-east.

The trend of most faults in the area, and to the north (Parson, 1979) is northeast-southwest, parallel to the Great Glen. These form part of the general fault pattern (Johnson and Frost, 1977) in the Central Highlands. Shear planes in the Newer Granites also possess this trend and a dominantly strike-slip movement, analogous to that of the Great Glen fault, is implied. It is also suggested that faulting continued after intrusion of the granite masses, dated at approximately 400 million years (see Section 6.6).

CHAPTER SIX-IGNEOUS ROCKS AND AMPHIBOLITES

6.1 Introduction

The Newer Granites (Read,1961) intrude the Killin area: the Foyers granite in the north and the Allt Crom granite in the south-east. The Corrieyairack granite also approaches within five kilometres of the southwestern corner of the area (Figure 39).

Figure 40 shows the subdivision into areas which is used todescribe the intrusions. It is difficult to map contacts precisely, hence those illustrated on Figure 40 are approximations. Field occurrences are thus limited to dykes and sheets, although the scale may differ considerably between and within each group.

Granitic intrusions are the most common, with subsidiary granodiorite and adamellite and rare tonalites. The relative abundance and the petrography of these rock types is similar in each sub-area, hence their descriptions are contained in one section. Classification of the intrusions is based on the distinctions of Carmichael, Turner and Verhoogen (1974), summarised below:

GRANITE:potash feldspar > plagioclase:biotite$\pm$hornblende or muscovite

GRANODIORITE:plagioclase > potash feldspar:biotite and/or hornblende

ADAMELLITE:potash feldspar and plagioclase subequal:biotite and/or hornblende

TONALITE:plagioclase:biotite and hornblende

Figure 39 Newer Granites bordering the Killin area

Figure 40 Four sub-areas affected by intrusive igneous rocks (as described in text)

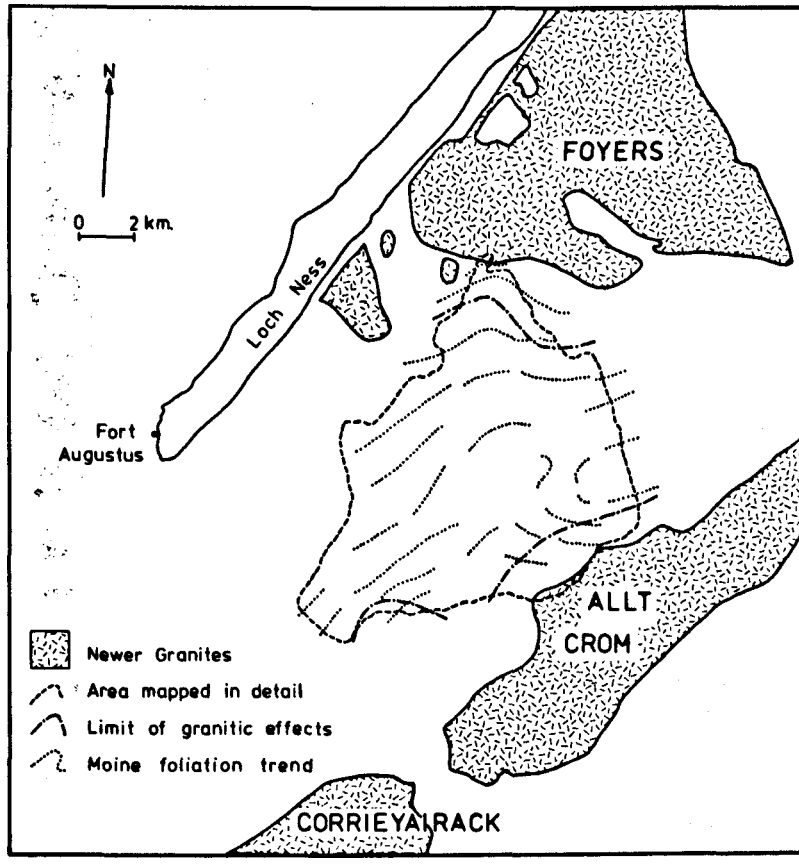
N
0 2 km.
FOYERS
Loch Ness
Fort Augustus
ALLT CROM
CORRIEYAIRACK
Newer Granites
Area mapped in detail
Limit of granitic effects
Moine foliation trend

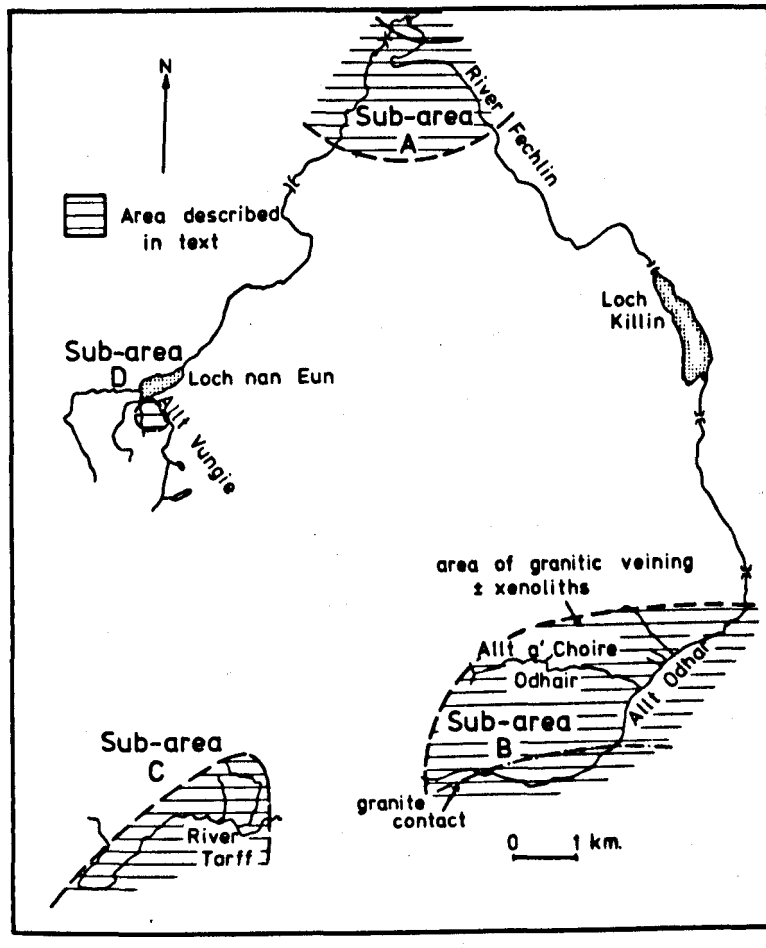
N
Area described in text
Sub-area A
River Fechlin
Loch Killin
Sub-area D
Loch nan Eun
Allt Vungie
area of granitic veining ± xenoliths
Allt a' Choire Odhair
Allt Odhar
Sub-area B
Sub-area C
River Tarff
granite contact
0 1 km.

6.2 Field Occurrence

6.2.1 Sub-area A

Figure 41 shows the distribution and trend of intrusions in sub-area A. Most are exposed in the River Fechlin. Broad granitic dykes occur in the northern part of the area, traceable for up to 100 metres and reaching 50 metres in width. These dykes are sheared along a north-east to south-west direction which imparts close joints to the granite. Secondary epidote and chlorite have developed along the joint planes.

Further south small dykes and sheets occur, commonly as thin (5 to 20 centimetres) homogeneous veins with sharp contacts. Little planar fabric or crystal orientation is developed, although larger bodies do possess a lensoid appearance. Since the fabric is poorly developed, it is unlikely to be the distensive foliation seen at Foyers (Marston,1971) but may be sheet jointing (Price,1966).

The larger granitic dykes contain metasedimentary inclusions (Plate 34) with randomly oriented semi-pelitic and semi-psammitic blocks reaching 25 centimetres in length. Within the 'granite contact' (Figure 41) larger metasedimentary xenoliths exist but it is not possible to completely determine their boundaries.

Inclusions usually retain their original shape although occasionally the 'splintered' end of a semi-pelitic block shows incipient assimilation with an increase in quartz and orthoclase content. Mafic schlieren are not developed.

Both granodiorite and adamellite dykes occur but it is not possible to determine relative ages from the observed field relationships.

Plate 34 Metasedimentary inclusions in granitic dyke

Plate 35 Euhedral sphene crystals in granitic sample

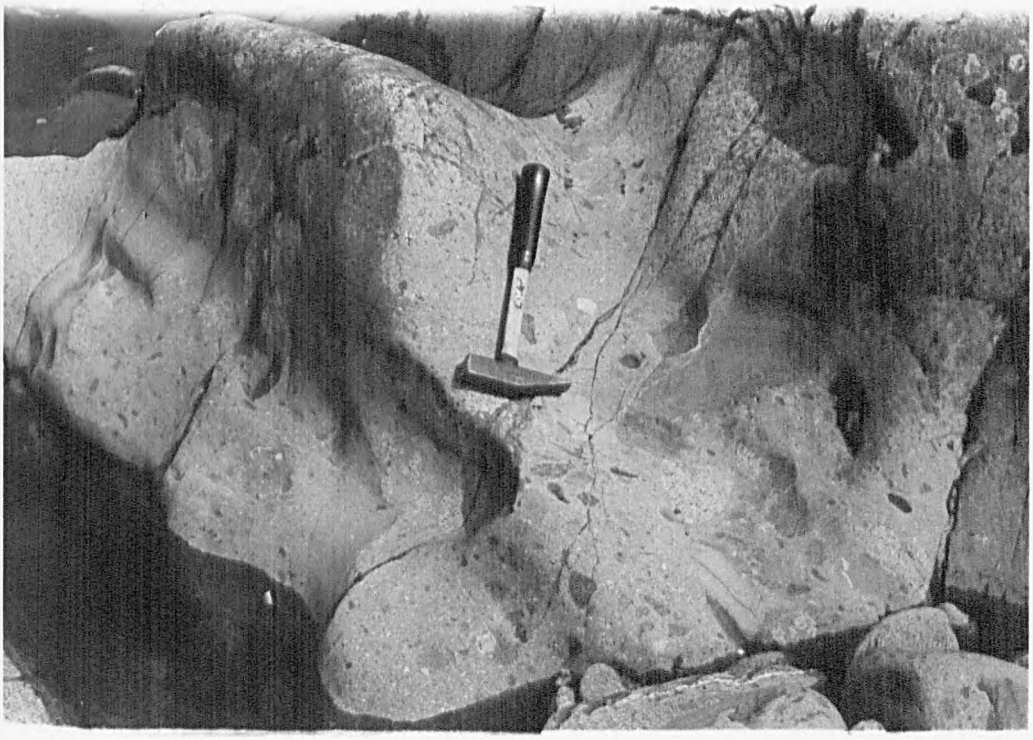

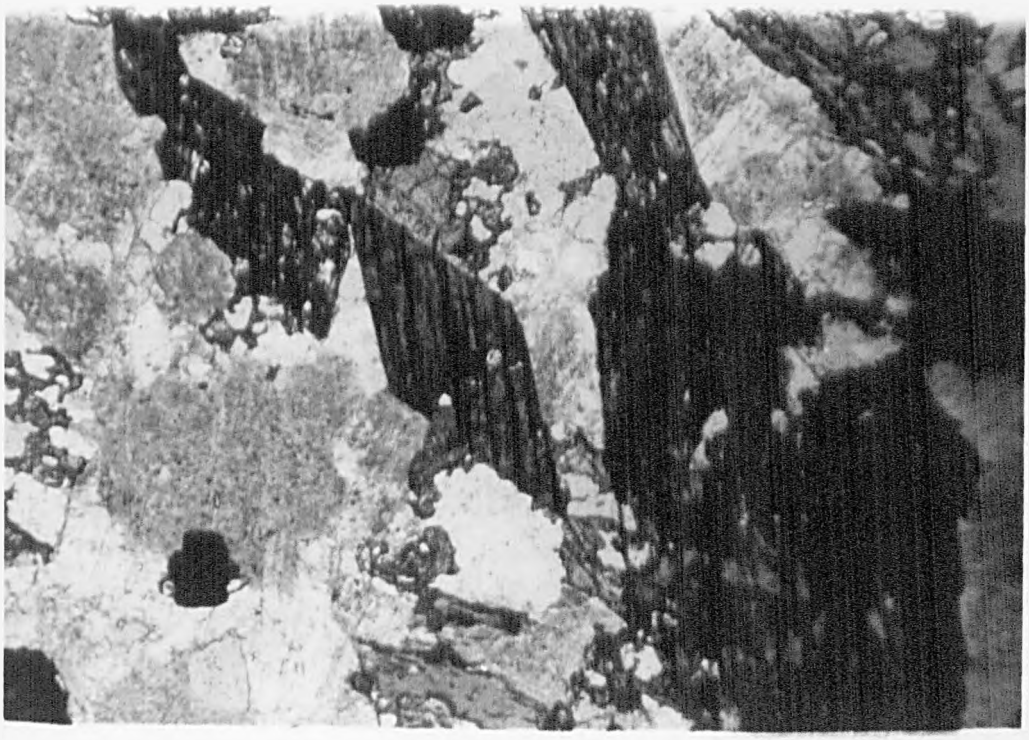

Figure 41 Igneous elements in Sub-area A

Figure 42 Igneous elements in Sub-area B
('contact' illustrated in Figure 40)

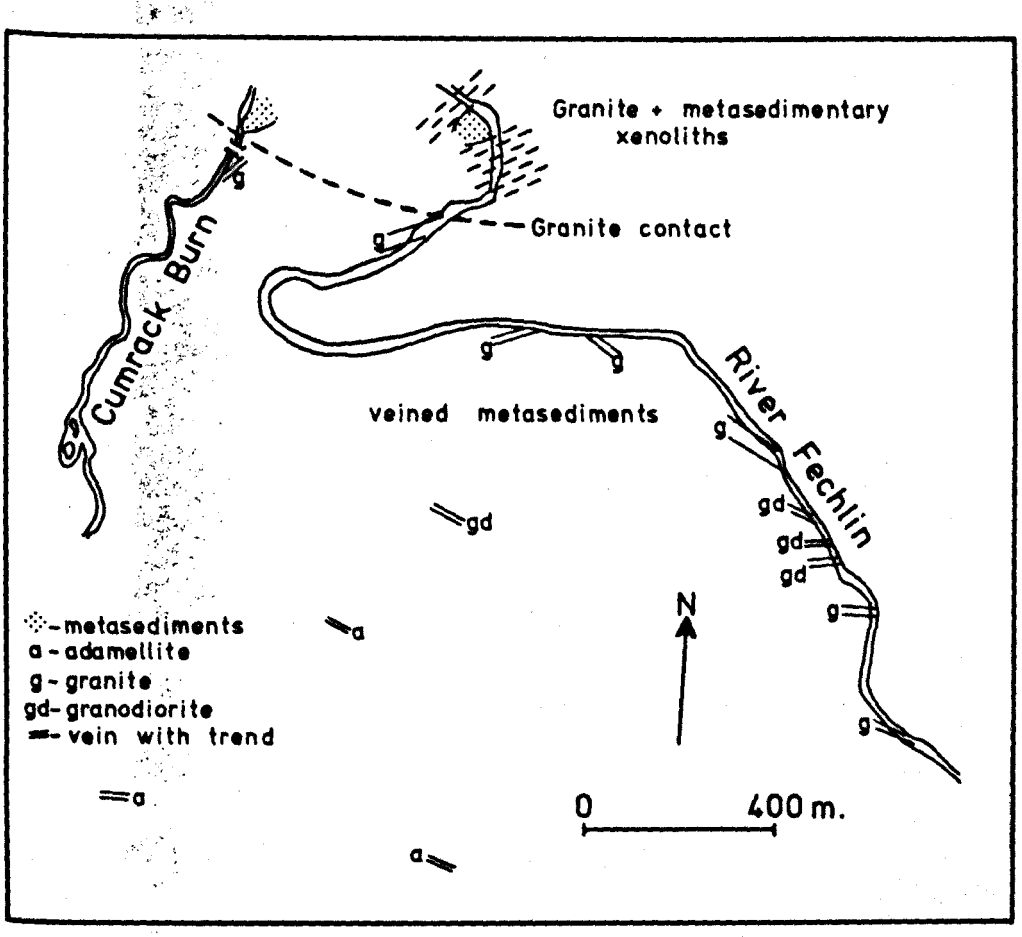
Granite + metasedimentary xenoliths
Granite contact
Cumrack Burn
River Fechlin
veined metasediments
gd
N
0
400 m.
-metasediments
a - adamellite
g - granite
gd - granodiorite
- vein with trend

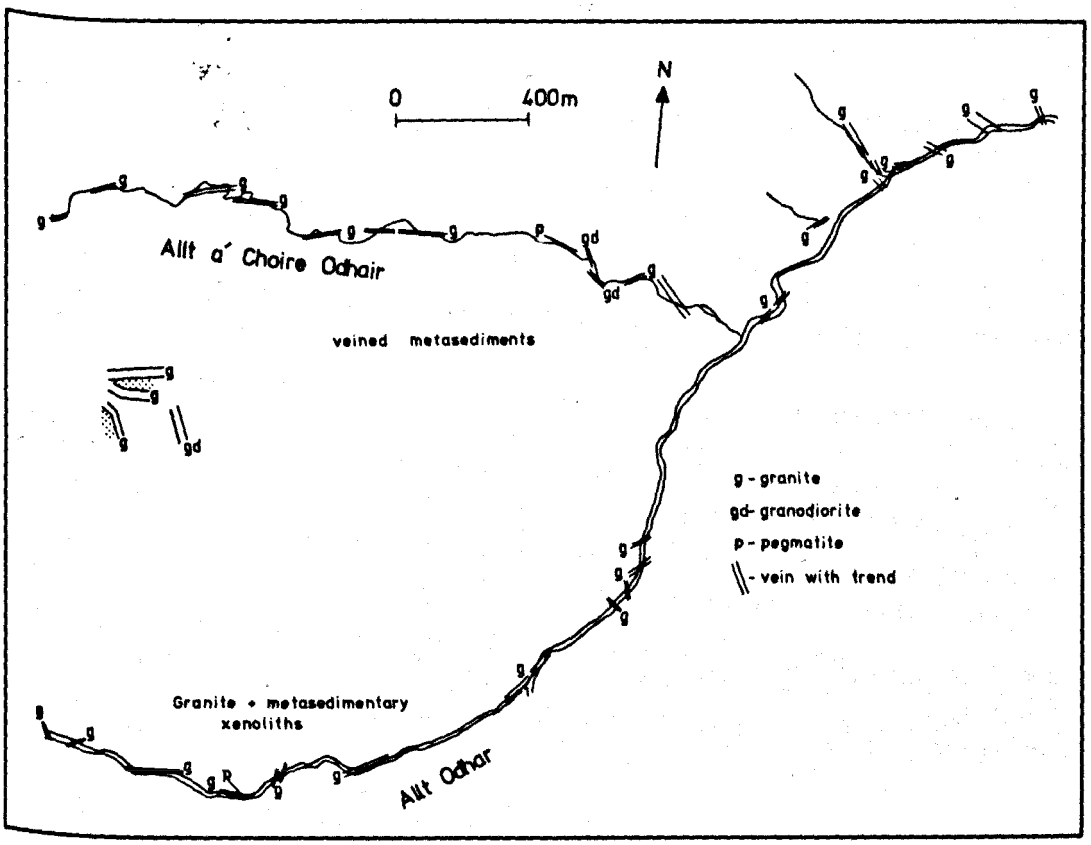
0
400m
N
Allt a' Choire Odhair
veined metasediments
g - granite
gd - granodiorite
p - pegmatite
- vein with trend
Granite + metasedimentary xenoliths
Allt Odhar

6.2.2 Sub-area B

The Allt Crom granite is exposed in this sub-area, but exposure is generally very poor. Where discernible the majority of exposures are dykes (Figure 42) and all but three are granitic. The remainder comprise two granodiorites and one microtonalite, and all occur as dykes.

All dykes vary from 50 centimetres to 10 metres in width and occur with concordant granitic sheets up to one metre thick, all showing sharp contacts (see Section 6.2.5). These intrusions have disrupted the regional foliation in the vicinity and have feldspathised the host lithologies. Larger dykes contain numerous xenoliths (>2.5 metres long) and with the granitic sheets tend to isolate large rafts of host lithologies (>10 metres in length). This is an area of veined metasediments noted originally by Anderson (1956), in which the host rocks first lose their orientation.

The larger dykes and sheets possess joints with a dominantly north-east to south-west trend. Two trends, 030 and 080 are defined by plotting on a rose diagram (Figure 43).

Pegmatites also occur in this sub-area, in the Allt Odhar and the Allt à Choire Odhar. These irregular, thin (<7 centimetres thick) veins contain quartz, muscovite, orthoclase and black tourmaline in approximately equal proportions.

6.2.3 Sub-area C

No major intrusions are exposed in this area- it consists of a concentration of dykes. Intrusions are all granitic, forming both dykes and sheets in exposures along the River Tarff. The exact northerly extent of the granitic

Figure 43 Joint rose diagram for granitic dykes and sheets

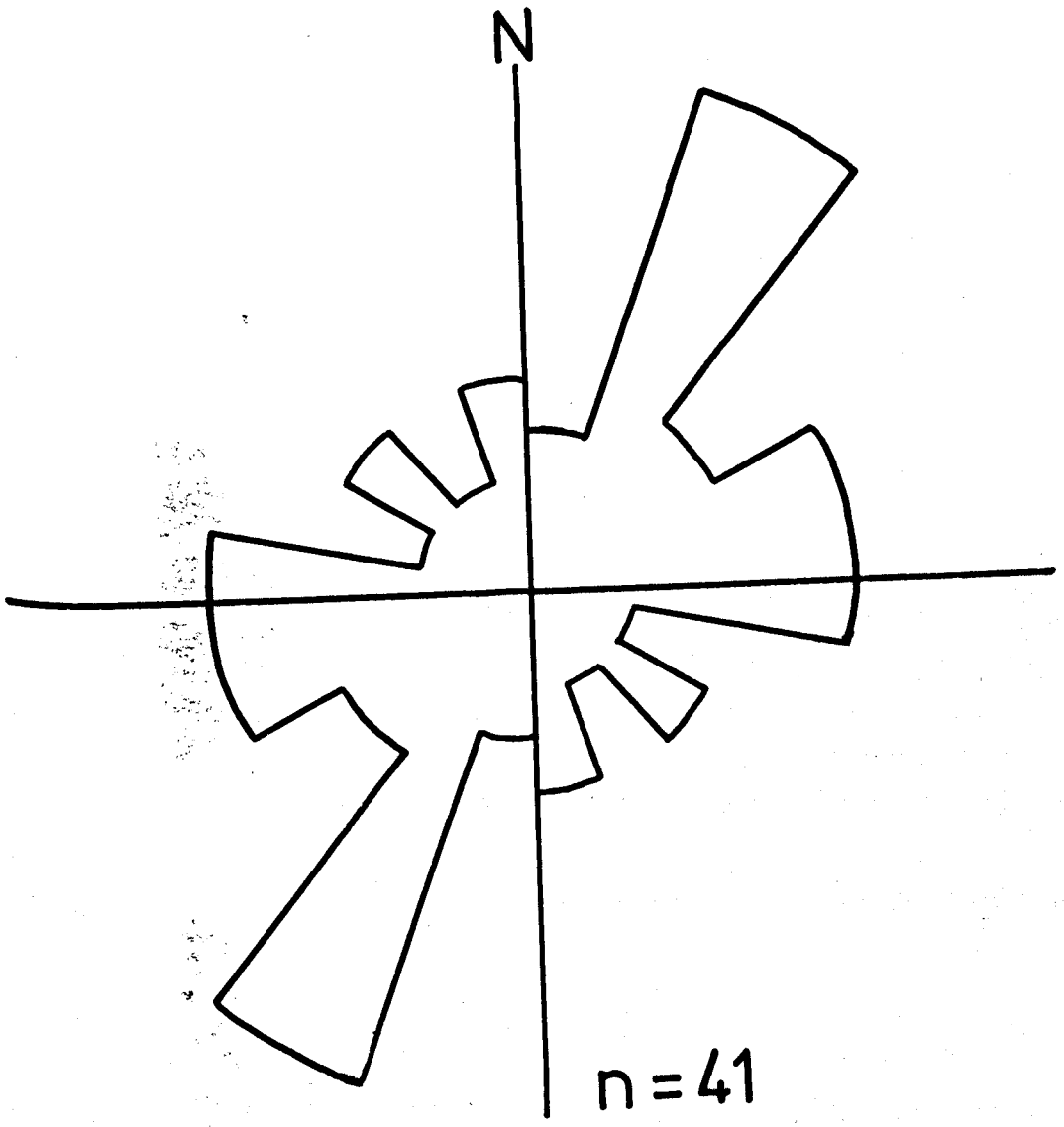
N
n = 41

intrusions is unknown due to lack of exposure but is probably limited since previously mapped granite sources are some distance away. Although it may be related to the Corrie-Yairack granite (op.cit.) to the south, it seems more likely that it is an offshoot of the closer Allt Crom granite.

The granite dykes reach 18 metres in width and granitic sheets up to one metre thick may be traceable for 45 metres. Joints are well developed and show two dominant trends at 055 and 160.

6.2.4 Sub-area D

In sub-area D a six metre thick dyke of dark red biotite granite occurs at the south-western end of Loch nan Eun (Figure 40). It exhibits sharp contacts and surrounding metasediments show feldspathisation. This occurrence is closest to the westerly offshoot of the Foyers granite (Figure 39) and this seems to be the most likely source.

6.2.5 Intrusion contacts

In all cases, intrusion contacts are sharp and there is no melting of country rock, except where small inclusions are contained within intrusions. This suggests that intrusion post-dated metamorphism as well as deformation in these rocks.

It is not possible to determine the precise relationship between the numerous dykes and the two major intrusions due to lack of suitable outcrop, but it seems likely that the dykes are offshoots of the larger bodies.

6.3 Petrography

Table 6.1 shows average modal analyses of selected rock types from sub-areas A and B.

6.3.1 Granites

The granites contain quartz either as large grains with undulose extinction and sub-grains (where the original grain has 'fractured'), or close-packed masses of smaller grains on boundaries between K-feldspar grains. Larger grains (up to 4.0 millimetres long and 2.0 millimetres wide) show curved to lobate boundaries, whilst the smaller ones form sub-rounded grains with an average diameter of 0.1 millimetres.

Plagioclase occurs predominantly as rectangular blades often with slightly rounded boundaries. Grains reach 3.5 millimetres in length and 1.5 millimetres in width and both multiple (albite) and combined Carlsbad-albite twins are common. Plagioclase compositions (Table 6.1) are determined using the symmetrical extinction method of Michel-Levy for multiple twins, and the combined twin method of Wright (1911) for Carlsbad-albite twins. A few untwinned grains also occur. Some grains are zoned but the cores are totally sericitised rendering determination of composition difficult. Rare anti-perthitic textures are present.

K-feldspar is represented by orthoclase, with subsidiary microcline, primarily in sub-area B. Rounded anhedral grains of orthoclase are often clouded by incipient alteration but Carlsbad twins are still discernible. Grains reach a maximum of 5 millimetres in length and 2 millimetres in width and some contain quartz and plagioclase inclusions. Myrmekitic

	1	2	3	4	5	6
Quartz	49.8	48.2	34.4	21.6	39.9	40.6
Plagioclase	13.6	23.0	15.2	29.8	15.0	25.1
An value	31	32	28	34	27	34
Orthoclase	23.9	25.6	29.1	16.0	30.7	23.5
Microcline	--	1.5	--	--	8.5	4.3
Epidote	--	--	4.0	11.9	tr	--
Muscovite	1.2	tr	tr	--	tr	0.4
Biotite	7.5	0.3	0.2	--	4.6	1.5
Hornblende	--	--	0.2	--	--	--
Chlorite	3.2	0.7	7.5	16.5	0.6	2.5
Opaques	0.4	--	2.3	0.1	0.5	1.9
Sphene	tr	tr	0.7	2.2	--	--
Apatite	tr	tr	tr	tr	tr	tr

Key: 1-granite of sub-area A

2-adamellite of sub-area A

3-sheared granites of sub-area A

4-sheared granodiorite of sub-area A

5-granite of sub-area B

6-adamellite of sub-area B

tr-trace

Table 6.1 Average Modal Analyses of Selected Igneous Rocks

intergrowths occur between adjacent grains of plagioclase and alkali feldspar by vermicular quartz intergrowing in plagioclase. Although several processes could be responsible for its formation (Phillips,1974), one of replacement seems most feasible.

Biotite is the dominant mafic mineral and often occurs as clusters associated with chlorite, both showing an undulation along their length. Biotite also occurs as small flakes some of which are rectangular, pleochroic from straw yellow to deep brown. Smaller flakes average 0.5 millimetres in length and may enclose thin 'slivers' of sphene measuring approximately 0.3 by 0.05 millimetres.

Opaque minerals consist of magnetite and haematite with very little pyrite. Scattered growths of ilmenite also occur, usually adjacent to magnetite or rimming sphene. Sphene occurs as isolated grains and is common in the sheared granites as euhedral crystals reaching 1.75 millimetres in length and 1.0 millimetre in width (Plate 35).

6.3.2 Adamellites

The adamellites are texturally very similar to the granites. Quartz occurs as large grains (3 by 2 millimetres) showing strained extinction, or as small grains forming aggregates. Some of the larger grains now comprise sub-grains. Quartz-quartz boundaries are dominantly lobate.

Plagioclase and alkali feldspar occur in approximately equal amounts and both contain scattered grains of sericite. Plagioclase often occurs as large grains (up to 4 by 1.5 millimetres) with Carlsbad-albite and some pericline twinning. Some grains also show normal zoning.

Orthoclase similarly occurs as large grains (up to 4

by 2 millimetres) or rounded grains with a diameter of 1.5 millimetres. Simple twins occur and zoning is apparent in a few grains. Lesser amounts of microcline occur as rounded grains (approximately 1.25 millimetres in diameter) exhibiting cross-hatch twinning and microperthitic textures.

Both muscovite and biotite are present, the former only as scattered flakes. Biotite is associated with chlorite and sphene and forms dark brown flakes with dark cleavage traces.

6.3.3 Granodiorites and tonalites

Quartz occurs in various grain sizes. Inequant grains show lobate boundaries (and are often associated with epidote) and small grains occur in thin crush zones between K-feldspar and epidote.

Plagioclase forms large grains (up to 4 by 2 millimetres) with albite twinning and some microfaulting of twin planes (Plate 36). Grains are commonly flecked with sericite. Some zoned anti-perthitic plagioclase occurs with a little micro-perthitic orthoclase. However, orthoclase occurs primarily as large (3 by 1.5 millimetres), slightly rounded grains with simple Carlsbad twins. Sericite flakes again produce a cloudy effect.

Epidote occurs in some samples, either as a 'web' associated with quartz or as small prisms forming aggregates and closely associated with chlorite. The epidote shows pleochroism from green to yellow and individual grains reach 0.4 millimetres in diameter. The chlorite is frequently adjacent to or enclosing calcite (see Section 6.4). Chlorite grains reach 3 millimetres in length and 1 millimetre in

Plate 36 Microfaulting of plagioclase grains

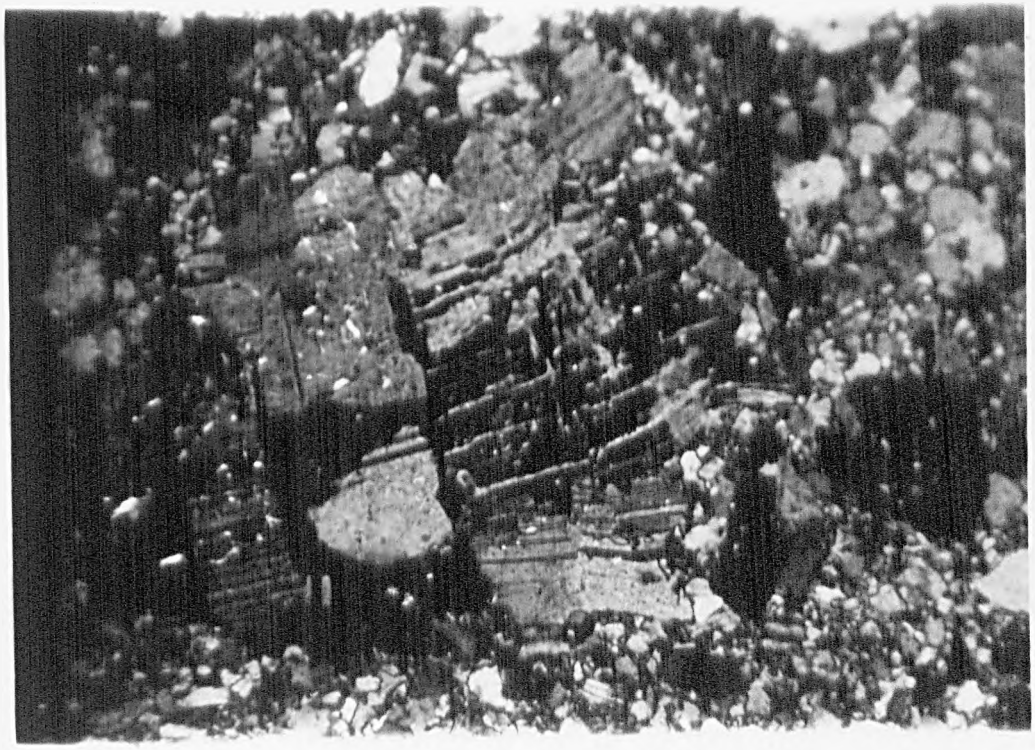

width.

Remaining components include sphene and opaque minerals. Sphene commonly forms rhombs reaching a length of 1.75 millimetres. Magnetite and pyrite usually form isolated grains (~0.2 millimetres in diameter), but are sometimes associated with sphene.

Tonalites do not form a very distinctive or common suite and therefore only brief mention is made here. Quartz occurs as predominantly small grains or subgrains, but larger grains do occur. Plagioclase is the commonest feldspar with subsidiary K-feldspar. Brown-green hornblende is present with biotite and a little magnetite.

6.3.4 Pegmatites

Pegmatites occur primarily in sub-area B and contain large (5 millimetres in length and 3 millimetres in width) quartz grains with undulose extinction and lobate boundaries. Muscovite occurs as large blades (6 millimetres x 4 millimetres) which may be kinked, and tourmaline (schorlite) occurs with cross-cutting fractures. Green-brown in thin section, the tourmaline contains quartz enclaves and either partially or totally encloses slightly perthitic K-feldspar. Small (0.7 millimetres x 0.4 millimetres) muscovite flakes are also included in the schorlite, the latter occurring as one crystal measuring 2 centimetres in length and 0.5 centimetres in width.

The pegmatites clearly cut the metasediments but their relation to the major intrusions is not apparent.

6.4 Shearing Effects

Physical effects of the shearing include microfaulting in plagioclase grains (Plate 36), and the production of 'micro-

crush' (mylonitic) zones. The zones reach 2 millimetres in width and 1 centimetre in length and contain small (< 0.02 millimetres) rounded grains of quartz, plagioclase, often with epidote, and late calcite (see Section 6.3.3). Some of the features, especially those seen in quartz, i.e. undulose extinction, subgrains and certain serrated grain boundaries, are analogous, if not compatible with the development of mylonitic characteristics (Bell and Etheridge, 1973).

The development of secondary minerals due to shearing is best seen in the granites of sub-area A. Biotite is almost completely absent and is replaced by dark green chlorite (penninite). Hornblende is also partially replaced by penninite and, closely associated with the latter, either partially or totally enclosed by it, are numerous grains of epidote. Individual rounded grains reach 0.5 millimetres in diameter but aggregates of prismatic epidote attain 1 millimetre in length and 0.75 millimetres in width and possess straight boundaries with some triple points. This latter feature suggests a relatively late formation under little stress.

Late veins of calcite are common and also present in very small amounts are tourmaline (dravite) and allanite, the latter occurring as small granules, pleochroic from pale brown to dark red-brown.

6.5 Marginal Effects

As previously noted (in Section 6.2.5), all dyke and sheet contacts are sharp, implying post-metamorphic intrusion. No new minerals are formed, but all lithologies show a hardening and feldspathization

(suggesting small-scale metasomatism) with an increase in orthoclase and quartz, producing a porphyroblastic texture. Small (< 5 centimetres long) pods of orthoclase and quartz are also formed and incipient recrystallisation is common.

Intrusions produce a disruption of the host-rock foliation which may be of the order of metres, depending upon the size on the intrusion. In thin section, the planar fabric delineated by biotite flakes is superceded by biotite flakes parallel to the contact and discordant to the earlier foliation, suggesting physical readjustment caused by the intrusion.

The lack of a thermal aureole on the larger granite contacts implies that the rocks in the Killin area may have been warm prior to intrusion, and that the country rocks may have been too Al-poor and Ca-rich for the formation of such minerals as andalusite and cordierite.

6.6 Ages of Intrusion

The potassium-argon ages which have been produced from the Newer Granites of this area suggest that emplacement occurred approximately 400 million years ago. Miller & Brown,(1965) and Brown, Miller & Grasty (1968) have produced the following ages:

Foyers Granite 404 ± 18 Ma (2 readings at different locations)

Foyers Tonalite 396 ± 18 Ma

Allt Crom Granite 404 ± 15 Ma

Foyers Tonalite 406 ± 8 Ma

Foyers Granodiorite 397 ± 8 Ma (2 readings)

Marston (1971) produced an emplacement order of tonalite, granodiorite and finally adamellite. The above figures would seem to confirm this and to fix the relative ages of the intrusions in the Killin area, although field evidence does not assist in elucidating the pattern.

6.7 Granophyre Suite

6.7.1 Occurrence

A suite of granophyre dykes occurs throughout the Killin area (Figure 44). These are distinguishable in the field by the occurrence of scattered mafic minerals set in a light coloured matrix. All samples are broadly granitic in composition with a predominance of orthoclase over plagioclase.

Hand specimens vary in colour from beige and grey to red and pink with darker mafic flecks. All intrusive contacts are discordant and abrupt but in some cases the granophyre does tongue into the country rock (Plate 37). The dykes vary in size from pods 2 metres square to dykes which average 10 or 12 metres in thickness and may reach 150 metres in length. Weathering of the lighter coloured samples produces an orange coloured hue which is distinctive and readily visible in the field.

All exposures are well jointed, commonly possessing three planes with one dominant and very closely spaced (< 2.5 centimetres) trending east-south-east/west-north-west. Figure 45 shows the dominant joint directions trending 025°, 085° and 145°. The first two trends are almost parallel to those in the granitic dykes in sub-area B.

The intrusion of these granophyres is late since their

Figure 44 Granophyre occurrences in the Killin area

Figure 45 Joint rose diagram for granophyres

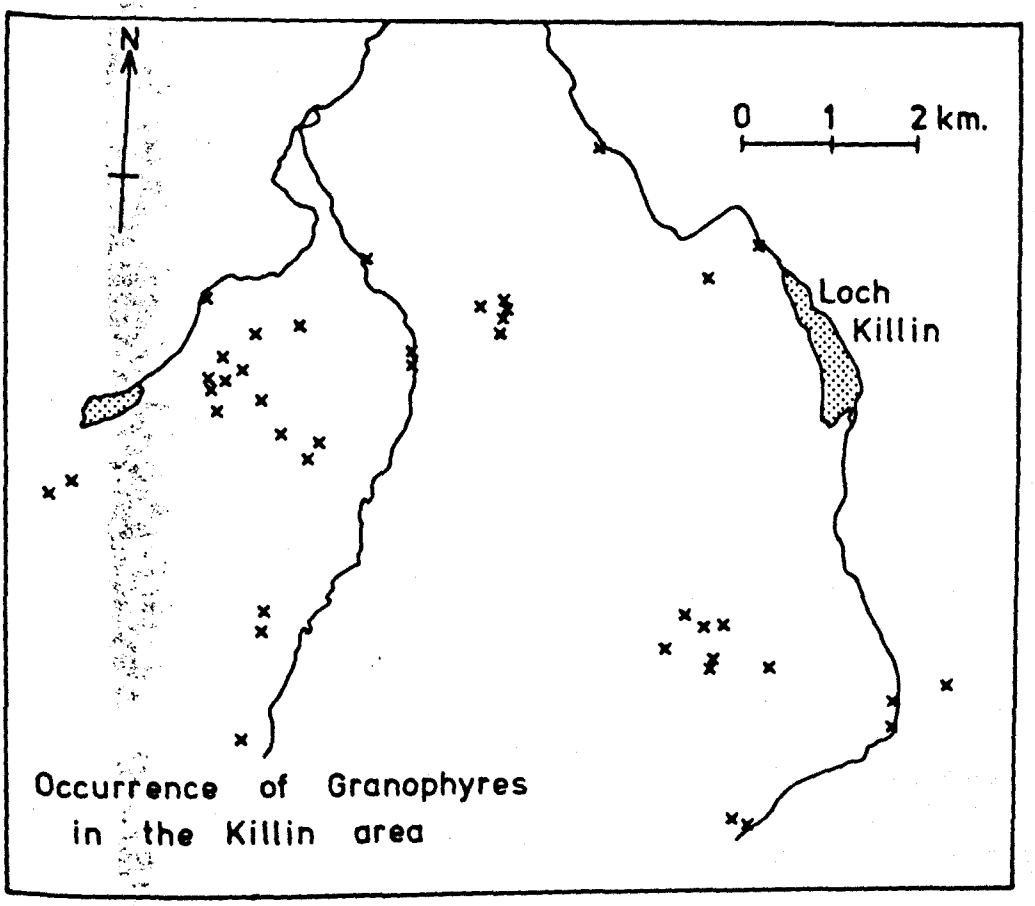

Occurrence of Granophyres in the Killin area

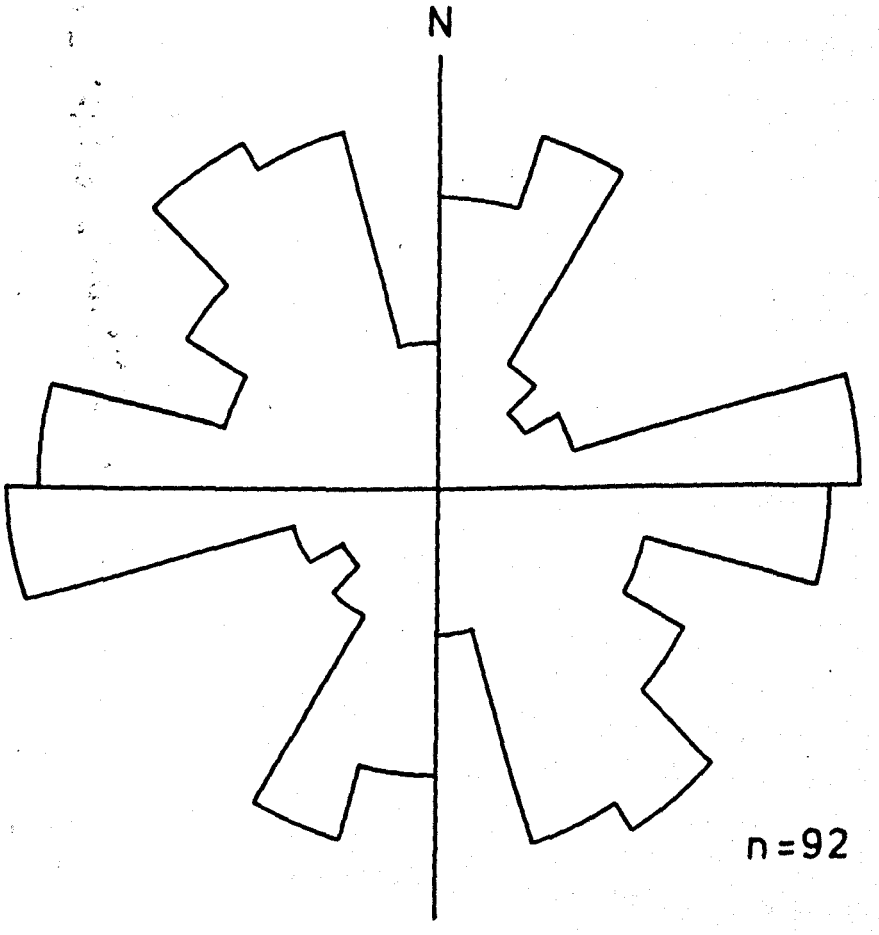

Plate 37 Contact of granophyre with country rock

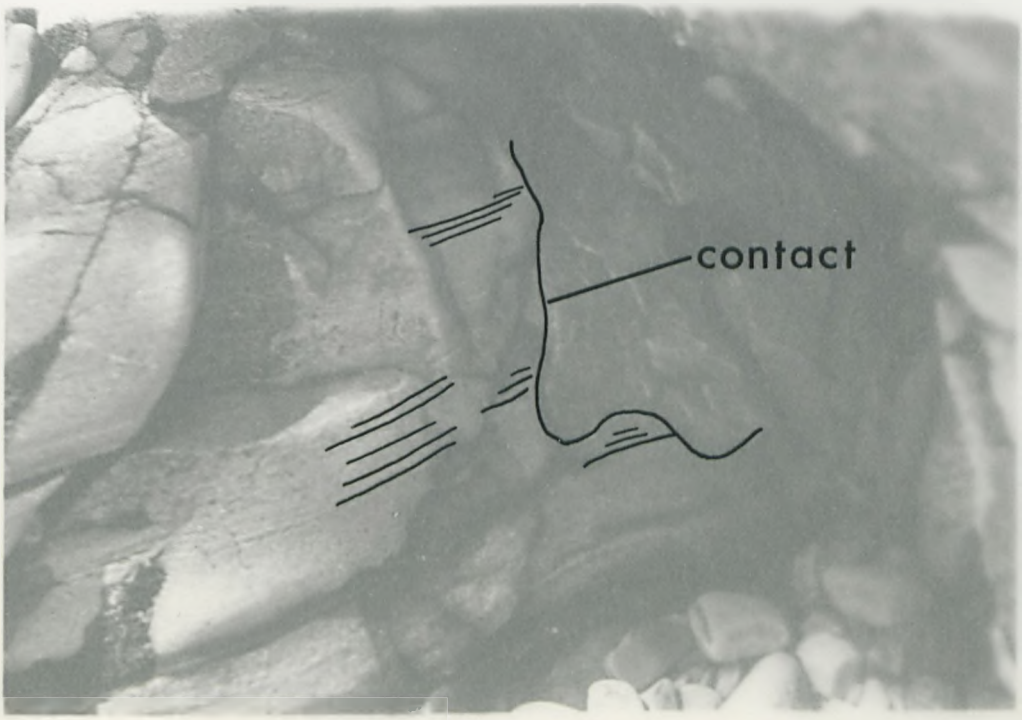
contact

field relations show them to post-date all tectonic deformation except for late faulting. Their late emplacement is substantiated by the lack of crystal orientation and the retention of the igneous granophyric texture.

There is no evidence to date the granophyres relative to the granites but a suite of felsites bordering the Great Glen has been dated at 380 million years by Dearnley (1967). Although no petrographic details are provided for the felsites (op. cit.), they may be compatible with the granophyres of the Killin area.

6.7.2 Petrography

Twelve samples have been studied in thin section. All but four samples contain phenocrysts and in each the groundmass is very similar, containing small (0.2 millimetres by 0.1 millimetres) quartz grains forming an interlocking matrix with orthoclase and plagioclase laths (up to 0.15 millimetres by 0.05 millimetres). The orthoclase and quartz form typical granophyric textures resulting in a matrix crowded with quartz hieroglyphs in some specimens. Spherulites are sometimes seen, with radiating crystals.

Up to five different minerals may occur as phenocrysts in any one rock. Table 6.2 shows the variation and the maximum sizes, grouped in individual samples.

PHENOCRYST	MAX. LENGTH (mm.)	% OF TOTAL PHENOCRYSTS
Plagioclase	6	100
Green biotite	5	32.5
Plagioclase, Orthoclase	6	68.5
Green biotite	4.5	25.5
Iron oxide	1.5	5.0
(Strained) quartz	2.5	38.5
Orthoclase and plagioclase	5.0	31.0
Orthoclase	3.0	60.0
(Strained) quartz	3.0	40.0
Albite, pericline plag.	3.0	10.0
Orthoclase (aggregate)	4.0	80.0
Quartz	2.0	10.0
Orthoclase and plagioclase(aggregate)	5.0	95.0
Green biotite	1.5	5.0
Orthoclase	2.5	50.0
Plagioclase	2.0	20.0
Quartz	2.0	30.0
Biotite	1.75	10.0
Perthitic K-feldspar	2.0	10.0
Sphene	1.0	1.0
Orthoclase (aggregate)	4.0	54.0
Plagioclase	3.5	25.0

Table 6.2

6.8 Younger Basalts

Two occurrences of younger igneous rocks were mapped. Both occur as thin (< 20 centimetres) sill-like bodies with sharp, planar contacts. They are traceable for only a few metres laterally.

Phenocrysts of augite (Plate 38) and andesine plagioclase reach 1 millimetre and 2 millimetres in length respectively. Other phenocrysts are chloritised and appear to pseudomorph olivine (Plate 39). The groundmass consists of very fine plagioclase laths of indeterminate composition.

The relatively late occurrence of the intrusions is indicated by the lack of deformation. However, chlorite may now form pseudomorphs of olivine, and although the clinopyroxene remains reasonably fresh, alteration has occurred.

Plate 38 Augite phenocryst in basalt

Plate 39 Chloritised olivine crystals in basalt

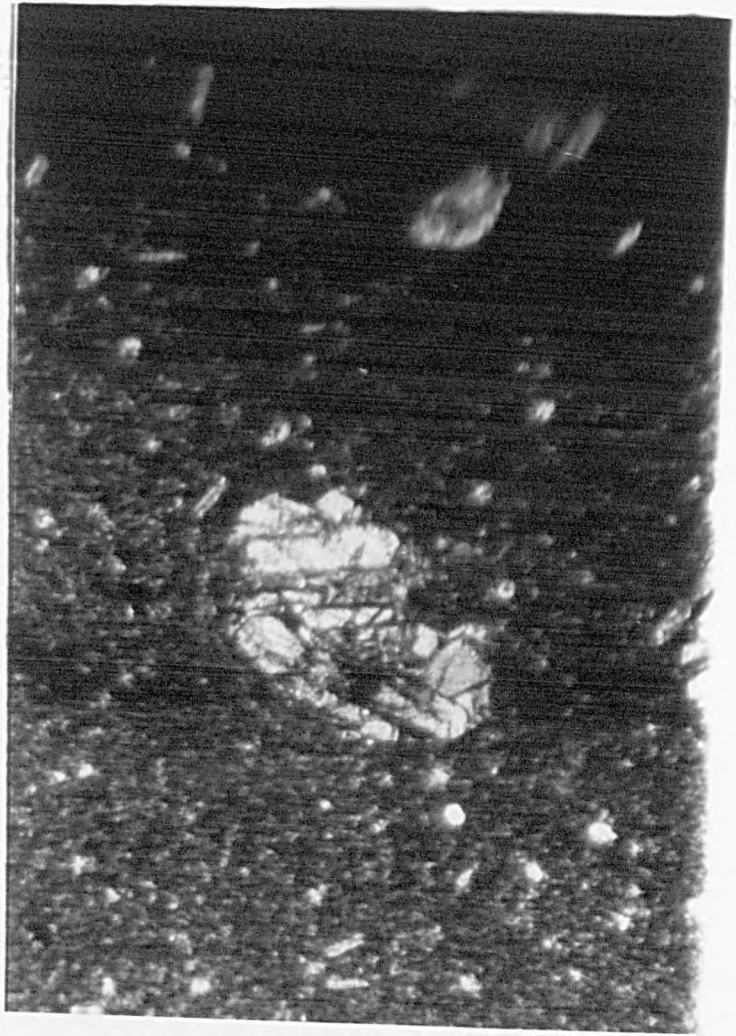

6.9 Amphibolites

Amphibolites are rare in the Killin area. Eleven samples have been collected (Figure 46) with an additional three from the margins of one amphibolite dyke.

The eleven samples can be divided into two groups based on field occurrence. The first group (Section 6.9.1) are concordant with the regional foliation and themselves possess a foliation. The second group (see Section 6.9.2) cut the regional foliation and later structures.

The amphibolites are also divided on chemical grounds (Section 7.5.3).

6.9.1 Foliated Amphibolites

These amphibolites occur either as thin, lensoid pods (< 2 metres long and 0.5 metres thick) or as larger sill-like features. All lie within the regional foliation but the development of a planar fabric within the amphibolites varies. Indeed, although the field evidence points to an early origin, the planar fabric may be weak. Hand specimens are typically olive green.

Minerals present are hornblende (with some tremolite), biotite which is often green, plagioclase, sphene, magnetite and pyrite. Epidote may also be present and calcite occurs, often as late, cross-cutting veinlets.

Bladed hornblende and tremolite may reach 4 millimetres in length, and commonly measure 2-3 millimetres long by 1-1.5 millimetres wide (Plate 40). They are often spongy with quartz inclusions and corroded edges show sericite rims. Rounded sphene (average diameter

Figure 46 Occurrence of amphibolites in the Killin area

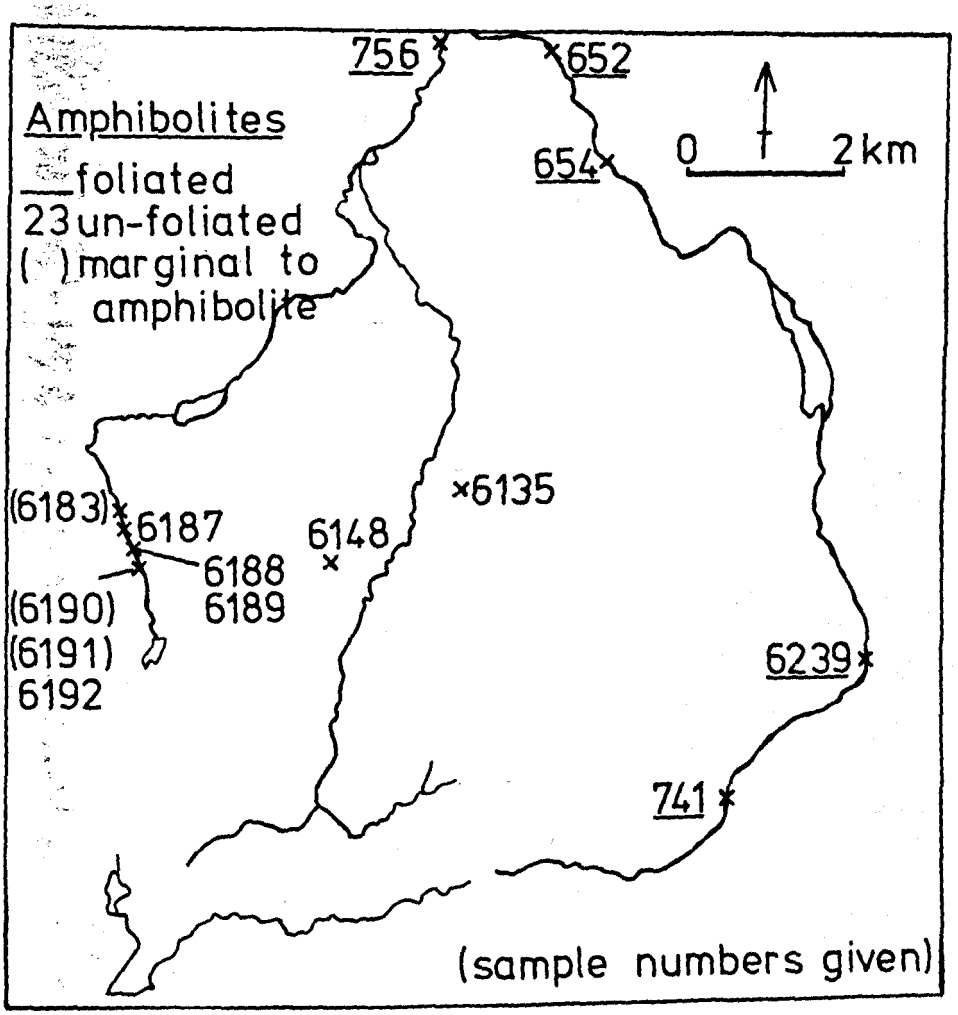
Amphibolites
foliated
23 un-foliated
( ) marginal to amphibolite
756
652
654
0
2km
(6183)
6187
6188
6189
(6190)
(6191)
6192
6148
6135
6239
741
(sample numbers given)

Plate 40 Hornblende and tremolite crystals from amphibolite sample

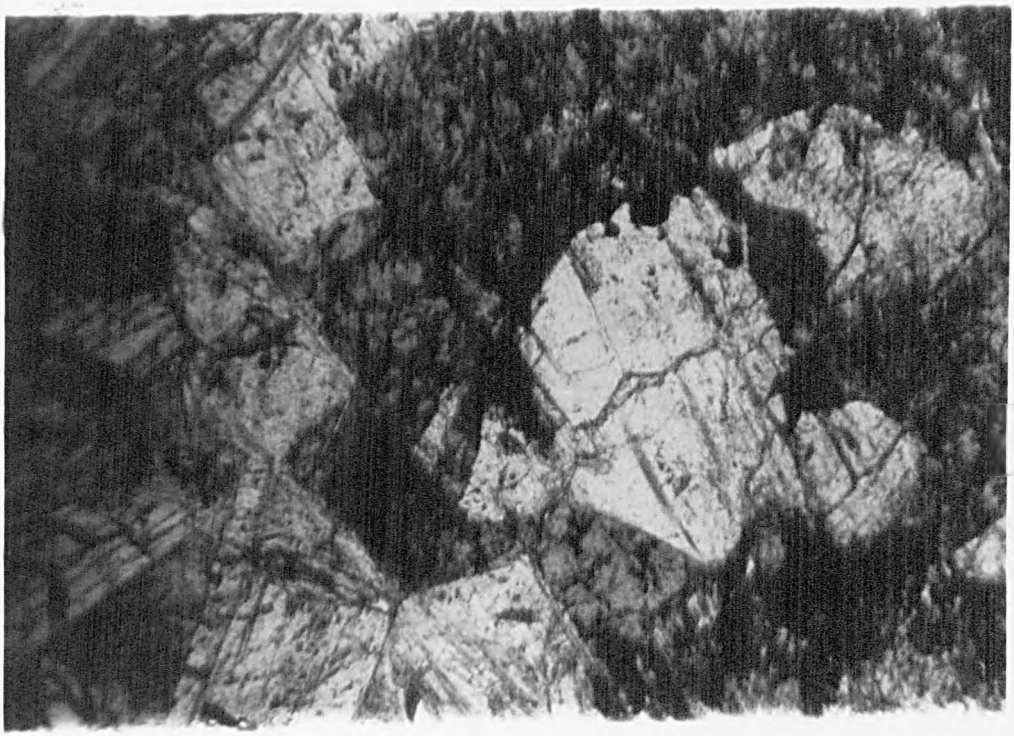

0.15 millimetres, but often larger) is common and is often associated with hornblende and tremolite.

Hornblende may also occur as small crystals averaging 0.3 millimetres in length and 0.1 millimetres in width, often with a granular habit. Sphene is again commonly associated with the hornblende as is biotite (< 0.4 millimetres long and 0.2 millimetres wide) which often exhibits a strong brown-green colour.Where both prismatic and basal hornblende crystals occur, quartz often forms an 'intersertal' mineral.

Where hornblende and tremolite occur together, the two are commonly intergrown. Hornblende usually forms a core surrounded by tremolite in physical continuity, although some crystals contain several zones exhibiting an alternation of hornblende and tremolite with lines of optical separation. These boundaries within mineral grains are attributed to a compositional break in this mineral series due to a miscibility gap (Shido & Miyashiro,1959; Klein,1969; Cooper & Lovering,1970).

Plagioclase occurs primarily in the matrix as small plates and laths. Grains reach 0.5 millimetres in length and 0.2 millimetres in width. Sericitisation of the grains is common.

Remaining components include pyrite, magnetite and small amounts of both chlorite and epidote. Garnet is notably absent.

6.9.2 Unfoliated Amphibolites

All samples in this category are seen to cut the F_1 foliation and four of the five samples are from the

Allt Vungie amphibolite which cuts F_2 generation folds (Plate 41). The dyke, which reaches approximately 7 metres in thickness, exhibits a massive, crystalline central area and slightly lensoid margins.

The fifth sample of this group does show what may be a very weak planar fabric but it nevertheless cuts the F_1 foliation. Its similarity to the Allt Vungie is noted chemically and it forms part of the meta-appinite suite (Winchester, 1976 and Section 7.5.3). Hand specimens in this category are predominantly pale to dark green in colour.

Minerals present are tremolite with hornblende, (brown) biotite, plagioclase, chlorite and opaque minerals. Very little sphene is present and epidote occurs in only one sample. Calcite again forms late, discordant veinlets.

Tremolite is the dominant amphibole. It occurs with hornblende either as large crystals (reaching 3 or 4 millimetres in length) or as small grains with a 'granular' habit. Biotite is commonly associated with amphibole, as is chlorite.

Quartz is present primarily as small (0.15 millimetres diameter) strained, inequant grains and plagioclase again occurs as small plates or laths.

Pyrite, and lesser amounts of magnetite, are also present.

6.9.3 Marginal effects

The samples described in this section are not amphibolites but occur along the margins of the Allt Vungie amphibolite. Minerals present include muscovite

Plate 41 Amphibolite dyke cutting F_2 generation folds

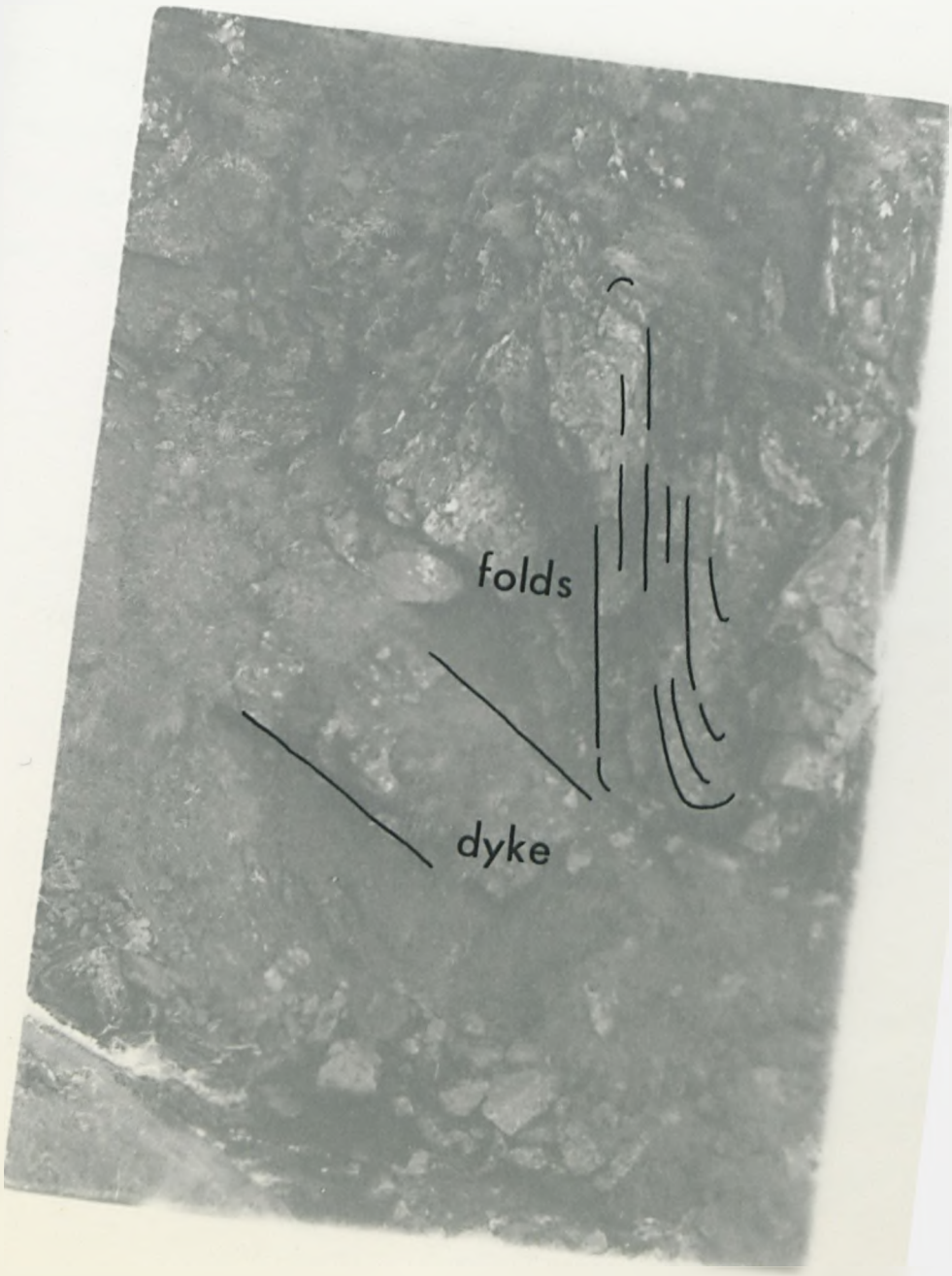
folds
dyke

with some biotite, K-feldspar, chlorite, quartz, calcite and magnetite. Little plagioclase is present and epidote occurs in only a very small amount in one sample.

In places a 'brecciated' texture is exhibited, with small blocks (< 1 centimetre) of quartz, orthoclase and chlorite crossed by thin bands of granular quartz.Within blocks there is a slightly lensoid appearance, accentuated by elongate quartz veins separated by thin chlorite laths. This texture is from the margin of the amphibolite and probably represents the brecciated host rock.

CHAPTER SEVEN-GEOCHEMICAL STUDY

Introduction

One hundred and fifteen samples have been analysed in an attempt to supplement the overall picture produced in the Killin area. Preparation of specimens for analysis and the subsequent methods and techniques employed (using X-ray fluorescence spectrometry) are outlined in Appendix 1. Where the number of samples in a group is low, the sample populations are used only as an indication of the chemical nature of a rock type.

Ten major element oxides have been determined, namely: SiO_2, Al_2O_3, Fe_2O_3, MgO, CaO, Na_2O, K_2O, TiO_2, MnO and P_2O_5. Some trace elements were also used for selected lithologies. For the metasediments Nb, Zr, Y, Sr, Rb, Ni and Cr have been determined. The same elements have also been determined for the amphibolite samples whilst only four have been used in studying the acid igneous rocks, namely Rb, Sr, Y and Zr. In discussion, the mean of a set of analyses is normally used. All analyses are available in Appendix 3.

CO_2 has not been determined and therefore constitutes part of the loss on ignition (Appendix 1). Iron has been determined only as total Fe_2O_3 and no correction has been made for the oxidation of the FeO component to Fe_2O_3.

Where mean values have been compared and are said to show 'significant' differences or otherwise, this is a statistical statement. In most cases Student's t-test has been used with a 95% limit hence the term is only used where valid (see Appendix 2).

7.1 Metasediment Chemistry-Major Elements

In studying the metasediments, a chemical and compositional distinction has been made between samples which are dominantly pelitic and dominantly psammitic. In this study the distinction is made at 66.00% SiO_2. This distinction in the Killin samples is an arbitrary one, the mean silica values for each lithology in each formation showing a break around this value (Table 7.1).

	FECHLIN	KNOCKCHOILUM	GLEN DOE	MONADHLIATH
Semi-pelitic	n=3 61.25	n=9 56.70	n=10 59.74	n=5 58.07
Semi-psammitic	n=2 70.83	n=4 69.40	n=9 68.90	n=2 66.73

Table 7.1 Mean SiO_2 Values in each Formation

This classification accords well with previous analyses (e.g. Shaw, 1956; Wedepohl, 1969) and therefore encompasses the pelites studied by Shaw (op.cit.) when the average silica content of 155 samples was 61.54% and also the mica schists used by Wedepohl (op.cit.) which contained approximately 60.00% SiO_2.

7.1.1 Semi-pelitic chemistry

A major use of mean values is to compare formations with each other for each oxide to see if any differences or similarities are suggested. Using the semi-pelitic samples comparisons can be made between the groups shown in

Table 7.2.

	FORMATION							
	FECHLIN		KNOCKHOILUM		GLEN DOE		MONADHLIATH	
n	3		9		10		5	
	$\bar{x}$	s	$\bar{x}$	s	$\bar{x}$	s	$\bar{x}$	s
SiO_2	61.26	5.92	56.70	4.43	59.74	4.10	58.07	4.61
Al_2O_3	17.17	2.56	18.77	2.05	16.83	2.18	18.94	2.44
Fe_2O_3	6.39	1.51	8.28	1.36	7.71	1.34	7.56	1.61
MgO	2.35	0.60	2.68	0.48	2.50	0.48	2.49	0.52
CaO	1.73	0.35	1.54	0.30	2.35	2.10	2.32	1.13
Na_2O	3.55	0.47	2.46	0.66	3.16	0.98	2.74	1.50
K_2O	4.07	0.28	4.88	0.97	3.32	1.18	3.86	2.19
TiO_2	0.76	0.18	0.95	0.13	0.88	0.15	0.94	0.14
MnO	0.10	0.03	0.13	0.02	0.16	0.07	0.19	0.04
P_2O_5	0.21	0.05	0.23	0.07	0.27	0.09	0.27	0.06

Table 7.2 Mean Values for Semi-pelitic Samples

These mean values show that there is little significant deviation between the principal formations. Only in two of the major oxides are any differences apparent namely K_2O and Na_2O. Between the Glen Doe and the Knockchoilum samples there is a significant difference in K_2O content reflecting a higher biotite and K-feldspar content in the Knockchoilum formation. The Knockchoilum formation means also show a slightly higher Fe_2O_3, MgO and Al_2O_3 which may also reflect higher biotite content.

The difference in Na_2O content between the Fechlin and Knockchoilum formations is considered significant and may relate to the plagioclase content variation.

7.1.2 Semi-psammitic chemistry

Table 7.3 illustrates the mean compositions of the psammitic samples in each formation.

	FECHLIN	KNOCKCHOILUM		GLEN DOE		MONADHLIATH
n	2	4		9		2
	$\bar{x}$	$\bar{x}$	s	$\bar{x}$	s	$\bar{x}$
SiO_2	70.83	69.40	2.76	68.90	0.74	66.73
Al_2O_3	13.81	13.87	1.38	13.33	0.98	15.18
Fe_2O_3	2.82	4.81	0.75	4.34	0.58	5.42
MgO	1.09	1.60	0.27	1.42	0.19	1.45
CaO	1.14	1.57	0.24	2.92	1.17	3.74
Na_2O	3.34	3.08	0.53	3.11	0.52	4.40
K_2O	4.01	2.93	0.45	2.15	0.57	0.94
TiO_2	0.44	0.68	0.09	0.64	0.06	0.71
MnO	0.07	0.09	0.02	0.12	0.03	0.34
P_2O_5	0.13	0.15	0.04	0.15	0.03	0.35
K_2O/Na_2O	1.20	0.95		0.69		0.21

Table 7.3 Mean Values for Semi-psammitic Samples

Although certain differences between the formations are apparent in Table 7.3 sample numbers are low for the Fechlin and Monadhliath formations. For this reason standard deviations relating to these formations have been omitted.

The gradual increase in SiO_2 and decrease in Al_2O_3 from the Fechlin formation down the sequence is noticeable. Associated with this trend, the Monadhliath formation contains

the highest Fe_2O_3, CaO and Na_2O contents. This reflects an overall more pelitic character higher up the sequence specifically due to a lower quartz and a higher biotite content in the Monadhliath formation.

Two minor distinctions are apparent in the CaO and K_2O contents. The higher CaO content of the Glen Doe samples (exceeded only by the mean content of the Monadhliath samples) reflects the plagioclase content and its calcic nature. Both sphene and epidote are either absent or occur as rare grains and therefore contribute little to this value. Free calcite is also uncommon in these samples.

Calc-silicate minerals forming discrete bands are widespread in both the Glen Doe and Monadhliath formations. In some cases however a similar rock type, a calcium-rich semipsammite, may contain plagioclase as the dominant calc-silicate mineral with occasional accessory clinozoisite present.

The higher K_2O content of the Knockchoilum formation (when compared to the Glen Doe formation) mirrors the difference in the pelitic samples. Again due to a higher biotite and K-feldspar content, this would seem to provide a relatively consistent distinction between the two formations. Further major differences between these two formations are lacking.

The Fechlin and Monadhliath samples will be mentioned briefly but only to provide preliminary indications of their compositions and apparent differences. The most noticeable differences are in the K_2O and Fe_2O_3 contents. The former is significantly higher in the Fechlin samples reflecting the increase in K-feldspar which is certainly partially due to the proximity of granite in the north-eastern part of the

area. The higher Fe_2O_3 of the Monadhliath formation is due to several factors. There is a higher biotite content in both samples and this is accompanied by an increase in opaque minerals (primarily magnetite). The third difference is that garnet persistently forms a minor constituent of the Monadhliath samples, unlike the other formations where it is either absent or present in only very small amounts. The garnet is also the likely mineral host for the much higher MnO content of the Monadhliath samples. TiO_2 also shows a marked increase in the Monadhliath formation relating to the sphene content and the much higher P_2O_5 content reflects the presence of numerous small apatite grains (both features being identifiable in thin section).

One further difference is the increase in CaO up the sequence reflecting the dominance of K-feldspar in the Fechlin formation and the higher proportions of calcic minerals in the Monadhliath formation including plagioclase and sphene.

7.1.3 Summary

In this brief study of forty-four samples, the analyses show few significant differences when applying the Student's t-test with 95% probability. For the ten major element oxides the four formations can therefore be considered to belong to the same sequence. There is apparently no break in continuity. The few differences that exist between the Knockchoilum and Glen Doe samples might suggest that both belong to the same formation which can then be subdivided on minor properties. One such easily determined

feature in the field is the presence of white or green calc-silicate bands.

Trace Elements

Thirty-five selected samples have been analysed for seven trace elements, namely Rb, Sr, Zr, Y, Nb, Ni and Cr to determine if any distinctions can be made between formations. All figures quoted are in parts per million.

7.1.4 Semi-pelitic chemistry

Table 7.4 shows the average concentrations in each of the seven elements for twenty-one semi-pelitic samples.

	n	Nb	Zr	Y	Sr	Rb	Ni	Cr	Rb/Sr
MONADHLIATH	4	15	214	34	295	163	36	116	0.55
GLEN DOE	7	17	224	42	311	137	37	112	0.44
KNOCKCHOILUM	8	17	168	36	242	188	43	114	0.78
FECHLIN	2	15	163	33	295	157	(34)	(86)	0.53

Table 7.4 Average Concentrations of Trace Elements in Semi-pelitic Samples.

From these data it is seen that no clear distinction can be made. The only difference is that the Monadhliath and Glen Doe formations possess higher mean Zr values than the Knockchoilum or Fechlin formations. However, the range of values obtained from individual analyses (Appendix 3) is too large to allow any significance to be attributed to these differences. Variations are more apparent in the

Rb/Sr ratios discussed in section 7.2.1.

7.1.5 Semi-psammitic chemistry

Similar variations are shown by the mean concentrations of semi-psammitic samples in three formations (Table 7.5). The Fechlin formation again shows lower mean Zr and Y concentrations. The steady decrease in these two trace elements is noticeable from the stratigraphically higher Glen Doe to the lower Knockchoilum and Fechlin formations. The Zr values may relate to lower zircon contents in the respective formations, but few other distinctions can be made.

	n	Nb	Zr	Y	Sr	Rb	Ni	Cr
GLEN DOE	9	17	265	32	367	89	28	81
KNOCKCHOILUM	3	16	225	29	263	101	30	85
FECHLIN	2	17	134	15	270	105	25	62

Table 7.5 Average Concentrations of Trace Elements in Semi-psammitic Samples.

7.2 Sediment Type and Minerals based on Analytical Information

Using both major and trace element analyses, attempts can be made to outline trends suggesting a possible parent sediment type for the Killin metasediments. No definite pairing of sediment to metasediment can be made but only a tentative and preliminary correlation.

Although there will probably have been some movement of components during metamorphism (primarily alkalis), most

elements can be considered relatively immobile (Elliot, 1973; Field and Elliot, 1974; Engel and Engel, 1962). The presence of sharp edges to most white calc-silicates would seem to point to a lack of widespread metasomatism.

7.2.1 Semi-pelitic lithologies

Table 7.2 shows the mean compositions of pelitic samples from the four Killin formations. The variation in components is clear when compared to the semi-psammitic averages and serves to illustrate the progressive chemical differences.

Table 7.6 compares the psammitic and pelitic means.

	PSAMMITIC	PELITIC	CHANGE RELATIVE
n	17	27	TO PELITIC
SiO_2	68.99	58.59	-
Al_2O_3	13.73	17.91	+
Fe_2O_3	4.40	7.73	+
MgO	1.43	2.54	+
CaO	2.49	2.01	-
Na_2O	3.28	2.89	-
K_2O	2.41	4.02	+
TiO_2	0.63	0.90	+
MnO	0.13	0.15	+
P_2O_5	0.17	0.25	+

Table 7.6 Psammitic and Pelitic Means

SiO_2 and CaO and Na_2O are the only three components to show a reduction related to quartz and feldspar changes.

The remaining components all show increases which can be largely attributed to the increase in mica. The dominance of MgO over CaO suggests that the original clay minerals probably included a high proportion of chlorite, and the presence of illite and montmorillonite may be indicated by the high Na_2O and K_2O contents.

The increase in Al_2O_3 will relate to the increase in clay minerals (and feldspar). The relatively large rise in Fe_2O_3 will also be related to the increase in clay minerals content. In the case of the accessory minerals, P_2O_5 shows a 50% increase in the pelitic mean reflecting greater abundance of detrital apatite. The MnO shows a slight increase and will occur primarily in garnet although since it is chemically similar to both Fe and Ca it could occur in other minerals including biotite and chlorite. TiO_2 shows a considerable increase in the pelitic mean related directly to the sphene content. This probably reflects a higher titanium content in the sediment contained in detrital rutile, possibly ilmenite, and clays.

Figure 47 illustrates the grouping of twenty-one semi-pelitic samples using the triangular plot of Moore and Dennen (1970). In this diagram, plots of the principal elements Si, Al and Fe are recalculated and can be related to the silica ranges for various rock types. Compositional fields on the diagram are those derived by Moore and Dennen.

The Killin samples indicate a spread between greywacke and shale sediment-type, no formation producing a very close grouping. The semi-pelites do not actually show features readily compatible with a greywacke composition (high Na_2O, near equal CaO and MgO) but the plot is any case

Figure 47 Triangular Si-Al-Fe plot for semi-pelitic samples (after Moore & Dennen,1970)

Figure 49 Triangular Si-Al-Fe plot for semi-psammitic samples (after Moore & Dennen,1970)

'Arkose' field derived from:Pettijohn,1949 & 1963;Middleton,1959 and Schwarcz,1966.

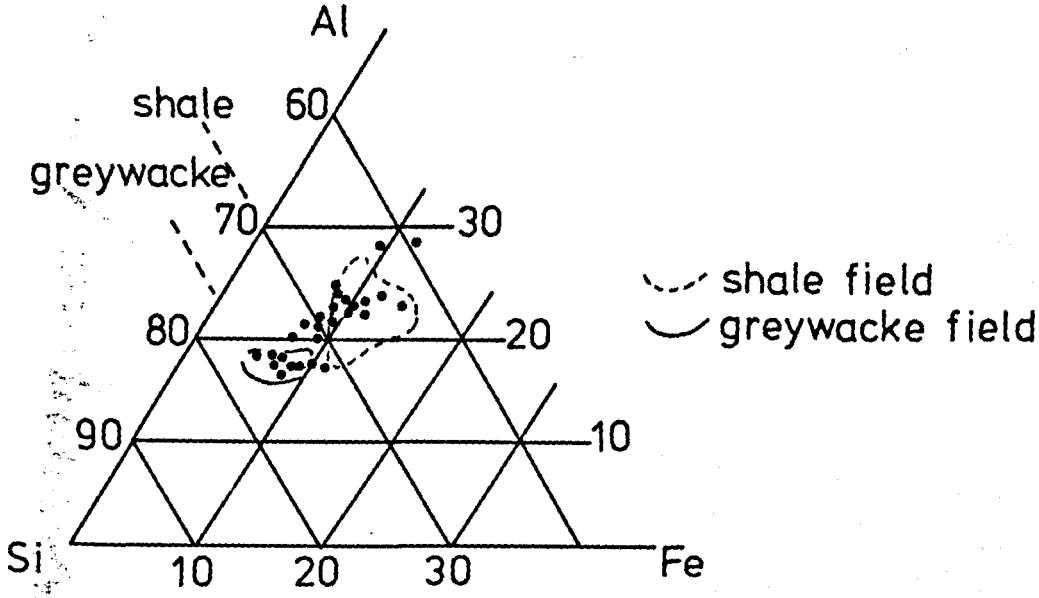
Al
shale
greywacke
60
70
30
80
20
90
10
Si
10
20
30
Fe
shale field
greywacke field

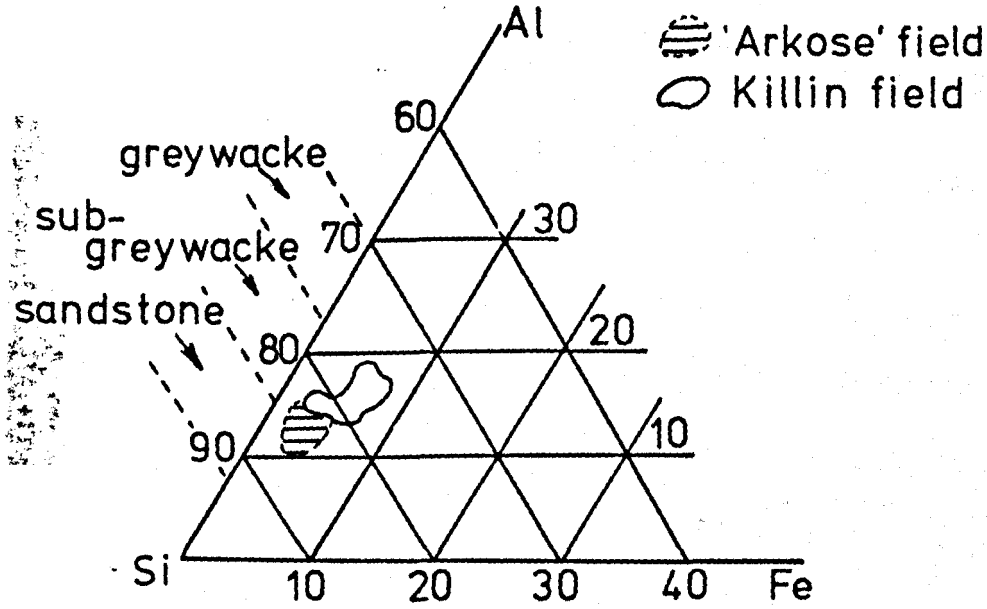
Al
'Arkose' field
Killin field
greywacke
sub-
greywacke
sandstone
60
70
30
80
20
90
10
Si
10
20
30
40
Fe

only an indication of possible parent type.

This is reflected by the trace element contents of the semi-pelitic samples both in absolute values and in relation to the semi-psammitic values. Table 7.7 shows three sets of trace element ratios.

	Sr/Y	Rb/Sr	$P_2O_5(x10^3)/Zr$
MONADHLIATH	8.7	0.55	1.26
GLEN DOE	7.4	0.44	1.21
KNOCKCHOILUM	6.7	0.78	1.37
FECHLIN	8.9	0.53	1.29

Table 7.7 Trace Element Ratios in Semi-pelitic Lithologies

The Sr/Y ratios illustrate the degree to which minerals will accept Sr but not Y i.e. the higher the ratio the higher the proportion of minerals into which Sr can enter such as feldspar (Pettijohn, Potter and Siever, 1972). High Sr/Y ratios therefore suggest a relatively high proportion of feldspar (although not as high as in the semi-psammites, Table 7.8). The Rb/Sr ratios reflect clay minerals (into which Rb enters). All values are below unity but are considerably higher than the semi-psammitic values, reflecting the increase in clay minerals. Although Rb is mobile (rendering the results likely to some modification) these values would suggest that the semi-pelites are relatively immature sediments in which some feldspar was retained, suggesting quite rapid erosion and deposition.

The P_2O_5/Zr ratios also provide information concerning the maturity of these parent sediments. P_2O_5 occurs

primarily in apatite and compared to zircon (accounting for the Zr) the mineral is less refractory and will be reduced by sedimentary sorting (Krynine, 1935). The ratios are constant between formations and are substantially higher than the semi-psammitic values. A combination of two factors is therefore suggested. Firstly, that the parent sediments were deposited quite rapidly and secondly that the original P_2O_5 content was high. The trace elements would therefore suggest quite rapid deposition. A shale would, as a parent sediment type, suggest an enrichment in clay minerals due to more extended weathering and sorting. It is therefore more likely that the greywacke-type trend shown by some samples is more indicative of the metasediment type.

The remaining traces offer little distinctive evidence. Analyses for chromium are few and, excluding the Fechlin formation, are constant. It can be expected that it will substitute for ferromagnesian minerals (as will nickel) i.e. in biotite and chlorite. The value of approximately 114 p.p.m. Cr is however lower than averages quoted for shales by Rankama & Sahama (1950) of up to 600 p.p.m. but very close to the value of 110 p.p.m. determined by Shaw (1954) for pelitic rocks.

Overall, the trace element data would seem to indicate few differences between formations suggesting that all are related and there are no undetected breaks in the succession.

7.2.2 Semi-psammitic lithologies

Table 7.3 illustrates K_2O/Na_2O ratios derived from mean values for the formations. These show a clear

trend decreasing from the basal Fechlin to the Monadhliath formation, suggesting a change from arkosic to greywacke sediment type. The Fechlin formation lithologies have been stated (see Section 6.5) to exhibit some features of small scale metasomatism close to granitic intrusions and it might therefore be expected to affect this ratio. However, even if the K_2O content had been increased by 20% the ratio would still have approached unity, maintaining the trend. It is thus envisaged that the value is sufficiently valid for the purposes of general comparison.

Figure 48 shows a graphical representation of the relevant major elements when used in the maturity diagram of Pettijohn, Potter & Siever (1972). Logarithmic ratios of SiO_2/Al_2O_3 and Na_2O/K_2O are plotted for each sample thus positioning it in one of the 'fields' derived from numerous analyses (op.cit.). The possibility of change in alkali contents in these metasediments renders the plot more approximate but it nevertheless provides an insight into the original sediment types. Also, bulk chemistry will be a combination of many factors, including source area geology, weathering, transport and matrix composition and this will render discrimination between sandstone types approximate. Such plots will however illustrate the uniformity or otherwise of the samples from different formations.

The diagram shows that most of the points fall on the greywacke side of the boundary between greywacke and lithic arenite suites, save for two which straddle the line. The Monadhliath mean value has a higher Na_2O content and therefore falls well within the greywacke field but, bearing in mind the possibility of minor variations, the remainder can

Figure 48 Maturity diagram for semi-psammitic samples (after Pettijohn,Potter & Siever,1972)

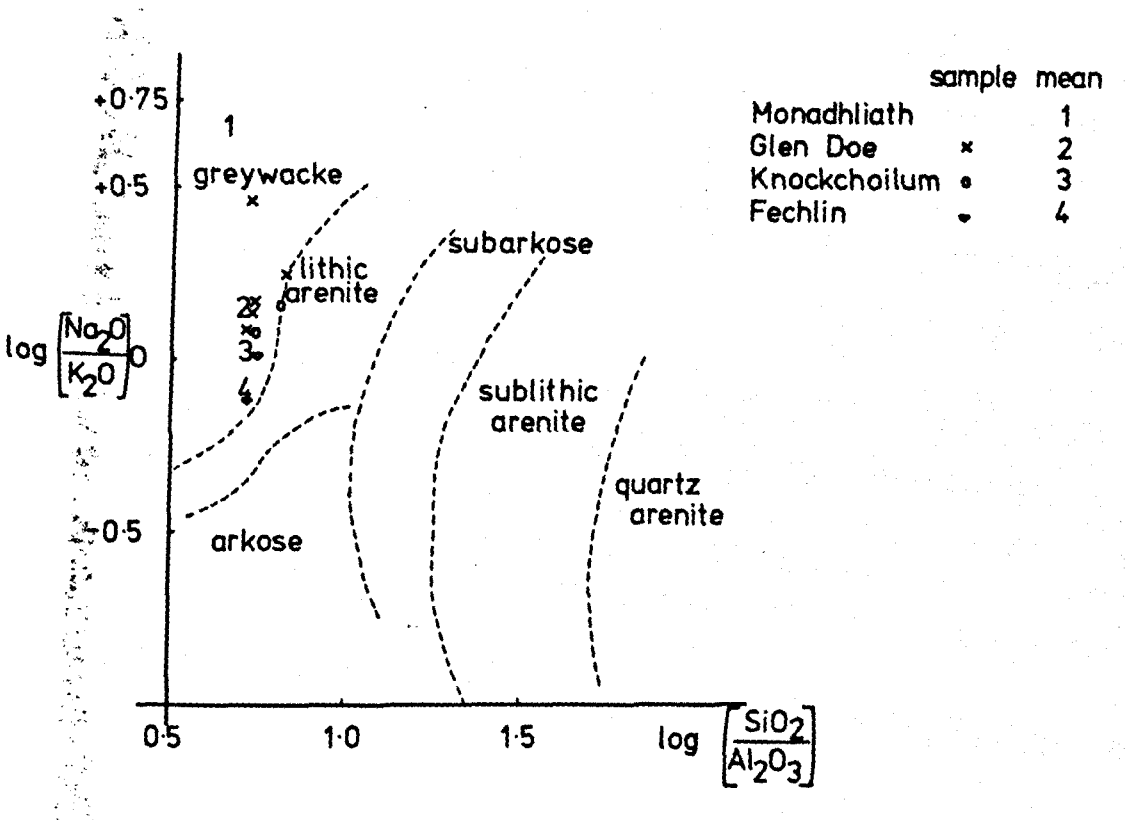
sample mean
Monadhliath 1
Glen Doe 2
Knockchoilum 3
Fechlin 4
+0·75
+0·5
-0·5
log [Na2O/K2O]
1
greywacke
lithic arenite
subarkose
sublithic arenite
quartz arenite
arkose
0·5
1·0
1·5
log [SiO2/Al2O3]

be said to border the lithic arenite field. It is clear however that there is a definite trend up the sequence based primarily on alkalis content. The SiO_2/Al_2O_3 ratios are considered near to constant save for the Monadhliath mean which has a slightly higher Al_2O_3 and lower SiO_2 content.

The Monadhliath formation has the highest mean Na_2O content suggesting a dominance of Na-feldspar due either to source variations or subsequent growth. This feature is compatible with a greywacke-type sediment and is also exhibited by the mean value of the Glen Doe formation. A further feature likely to be shown by this sediment type is the near equal contents of CaO and MgO (from mean composition table, page 15 of Pettijohn,1963). This is due to a higher chlorite content in the matrix, but only the Knockchoilum formation falls into this category.

These chemical characteristics indicate the possible original sediment which the Killin metasediments may represent, based on four of the major elements analysed. However, this indication gained is far from definite and a confirmation is therefore sought, using the triangular diagram with Si, Al and total Fe forming the end-members (Moore & Dennen, 1970). To enable comparison to be drawn, an arkose 'field' is incorporated, constructed from four data sources.

Figure 49 shows the triangular diagram with the Killin sample 'field' plotted. The clustering is clear and borders the greywacke and subgreywacke fields and thus presents a similar conclusion to that derived from the maturity diagram.

Trace elements can be used and produce information concerning the maturity of the parent sediments. Using Sr and Y values from Table 7.5, Sr/Y ratios can be determined for

all but the Monadhliath formation. The Fechlin formation has the highest (Table 7.8) Sr/Y ratio suggesting a high proportion of minerals into which Sr but not Y could enter. This would suggest a high feldspar content (also suggested by the low Rb/Sr ratio), rapid erosion and deposition, and therefore relative immaturity (since feldspar is likely to breakdown under normal weathering).

	Sr/Y	$P_2O_5(x10^3)/Zr$	Rb/Sr
FECHLIN	18.0	0.97	0.39
KNOCKCHOILUM	9.1	0.67	0.38
GLEN DOE	11.5	0.57	0.24

Table 7.8 Trace Element Ratios in Semi-psammitic Lithologies

The Glen Doe formation possesses the highest Sr value and this may imply a calcareous cement as suggested in the high CaO of the Monadhliath formation.

The relative immaturity of the Fechlin formation is again suggested using the P_2O_5/Zr ratios (Table 7.8). P_2O_5 occurs primarily in apatite and Zr in zircon but since the former is less refractory (Krynine, 1935) than the latter it will be reduced by sedimentary sorting. A lower ratio may therefore reflect a more mature sediment or possibly sediment eroded from a sedimentary source rock. The latter proposal would seem less likely since the formations tend to show gradual compositional changes and an overall grouping suggesting little basic change in source material.

The psammitic metasediments would therefore seem to represent relatively immature (although no distinction can

be made between textural and compositional immaturity) sediments which were probably rapidly deposited, and which resemble in composition a suite of greywacke to lithic arenite sandstone types.

7.2.3 Comparative chemistry

In this section the Killin mean analyses, for both semi-pelites and semi-psammites, are compared with average compositions of sediments (Table 7.9). The table shows that these mean compositions can be used only as a broad indication since minor differences abound. The Killin pelitic samples resemble the shales of Van der Kamp et al. (1976) save for a higher Na content. The composite analysis of Wedepohl (1969) which comprises results from Clarke (1924), Goldschmidt (1933), Minami (1935) and Shaw (1956) presents similarities in SiO_2, MgO, and CaO but has a substantially different Na_2O/K_2O ratio (Table 7.10).

The pelitic samples from Killin possess a Na_2O/K_2O ratio higher than all other shale values and although they do not show the dominance of Na_2O over K_2O expected of greywackes they may form an intermediate between these two groups.

The Killin psammitic samples show similarities to both groups of greywackes with respect to the Na_2O/K_2O ratios but do not show the parity of CaO and MgO expected of greywackes. They resemble more the arkoses of Van der Kamp et al. (1976). These samples therefore fall between pure arkoses and greywackes and show characteristics of both lithologic types.

n	A 27	(1) 14	(2) 277	(3) 155
SiO_2	58.58	58.87	58.9	61.54
Al_2O_3	17.91	17.12	16.7	16.95
Fe_2O_3(tot.)	7.73	7.64	6.9	6.65
MgO	2.54	2.83	2.6	2.52
CaO	2.01	1.98	2.2	1.76
Na_2O	2.89	1.71	1.6	1.84
K_2O	4.02	3.56	3.6	3.45
TiO_2	0.90	0.86	0.78	0.82
MnO	0.15	0.08	0.09	-
P_2O_5	0.25	0.14	0.16	-

n	(4) 23	(5) 61	(6)	(7) 26	B 17
SiO_2	64.43	66.7	66.1	69.62	68.99
Al_2O_3	15.48	13.5	8.1	12.84	13.73
Fe_2O_3(tot.)	6.54	5.5	5.3	3.60	4.40
MgO	3.12	2.1	2.4	1.73	1.43
CaO	2.22	2.5	6.2	2.67	2.49
Na_2O	3.74	2.9	0.9	3.07	3.28
K_2O	2.44	2.0	1.3	2.74	2.41
TiO_2	0.62	0.6	0.3	0.44	0.63
MnO	0.14	0.1	0.1	0.06	0.13
P_2O_5	-	0.2	0.1	0.14	0.17

Table 7.9 Comparison of Killin analyses to sediments

(see Table 7.10 for key to columns)

	A	(1)	(2)	(3)	
Na_2O/K_2O	0.68	0.48	0.44	0.53	
CaO/MgO	0.79	0.69	0.84	0.69	
SiO_2/Al_2O_3	3.27	3.44	3.53	3.63	
	(4)	(5)	(6)	(7)	B
Na_2O/K_2O	1.53	1.45	0.69	1.12	1.35
CaO/MgO	0.71	1.19	2.58	1.54	1.74
SiO_2/Al_2O_3	4.16	4.94	8.16	5.42	5.02

Table 7.10 Comparison of Major Element Ratios

Key to Sources:

A -Killin semi-pelites

B -Killin semi-psammites

(1)-Shales,Van der Kamp *et al*.(1976)

(2)-Shales,composite by Wedepohl (1969) including Shaw (1956)

(3)-Pelites,composite by Shaw (1956)

(4)-Greywackes,Condie (1967)

(5)-Greywackes,Pettijohn (1963)

(6)-Lithic arenites,Pettijohn (1963)

(7)-Arkoses,Van der Kamp (1976)

7.3 Comparative Moine/Dalradian Chemistry

The trace element analyses of the Killin samples can be compared to similar Dalradian and Moine lithologies to highlight any differences. A plot of the pelitic samples using Rb and Sr results is shown in Figure 50. Means of analyses are taken from other pelitic schists from the Moinian and Dalradian.

Average and individual compositions of various Moine and Lower Dalradian rocks show little overlap when Rb is plotted against Sr. On this basis Lambert, Winchester & Holland (1981). have been able to draw an optimum line dividing the fields of Dalradian and Moinian rocks. This difference probably relates to original compositions with a higher clay content (and therefore Rb content) in the Dalradian pelites.

The Killin samples show a very strong affinity for the Moinian field, with higher Sr values. In most cases the Sr/Rb ratio exceeds 1.00. This suggests that the Killin pelites originated from shales with a high concentration of detrital feldspar whereas the Dalradian samples contained a higher proportion of clay minerals (higher Rb than Sr). The slates of the Dalradian, however, represent part of a rhythmic sequence occurring primarily as black mud which has undergone chemical weathering (Hickman,1975). The higher clay minerals content could also imply derivation from a sedimentary source.

This would appear to be the main difference between the two supergroups although other minor distinctions can be postulated. Y seems to be lower in Moinian samples whilst

Figure 50 Plot of Rb and Sr values for Killin pelitic samples (marked thus:x)

Reference values:

Solid circles
1-Basal Morar Pelite (n=25)
2-Morar Pelite (n=39)
3-Glenfinnan Pelite (n=23)
4-Loch Eil Pelite (n=6)

(from Lambert, Winchester & Holland, 1981)

Open circles
1-Glen Creran
2-Allt Eilidh
3-Glen Roy
} (n=55)
4-Ballachulish Slate (n=35)
5-Cuil Bay Slate (n=15)

(from Hickman, 1975)

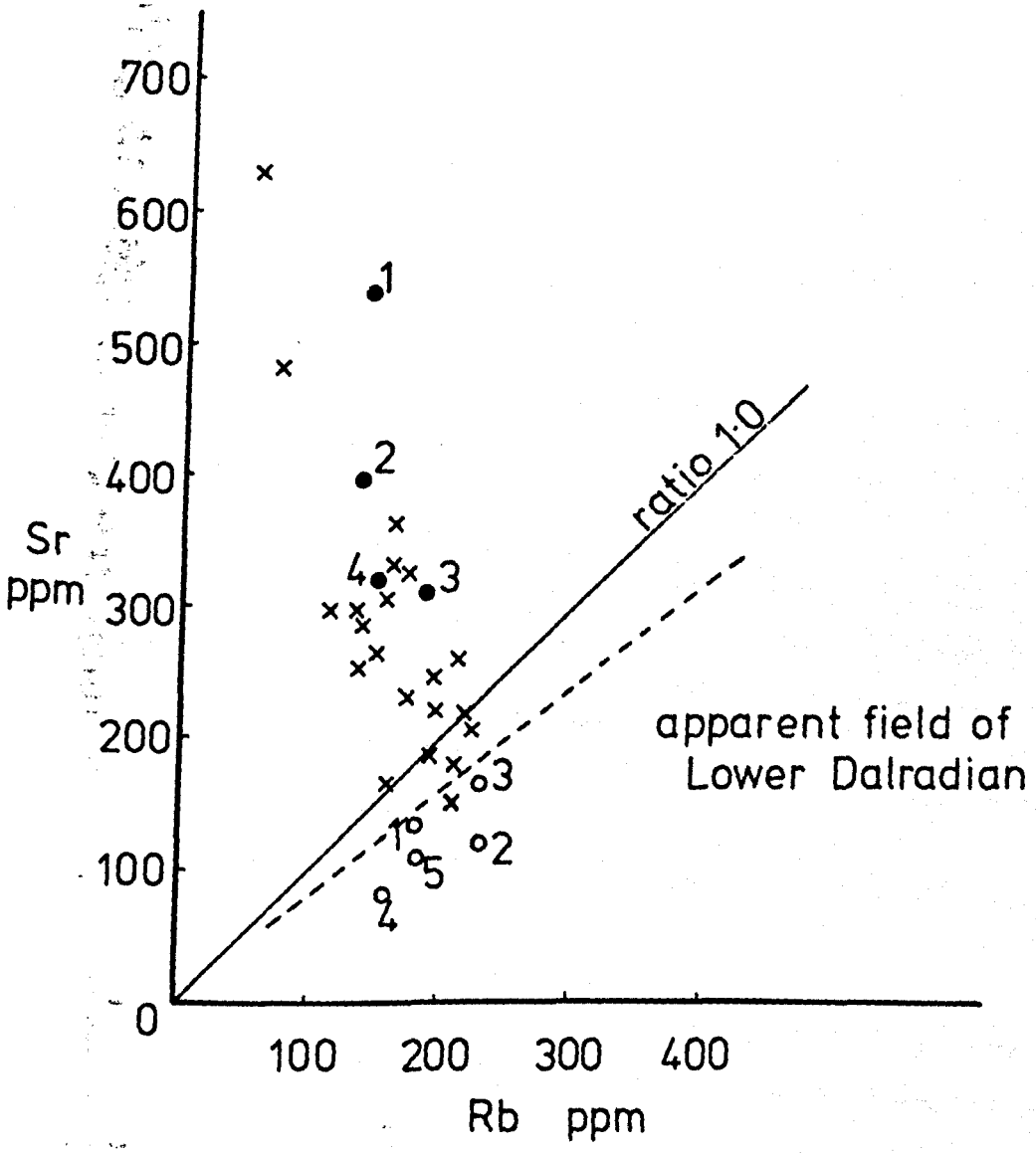
700
600
500
400
300
200
100
0
Sr
ppm
100
200
300
400
Rb ppm
ratio 1·0
apparent field of
Lower Dalradian
1
2
3
4
3
2
5
4

P_2O_5 is higher in the Dalradian reflecting more differentiated sediments (Lambert & Holland,1974).

Almost all the Killin samples fall into the Moine field indicating chemical affinities with the Moine. There is therefore no justification for placing these metasediments in the Dalradian.

7.4 Calc-silicate Chemistry:Major Elements

7.4.1 Differences between white and green types

43 samples of both types of calc-silicate have been analysed to determine their chemical differences. Table 7.11 illustrates the mean composition of all samples in both groups.

	Green Type		White Type	
	8		35	
	x	s	x	s
SiO_2	63.14	(3.36)	62.16	(3.53)
Al_2O_3	14.12	(1.56)	16.58	(1.13)
Fe_2O_3	4.04	(0.48)	4.68	(0.93)
MgO	1.51	(0.13)	1.52	(0.35)
CaO	9,89	(2.79)	8.95	(2.37)
Na_2O	1.39	(1.03)	1.94	(0.90)
K_2O	2.20	(1.20)	0.81	(0.61)
TiO_2	0.65	(0.07)	0.69	(0.08)
MnO	0.27	(0.07)	0.37	(0.11)
P_2O_5	0.20	(0.05)	0.31	(0.18)

Table 7.11 Mean Compositions of White and Green Calc-silicates

The mean compositions define three statistically significant differences namely in the Al_2O_3, K_2O and MnO contents. Slight differences are apparent in other oxides (Fe_2O_3, CaO and Na_2O) but these were not found to be significant using Student's t-test.

The occurrence of actinolitic amphibole and diopside in the green calc-silicates instead of the hornblende characteristic of the white calc-silicates accounts for many of the differences. The lower alumina content of the green calc-silicates relects the more minor role played by hornblende when compared to actinolite. The latter would also seem to contribute to the absence or scarcity of garnet which is a feature of the green calc-silicates.

The higher Al_2O_3 of the white calc-silicates may also be reflected in the presence of clinozoisite which is more abundant than is epidote in green calc-silicates.

The loss on ignition shows a substantial difference between the two groups. For the green and white types the losses are respectively 2.80% and 1.60%, reflecting principally the presence of more abundant calcite in the green calc-silicates.

7.4.2 Chemical differences within the white group

Within the white calc-silicates three groups can be defined by different phase assemblages and these correspond to similar assemblages (see Section 4.1.1) initially suggested by Kennedy (1949). The number of samples is weighted in favour of the andesine-hornblende bearing group since this type is the most common throughout the Killin area. The remaining two groups also contain hornblende

but are distinguished by the presence of biotite in one and bytownite in the second, mineralogical variations attributed to differences in metamorphic grade (Kennedy,1949).

Table 7.12 illustrates the mean compositions of calc-silicates containing the different phase assemblages within the white group. Comparison of the first two groups produces only one significant difference. The group containing hornblende and andesine has a lower K_2O content compared with the group containing hornblende and biotite. This is readily explained by the replacement of biotite by hornblende with an increase in metamorphic grade and a consequent removal of K_2O.

	Hb & Bi		Hb & And		Byt & Hb
	5		28		2
	$\bar{x}$	s	$\bar{x}$	s	$\bar{x}$
SiO_2	60.11	(4.82)	62.55	(3.17)	62.62
Al_2O_3	16.51	(1.26)	16.57	(1.15)	16.84
Fe_2O_3	4.81	(0.61)	4.71	(0.98)	3.91
MgO	1.63	(0.23)	1.51	(0.37)	1.26
CaO	9.05	(4.05)	8.86	(1.92)	9.92
Na_2O	2.09	(0.95)	1.99	(0.88)	0.94
K_2O	1.52	(0.70)	0.69	(0.52)	0.73
TiO_2	0.70	(0.06)	0.69	(0.08)	0.63
MnO	0.35	(0.07)	0.38	(0.12)	0.42
P_2O_5	0.46	(0.37)	0.29	(0.10)	0.28

Table 7.12 Comparison of White Calc-silicate Assemblages

The change from hornblende-andesine to bytownite-hornblende assemblages is accompanied by few changes. Owing to their scarcity in the field, only two bytownite-bearing calc-silicates are used. Of the two differences apparent therefore (i.e. Fe_2O_3 and Na_2O contents), it is possible that the Fe_2O_3 variation may be due either to sampling effects or statistical variation, and this may also apply to some extent to the Na_2O variation. The lower Na_2O value in the bytownite-bearing group may mirror the less sodic nature of the plagioclase, reflecting the increase in grade.

7.4.3 Chemical differences within the green group

Since fewer analyses are available for green calc-silicates than for the white ones, it is less easy to define chemical differences. Individual analyses show a large range of values for particular oxides, notably CaO, Na_2O and K_2O. This renders meaningful comparisons of groups difficult.

Unlike the white calc-silicates, groups based on phase assemblages are less well established. Two 'associations' can be chosen however for samples containing either biotite or pyroxene, amphibole being common to both. Table 7.13 shows mean analyses for these two groups.

Differences are apparent in the Al_2O_3, Fe_2O_3, CaO and Na_2O values. (Note. Because of low numbers of samples and high variations, Student's t-test has not been applied in this case. Differences are therefore not statistically significant). The difference in CaO content is due to the variability of the analyses and also the presence of calcite in some samples, reflected by higher losses on ignition.

	Bi-bearing	Px-bearing
n	3	4
SiO_2	61.00	64.03
Al_2O_3	14.96	13.38
Fe_2O_3	4.32	3.79
MgO	1.55	1.49
CaO	9.26	10.78
Na_2O	1.49	1.10
K_2O	2.47	2.32
TiO_2	0.69	0.61
MnO	0.29	0.28
P_2O_5	0.22	0.18

Table 7.13 Mean Compositions of Biotite and Pyroxene-bearing Green Calc-silicates

The higher Al_2O_3 of the biotite-bearing group probably relates directly to the presence of this mineral and the higher Fe_2O_3 may reflect the varying proportions of ferromagnesian minerals. The difference in Na_2O content is probably linked to changes in plagioclase composition. However, since sericitisation of the plagioclase is a feature of these green calc-silicates, it is not possible to confirm or refute this.

Summary: Minor chemical differences are therefore apparent between the green and white calc-silicates and within the green calc-silicates. The white calc-silicates do show chemical differences between different assemblages which can be attributed to an increase in metamorphic grade.

7.5 Amphibolite Chemistry

Amphibolites are not common in the Killin area and only six samples have been analysed. These can be divided on morphology, two structurally 'early' samples occurring as foliated pods in the Fechlin Psammite and four 'late' samples occurring as more massive dyke-like bodies in which foliation or preferred orientation of minerals is lacking. The latter samples all occur in the Glen Doe Semi-psammite.

7.5.1 Major element chemistry

The mean major elements concentration in the two groups are shown in Table 7.14.

	Foliated	Unfoliated
	2	4
SiO_2	45.15	45.96
Al_2O_3	13.74	9.25
Fe_2O_3	13.64	9.34
MgO	7.51	16.35
CaO	9.54	8.43
Na_2O	0.64	0.80
K_2O	3.61	1.56
TiO_2	2.80	0.76
MnO	0.25	0.18
P_2O_5	0.35	0.21

Table 7.14 Mean Compositions of Amphibolite Groups

Differences are readily apparent on studying the compositions but none have been qualified statistically because of the low number of samples and the range in particular oxides, notably MgO and Fe_2O_3 (illustrated in Figures 51 and 52). Major differences between groups are nevertheless apparent for MgO, Fe_2O_3 and TiO_2. More minor variations are noted in K_2O, MnO and P_2O_5 values. Average SiO_2 values are similar.

The high TiO_2 content of the foliated group is reflected by numerous grains of sphene apparent in thin section. Variation in the Fe_2O_3 and MgO values is related to the relative proportions of hornblende and tremolite in the samples. Hence the tremolite-rich, unfoliated specimens have higher MgO contents than the foliated amphibolites, even though the latter contain both hornblende and biotite.

The lower alumina content of the unfoliated group can also be related to the high tremolite and low biotite contents when compared to the foliated amphibolites. A high K_2O content in the two foliated samples also reflects their content of biotite. The overall composition of the four unfoliated samples is similar to the meta-appinites noted intruding the Moines west of the Great Glen Fault (Winchester, 1976). Many components show similar values to those analysed by Winchester (op.cit.), namely SiO_2, Fe_2O_3, MgO, CaO and TiO_2. Four of these oxides have been used to superimpose the Killin samples on variation diagrams used by Winchester (op.cit.). The similarity in composition is noticeable for two of the three diagrams from the meta-appinite field.

Figure 51 Variation diagrams for Killin foliated and unfoliated amphibolite samples.
Meta-appinite fields from Winchester (1976)
The dotted line in part (c) is explained in the text.

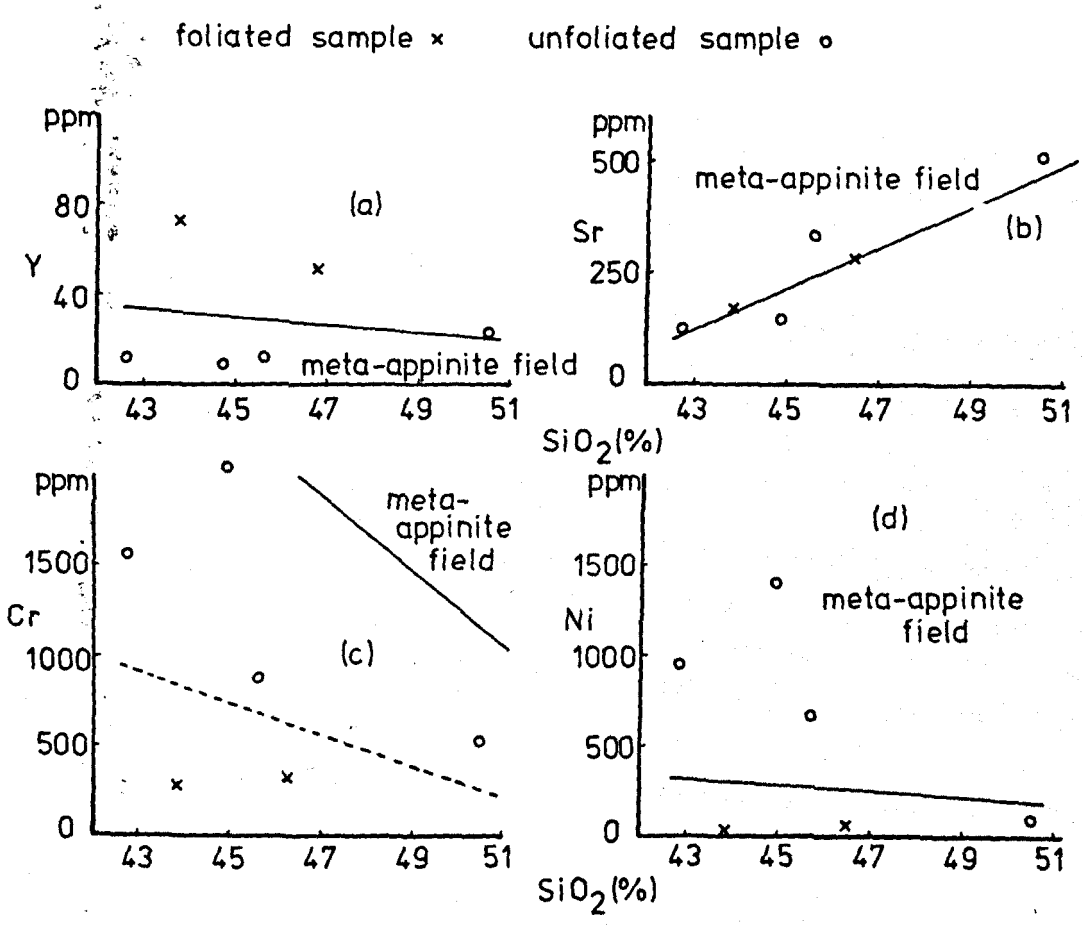
foliated sample ×
unfoliated sample o
ppm
80
Y
40
0
(a)
meta-appinite field
43
45
47
49
51
ppm
500
Sr
250
0
meta-appinite field
(b)
SiO2(%)
ppm
1500
Cr
1000
500
0
meta-
appinite
field
(c)
ppm
1500
Ni
1000
500
0
(d)
meta-appinite
field
SiO2(%)

Figure 52 Variation diagrams for Killin foliated and unfoliated amphibolite samples
Meta-appinite fields from Winchester (1976)

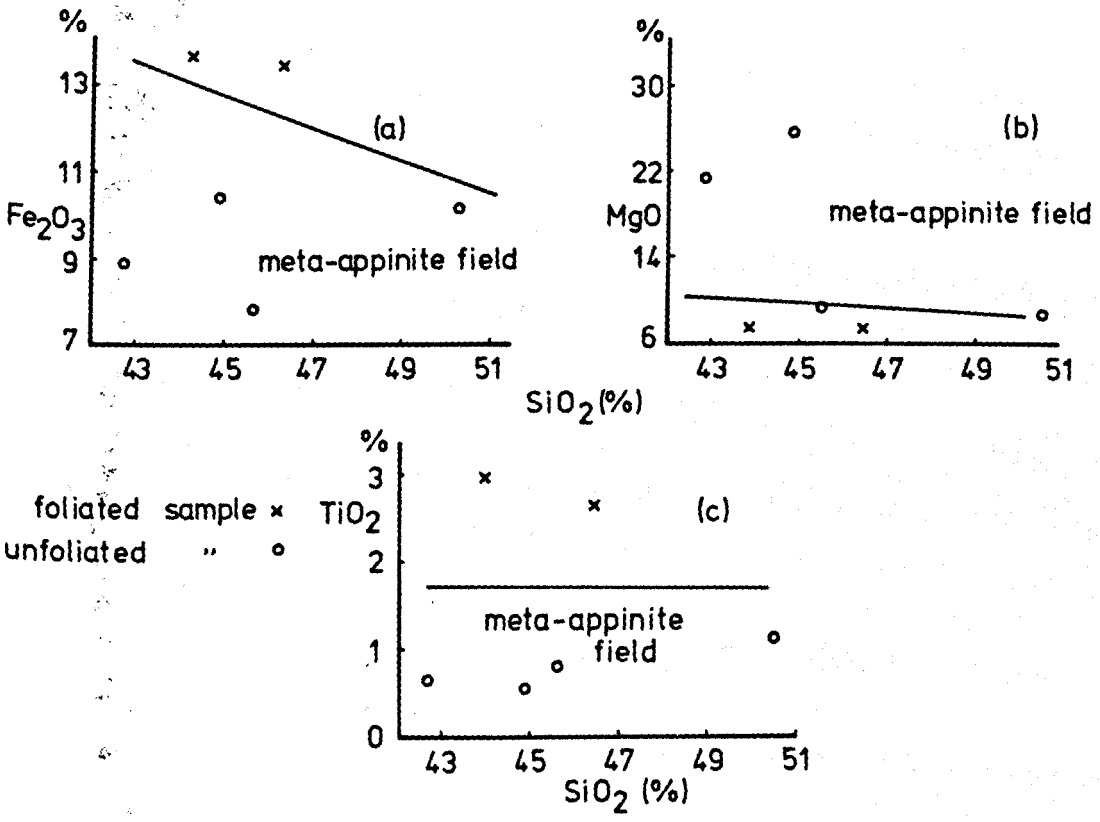
%
13
11
Fe_2O_3
9
7
(a)
meta-appinite field
43
45
47
49
51
%
30
22
MgO
14
6
(b)
meta-appinite field
SiO_2(%)
foliated sample ×
unfoliated " o
%
3
2
1
0
TiO_2
(c)
meta-appinite field
SiO_2 (%)

7.5.2 Trace element chemistry

The division of the amphibolites into two groups, termed foliated and unfoliated, is substantiated by a brief survey of the trace element values (Table 7.15).

To try and categorise these amphibolites using trace element data is difficult due to the small number of samples. The igneous origin of the samples is determined by their field occurrence and the distinction between the two groups suggested by their major element chemistry can be emphasised using certain plots which confirm the later, unfoliated group as belonging to the meta-appinite suite.

	sample	Nb	Zr	Y	Sr	Rb	Ni	Cr
Foliated	652	11	231	51	285	79	79	314
	654	9	315	76	172	254	45	269
Unfoliated	6148	9	141	27	511	21	81	504
	6187	7	32	12	118	75	993	1573
	6189	1	67	14	328	66	654	871
	6192	17	42	13	139	5	1389	2102

Table 7.15 Trace Element Content of Amphibolites and Meta-appinites

In each case the Killin samples are plotted using the variation diagrams of Winchester (1976) and four trace elements are used namely, Y,Sr, Cr and Ni (Figure 51). The diagrams illustrate the chemical differences between the amphibolites and meta-appinites. In the case of Cr,

the dividing line occurs at a lower value for the Killin samples, although this line (dashed in Figure 51,c) could equally have been drawn using Winchester's data. Although some of the plots show one point straddling the line dividing the two fields, it is clear that the later unfoliated group has a trace element chemistry broadly similar to that of the meta-appinites discussed by Winchester (op.cit.).

The chemistry of the two foliated amphibolites suggests a broadly basaltic composition, but further classification must be very tentative. Plotting SiO_2 against total alkalis (Macdonald & Katsura,1964) places both samples in the alkaline field, although this may prove unreliable if chemical change accompanied metamorphism. Both bodies are relatively small and as their K_2O contents greatly exceed that of average basalt, introduction of K_2O during metamorphism seems probable.

Further discriminative plots may be employed (Floyd & Winchester,1975) using elements which may normally be considered immobile during amphibolite facies metamorphism (Engel & Engel,1962; Elliot,1973; Field & Elliot,1974). TiO_2 vs. Zr/P_2O_5 and Nb/Y vs. Zr/P_2O_5 discriminant plots used by Winchester & Floyd (1976) suggest that the foliated amphibolites originated as subalkaline basalts.

7.5.3 Conclusions

Two groups are thus discernible, not only from their field relationships but also by their chemistry. The larger group is probably related to the suite of meta-appinites mentioned by some authors (Richey,1938;Johnson & Dalziel,1966; Winchester,1976) and found intruding all the

Moine divisions of the Western Highlands.

The second and smaller group of foliated amphibolites show similarities to amphibolites elsewhere in the Moines west of the Great Glen Fault. However, with so small a sample, no more definite conclusion can be reached.

7.6 Acid Igneous Rock Chemistry

In a study of the acid igneous rocks, samples thought to be related to the Foyers and Allt Crom granites were analysed together with samples from two suites of granophyres.

Comparisons are made within both the granite and granophyre groups and the two lithologies are compared in order to discover what differences or affinities exist.

7.6.1 Granites-major element chemistry

The granites were collected from areas heavily intruded by dykes from the Foyers and Allt Crom granites. Since only two samples from each type are available, these results can merely be used as an indication of the group chemistry. However, the mean compositions do show some differences worthy of mention (Table 7.16). Differences are seen in all components and all are marked (deemed significant) save for three, namely SiO_2, Al_2O_3 and MgO. Although the MgO comparison does not satisfy the 95% confidence limit it is clear that there is some minor difference in content. The apparent compatability shown by the test may well be due to the low sample numbers.

The higher Fe_2O_3 and MgO contents of the Foyers mean reflects two features of this group. Firstly, the biotite

	Foyers	Allt Crom
n	2	2
SiO_2	73.50	70.02
Al_2O_3	12.50	15.06
Fe_2O_3	3.27	1.73
MgO	1.16	0.62
CaO	2.30	1.03
Na_2O	3.01	4.28
K_2O	1.62	4.77
TiO_2	0.55	0.28
MnO	0.09	0.04
P_2O_5	0.13	0.09
Rb	69	67
Sr	307	496
Y	20	10
Zr	197	155
Rb/Sr ratio	0.22	0.14

Table 7.16 Mean Compositions of Granite Samples-Major and Trace Elements

content is higher in the Foyers samples and secondly they contain more chlorite.

The Allt Crom mean shows the higher alkali content, the more pronounced difference lying with the K_2O content, which reflects the greater role played by orthoclase in these samples. A slightly higher proportion of plagioclase is recorded in the Allt Crom samples and this is reflected by the higher Na_2O value. The remaining minor components reflect variations in the accessory minerals.

These differences, although only tentative, suggest that the two compositions are unlikely to be related or to lie on the same differentiation trend.

7.6.2 Granites-trace element chemistry

The concentrations of the trace elements Rb, Sr, Y and Zr have been determined for the Foyers and Allt Crom granitic dykes (Table 7.16). Low sample numbers detract from the value of these figures which do however indicate that there are clear differences between the means.

The substantially higher Sr value of the Allt Crom granitic dykes is probably related to a higher plagioclase feldspar content. Both Y values are low but the Foyers value is twice that of the Allt Crom, reflecting a higher proportion of calcic minerals e.g. hornblende and sphene. A higher sphene content relates to the high TiO_2 content of the Foyers group (Section 7.6.1 and Table 7.16)

7.6.3 Granophyres-major element chemistry

The ten granophyre samples are clearly divisible into two groups based on their chemistry. There exists no

geographical pattern of distribution and the samples bear no relationship to the major granites, each group showing a broad scatter of locations.

Table 7.17 illustrates the mean compositions of the two groups. The samples were not subjected to Student's t-test but evident differences exist in all the components save for SiO_2, Al_2O_3 and MnO.

These chemical differences mirror the petrological differences which lie in the phenocryst type. Group 2 samples contain biotite (and secondarily chlorite), sphene and to a lesser extent hornblende whilst group 1 samples contain only quartz, feldspar and rare biotite phenocrysts (see Section 6.7.2).

7.6.4 Granophyres-trace element chemistry

The two groups of granophyres are again easily separated by their trace element values (Table 7.17). In each case, the group 2 samples show substantially higher values. These can be related directly to the phenocrysts of this smaller group. The Y reflects a higher proportion of calcic minerals i.e. sphene and hornblende, whilst the Sr relates to the plagioclase feldspar content. The Rb value must be accommodated mainly in the increased number of biotite phenocrysts. Thus these results mirror the petrographic details and the major element chemistry.

The two Rb/Sr ratios can be compared with similar ratios from the two sets of granitic dykes. Although the group 2 value is close to that of the Foyers mean, any affinities would seem to be negated by the lack of any geographical relationship. The group 1 Rb/Sr value shows no affinity with either set of granitic dykes.

	Group 1		Group 2	
n	8		2	
	$\bar{x}$	s	$\bar{x}$	s
SiO_2	74.75	(0.90)	70.59	(3.08)
Al_2O_3	14.12	(0.22)	13.62	(1.80)
Fe_2O_3	0.32	(0.14)	3.26	(0.09)
MgO	0.17	(0.04)	1.11	(0.11)
CaO	0.41	(0.14)	1.95	(0.31)
Na_2O	4.79	(0.15)	3.76	(0.82)
K_2O	4.40	(0.39)	2.86	(1.16)
TiO_2	0.12	(0.01)	0.56	(0.04)
MnO	0.03	(0.01)	0.07	(0.01)
P_2O_5	0.02	(0.01)	0.15	(0.04)
Rb	63		99	
Sr	213		416	
Y	7		17	
Zr	57		204	
Rb/Sr ratio	0.30		0.24	

Table 7.17 Mean Compositions of Granophyre Samples-Major and Trace Elements

7.6.5 Granite/granophyre comparative chemistry

In a comparison of the mean compositions of all granites and the larger group of granophyres, sufficient important differences occur to suggest that they are not related. Where differences occur, they are large enough to validate such a grouping. The comparison is shown in Table 7.18.

	Granites		Granophyres	
	4		8	
	$\bar{x}$	s	$\bar{x}$	s
SiO_2	71.76	(2.55)	74.75	(0.90)
Al_2O_3	13.78	(1.58)	14.12	(0.22)
Fe_2O_3	2.50	(0.82)	0.32	(0.14)
MgO	0.89	(0.30)	0.17	(0.04)
CaO	1.67	(0.65)	0.41	(0.14)
Na_2O	3.64	(0.66)	4.79	(0.15)
K_2O	3.19	(1.61)	4.40	(0.39)
TiO_2	0.42	(0.14)	0.12	(0.01)
MnO	0.06	(0.02)	0.03	(0.01)
P_2O_5	0.11	(0.02)	0.02	(0.01)

Table 7.18 Mean Compositions of Granites and Group 1 Granophyres

The differences are considered significant using Student's t-test at the 95% confidence level. Only two oxides, Al_2O_3 and K_2O can be considered to belong to the same population. The composition of the granophyres reflects that they contain primarily quartz and K-feldspar and very few other

minerals. Little or no biotite is present, shown by the very low iron and magnesium values, the high potassium relating more to the presence of K-feldspar. Little sphene is recorded in the granophyres, indicated by a low TiO_2 value.

A comparison of both granophyre groups to the two groups of granites is made in Table 7.19 for the oxides which exhibit the major differences.

	GRANITES		GRANOPHYRES	
	FOYERS	ALLT CROM	GROUP 1	GROUP 2
n	2	2	8	2
Fe_2O_3	3.27	1.73	0.32	3.26
MgO	1.16	0.62	0.17	1.11
CaO	2.30	1.03	0.41	1.95
Na_2O	3.01	4.28	4.79	3.76
K_2O	1.62	4.77	4.40	2.86

Table 7.19 Comparison of Selected Oxides for Granites and Granophyres

It is clear that the group 1 granophyre is comparable only to the Allt Crom samples and then only in total alkali content. The smaller group 2 does show a greater resemblance, although still slight, to the Foyers samples. However, it does seem clear that no one group, whether granite or granophyre can be said to belong to the same population (summarised diagrammatically in Figure 5 3).

Figure 53 Comparative plots of granites and granophyres using selected major elements

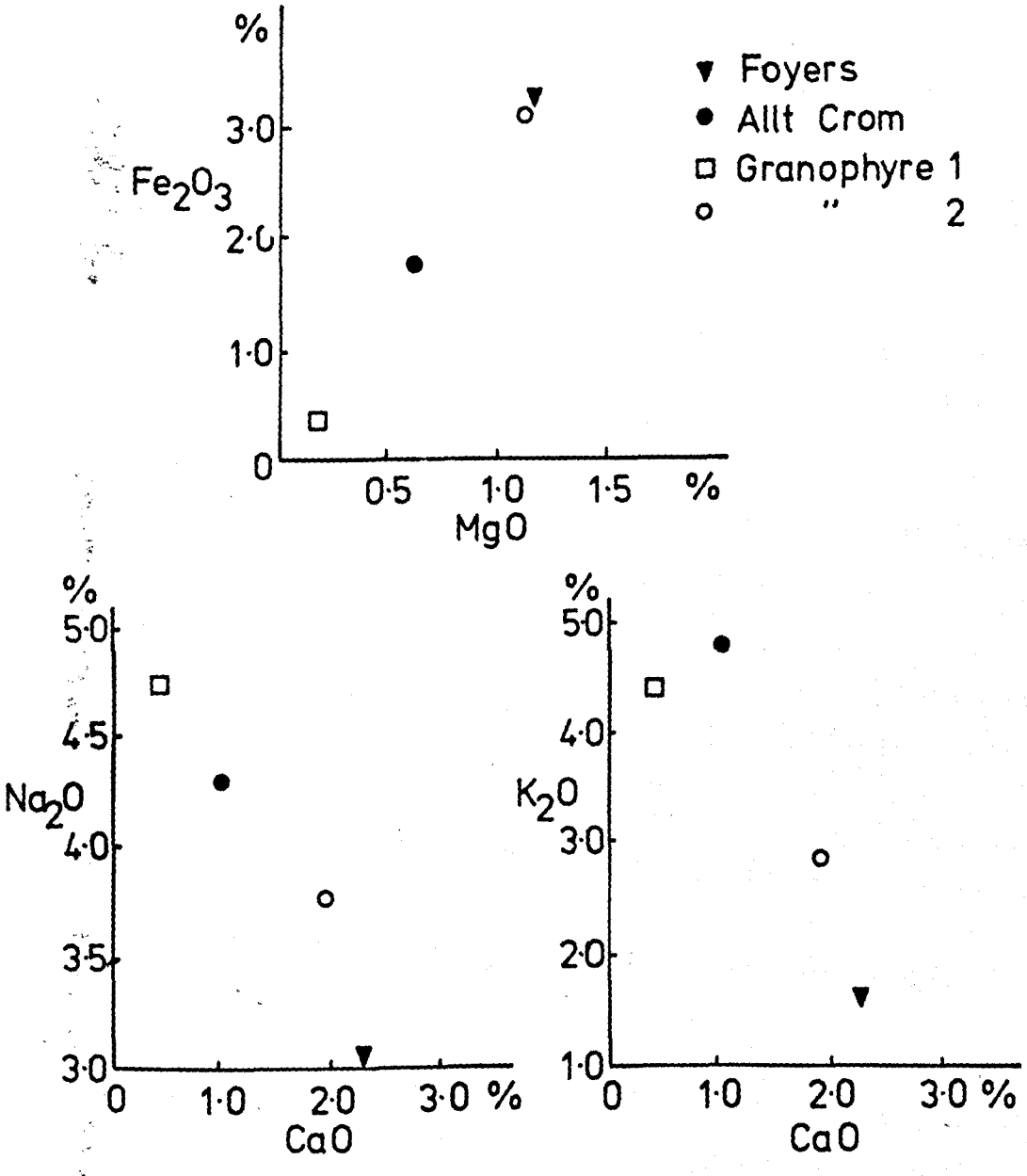
%
3·0
2·0
1·0
0
Fe_2O_3
0·5
1·0
1·5
%
MgO
Foyers
Allt Crom
Granophyre 1
" 2
%
5·0
4·5
4·0
3·5
3·0
Na_2O
0
1·0
2·0
3·0 %
CaO
%
5·0
4·0
3·0
2·0
1·0
K_2O
0
1·0
2·0
3·0 %
CaO

7.6.6 Miscellaneous sample

Sample 713 shows some similarities to the group 2 granophyres but is intermediate in composition and is classified as a microdiorite. Table 7.20 compares the microdiorite to the group 2 granophyres.

	Sample 713	Group 2 Granophyres
SiO_2	59.94	70.59
Al_2O_3	15.66	13.62
Fe_2O_3	6.24	3.26
MgO	2.96	1.11
CaO	2.16	1.95
Na_2O	4.51	3.75
K_2O	4.02	2.86
TiO_2	1.16	0.56
MnO	0.10	0.07
P_2O_5	0.62	0.15

Table 7.20 Comparison of the Microdiorite to the Group 2 Granophyres

The microdiorite shows a substantially higher Fe_2O_3 and MgO content and slightly higher CaO content. This sample contains large biotite phenocrysts, which is also reflected in a higher K_2O content. Large, euhedral sphenes are also apparent, mirrored by a very high TiO_2 content.

7.6.7 Summary

Two features therefore emerge. The two sets of granite dykes may not be direct descendants of the same

parent since their chemistry is substantially different. Secondly, the granophyres cannot readily be associated with either granite suite. This would suggest that the granophyres either form part of a completely different suite or a substantially differentiated group rich in silica and alkalis.

CHAPTER EIGHT-METAMORPHISM IN THE KILLIN AREA

8.1 Introduction

The term metamorphism is here used to encompass all changes that reflect altering physical and chemical conditions. It is really to be applied when the total rock composition is unaltered, but in fact most metamorphic processes involve some chemical change and metasomatism is therefore included.

This principle is illustrated on a small scale in Killin by individual white calc-silicate bands where evidence of metasomatism is apparent at the margins of the bands. Hence for some elements the system must be open. However, on a large scale, taking for example, all the rocks involved, chemical changes seem to be very limited and metamorphism can be regarded as being broadly isochemical.

Regional metamorphism has affected the whole Killin area. Only the granite rocks are unaffected as they were intruded after the last metamorphic event. In various metasedimentary lithologies minerals are present which indicate the grade of metamorphism. The relative timing of mineral growth can be related to different deformational episodes.

8.2 Evidence of Metamorphic Grade

8.2.1 Pelites

Garnet is present throughout the Killin area primarily in biotite-bearing pelitic and semi-pelitic rocks. No alumino-silicate index minerals defining other

Barrow zones were found in the area. This renders precise determination of grade difficult, using the index minerals of the Barrovian zonal sequence. This difficulty has been noted by Butler (1965) in Ardnamurchan, and occurrences of alumino-silicate minerals such as staurolite, kyanite and sillimanite have been found to be rare throughout the Moine and Central Highlands even where alternative evidence suggests that the pressure and temperature conditions would have favoured the growth of such minerals in a rock of suitable composition. Sporadic occurrences of these minerals are known (Barrow et. al.,1913; Horne and Hinxman, 1914; Hinxman and Anderson,1915; Bosworth,1925; Read,1931; Drever,1940; Anderson,1947a and 1956; Clifford,1957; Fleuty,1961; Tobisch,1963; Dalziel and Brown,1965; Dalziel, 1966; Poole,1966 and Winchester,1972) but the greater CaO content of Moine pelitic and semi-pelitic rocks usually precludes their occurrence (Winchester,1974a). The absence of these minerals in the Killin area, therefore, does not preclude the possibility that the metamorphic grade may have been high enough to favour their formation in rocks of a suitable composition. The evidence from the phase assemblages in pelitic rocks therefore only provides a broad suggestion that the entire area was subject to amphibolite-facies regional metamorphism.

8.2.2 Amphibolites

Wiseman (1934) interpreted the absence of biotite in amphibolites as indicative of kyanite grade. The foliated amphibolites of the Killin area contain some green biotite and the unfoliated group contains some brown

biotite. The latter is in some instances replacing hornblende and may therefore be partially a retrogressive product. The later unfoliated amphibolites cut across folds of F_2 age and their mineralogy therefore relates to post-F_2 metamorphism.

Wiseman (op cit.) further interpreted hornblende and andesine (± epidote, biotite and garnet) as being characteristic of the amphibolite facies. Plagioclase in many of the Killin samples is too sericitised for its composition to be determined but of those samples where determination is possible, andesine is present in some instances. This may tentatively place the Killin samples in the amphibolite facies.

8.2.3 White calc-silicates

(a) mineralogical variations: A greater range of mineral assemblages is exhibited by the white calc-silicate bands in the Killin area. As noted in the Western Moines, the calc-silicates have provided the most precise indication of metamorphic grade and evidence of variations of grade within the area. The mineralogical assemblages in the white calc-silicates from Killin have been classified in Chapter three and their geographical distribution is illustrated in Figure 8.

White calc-silicates have been used previously (Kennedy, 1949; Tanner, 1976; Winchester, 1972 and 1974 b and c) in an attempt to determine metamorphic grade in the Western Moines. Based on the calc-silicate mineralogy, zones have been drawn and can similarly be constructed in the Killin area (zones are outlined in Chapter four). The zones, determined by the occurrence or disappearance of index

minerals are designated thus:

(i) biotite and hornblende

(ii) hornblende

(iii) bytownite and hornblende

The noticeable feature is that in isochemical calc-silicates, bytownite-bearing samples are found only in the east, near Loch Killin, thus indicating higher grade. By including samples from east of Loch Killin, (collected by Winchester and analysed by Winchester and K.H.W.) assemblages containing pyroxene enable a fourth zone to be indicated. The mineral assemblages progress from west to east through biotite and hornblende to pyroxene and therefore suggest an eastwards increase in grade. The area exhibits a topographic range of up to 500 metres and this permits construction of a three dimensional picture of the zonal pattern.

(b) Chemical controls: The method of using calc-silicates to assess metamorphic grade has been used by Winchester (1972,1974c) in northern Ross-shire. It was then found that the CaO/Al_2O_3 ratio exercised the most direct influence upon the mineral assemblages of any particular grade, probably because most reacting phases are calcium-aluminium silicates i.e. hornblende, clinozoisite and plagioclase. Other components, such as MgO and K_2O, might be expected to control the assemblages to some extent, but they occur in relatively low concentrations (particularly K_2O which is often well under 1.0% of the rock) and appear to have little effect. However, K_2O does exhibit local mobility at the contacts of calc-silicate bands and pelites, producing a biotite-rich selvage zone.

Some overall discrepancy may exist due to potential error in CaO/Al_2O_3 ratios and the minor effect of other components. However, these appear to affect the conclusions only slightly.

Few calc-silicates were used which contained free calcite (none with calcite >1.5 vol.%). The presence of calcite shows no particular affinity with any one assemblage and is probably controlled by the partial pressure of CO_2. Hence exclusion of calcite-bearing calc-silicates limits the occurrence of minerals favoured preferentially by a high PCO_2 and eliminates the 'favouring' of Ca-bearing minerals.

(c) Isograds and isograd surface: Tilley (1924) defined isograd as 'a line joining points of similar pressure/temperature values in metamorphic rocks'. The production of various minerals must, however, be dependent on the whole rock composition.

Atherton (1965) divided isograds into two types based on the first appearance of an index mineral, or on the disappearance of a particular phase.

In the Killin area, the isograds are based primarily on two factors: the occurrence (and therefore disappearance) of specific minerals, and related whole rock compositions. The former includes the appearance of hornblende and bytownite, the latter mineral to some extent changing composition with grade. Bytownite is the term applicable to plagioclase which has the compositional range An_{70} to An_{90}. However, in the white calc-silicate group, bytownite is used loosely to include plagioclase with An content exceeding An_{68}. This is on the calcic side of a composit-

ional 'gap' shown by plagioclase in the white calc-silicate group (Section 4.1.4).

The area to the east of Loch Killin, although strictly outside the area covered by this thesis, afforded the best opportunities for accurate determination of metamorphic grade, because well-developed calc-silicates were widely distributed in an area with high relief and extensive outcrop.

Using several samples from one location the critical CaO/Al_2O_3 ratios controlling phase assemblages can be determined at each location, for example dividing samples in which bytownite is developed from those with less calcic plagioclase. Increase in grade allows development of bytownite in progressively less calcic calc-silicates. Where the critical CaO/Al_2O_3 ratios are the same, these locations have been interpreted as lying on the same isograd.

At four locations southeast of Loch Killin the critical ratio above which bytownite is developed is 0.5 and this can be used to determine the 0.5 bytownite isograd surface. Using a geometrical construction (Figure 54) the orientation of the isograd surface can be determined by constucting two triangles. This indicates that the attitudes of the isograd surfaces are 352° strike, 11° westerly dip and 358° strike, 15° westerly dip in the eastern and western examples respectively. Since these two results show an aggreement well within the expected error it has been assumed that the attitude of the isograd surface in the area is consistent. Therefore the average for the 0.5 bytownite isograd surface (a strike of 355° and a

Figure 54 Calculation of the angle of dip of the 0.5 bytownite isograd. X denotes a sampling location with the elevation in metres (from Winchester & Whittles, 1979)

Figure 55 Section illustrating dip of isograd surfaces (from Winchester & Whittles, 1979)

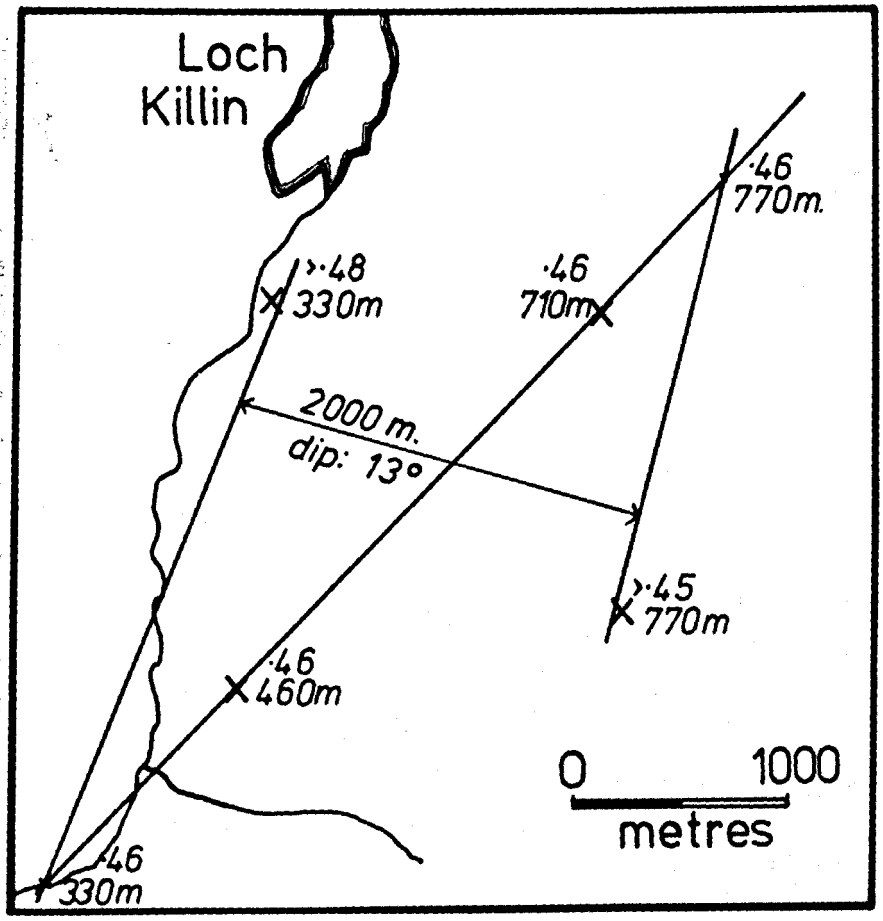
Loch
Killin
·46
770m.
·48
330m
·46
710m
2000 m.
dip: 13°
·45
770m
·46
460m
0
1000
metres
·46
330m

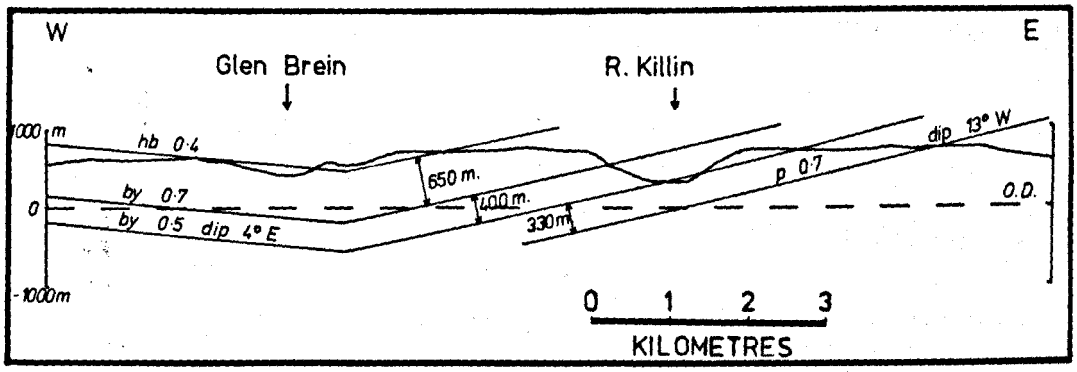
W
E
Glen Brein
R. Killin
1000 m
0
-1000m
hb 0·4
by 0·7
by 0·5 dip 4° E
650 m.
400 m.
330m
p 0·7
dip 13° W
O.D.
0 1 2 3
KILOMETRES

westerly dip of 13°) has been interpreted as the closest approximation to the actual attitude in this area.

Since the metamorphic grade increases eastwards and downwards, the metamorphic zones are seen to be uninverted in contrast to those in northern Ross-shire (Winchester, 1972,1974c). Using the same method, further isograd strike lines can be constructed and Figure 55 shows a cross-section, illustrating the separation between the isograds. The pyroxene 0.7 isograd is calculated east of Loch Killin on Doire Meurach and is separated by 330 metres from the 0.5 bytownite isograd. The separation between the bytownite 0.5 and 0.7 isograds is shown in the cross-section and by coincident structure contours as 400 metres.

Further west near Glen Brein primary biotite is recorded in the least calcic calc-silicates and the isograd is defined along the eastern edge of the area, as the occurrence of biotite in calc-silicates with a ratio of up to 0.4. Assuming parallelism with the other isograds, approximately indicated by the calc-silicates in Glen Brein, it is separated from the 0.7 bytownite isograd surface by 650 metres (Figure 55). If this westerly dip of 13°, determined from information east of Glen Brein is maintained further west, the calc-silicates occurring west of Glen Brein would also contain biotite. However, hornblende and not biotite is recorded in all calc-silicates to the west collected from many different elevations, and this suggests that a slight increase in grade occurs westwards. To produce an isograd dip, petrological constraints are used. Bytownite is not present

hence the dip cannot be high and since biotite is not present west of Glen Brein, then to achieve this with the structure contours, an optimum easterly dip of approximately 4^{o} is determined. Figure 56 shows the resultant structure contour map. This shows a simple structure with a 'metamorphic synform' inferred east of Glen Brein which plunges northwards at approximately 2^{o}. Other (minor) folds may be present, but the evidence is not sufficiently precise to prove their existence.

The overall trend of the 'metamorphic synform', roughly north-south, is subparallel to the trend of F_3 fold axes and discordant to the first and second generation folds. The evidence therefore suggests that the F_3 folding postdated the establishment of the isograds. Later metamorphic episodes were of low grade and evidence suggests that the M_3 and M_4 only just reached the Lower Greenschist facies (biotite and chlorite formed respectively- see Section 8.3.1).

(d) Calc-silicate zones: The definition of the bytownite and pyroxene isograds as the occurrence of these minerals in calc-silicates with a ratio of 1.0 (Winchester, 1974b) is not applicable in the Killin area since only one sample exceeds this ratio. More applicable isograds are thus defined in calc-silicates with a CaO/Al_2O_3 ratio of 0.7 (Winchester and Whittles, 1979).

The calc-silicate zones are therefore defined as below:

Pyroxene: pyroxene present in all calc-silicates with a CaO/Al_2O_3 ratio which exceeds 0.7
(only occurs east of the Killin area)

Bytownite: bytownite present in all calcite-free calc-

Figure 56 Structure contour map of isograds in the Killin area (from Winchester & Whittles, 1979)

Figure 57 Zonal map of the Killin area (from Winchester & Whittles, 1979)

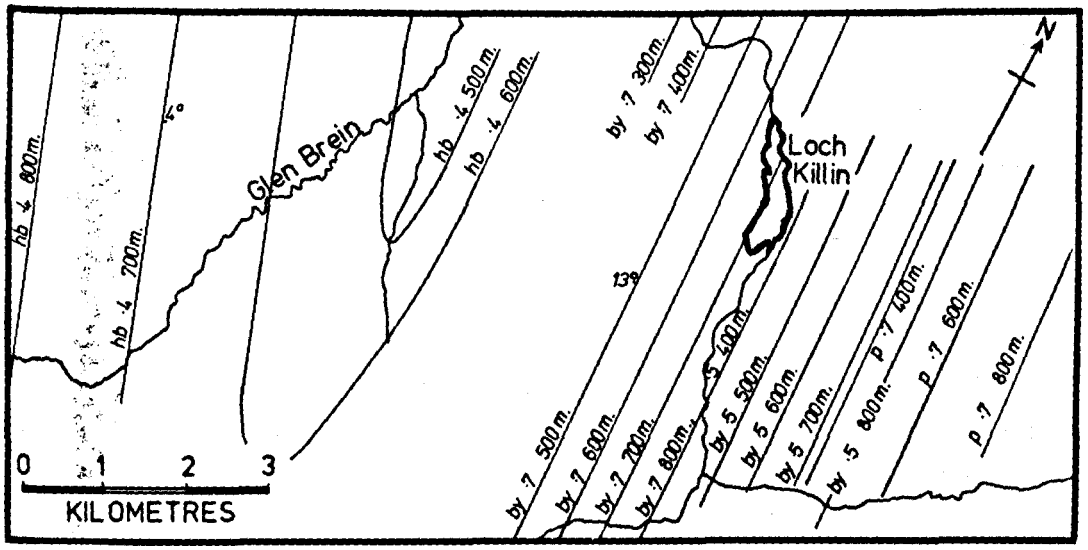
hb 4 800m.
hb 4 700m.
4°
Glen Brein
hb 4 500m.
hb 4 600m.
by 7 300m.
by 7 400m.
Loch Killin
13°
by 7 500m.
by 7 600m.
by 7 700m.
by 7 800m.
by 5 400m.
by 5 500m.
by 5 600m.
by 5 700m.
by 5 800m.
p 7 400m.
p 7 600m.
p 7 800m.
N
0 1 2 3
KILOMETRES

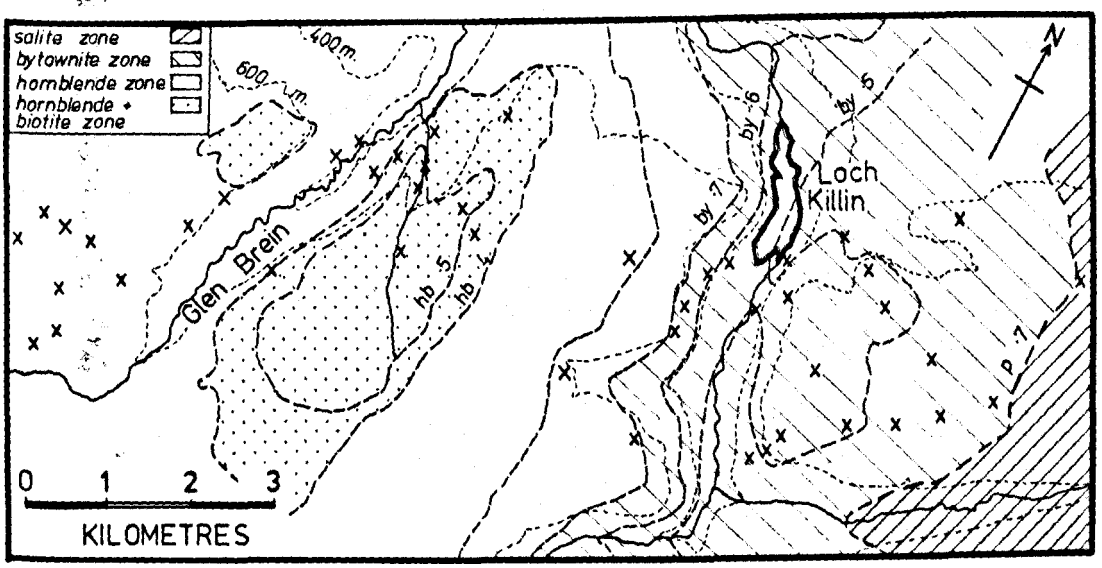
salite zone
bytownite zone
hornblende zone
hornblende + biotite zone
400m.
600m.
Glen Brein
hb 5
hb 4
by 6
by 5
by 7
Loch Killin
p 7
N
0 1 2 3
KILOMETRES

silicates with a CaO/Al_2O_3 ratio which exceeds 0.7

Hornblende: hornblende present in all calcite-free calc-silicates with a CaO/Al_2O_3 ratio which exceeds 0.4 (Winchester,1974b).

Hornblende and Biotite: this forms a transitional zone where both hornblende or biotite may be present in calc-silicates with CaO/Al_2O_3 ratios which exceed 0.4

The last zone was found by Winchester (1974c) to be 400 metres thick in northern Ross-shire, but in the Killin area its full thickness cannot be determined. Figure 57 shows isograd traces and the intervening zones as actual ground traces. The interval between the hornblende and pyroxene isograds is shown to be less than 1400 metres, assuming that the isograd surfaces have an average westerly dip of 13° around Loch Killin, as calculated using bytownite-bearing assemblages.

8.2.4 Correlation of Barrovian and calc-silicate zones

Correlation of calc-silicate zones with Barrovian zones is imprecise because, as previously noted, the aluminium silicate index minerals are frequently absent from Moinian and Killin pelites. Tentative correlations have been made based on isolated occurrences of kyanite, staurolite and sillimanite (Winchester,1972). Comparison of calc-silicate assemblages with sources of index minerals from pelitic zones by Tanner (1976) suggested that pyroxene-bearing calc-silicates could be equated with the sillimanite zone. Less decisive evidence was available for Tanner's bytownite/hornblende zone, possible equivalents

including three pelitic zones (sillimanite, kyanite and staurolite). However, most available information seemed to indicate an equivalent in the kyanite zone.

Kennedy (1949) produced similar results, equating his pyroxene with the Barrovian sillimanite zone and the biotite and zoisite zone with the Barrovian garnet zone. Winchester (1974b) correlated the hornblende isograd with the kyanite isograd and although the former occurs in the Killin area, a definite correlation of isograds should be avoided.

8.3 Structural Correlation and Timing of Metamorphic Events

It has already been stated that isograd surfaces deduced from the distribution of calc-silicate assemblages have apparently (cf. 8.2.3 (d)) been folded by D_3 folds. This conforms with the microstructural evidence which can be used to date the growth periods of major minerals.

This growth pattern which indicates two major periods of mineral growth is reflected in pelitic assemblages and is summarised in Table 8.1.

	Deformational Episode			
	1	2	3	4
				——→time
gt	g——	r & g	g	
bi	g——		g	PELITES
mus	g——			
chl			g	
hb	g—	g		WHITE
clzo	g—	g?		CALC-SILICATES
gt	g—	g?		
clpx	g—			
hb	g—			GREEN
act	——g——			CALC-SILICATES
gt	g—			
clzo + ep			g	

Table 8.1 Schematic Representation of the Major Features involved in the Timing of Metamorphism

Key: g=growth;r&g=rotation and growth
gt=garnet;bi=biotite;mus=muscovite;chl=chlorite;
hb=hornblende;clzo=clinozoisite;clpx=clinopyroxene;
act=actinolitic amphibole;ep=epidote

Two principal metamorphic peaks are indicated, M_1 apparently extending from before until just after the first phase of deformation. M_2 is very similar in grade and indeed a metamorphic 'plateau' may have existed to some extent between D_1 and D_2 since garnet growth appears to have continued between the two fold phases. The 'grade' during and until after the F_2 event must have remained high since the structural evidence indicates post-F_2 intrusion of the dykes in the Glen Doe semi-psammite. The dykes now exist as amphibolite bodies.

There is scant evidence for post-M_2 metamorphism. Localised retrogression is sporadically evident with muscovite and chlorite development, either axial planar to F_3 folds or replacing phases formed in the M_2 event.

8.3.1 Evidence from pelites

Psammitic metasediments do show many features which verify the association of minerals with structural deformations noted in pelites. However, the picture is less obvious as the increased competence due to greater quartz content renders these metasediments less able to adjust to deformation than their pelitic counterparts.

Within the pelites, many garnets are zoned, suggesting that growth occurred in several stages. Many also contain inclusion trails and these help establish the relative timing of metamorphic events and principal deformational episodes. However, not all garnets exhibit inclusion trails and many occur as small idioblastic grains, rarely disturbing the foliation, indicating static post-tectonic growth. Growth appears to have continued up to the D_3 phase of deformation.

Three samples with zonal growth and inclusions are described and each is enveloped by aligned mica flakes which outline the S_1 foliation and show later folding. Plate 42 exhibits a garnet from a sample which is composed of quartz, chlorite and garnet. The outcrop occurs as an elongate pod which is discordant to the S_1 foliation but partially folded (therefore suggesting rotation in D_2).

The features it exhibits suggest a syn-F_2 rotational core with a post-F_2 homogeneous rim.

Plate 43 (which is represented diagrammatically in Figure 58) illustrates a pretectonic and rotated core surrounded by a syntectonic ring with curved inclusion trails. The outer rim contains no inclusions and is probably post-tectonic. This would suggest that garnet growth continued up to and after the F_2 event. This is also suggested by the third example illustrated in Plate 44. Several zones can be determined, although interpretation may not be definitive. The growth periods can probably be assigned to post-F_1 rotation, growth during F_2 folding and growth post-dating F_2 folding.

Biotite occurs, with minor muscovite, as oriented flakes defining the S_1 foliation. Crystal growth was therefore largely syn-tectonic with the first period of deformation. Subsequent development is only reflected in the growth of some biotite and muscovite flakes parallel to the axial planes of some F_3 crenulations. Thus the latest growth is syn-F_3. Some grains are kinked by F_4 kink bands (as illustrated in Plates 26 and 27). Occasionally randomly oriented biotite grains are seen to occupy the nose of a minor fold and this may be an example of post-tectonic polygonisation (Spry, 1969). No mineral growth can be clearly associated with the F_4 episode of folding.

Plate 42

Inclusion trails in garnets

Plate 43

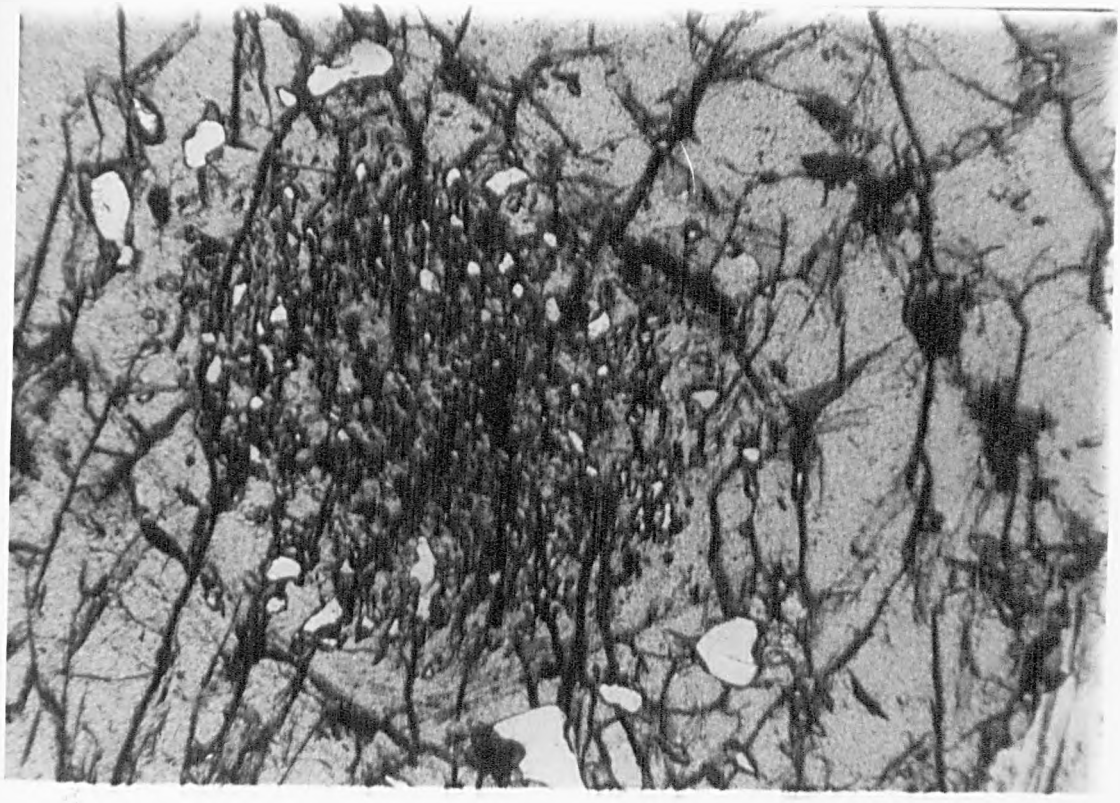

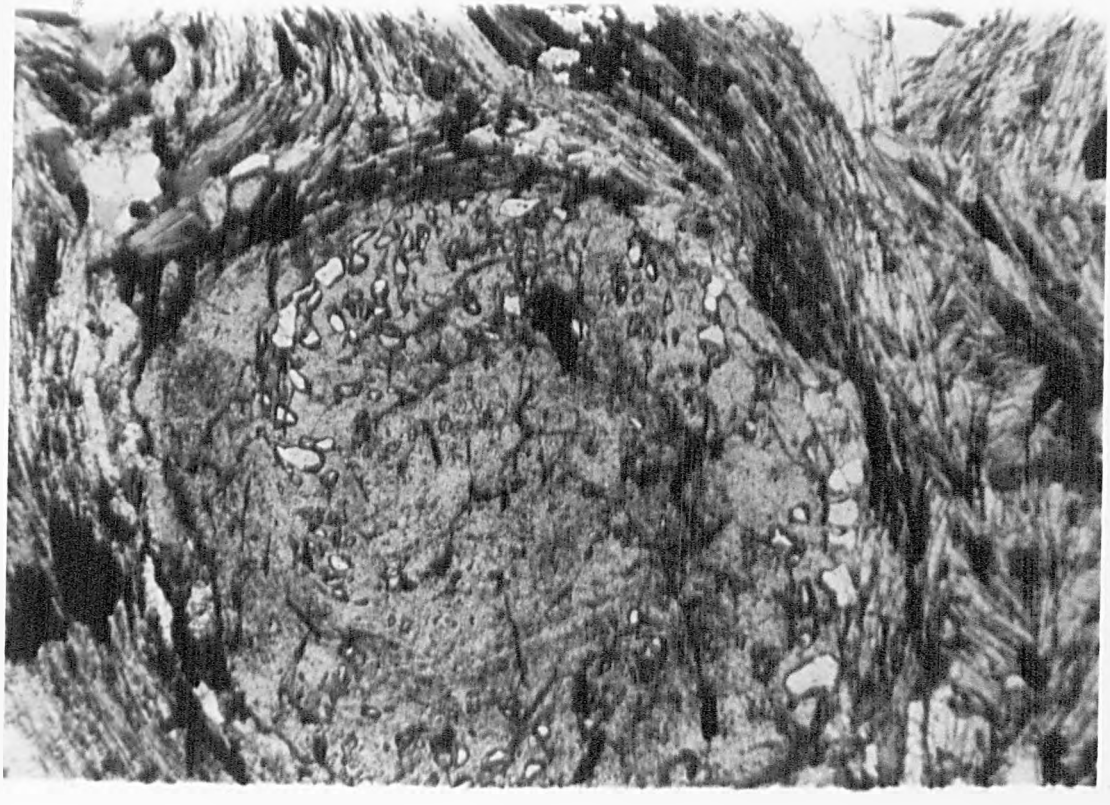

Figure 58 Outline of garnet growth zones (from Plate 43)

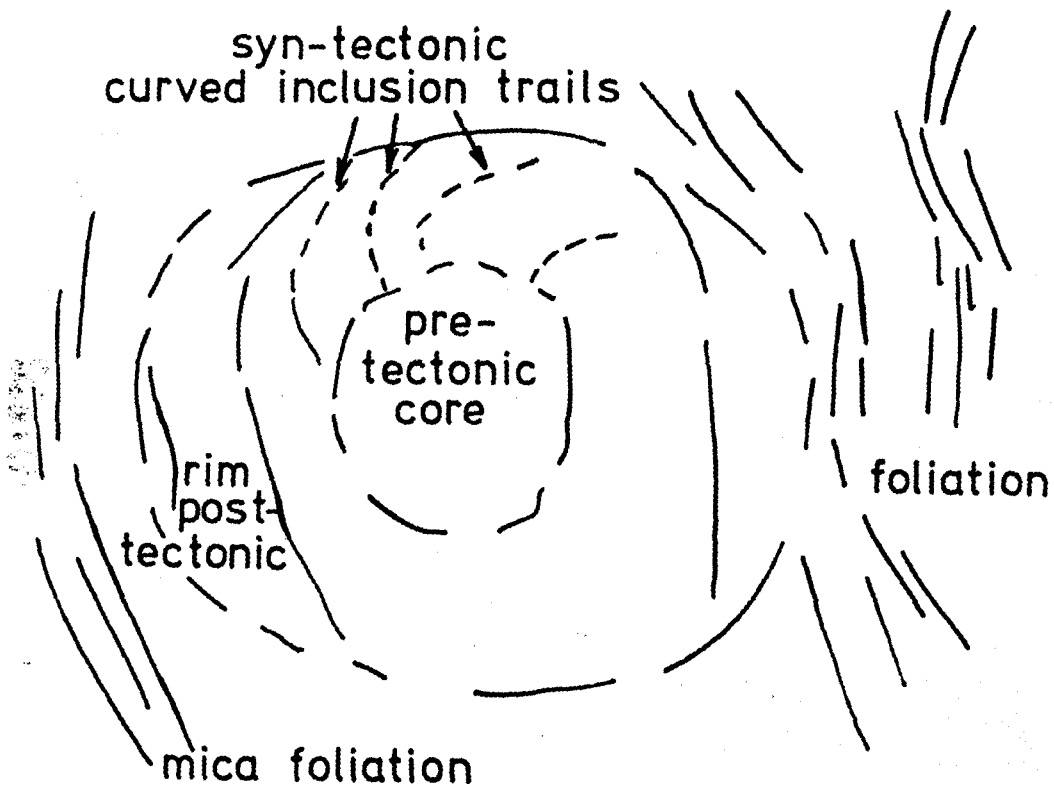
syn-tectonic
curved inclusion trails
pre-
tectonic
core
rim
post-
tectonic
foliation
mica foliation

Plate 44 Zoned garnet with inclusion trails

Plate 45 Post-tectonic chlorite overgrowing mica crystals

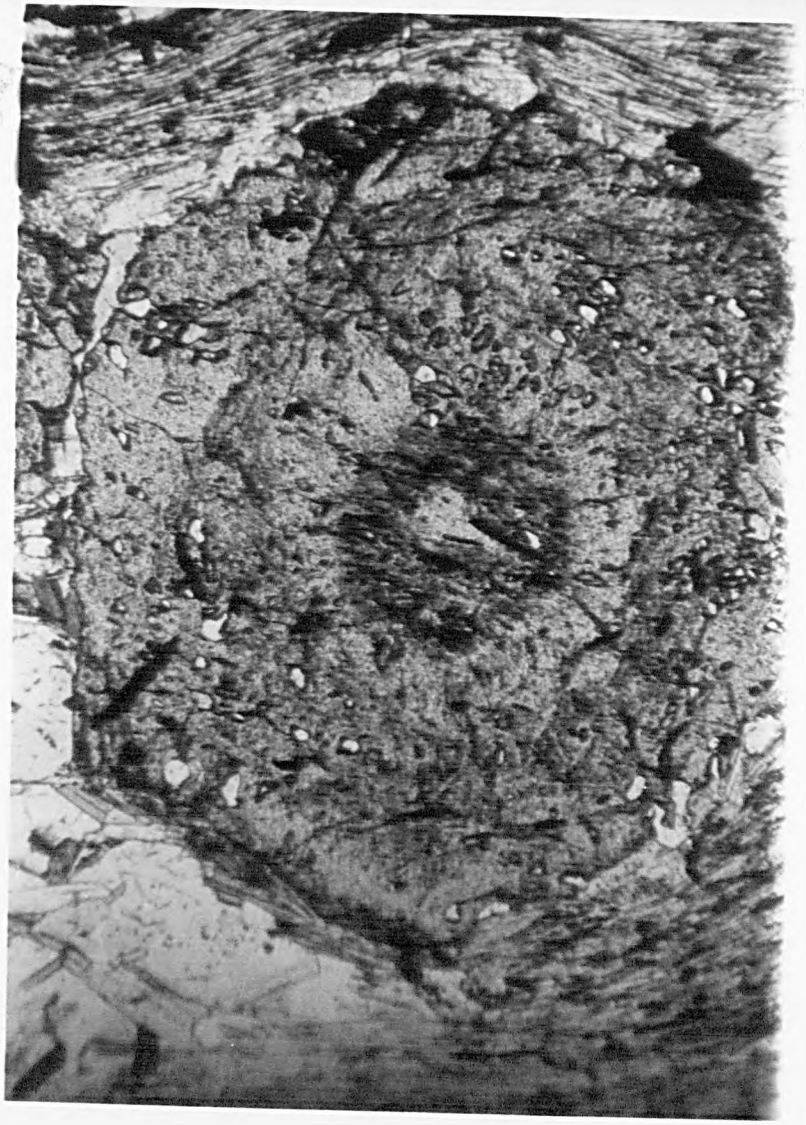

Chlorite is restricted to late growth and all examples exhibit post-tectonic growth. Plate 45 illustrates grains overgrowing micas oriented by F_3 crenulations. Since the effect of post-F_3 deformation is limited, it is not possible to specifically date the growth of chlorite further than a post-F_3 age.

Although opaque grains are common, they are rarely deformed. Plate 46 illustrates one exception with predominantly small grains of magnetite outlining an F_3 crenulation. The larger grains only partly reflect the crenulation form, indicating their relative competence.

8.3.2 Evidence from white calc-silicates

Hornblende, clinzoisite and garnet are the three minerals which provide most information. Although quartz and plagioclase (the latter often sericitised) are present, they provide little textural information. Quartz grains are slightly elongated within the S_1 foliation indicating pre to syn-tectonic growth. Evidence for later growth is scarce but there is polygonisation of larger grains.

Hornblende prisms define the S_1 foliation and this strong alignment suggests predominantly syn-tectonic growth. Early garnets are enclosed by hornblende and the latter also encloses pressure shadows of quartz which have subsequently polygonised. Later hornblende growth is limited to a few examples of growth along S_2 planes. The apparent lack of physical response to later deformations is a result of the relative competence of calc-silicate bands compared to the adjacent semi-pelitic or semi-psammitic rocks.

Clinozoisite blades and grains parallel the attitude of

Plate 46 Opaque grains outlining an F_3 crenulation

hornblende. Syn-tectonic grains contribute to the S_1 foliation and also enclose garnets. Later growth is restricted to scattered grains growing across the S_1 foliation and granules impinging on earlier blades. The scarcity of this feature renders correlation with a tectonic event difficult, but it would seem to show a similar development to that of hornblende.

Garnet growth in the calc-silicates is primarily syn-F_1 since it is enclosed by aligned hornblende prisms and bladed clinozoisite. Rare quartz inclusion trails may indicate a pre-F_1 growth. The inclusions, which form straight trails, are discordant to the S_1 fabric and in one instance present a tripartite division based on inclusion size (see Section 5.8.1). Later growth is indicated by small garnets in some calc-silicates. It is difficult to be certain about the period of growth due to the lack of features readily equated with later tectonic events. Since the smaller grains usually contain fewer inclusions (than the larger garnets) and often impinge upon biotite in the foliation, it may be assumed that they are at least post-F_1 in age.

8.3.3 Evidence from green calc-silicates

Evidence relating mineral growth to structural phases is again limited to a few minerals, namely amphibole, garnet and to a minor extent clinopyroxene and epidote. Growth of quartz and plagioclase is very similar to that exhibited in the white calc-silicates but sericitisation of the feldspar is much more prevalent thus obliterating textural relationships to a large degree.

Clinopyroxene growth is apparently syn-F_1 since the isolated tabular grains are all aligned within the foliation.

Response to subsequent deformation is difficult to discern, save for some slight fracturing.

Amphibole occurs as both hornblende and actinolitic amphibole. The former shows alignment with the S_1 fabric and often alternates with 'bands' of elongate quartz grains and sericite 'stringers' (after plagioclase). Actinolitic amphibole nucleates on grains of clinopyroxene (and appears to be derived from it) and assumes an orientation discordant to S_1 and aligned with the weak S_2 fabric (Plate 15 and section 3.4.3).

This syn-F_2 development is the latest growth of amphibole in the green calc-silicates and this may suggest that F_2 was slightly less intense than F_1.

Garnet is rare or absent from many green calc-silicates. When present it occurs only in skeletal form or as isolated granules (see Table 3.4). To determine a relative age is therefore difficult, but the skeletal texture suggests early growth followed by replacement. In many instances the garnet 'grains' are enclosed either partially or totally by 'webs' of epidote and clinozoisite. This is a late feature and is apparently unaffected by any deformation and must certainly be post-F_3.

8.4 Conclusions on Timing and Metamorphic Grade

From the foregoing sections, several conclusions can be drawn concerning the metamorphism of the Killin area.

i) The metamorphic grade increases from west to east in the eastern part of the area and is broadly constant in the west.

ii) The metamorphic zones constructed are not inverted,

and their thicknesses can be directly measured where white calc-silicates are present.

iii) The metamorphic zones are apparently folded by the F_3 generation folds and so relate to M_2.

iv) Two major metamorphic peaks were produced. The first peak accompanied F_1 and post-dated it a little. The second peak similarly accompanied F_2. This pattern is illustrated by the pelites and to a lesser extent by the white calc-silicates. The green calc-silicates indicate two periods of growth but no clear sequence of zonal phase assemblages can be seen in this particular suite.

v) In the pelitic lithologies a third low-grade metamorphic event (M_3) accompanied F_3.

vi) The M_3 event apparently had scant effect on the calc-silicate isograds established in M_2.

vii) Thermal effects of the post-tectonic granites were slight and would suggest that the rocks were still warm at the time, or under pressure (see also Sections 6.2.5 and 6.5).

APPENDIX ONE-TECHNIQUES AND METHODS OF COLLECTION, PREPARATION AND ANALYSIS OF SAMPLES

115 samples from the Killin area were analysed using X-ray fluorescence spectrometry. This technique was used in preference to classical chemical methods due primarily to the greater speed of analysis. Errors are considered to be greater in the rapid analysis method but the accuracy is considered sufficient for this first insight into the geochemistry of these metasediments. Several publications describe in detail the equipment, sample preparation, analysis and calculations (Leake et al.,1969; Norrish & Chappell, 1967) hence the following sections present basic relevant information.

A1.1 Sample Collection

Fresh field samples (approximately one kilogram minimum weight) were obtained for analysis. Distribution of samples was determined by amount of exposure in many parts of the area, but it was attempted with the more common lithotypes to collect representative samples of the lithologic units. River and stream sections presented ideal access for specimen collection and many samples are from such locations.

Depending upon the grain size, a particular minimum weight was prepared from the field sample in order that a representative analysis be produced. For grain sizes up to 1 millimetre, 500 grams of sample were taken and for grain sizes up to 10 millimetres, 1000 grams. Some calc-silicate bands collected for analysis were thin (<1.5 centimetres thick) and large amounts had to be taken to allow for the removal of adjoining rock-types. To facilitate the removal

of the adjoining rock, many samples were sawn into thin slices thus allowing splitting along the margin of the calc-silicate.

A1.2 Preparation of Sample

Any weathered faces were removed either using a rock-splitter or a rock-cutting circular saw. The sample was then reduced to small ($\leqslant$2 centimetre) blocks using a Denbigh fly-press rock splitter and further ground to gravel (5 millimetres and less) in a Sturtevant 5" x 2" jaw crusher. After homogenisation by successive cone-and-quartering, one quarter of the sample was selected. The gravel was reduced to a powder (120 mesh) using a Tema disc mill. The mill reduces the charge of approximately 100-125 grams to powder by eccentric movements of two rings and a central barrel of tungsten carbide (Widia) within the shallow pot.

The powder was then poured onto a clean sheet of paper and thence decanted into a sample bag or jar. The mill and tungsten carbide rings were cleaned using a vacuum, clean cloths, fine-bristled brushes and tissues. Every attempt was made to keep machinery as clean as possible to avoid contamination.

For X-ray analysis the powder (approximately 20 grams) was homogenised (to 200 mesh) in a Glen Creeston M280 tungsten carbide ball mill for a further 30 minutes.

A1.3 Determination of Loss on Ignition

After leaving overnight in an oven (at 110°C), one gram of homogenised powder was accurately (to within 0.01%) weighed out into a platinum dish. Batches of six dishes, each containing a different sample, were placed in a furnace at

1000°C for 30 minutes and each was partially covered with a platinum lid. After the correct time, the dishes were removed from the furnace and quickly transferred to a desiccator. After allowing to cool for 20 minutes each sample was weighed again and the weight loss noted.

To check the reproducibility of this process, six samples were chosen at random for a repeat measurement. These comprised amphibolites (with higher than average losses), semi-psammites and a semi-pelite. The average variation was 5.25% for the six samples.

A1.4 Preparation of Discs for Analysis by X.R.F.

The homogenised powder was prepared for analysis in two ways, either as a pressed pellet or a fused disc. The former method, using unignited powder was used for analysis of trace elements and sodium. A powder sample was preferable for trace elements due to their low concentrations, and any sample dilution would result in a sensitivity loss.

The pellets were prepared by thoroughly mixing 6 grams of the powder in an agate mortar with a few drops of binding agent, Mowiol N90/98 (produced by Hoechst Chemicals Ltd.). The powder-cement mix was then compressed in a cylindrical dye faced on either side by polished tungsten carbide coated plattens. The disc assembly was subjected to 5 tons weight for one minute and 25 tons weight for a further four minutes. After drying overnight at 110°C, the pellet was ready for analysis. Such pellets were very useful since the surfaces were smooth and both sides could be analysed.

The fused discs with which most of the major elements were determined, were produced using a technique modified

from that used by Norrish & Hutton (1969). 0.5 grams of ignited powder were mixed with 2.5 grams of lithium metaborate flux ($LiBO_2$, Spectroflux SP 100A) and then fused in a platinum crucible over a meker burner until quiescent and homogeneous. The melt was then poured onto a brass die on a hotplate (at a temperature of 230°C) and immediately chilled to glass by stamping and cooling with an aluminium plunger. The resulting glass disc was contained within a ring of copper wire, previously mounted on the die.

The fusion method was used to avoid the influence of differing particle sizes and to help overcome effects due to variations in absorption coefficients. Lithium metaborate also readily dissolved all silicate powders. (Absorption coefficients, in this case the mass-absorption coefficient, have fixed values for a given element for a particular wavelength of X-rays and refer to the absorption of incident X-rays in the sample being analysed).

A1.5 Methods of Analysis

Each sample, whether fused disc or pressed powder pellet was analysed using the Philips PW 1212 fully automatic sequential X-ray spectrometer in the Department of Geology at Keele University.

An approach similar to that used by Leake et al.(1969) was adopted. For major elements, the fused discs were analysed for a minimum of three cycles and the mean of these recorded. For pressed powder pellets, both sides of the sample were analysed, usually for at least two cycles. The thickness of the powder pellets exceeds the critical depth of penetration by the X-rays and each side effectively

forms a duplicate sample.

Counts were made on both peaks and backgrounds and the net counts (peak-background) were used, with or without additional corrections for matrix effects. Jenkins & de Vries (1967) provide full details of this approach.

In all cases, calibrations were achieved by analysing selected international standards (Flanagan, 1974) concurrently. Keele departmental spikes were also used. The international standards used included W-1, PCC-1, BCR-1 and AGV-1. Apparent fluorescent values were obtained following an approach similar to that of Harvey et al. (1973). Inter-element corrections were made using the method of Norrish & Hutton (1969).

Calibration of the trace element data was achieved using international standards, with mass absorption corrections being applied when necessary. The method of Reynolds (1963) was followed for Rb, Sr, Y and Zr determination.

Instrumental precision has been gauged using replicate analyses of the same rock samples over a period of time. For this particular study, several analyses were made of two standards, KUI-3 (Keele departmental) and W-1 (International). Duplicate analyses of Killin samples were also made and conformed to the figures presented in Table A1.1. The coefficient of variation (or relative deviation) can be used to compare sets of results on a percentage basis.

Seven major elements have been particularly chosen for this exercise due to their greater usage in the geochemical study (Chapter 7).

The precision is generally poorer for elements present in small or trace amounts and this applies to the lower

concentrations in Table A1.1.

	mean	range	standard deviation	coefficient of variation (%)
SiO_2	70.120	0.919	0.40	0.57
Al_2O_3	15.20	0.079	0.03	0.20
Fe_2O_3	10.982	0.117	0.043	0.39
CaO	1.843	0.069	0.03	1.62
K_2O	4.133	0.024	0.01	0.24
TiO_2	0.520	0.014	0.06	1.15
MnO	0.176	0.009	0.004	2.27

Table A1.1 Summary of Precision (W-1 used for Fe and Mn, KUI-3 for remainder)

Accuracy is the extent to which an analysis is capable of giving the 'correct' value for a known sample. To this end, analyses of international standards are used and compared to the recommended values. Table A1.2 compares the accepted values (for the seven major elements already used) with repeat analyses performed during this study for the W-1 standard.

All the oxides show good agreement save for the lower concentrations, where small changes appear relatively large. It may be that the results overall are slightly low since all elements but MnO show a comparatively low value. The variation is, however, low and constant.

It does seem that this method of analysis is more than adequate for most elements where rapid analysis of many samples is required.

	W-1	comparative values	relative variation(%)
SiO_2	52.64	51.58	-2.01
Al_2O_3	15.00	14.65	-2.33
Fe_2O_3	11.09	10.98	-0.99
CaO	10.96	10.95	-0.09
K_2O	0.64	0.60	-6.25
TiO_2	1.07	1.05	-1.87
MnO	0.17	0.18	+5.88

Table A1.2 Summary of Accuracy

APPENDIX TWO-STATISTICAL ANALYSIS

A2.1 Introduction to Student's t-test

A full description (see for example Till, 1974) and derivation is not necessary here but the basic information is provided.

The t-test is a statistical testing hypothesis based on the t-distribution. Student (a pseudonym for the statistician Gosset) defined the t-distribution for sample means. Values of t can be calculated for all possible random samples from a normal distribution. The curve thus produced closely resembles a normal curve (an equal distribution of values about the population mean producing a symmetrical curve).

The t-distribution can be used to test populations whose standard deviations are unknown to predict the population mean. Hence the average (or population mean) can be predicted from a small group of samples, assuming these samples are from a normally distributed population.

That part of the t-curve can be found which contains 95% of its area and this area can be taken symmetrically about the mean, leaving 2.5% of the area at each side or tail of the distribution. Random samples can then be compared to this distribution and since 95% of all possible t-values are within the curve, the probability of t being outside that range is 0.05.

A t-test is therefore used to determine if there is a significant difference between two groups of values. A hypothesis (called the Null Hypothesis) is set up to compare population means. The question is thus posed-how probable

is it that our two samples represent identical populations. The purpose is to find out with what confidence the hypothesis can be accepted or rejected. The calculated value of t can then be compared with t values from statistical tables to determine acceptance or rejection.

A2.2 Application to Analyses

Student's t-test has been applied to chemical analyses of rock samples from the Killin area. A group of rock analyses forms the random sample from a population (equivalent to the formation as a whole) and two samples are compared for a particular element oxide. In this way, all the components for groups of samples can be compared to determine whether the samples can be considered to belong to the same population.

The t-test was undertaken by a Digico M16E computer in the Department of Geology at Keele University. Insertion of the values within the two samples under consideration produced mean and standard deviation values. The computed t-value was compared to the value from statistical tables and the hypothesis that the two samples form part of the same population was accepted or rejected at the 95% level.

These results were used, where appropriate, as an aid in the geochemical discussions of Chapter 7.

APPENDIX THREE

The following pages list major element analyses of samples used in this study. Each entry lists ten oxides and is preceded by the formation and sample number below which the grid reference is provided. The four formations are abbreviated thus;

F-Fechlin

K-Knockchoilum

G-Glen Doe

M-Monadhliath

LOI refers to the loss on ignition. The samples are grouped by lithology and numerically within these suites. Specific groups referred to in the text are listed below;

Amphibolites-foliated:F652,F654

-unfoliated:G6148,G6187,G6189,G6192

Granophyres-Group 1:K6251,K6253,G6144,G6215,G76, G722,M6211,M6230

-Group 2:K6233,G725

Granites-Fechlin samples represent Foyers

-Knockchoilum samples represent Allt Crom

White calc-silicate groups are listed in Table 3.1. Trace element data are listed after the major element analyses.

Semi-Pelitic

	F 626	F 648	F 681	K 634	K 660	K 666
	496140	490145	489141	497137	502128	504126
SiO_2	52.90	65.88	65.00	56.52	56.15	55.94
Al_2O_3	20.79	15.43	15.30	18.28	18.77	19.89
Fe_2O_3	8.52	5.42	5.23	9.11	8.21	7.28
MgO	3.19	1.97	1.88	2.85	2.59	2.18
CaO	2.23	1.52	1.45	1.23	2.18	1.68
Na_2O	4.19	3.06	3.40	2.09	2.14	2.98
K_2O	4.45	3.95	3.80	5.12	4.27	5.21
TiO_2	1.01	0.63	0.63	0.93	0.88	0.98
MnO	0.15	0.08	0.08	0.14	0.14	0.11
P_2O_5	0.29	0.17	0.17	0.15	0.22	0.27
LOI	1.70	1.20	1.10	1.90	2.60	1.80
TOTAL	99.42	99.31	98.04	98.42	98.15	98.32

	K 687	K 695	K 6123	K 6220	K 6250	K 6255
	477115	478119	492123	486064	524058	517055
SiO_2	58.06	64.07	60.76	47.86	52.04	58.92
Al_2O_3	18.43	15.67	17.76	23.63	19.10	17.38
Fe_2O_3	8.45	6.43	6.82	9.29	11.14	7.85
MgO	2.86	2.16	2.33	3.01	3.77	2.41
CaO	1.51	1.41	1.45	1.23	1.29	1.89
Na_2O	2.58	1.90	2.49	1.65	2.27	4.03
K_2O	4.74	4.07	5.04	6.83	5.56	3.16
TiO_2	0.90	0.73	0.85	1.16	1.12	1.02
MnO	0.12	0.10	0.11	0.15	0.18	0.13
P_2O_5	0.22	0.18	0.21	0,42	0.20	0.20
LOI	2.07	1.50	1.70	2.90	2.05	1.85
TOTAL	99.94	98.22	99.52	98.13	98.72	98.74

	G 611	G 676A	G 6118	G 6176	G 6177	G 6182
	521113	518120	510112	442088	442087	442085
SiO_2	55.49	55.31	64.03	61.90	62.00	55.17
Al_2O_3	18.94	21.57	15.52	15.16	16.68	18.65
Fe_2O_3	8.97	6.92	6.48	8.62	6.82	9.82
MgO	2.87	1.80	2.28	2.92	2.35	3.27
CaO	1.39	1.38	1.34	1.49	1.42	1.04
Na_2O	1.58	1.85	3.19	2.84	2.69	3.66
K_2O	5.36	4.61	3.69	3.17	4.20	3.39
TiO_2	0.93	1.13	0.75	0.79	0.81	1.02
MnO	0.13	0.18	0.10	0.14	0.10	0.14
P_2O_5	0.18	0.40	0.17	0.24	0.22	0.37
LOI	2.20	3.20	1.90	2.00	1.25	2.60
TOTAL	98.04	98.35	99.45	99.27	98.54	99.13

	G 6184	G 6185	G 79	G7525A	M 617	M 694
	443084	443083	467076	479089	525101	488094
SiO_2	64.12	63.86	53.43	62.13	51.22	57.70
Al_2O_3	15.25	14.68	17.37	14.47	23.03	18.83
Fe_2O_3	5.82	6.42	7.81	9.42	8.02	8.47
MgO	2.15	1.81	2.55	2.98	2.57	2.77
CaO	1.64	2.30	8.43	3.04	1.14	1.54
Na_2O	3.28	4.51	4.88	3.10	1.34	1.72
K_2O	3.39	1.47	2.17	1.75	6.82	4.82
TiO_2	0.70	0.72	1.09	0.85	1.19	0.87
MnO	0.11	0.19	0.14	0.37	0.19	0.14
P_2O_5	0.19	0.28	0.40	0.20	0.33	0.27
LOI	1.50	3.20	2.08	0.70	3.30	2.05
TOTAL	98.15	99.44	100.35	99.01	99.15	99.18

	M 6115	M 6137	M 7553
	525078	487086	456053
SiO_2	55.98	65.12	60.34
Al_2O_3	19.39	15.49	17.98
Fe_2O_3	9.45	4.71	7.14
MgO	3.09	1.53	2.50
CaO	1.56	3.54	3.84
Na_2O	1.51	4.62	4.53
K_2O	5.03	0.97	1.68
TiO_2	0.99	0.79	0.88
MnO	0.17	0.26	0.19
P_2O_5	0.32	0.26	0.16
LOI	2.53	1.90	0.50
TOTAL	100.02	99.21	99.74

Semi-Psammitic

	F 627	F 6171	K 633	K 638	K 6245	K 6249
	497139	496142	497138	501136	527059	524058
SiO_2	69.84	71.81	67.16	74.04	67.45	68.96
Al_2O_3	13.20	14.42	15.67	11.82	13.69	14.30
Fe_2O_3	4.80	0.84	5.55	3.55	5.07	5.08
MgO	1.76	0.42	1.80	1.15	1.65	1.80
CaO	1.50	0.78	1.87	1.61	1.57	1.21
Na_2O	2.89	3.79	2.63	3.20	3.89	2.58
K_2O	2.90	5.12	2.94	2.23	3.03	3.50
TiO_2	0.67	0.20	0.83	0.61	0.65	0.63
MnO	0.08	0.05	0.12	0.08	0.08	0.08
P_2O_5	0.14	0.12	0.17	0.11	0.20	0.12
LOI	0.80	1.00	1.70	0.70	2.35	1.15
TOTAL	98.58	98.55	100.54	99.10	99.63	99.41

	G 64	G 65	G 69	G 613	G 616	G 671
	525107	523109	528110	518113	522109	506124
SiO_2	68.59	69.82	69.07	68.31	69.31	67.16
Al_2O_3	14.06	12.89	13.16	14.13	13.10	14.21
Fe_2O_3	3.72	4.30	3.71	4.71	4.19	5.54
MgO	1.15	1.52	1.26	1.69	1.41	1.72
CaO	3.23	1.63	3.40	1.34	2.31	2.77
Na_2O	3.18	3.32	2.80	3.21	3.24	2.71
K_2O	1.81	2.79	1.91	3.10	2.75	2.30
TiO_2	0.53	0.65	0.59	0.64	0.63	0.78
MnO	0.12	0.08	0.12	0.09	0.09	0.14
P_2O_5	0.17	0.13	0.16	0.15	0.11	0.21
LOI	1.90	1.20	2.70	1.50	2.00	1.50
TOTAL	98.46	98.33	98.88	98.87	99.14	99.04

	G 673B	G 6129	G 6163	M 6217	M 6219
	511117	464109	451088	456054	466059
SiO_2	69.37	69.29	69.22	66.97	66.48
Al_2O_3	14.09	13.46	10.92	15.46	14.89
Fe_2O_3	4.72	4.50	3.66	6.05	4.79
MgO	1.52	1.37	1.18	1.68	1.22
CaO	4.33	2.12	5.12	3.31	4.17
Na_2O	2.16	4.22	3.12	4.48	4.32
K_2O	1.56	1.40	1.76	1.14	0.74
TiO_2	0.68	0.66	0.64	0.64	0.77
MnO	0.19	0.11	0.13	0.27	0.40
P_2O_5	0.16	0.13	0.12	0.23	0.47
LOI	1.50	1.30	4.10	0.70	0.60
TOTAL	100.28	98.56	99.97	100.93	98.85

White Calc-silicates

	G 669	G 673	G 674	G 6213	G 75	G 710
	506126	511117	511118	466073	478088	467076
SiO_2	63.79	71.31	64.96	66.18	57.89	51.83
Al_2O_3	15.42	13.23	16.59	14.37	17.76	15.18
Fe_2O_3	5.50	4.77	3.52	4.24	6.12	4.70
MgO	1.56	1.45	1.37	1.43	2.13	1.92
CaO	4.74	4.63	5.02	9.41	10.53	15.43
Na_2O	3.66	2.56	3.01	1.54	1.61	2.28
K_2O	1.83	1.18	2.54	0.34	0.64	1.06
TiO_2	0.77	0.72	0.66	0.59	0.77	0.65
MnO	0.31	0.19	0.23	0.30	0.43	0.45
P_2O_5	1.19	0.17	0.19	0.19	0.25	0.25
LOI	1.60	1.10	2.00	2.00	2.27	7.06
TOTAL	100.37	101.31	100.09	100.59	100.40	100.86

	G 757	G7525B	G 7526	G 7527	G 7555	M 67
	455049	479089	479089	479089	454050	532098
SiO_2	63.13	56.76	58.01	58.03	64.20	62.72
Al_2O_3	15.38	18.01	17.96	17.80	15.72	17.12
Fe_2O_3	3.20	6.06	6.14	6.12	5.43	5.28
MgO	1.14	2.12	2.12	2.12	1.74	1.61
CaO	9.48	10.77	8.73	10.81	5.99	6.60
Na_2O	2.73	2.08	2.83	1.72	2.84	0.69
K_2O	0.23	0.24	0.56	0.31	0.74	2.50
TiO_2	0.66	0.77	0.81	0.77	0.77	0.66
MnO	0.33	0.43	0.43	0.44	0.46	0.35
P_2O_5	0.21	0.26	0.26	0.27	0.35	0.37
LOI	4.10	0.60	0.90	0.90	0.90	1.80
TOTAL	100.59	98.10	98.75	99.29	99.14	99.70

	M 692	M 6111	M 6142	M 6143	M 6155	M 6156
	487091	523088	482086	484090	519089	513076
SiO_2	59.74	64.67	60.85	61.42	63.17	63.23
Al_2O_3	18.45	16.21	16.26	16.91	16.60	15.85
Fe_2O_3	4.43	3.75	5.67	4.58	4.52	5.44
MgO	1.44	1.26	1.76	0.96	1.69	1.90
CaO	12.72	6.36	8.19	7.83	9.38	6.50
Na_2O	0.79	1.89	2.97	3.19	0.49	2.68
K_2O	0.61	1.77	0.51	0.64	1.48	0.56
TiO_2	0.65	0.79	0.71	0.86	0.73	0.75
MnO	0.42	0.23	0.34	0.60	0.38	0.27
P_2O_5	0.38	0.22	0.24	0.53	0.31	0.23
LOI	1.20	1.20	0.60	1.10	1.80	0.80
TOTAL	100.83	98.35	98.10	98.62	100.55	98.22

	M 6157	M6157A	M 6207	M 6208	M 6209	M 6210
	513076	513076	455065	455065	455065	460063
SiO_2	61.69	62.94	61.73	64.54	66.69	57.55
Al_2O_3	16.72	16.37	17.28	16.42	15.72	18.64
Fe_2O_3	4.77	4.13	4.23	4.08	3.87	4.84
MgO	1.51	1.35	1.38	1.25	0.98	1.81
CaO	9.32	9.26	10.00	8.04	10.12	12.12
Na_2O	1.09	0.91	1.74	2.55	0.76	1.94
K_2O	0.54	0.65	0.29	0.44	0.25	0.46
TiO_2	0.74	0.68	0.55	0.52	0.69	0.65
MnO	0.29	0.25	0.44	0.33	0.36	0.39
P_2O_5	0.27	0.30	0.23	0.26	0.09	0.28
LOI	1.10	1.80	0.90	1.00	1.10	2.10
TOTAL	98.04	98.64	98.77	99.43	100.63	100.78

	M 6216	M 6221	M 6223	M 6224	M 6225	M 6228
	454068	476071	523094	525095	525095	524071
SiO_2	61.20	67.86	61.91	59.75	65.48	63.12
Al_2O_3	17.73	15.75	16.05	16.74	16.93	16.83
Fe_2O_3	5.25	3.11	3.42	4.10	3.71	3.64
MgO	1.74	0.75	1.21	1.31	1.21	1.24
CaO	8.64	7.99	9.09	11.98	7.86	10.40
Na_2O	2.77	2.55	2.11	0.71	1.16	0.69
K_2O	0.50	0.17	1.04	0.81	0.65	1.34
TiO_2	0.76	0.54	0.65	0.68	0.57	0.66
MnO	0.37	0.32	0.26	0.47	0.36	0.28
P_2O_5	0.28	0.27	0.19	0.30	0.26	0.23
LOI	0.80	0.70	3.00	2.40	0.80	1.60
TOTAL	100.04	100.01	98.93	99.25	98.99	100.03

	M 73	M 765	M 7552	M 7553	M 7554
	474076	447062	456053	456053	456053
SiO_2	59.60	62.76	60.32	63.27	64.90
Al_2O_3	16.74	17.75	17.61	16.69	15.40
Fe_2O_3	6.98	4.49	4.41	4.23	5.13
MgO	2.08	1.57	1.46	1.18	1.36
CaO	10.70	6.24	9.75	11.60	6.87
Na_2O	1.21	3.53	1.81	0.67	2.22
K_2O	0.17	1.63	0.68	0.51	0.60
TiO_2	0.72	0.71	0.63	0.65	0.58
MnO	0.81	0.28	0.40	0.38	0.51
P_2O_5	0.33	0.44	0.54	0.43	0.30
LOI	1.15	1.15	2.40	1.20	0.90
TOTAL	100.49	100.55	100.01	100.79	98.77

Green Calc-silicates

	F 651	F 653	K 686	K 699	K 6104	K 745
	494143	496142	477116	486116	492136	472053
SiO_2	62.89	64.82	64.34	54.69	64.07	66.03
Al_2O_3	15.75	11.22	14.64	14.18	11.90	14.58
Fe_2O_3	4.18	3.72	4.20	4.77	3.06	4.23
MgO	1.62	1.51	1.59	1.67	1.23	1.48
CaO	11.61	9.45	9.14	14.78	12.92	8.24
Na_2O	0.85	0.60	2.87	0.86	0.07	2.30
K_2O	0.77	3.93	1.63	1.61	2.93	0.93
TiO_2	0.73	0.65	0.55	0.66	0.52	0.70
MnO	0.25	0.26	0.27	0.36	0.31	0.21
P_2O_5	0.27	0.17	0.16	0.28	0.13	0.19
LOI	1.10	2.20	0.50	5.70	4.70	1.90
TOTAL	100.02	98.53	99.90	99.56	101.84	100.79

	K 752	K 755
	470052	442028
SiO_2	65.48	62.83
Al_2O_3	15.44	15.26
Fe_2O_3	4.34	3.84
MgO	1.51	1.46
CaO	6.36	6.64
Na_2O	2.85	0.75
K_2O	1.74	4.06
TiO_2	0.70	0.70
MnO	0.16	0.36
P_2O_5	0.17	0.20
LOI	1.80	4.48
TOTAL	100.55	100.58

Amphibolites

	F 652	F 654	G 6148	G 6187	G 6189	G 6192
	496142	496143	469078	444082	440081	444080
SiO_2	46.40	43.89	50.53	42.74	45.62	44.93
Al_2O_3	13.54	13.93	12.57	7.38	10.04	6.99
Fe_2O_3	13.52	13.76	10.20	8.95	7.78	10.43
MgO	7.44	7.58	8.67	21.33	9,56	25.83
CaO	9.96	9.11	8.88	8.32	10.65	5.85
Na_2O	0.98	0.30	1.98	0.02	0.95	0.25
K_2O	2.05	5.17	1.74	2.33	1.91	0.26
TiO_2	2.61	2.99	1.10	0.61	0.77	0.55
MnO	0.26	0.24	0.21	0.16	0.18	0.16
P_2O_5	0.30	0.39	0.34	0.07	0.25	0.19
LOI	2.00	1.90	2.60	8.90	11.70	5.90
TOTAL	99.06	99.26	98.82	100.81	99.41	101.34

Marginal to Amphibolites

	G 6183	G 6191	G 714
	443084	445081	471111
SiO_2	67.92	50.69	58.54
Al_2O_3	12.64	18.04	17.99
Fe_2O_3	3.32	6.62	7.68
MgO	2.42	2.57	2.79
CaO	1.61	5.30	0.94
Na_2O	4.26	0.04	3.58
K_2O	2.80	5.14	4.54
TiO_2	0.62	0.97	0.96
MnO	0.09	0.11	0.12
P_2O_5	0.17	0.22	0.22
LOI	2.50	8.40	2.30
TOTAL	98.35	98.10	99.66

Granites

	F 657	F 658	K 6235	K 6244
	496142	496143	524059	529061
SiO_2	70.86	76.14	69.97	70.06
Al_2O_3	13.81	11.18	15.08	15.03
Fe_2O_3	3.66	2.88	1.61	1.84
MgO	1.34	0.97	0.64	0.60
CaO	2.42	2.18	1.18	0.88
Na_2O	3.26	2.75	4.30	4.25
K_2O	1.97	1.27	4.43	5.10
TiO_2	0.55	0.55	0.30	0.26
MnO	0.09	0.08	0.04	0.04
P_2O_5	0.14	0.12	0.08	0.09
LOI	1.00	0.80	0.50	0.85
TOTAL	99.10	98.92	98.13	99.00

Granophyres

	K 6233	K 6251	K 6253	G 6144	G 6215	G 76
	524059	521054	518055	492111	447091	468076
SiO_2	73.66	75.21	73.49	74.33	74.28	75.96
Al_2O_3	11.82	14.49	13.96	13.67	14.17	14.17
Fe_2O_3	3.35	0.51	0.14	0.22	0.50	0.34
MgO	1.00	0.22	0.15	0.19	0.23	0.08
CaO	2.26	0.44	0.34	0.39	0.53	0.34
Na_2O	2.94	4.56	5.00	4.80	4.70	4.81
K_2O	1.70	4.06	4.00	4.43	5.18	4.46
TiO_2	0.52	0.11	0.11	0.10	0.15	0.11
MnO	0.07	0.04	0.02	0.02	0.06	0.03
P_2O_5	0.11	0.01	0.02	0.01	0.02	0.01
LOI	1.70	1.10	2.30	0.80	0.55	0.67
TOTAL	99.13	100.70	99.53	98.96	100.37	100.99

	G 722	G 725	M 6211	M 6230
	461111	506117	464064	521072
SiO_2	76.05	67.51	74.94	73.72
Al_2O_3	14.12	15.41	14.21	14.18
Fe_2O_3	0.45	3.17	0.22	0.20
MgO	0.17	1.22	0.17	0.18
CaO	0.23	1.64	0.33	0.68
Na_2O	4.81	4.58	4.65	5.01
K_2O	4.44	4.02	4.47	4.12
TiO_2	0.12	0.60	0.11	0.11
MnO	0.03	0.07	0.02	0.02
P_2O_5	0.02	0.19	0.02	0.01
LOI	0.70	2.10	0.70	0.90
TOTAL	101.14	100.51	99.84	99.13

Microdiorite

	G 713
	468100
SiO_2	59.94
Al_2O_3	15.66
Fe_2O_3	6.24
MgO	2.96
CaO	2.16
Na_2O	4.51
K_2O	4.02
TiO_2	1.16
MnO	0.10
P_2O_5	0.62
LOI	1.90
TOTAL	99.27

Quartzites (for information)

	G 6138	M 623	M 6161	M 6206
	488082	525096	516076	449055
SiO_2	92.29	81.21	74.12	94.30
Al_2O_3	3.89	10.07	15.42	4.13
Fe_2O_3	0.34	1.04	Tr	Tr
MgO	0.29	0.40	0.41	0.17
CaO	0.12	2.32	0.06	0.17
Na_2O	1.09	1.83	0.04	1.63
K_2O	0.88	2.21	5.74	0.57
TiO_2	0.09	0.29	0.11	0.09
MnO	0.01	0.02	Tr	0.01
P_2O_5	0.03	0.05	0.02	0.03
LOI	0.50	1.80	2.40	0.70
TOTAL	99.53	101.24	98.32	101.80

White Calc-silicates*

	7535	7536	7537	7538	7539	7540
	554113	564112	564112	564112	562095	553096
SiO_2	65.10	62.70	63.68	78.68	66.63	60.97
Al_2O_3	16.25	17.91	16.33	10.95	15.25	17.03
Fe_2O_3	5.03	3.27	3.44	1.54	4.63	5.01
MgO	1.51	0.82	1.08	0.39	1.37	1.78
CaO	5.50	13.15	11.58	5.79	6.68	6.43
Na_2O	3.59	0.66	1.02	0.70	0.91	4.39
K_2O	0.96	0.20	0.16	0.03	1.06	2.36
TiO_2	0.70	0.54	0.73	0.39	0.75	0.74
MnO	0.34	0.35	0.31	0.27	0.28	0.31
P_2O_5	0.25	0.43	0.29	0.07	0.20	0.26
LOI	0.70	0.70	0.80	0.70	0.70	1.60
TOTAL	99.93	100.73	99.42	99.51	98.45	100.88

	7542	7543	7544	7545	7546	7547
	553096	553096	547100	547100	547100	542103
SiO_2	63.79	60.15	63.96	62.27	60.01	61.24
Al_2O_3	16.90	18.63	16.97	17.55	16.43	16.72
Fe_2O_3	3.78	4.95	4.04	3.46	4.66	6.52
MgO	1.29	1.55	1.27	1.34	1.73	2.17
CaO	9.02	9.44	8.01	10.34	11.18	8.51
Na_2O	1.15	1.01	1.15	0.59	0.61	1.12
K_2O	0.47	0.94	1.20	1.59	0.81	0.97
TiO_2	0.74	0.73	0.68	0.71	0.69	0.74
MnO	0.28	0.31	0.32	0.32	0.41	0.38
P_2O_5	0.22	0.30	0.32	0.27	0.25	0.24
LOI	0.90	0.90	1.70	2.40	2.60	0.90
TOTAL	98.54	98.91	99.62	100.84	99.38	99.51

* These calc-silicates are from outside the area, but were used in Chapter 8 for the metamorphic study (samples collected by J.A.W. and analysed by K.H.W.).

	7548	7549	7550	7551
	542103	542103	542103	536106
SiO_2	58.03	57.35	58.87	59.35
Al_2O_3	18.37	18.12	16.23	16.84
Fe_2O_3	7.69	4.03	4.23	5.57
MgO	2.80	1.56	1.65	1.75
CaO	5.71	11.54	12.65	11.09
Na_2O	1.13	1.44	0.91	0.80
K_2O	3.02	2.21	1.45	1.24
TiO_2	0.82	0.64	0.64	0.67
MnO	0.39	0.40	0.41	0.56
P_2O_5	0.27	0.34	0.24	0.25
LOI	1.50	2.20	3.10	2.40
TOTAL	99.73	99.83	100.38	100.52

Below are listed trace element concentrations for the samples which are referred to and used in Chapter 7. All values are in parts per million. Samples are listed by lithology first and numerical order second (the latter within formations).

		Nb	Zr	Y	Sr	Rb	Ni	Cr
Semi-Pelitic								
Fechlin	626	14	181	44	326	165	--	--
	648	16	145	23	265	150	34	86
Knockchoilum	634	16	145	32	223	216	43	110
	660	14	132	33	228	171	45	111
	666	19	177	43	360	163	48	120
	687	19	158	23	328	167	42	112
	695	17	165	31	168	158	35	95
	6123	15	224	38	246	191	41	102
	6220	20	203	50	177	211	39	136
	6250	13	141	39	205	221	51	128
Glen Doe	611	14	154	38	261	210	46	119
	676A	19	195	55	254	135	33	141
	6118	16	180	36	295	138	38	93
	6176	18	222	34	282	140	37	99
	6177	19	211	44	308	153	40	99
	6182	16	180	50	297	114	42	143
	6185	18	433	33	487	73	30	86
Monadhliath	617	22	197	36	150	207	35	139
	694	12	157	26	218	194	28	108
	6115	10	130	35	181	194	47	127
	6137	17	372	37	632	57	33	91

		Nb	Zr	Y	Sr	Rb	Ni	Cr
Semi-Psammitic								
Fechlin	627	16	206	25	260	106	33	84
	6171	18	61	12	280	105	17	40
Knockchoilum	633	19	226	31	240	103	32	100
	638	16	292	23	311	79	26	74
	6249	14	156	32	237	121	31	82
Glen Doe	64	18	210	35	356	80	29	79
	65	16	247	34	287	102	28	78
	69	17	215	22	420	78	28	77
	613	17	192	26	320	100	32	80
	616	15	223	29	432	86	29	83
	671	19	257	36	318	114	31	94
	673B	18	391	37	496	88	27	81
	6129	18	322	32	381	79	26	79
	6163	14	325	37	295	74	25	75
Amphibolites-all information is provided in the text Rocks marginal to amphibolites are listed here for information.								
Glen Doe	6183	9	239	26	157	98	35	84
	6191	19	320	46	134	194	97	124
	714	13	198	33	240	156	44	114
Granitic								
'Foyers'	657		165	20	348	80		
(intrudes	658		229	21	266	57		
Fechlin)								
'Allt Crom'	6235		143	8	528	69		
(intrudes	6244		166	12	464	64		
Knockchoilum)								

		Zr	Y	Sr	Rb
Granophyres					
Group 1					
Knockchoilum	6251	51	6	272	73
	6253	53	5	253	74
Glen Doe	6144	47	5	179	92
	6215	104	13	82	106
	76	50	6	158	81
	722	49	5	224	80
Monadhliath	6211	52	6	247	86
	6230	49	10	290	68
Group 2					
Knockchoilum	6233	207	19	385	64
Glen Doe	725	201	15	446	133

REFERENCES

ALLEN, J.R.L. 1965. The sedimentation and palaeography of the Old Red Sandstone of Anglesey, North Wales. Proc. Yorks. Geol. Soc., 35, 139-185.

ALLEN, J.R.L. 1977. The possible mechanics of convolute lamination in graded sand beds. Jl. geol. Soc. Lond., 134, 19-31.

ANDERSON, J.G.C. 1947. The geology of the Highland Border, Stonehaven to Arran. Trans. Roy. Soc. Edinb., 61, 497-515.

ANDERSON, J.G.C. 1947a. The Kinlochlaggan Syncline, Southern Inverness-shire. Trans. geol. Soc. Glasg., 21, 97-115.

ANDERSON, J.G.C. 1948. Stratigraphical nomenclature of Scottish metamorphic rocks. Geol. Mag., 85, 89-96.

ANDERSON, J.G.C. 1956. The Moinian and Dalradian rocks between Glen Roy and the Monadhliath Mountains. Trans. Roy. Soc. Edinb., 63, 15-36.

ATHERTON, M.P. 1965. The Chemical Significance of Isograds. In: Pitcher, W.S. & Flinn, G.W. (eds.) Controls of Metamorphism. Oliver & Boyd, Edinburgh, 368p.

BAILEY, E.B. 1934. West Highlands Tectonics: Loch Leven to Glen Roy. Q. Jl. geol. Soc. Lond., 90, 462-524

BARROW, G., HINXMAN, L.W., CUNNINGHAM CRAIG, E.H. & KYNASTON, H. 1913. The geology of Upper Strathspey, Gaick and the Forest of Atholl. Mem. geol. Surv. Gt. Br., 64.

BARTH, T.F.W. 1936. Structural and petrologic studies in Dutchess County, New York. Pt.II. Petrology and metamorphism of the Palaeozoic Rocks. Bull. Geol.

Am., 47, 775.

BELL, T.H. & ETHERIDGE, M.A. 1973. Microstructure of Mylonites and their descriptive terminology. Lithos, 6, 337-348.

BOSWORTH, T.O. 1925. The Pre-Tertiary Geology of Mull, Loch Aline and Oban. Mem. Geol. Surv. U.K.

BOUMA, A.H. 1962. Sedimentology of Some Flysch Deposits. Elsevier, Amsterdam. 168p.

BROOK, M., POWELL, D. & BREWER, M.S. 1977. Grenville events in Moine rocks of the Northern Highlands, Scotland. Jl. geol. Soc. Lond., 133, 489-496.

BROWN, P.E., MILLER, J.A. & GRASTY, R.L. 1968. Isotopic ages of late Caledonian granitic intrusions in the British Isles. Proc. Yorks. Geol. Soc., 36, 251-276.

BUTLER, B.C.M. 1965. A chemical study of some rocks of the Moine Series of Scotland. Q. Jl. geol. Soc. Lond., 121, 163-208

CARMICHAEL, D.M. 1970. Intersecting isograds in the Wheatstone Lake area. J. Petrology, 11, 147-181.

CARMICHAEL, I.S.E., TURNER, F.J. & VERHOOGEN, J. 1974. Igneous Petrology. McGraw Hill, New York.

CLARKE, F.W. 1924. Data of Geochemistry. 5th. ed. U.S. Geol. Surv. Bull., 770.

CLIFFORD, T.N. 1957. The stratigraphy and structure of part of the Kintail district of southern Ross-shire: In relation to the northern Highlands. Q. Jl. geol. Soc. Lond., 113, 57-92.

COBBOLD, P.R., COSGROVE, J.W. & SUMMERS, J.M. 1971. Development of internal structures in deformed, anisotropic rocks. Technophysics, 12, 23-53

CONDIE, K.C. 1967. Geochemistry of early Precambrian greywackes from Wyoming. Geochim. cosmochim. Acta, 31, 2135-49.

COOPER, A.F. & LOVERING, J.F. 1970. Greenschist amphiboles from Haast River, New Zealand. Contrib. Mineral. Petrol., 27, 11-24.

COSGROVE, J.W. 1976. The formation of crenulation cleavage. Jl. geol. Soc. Lond., 132, 155-178.

DALZIEL, I.W.D. 1966. A structural study of the granitic gneiss of western Ardgour, Argyll and Inverness-shire. Scott. J. geol., 2, 125-152.

DALZIEL, I.W.D. & BROWN, R.L. 1965. The structural dating of the sillimanite-grade metamorphism of the Moines in Ardgour (Argyll) and Moidart (Inverness-shire). Scott. J. geol., 1, 304-11.

DEARNLY, R. 1967. Metamorphism of minor intrusions associated with the Newer Granites of the Western Highlands of Scotland. Scott. J. geol., 3, 449-459.

DEER, W.A.,HOWIE, R.A. & ZUSSMAN, J. 1962. Rock-Forming Minerals. Vol. 1 Ortho and Ring Silicates. Longman 333p.

DREVER, H.I. 1940. The geology of Ardgour, Argyllshire. Trans. Roy. Soc. Edinb., 60, 141-170.

ELLIOT, D. 1965. The quantitative mapping of directional minor structures. J. Geol., 73, 865-880.

ELLIOT, R.B. 1973. The chemistry of Gabbro/Amphibolite transitions in Southern Norway. Contrib. Mineral. Petrol., 38, 71-79

ENGEL, A.E.J. & ENGEL, C.G. 1962. Progressive metamorphism of amphibolite, north-west Adirondack Mountains,

New York. In: Buddington Volume, Geol. Soc. Am. Bull., 37-82.

FAIRBAIRN, H.W. 1949. Structural Petrology of Deformed Rocks. Addison-Wesley, Reading, Mass., 344p.

FERRY, J.M. 1976. Metamorphism of calcareous sediments in the Waterville-Vassalboro area, south-central Maine. Mineral reactions and graphical analysis. Am. J. Sci., 276, 841-882.

FIELD, D. & ELLIOT, R.B. 1974. The chemistry of Gabbro/Amphibolite transitions in Southern Norway. Contrib. Mineral. Petrol., 47, 63-76.

FLANAGAN, F.J. 1974. Reference samples for the earth sciences. Geochim. cosmochim. Acta, 38, 1731-1744.

FLEUTY, M.J. 1961. The 3 fold-systems in the metamorphic rocks of Upper Glen Orrin, Ross-shire and Inverness-shire. Q. Jl. geol. Soc. Lond., 117, 447-479.

FLEUTY, M.J. 1964. The description of folds. Proc. Geol.Ass., 75, 461-492.

FLOYD, P.A. & WINCHESTER, J.A. 1975. Magma type and tectonic setting discrimination using immobile elements. Earth Planet. Sci. Lett., 27, 211-218.

GAY, N.C. & WEISS, I.E. 1974. The relationship between principal stress directions and the geometry of kinks in folded rocks. Tectonophysics, 21, 287-300.

GHENT, E.D. & DE VRIES, C.D.S. 1972. Plagioclase-garnet-epidote equilibria in hornblende-plagioclase bearing rocks from the Esplanade Range, British Columbia. Can. J. Earth Sci., 9, 618-635.

GILETTI, B.J., MOORBATH, S. & LAMBERT, R.St.J. 1961. A geochronological study of the metamorphic complexes of the Scottish Highlands. Q. Jl. geol. Soc. Lond., 117, 233-272.

GOLDSCHMIDT, V.M. 1915. Geologisch-petrographische Studien in Hochgebirge des Sudlichen Norwegan P III. (Trondhjem-Gebiet). Vidensk. Selsk. Skr. I. Mat-naturv., K-10, 1-37.

GOLDSCHMIDT, V.M. 1933. Grundlagen der quantitativen Geochemie. Fortschr. Mineral. Krist. Petrogr., 17, 112.

GRAY, D.R. 1977. Morphologic classification of crenulation cleavage. J. Geol., 85, 229-235.

HARLAND, W.B. et al. 1972. A concise guide to stratigraphical procedure. Jl. geol. Soc. Lond., 128, 295-305.

HARVEY, P.K., TAYLOR, D.M., HENDRY, R.D. & BANCROFT, F. 1973. An accurate fusion method for the analysis of rocks and chemically related materials by X-ray fluorescence spectrometry. X-Ray Spectry., 2, 33-44.

HASELOCK, P.J. & WINCHESTER, J.A. (in press). The stratigraphic relationship of the Leven Schists and Monadhliath Schists in the Central Highlands of Scotland. J. Geol.

HEWITT, D.A. 1973. The metamorphism of micaceous limestones from south-central Connecticut. Am. J. Sci., 273A (Cooper Vol.), 444-467.

HICKMAN, A.H. 1975. The stratigraphy of late Precambrian metasediments between Glen Roy and Lismore. Scott. J. Geol., 11, 117-142.

HINXMAN, L.W., ANDERSON, E.M. et al. 1915. The geology of mid-Strathspey and Strathdearn. Mem. Geol. Surv. Scot., 74.

HOBBS, B.E., MEANS, W.D. & WILLIAMS, P.F. 1976. An Outline of Structural Geology. J.Wiley, New York. 571p.

HORNE, J. & HINXMAN, L.W. 1914. The geology of the country around Beauly and Inverness. Mem. Geol. Surv. Scot., 83.

HÖY, T. 1976. Calc-silicate isograds in the Riondel area, S.E. British Columbia. Can. J. Earth Sci., 13, 1093-1104.

HUDDLESTON, P.J. 1973. Fold morphology and some geometrical implications of theories of fold development. Tectonophysics, 16, 1-46.

INGRAM, R.L. 1954. Terminology for the thickness of stratification and parting units in sedimentary rocks. Geol. Soc. Am. Bull., 65, 937-938.

JENKINS, R. & DE VRIES, J.L. 1967. Practical X-Ray Spectrometry. Macmillan, London. 109p.

JOHNSON, H.D. 1977. Shallow marine sand bar sequences: an example from the late Precambrian of North Norway. Sedimentology, 24, 245-270.

JOHNSON, H.D., LEVELL, B.K. & SIEDLECKI, S. 1978. Late Precambrian sedimentary rocks in East Finnmark, north Norway and their relationship to the Trollfjord-Komagelv fault. Jl. geol. Soc. Lond., 135, 517-533.

JOHNSON, M.R.W. & DALZIEL, I.W.D. 1966. Metamorphosed lamprophyres and the late thermal history of the Moines. Geol. Mag., 103, 240-249.

JOHNSON,M.R.W. & FROST,R.T.C. 1977.Fault and lineament patterns in the Southern Highlands of Scotland. Geol. en Mijnb.,287-294.

JOHNSTONE,G.S., SMITH,D.I. & HARRIS,A.L. 1969. The Moinian Assemblage of Scotland. Mem.Am.Ass.Petrol.Geol.,12, 159-180.

JOHNSTONE,G.S. 1975. The Moine Succession. In:Harris,A.L. et al.(eds.) A Correlation of Precambrian rocks in the British Isles.Spec.Rep.geol.Soc.Lond.,6.

KENNEDY,W.Q. 1949. Zones of progressive regional metamorphism in the Moine Schists of the Western Highlands of Scotland. Geol.Mag., 86, 43-56.

KLEIN,C. 1969. Two-amphibole assemblages in the system actinolite-hornblende-glaucophane.Am.Min., 54, 212-237.

KRYNINE,P.D. 1935. Arkose deposits in the humid tropics. A study of sedimentation in Southern Mexico. Am.J.Sci., 29, 353-363.

KUENEN,Ph.H. 1953. Significant features of graded bedding. Bull.Am.Ass.Pet.Geol., 37, 1044-1066.

KUENEN,Ph.H. 1958. Experiments in Geology. Trans.geol.Soc. Glas., 23, 1-28.

LAMBERT,R.St.J. & HOLLAND,J.G. 1974. Yttrium geochemistry applied to petrogenesis utilising Ca-Y relationships in minerals and rocks.Geochim. cosmochim. Acta,38, 1393-1414.

LAMBERT,R.St.J., WINCHESTER,J.A. & HOLLAND,J.G. 1981. Comparative geochemistry of pelites from the Moinian and Appin Group (Dalradian) of Scotland.Geol.Mag.,118,477-90.

LEAKE,B.E. et al. 1969. The chemical analysis of rock powders by automatic X-ray fluorescence. Chem.Geol., 5, 7-86.

LONG, L.E. & LAMBERT, R.St.J. 1963. Rb-Sr isotopic ages from the Moine Series. In: Johnson, M.R.W. & Stewart, F.H. (eds.) The British Caledonides. Oliver & Boyd, Edinburgh.

MACDONALD, G.A. & KATSURA, T. 1964. Chemical composition of Hawaiian lavas. J. Petrology, 5, 82-133.

MACGREGOR, A.G. 1948. Resemblances between Moine and Sub-Moine metamorphic sediments in the Western Highlands of Scotland. Geol. Mag., 85, 265-275.

MCKEE, E.D. & WEIR, G.W. 1953. Terminology for stratification and cross-stratification in sedimentary rocks. Geol. Soc. Am. Bull., 64, 381-390.

MARSTON, R.J. 1971. The Foyers granitic complex, Inverness-shire, Scotland. Q. Jl. geol, Soc. Lond., 126, 331-368.

MIDDLETON, G.V. 1959. Chemical composition of sandstones. Geol. Soc. Am. Bull., 70, 1645.

MILLER, J.A. & BROWN, P.E. 1965. K-Ar age studies in Scotland. Geol. Mag., 102, 106-134.

MINAMI, E. 1935. Selen-Gehalte von europäischen und japanischen Tonschieferen. Nachr. Ges. Wiss. Göttingen. Math.-physik, 4, 143.

MOORBATH, S. 1969. Evidence for the age of deposition of the Torridonian sediments of northwest Scotland. Scott. J. Geol., 5, 154-170.

MOORE, B.R. & DENNEN, W.H. 1970. A geochemical trend in Si-Al-Fe ratios and the classification of clastic sediments. J. Sed. Petrol., 40, 1147-1152.

MOULD, D.D.C.P. 1946. The geology of the Foyers 'granite' and the surrounding country. Geol. Mag., 83, 249-265.

MUECKE, G.K. 1969. Petrogenesis of granulite facies rocks from the Lewisian of north-west Scotland. Unpublished D.Phil. thesis, University of Oxford.

NARAYANAN KUTTY, T.R. & ANANTHA IYER, G.V. 1977. Chemical petrology of calc-silicate rocks and associated metamorphics around Sakarsanahalli Kolar. Ind. J. Earth Sci., 4, 141-159.

NORRISH, K. & CHAPPELL, B.W. 1967. X-ray Fluorescence Spectrography. In: Zussman, J.(ed.) Physical Methods in Determinative Mineralogy. Academic Press, London, 161-214.

NORRISH, K. & HUTTON, J.T. 1969. An accurate X-ray spectrographic method for the analysis of a wide range of geological samples. Geochim. cosmochim. Acta, 33, 431-453.

PARSON, L.M. 1979. The state of strain adjacent to the Great Glen Fault. In: Harris, A.L., Holland, C.H. & Leake, B.E. (eds.) The Caledonides of the British Isles-Reviewed. Spec. Publ. Geol. Soc. Lond.

PETTIJOHN, F.J. 1949. Sedimentary Rocks. Harper & Bros. New York.

PETTIJOHN, F.J. 1963. Chemical composition of sandstones-excluding carbonate and volcanic sands. U.S. Geol. Survey Prof. Paper, 440-S, 19p.

PETTIJOHN, F.J., POTTER, P.E. & SIEVER, R. 1972. Sand and Sandstone. Springer-Verlag, New York. 618p.

PHILLIPS, F.R. 1974. Myrmekite-100 years later. Lithos, 7, 181-194.

PIASECKI, M.A.J. 1975. Tectonic and metamorphic history of the Upper Findhorn, Inverness-shire, Scotland. Scott. J. Geol., 11, 87-115.

PIASECKI, M.A.J. 1980. New light on the Moine rocks of the Central Highlands of Scotland. Jl. geol. Soc. Lond., 137, 41-60.

PIASECKI, M.A.J. & VAN BREEMEN, O. 1979. The 'Central Highland Granulites': cover-basement tectonics in the Moine. In: Harris, A.L., Holland, C.H. & Leake, B.E. (eds.) The Caledonides of the British Isles-Reviewed. Spec. Publ. Geol. Soc. Lond.

PIASECKI, M.A.J. & VAN BREEMEN, O. 1979a. A Morarian age for the 'younger Moines' of central and western Scotland. Nature, Lond., 278, 734-736.

POOLE, A.B. 1966. The stratigraphy and structure of Northeast Morar, Inverness-shire. Scott. J. Geol., 2, 38-53.

POWELL, D. 1964. The stratigraphical succession of the Moine Schists around Lochailort and its regional significance. Proc. Geol. Ass., 75, 223-246.

PRICE, N.J. 1966. Fault and Joint Development in Brittle and Semi-brittle Rock. Pergamon Press, Oxford. 176p.

RAMDOHR, P. 1969. Ore Minerals and Their Intergrowths. Pergamon Press, Oxford.

RAMSAY, J.G. 1962. The geometry and mechanics of formation of 'similar' type folds. J. Geol., 70, 309-327.

RAMSAY, J.G. 1967. Folding and Fracturing of Rocks. McGraw Hill, New York, 568p.

RAMSAY, J.G. & SPRING, J. 1962. Moine Stratigraphy in the Western Highlands of Scotland. Proc. Geol. Ass., 73, 295-326.

RANKAMA, K. & SAHAMA, Th.G. 1950. Geochemistry. Chicago University Press.

READ, H.H. 1931. The Geology of Central Sutherland. Mem. Geol. Surv. Scot., 108 & 109.

READ, H.H. 1961. Aspects of Caledonian magmatism in Britain. L'pool Manch. Geol. J., 2, 653-683.

REINECK, H.E. & SINGH, I.B. 1975. Depositional Sedimentary Environments. Springer-Verlag, New York, 439p.

REYNOLDS, R.C. 1963. Matrix corrections in trace element analysis by X-ray fluorescence estimation of the mass absorption coefficient by Compton scattering. Am. Min., 48, 1133-1143.

RICHEY, J.E. 1938. Mem. Geol. Surv. Summ. Prog. for 1937, 72.

SANDERS, J.E. 1965. Primary sedimentary structures formed by turbidity currents and related resedimentation mechanisms. In: Middleton, G.V. (ed.) Primary Sedimentary Structures and their Hydrodynamic Interpretation. Soc. Econ. Pal. Min. Spec. Publ. 12, 192-219.

SCHWARCZ, H.P. 1966. Chemical and mineralogic variations in an arkosic quartzite during progressive regional metamorphism. Geol. Soc. Am. Bull., 77, 509-532.

SHAW, D.M. 1954. Trace elements in pelitic rocks. 1:Variations during metamorphism. 2:Geochemical variations. Geol. Soc. Am. Bull., 65, 1151-1182.

SHAW, D.M. 1956. Geochemistry of pelitic rocks. Part III: Major elements and general geochemistry. Geol. Soc. Am. Bull., 67, 919-934.

SHIDO, F. & MIYASHIRO, A. 1959. Hornblende of basic metamorphic rocks. J. Fac. Sci. Univ. Tokyo, 12, 85-102.

SPRY, A. 1969. Metamorphic Textures. Pergamon Press, Oxford, 350p.

STORRE, B. & NITSCH, K.H. 1972. Die Reaktion, 2 zoisit + 1 CO_2 = 3 Anorthit + 1 Calcit + 1 H_2O. Beitr. Mineral. Petrog., 35, 1-10.

STRENS, R.G.J. 1965. Stability and relations of the Al-Fe epidotes. Min. Mag., 35, 464-475.

TANNER, P.W.G. 1970. The Sgurr Beag Slide- a major tectonic break within the Moinian of the Western Highlands of Scotland. Q. Jl. geol. Soc. Lond., 126, 453-463.

TANNER, P.W.G. 1976. Progressive regional metamorphism of thin calcareous bands from the Moinian rocks of north-west Scotland. J. Petrology, 17, 100-134.

THOMPSON, A.B. 1975. Mineral reactions in a calc-mica schist from Gassetts, Vermont, U.S.A. Contrib. Mineral. Petrol., 53, 105-127.

THOMPSON, P,H. 1973. Mineral zones and isograds in 'impure' calcareous rocks, an alternative means of evaluating metamorphic grade. Contrib. Mineral. Petrol., 42, 63-80.

TILL, R. 1974. Statistical Methods for the Earth Scientist- an introduction. Macmillan, London, 154p.

TILLEY, C.E. 1924. The facies classification of metamorphic rocks. Geol. Mag., 61, 167.

TOBISCH, O.T. 1963. The structure and metamorphism of the Moinian rocks in the Glen Cannich-Fasnakyle Forest areas, Inverness-shire, Scotland. Unpublished Ph.D. thesis, University of London.

TURNER, F.J. & WEISS, L.E. 1963. Structural Analysis of Metamorphic Tectonites. McGraw Hill, New York, 545p.

VAN DER KAMP, P.C., LEAKE, B.E. & SENIOR, A. 1976. The petrography and geochemistry of some Californian arkoses with application to identifying gneisses of metasedimentary origin. J.Geol., 84, 195-212.

VIDALE, R.J. 1969. Metasomatism in a chemical gradient and the formation of calc-silicate bands. Am. J. Sci., 267, 857-874.

VIDALE, R.J. & HEWITT, D.A. 1973. 'Mobile' components in the formation of calc-silicate bands. Am. Min., 58, 991-997.

WEDEPOHL, K.H. 1969. Handbook of Geochemistry. Springer-Verlag, New York.

WHITTEN, E.H.T. 1966. Structural Geology of Folded Rocks. Rand McNally & Co. U.S.A. 678p.

WILSON, G., WATSON, J. & SUTTON, J. 1953. Current bedding in the Moine Series of north-western Scotland. Geol. Mag., 90, 377-387.

WINCHESTER, J.A. 1970. The Geology of Fannich Forest. Unpublished D.Phil. thesis, University of Oxford.

WINCHESTER, J.A. 1972. The petrology of Moinian calc-silicate gneisses from Fannich Forest, and their significance as indicators of metamorphic grade. J. Petrology, 13, 405-424.

WINCHESTER, J.A. 1974a. The control of whole-rock content of CaO and Al_2O_3 on the occurrence of the aluminosilicate polymorphs in amphibolite facies pelites. Geol. Mag., 111, 205-211.

WINCHESTER, J.A. 1974b. The zonal pattern of regional metamorphism in the Scottish Caledonides. Jl. geol. Soc. Lond., 130, 509-524.

WINCHESTER, J.A. 1974c. The three-dimensional pattern of polyphase metamorphism in the Moinian assemblage of Northern Ross-shire. J. Geol., 82, 637-649.

WINCHESTER, J.A. 1975. Epidotic calc-silicates of Arnipol type-a widely distributed minor sedimentary facies of the Moinian assemblage, Scotland. Geol. Mag., 112, 175-181.

WINCHESTER, J.A. 1976. Different Moinian amphibolite suites in northern Ross-shire. Scott. J. Geol., 12, 187-204.

WINCHESTER, J.A. & FLOYD, P.A. 1976. Geochemical magma type discrimination: Application to altered and metamorphosed basic igneous rocks. Earth Planet. Sci. Lett., 28, 459-469.

WINCHESTER, J.A. & WHITTLES, K.H. 1979. The pattern of three-dimensional metamorphism in the Killin area, Inverness-shire:a direct method of determining the thickness of metamorphic zones in the Caledonides. In:Harris, A.L., Holland, C.H. & Leake, B.E. (eds.) The Caledonides of the British Isles-Reviewed. Spec. Publ. Geol. Soc. Lond.

WISEMAN, J.D.H. 1934. Central and south-west Highland epidiorites. Q. Jl. geol. Soc. Lond., 90, 354.

WRIGHT, F.E. 1911. The Methods of Petrographic-microscopic Research. Carnegie Inst. Pub. 158.

THE SOLID GEOLOGY OF THE AREA WEST OF LOCH KILLIN, INVERNESS-SHIRE.

Gradational Lithological Boundary ------

Inferred ---?---

Subsidiary Lithological Boundary ——

Inferred ·····

Subsidiary Lithologies — Quartzite

— Pelite

Intrusive:

Newer Granites + + + +

Granitic Dykes and Sheets

Granophyric Dykes

Granite Contact ----

Inferred ---?---

Metasediment Foliation, with dip: 56 vertical: ⊢

Fault —·—·—

Foyers Granite (with xenoliths)

ALLUVIUM

Allt Breinegg

Cumrack Burn

dam

River Fechlin

Loch nan Eun

Allt Yungie

Allt Doe

River Tarff

Glen Tar

Foyers Granite

Fechlin Psammite

Knockchoilum Semi-psammite

Glen Doe Semi-psammite

Monadhliath Semi-pelite

Glen Doe Semi-psammite

Knockchoilum Semi-psammite

Allt Crom Granite

N

0 1 2 km

0 40 km.

Inverness

43 44 45 46 47 48 50

12 13 14 05 04 03

Allt Breinead

Glen Brein

Loch Killin

River Killin

Allt a' Choire Odhair

Allt Odhar

Allt Crom Granite
(with xenoliths)

NO EXPOSURE

N

kilometres

0 1 2

0 200 400 600 800
metres

National Grid